HIGH FIELD ELECTROMAGNETS

by

P.O.CARDEN

A collection of papers submitted for the degree of Doctor of Philosophy of the Australian National University by submission of published work.

October 1975

P. Carden.

THE RELATION BETWEEN PUBLICATIONS

The publications being submitted are:

1. High field magnet laboratory at Canberra - Carden - Proc. I.E.E., vol 115, No.5, pp. 711-715, May 1968.

2. Features of the high-field magnet laboratory at the Australian National University, Canberra - Carden - EP-RR 19, January, 1967.

3. Mechanical stresses in bonded plane helical solenoids with arbitrary external field - Carden - Journal of scientific instruments (Journal of Physics E), series 2, vol.1, pp. 437-443, 1968.

4. Mechanical stresses in an infinitely long homogeneous Bitter solenoid with finite external field - Carden - EP-RR 12, January, 1967.

5. The design and construction of a Bitter solenoid having a 26 cm diameter bore and generating 16.5 Tesla with 26 MW of power - Carden - Third International Conference on magnet technology, Carden, Hamburg, 1970.

6. The limitations of homogeneous plane helical solenoids in high field applications - Carden - Third international conference on magnet technology, Hamburg, 1970.

7. Instrumentation of the Australian National University 300 kilogauss experimental magnet - Carden, Whelan, R.E. - EP-RR 25, December, 1969.

8. Design principles relating to the strength and structure of the A.N.U. 30T electromagnet - Carden - Journal of Physics E, vol. 5, pp 654-656, 1972.

9. Design and construction of the inner solenoid of the A.N.U. 30 T electromagnet - Carden - Journal of Physics E, vol 5, pp 663-666, 1972.

10. Design and construction of the outer solenoid of the A.N.U. 30 T electromagnet - Carden - Journal of Physics E, vol. 5, pp. 657-662, 1972.

11. Testing the A.N.U. 30 T high field magnet at Canberra - Carden - Journal of Physics E, vol. 5, pp. 667-668, 1972.

12. The ultimate possibilities of quasi continuous high field electromagnets - Carden, Collins, A.M. - Journal of Physics E, vol 7, pp. 750-756, 1974.

13. Exceptional aspects of high power resistive solenoids in relation to their use in hybrid magnet systems. Hudson, P.A., Hanley,P.E.,Carden - Fifth international conference on magnet technology, Frascati (Rome) April 1975.

14. A method of bonding metal to metal or other materials - Australian patent no. 44033/68 - Carden, Harris, J.C., Ladyzhynsky,Y. (assigned to the A.N.U. - now lapsed)

Those publications designated EP-RR are Department of Engineering Physics Research Reports.

Of the above only numbers 7, 12, and 13 are under joint authorship. Number 7 divides naturally into two aspects, theoretical and technical. Mr. Whelan was responsible for the latter and I for the former and for the writing of the paper. In the case of number 12, Mr. Collins did the programming and the computing. The scope, methodology and the writing were due to me. Number 13 was written in England by Hudson and Hanley. I was included because the specific hybrid magnet referred to contained a resistive solenoid designed and built in Australia by a team under my

leadership. With regard to number 14, the joint authors comprised the research group under my direction.

The fourteen papers cited relate to an enterprise whose goal was the establishment of a high magnetic field facility and the development of a long duration magnet more powerful than existed elsewhere in the world. The achievement of this goal was expected to be of great value in making possible new lines of research in solid state physics and the work was well supported by a number of prominent physicists in Australia and England. The feasibility of the project depended entirely on the existence within the Department of Engineering Physics of the unique energy storage device known as the Canberra homopolar generator.

Quasi-continuous fields of 21 Tesla were available at the time (1966) at the National Magnet Laboratory of the Massachusettes Institute of Technology. The term quasi-continuous is used to indicate that the magnet producing the field is capable of producing it for the order of hours provided the electrical energy input and the coolant flow are maintained but that normally the magnet is energised for only a matter of seconds because of the limited capacity of the energy source.

The goal here referred to aimed at generating a 30 Tesla field in a spherical volume of 5 cm diameter (the same as the M.I.T. magnet for reasons of standardisation of insertion equipment). Such intense fields may only be produced - even now - by resistive solenoids i.e. by passing very large amounts of electrical power into a solenoid shaped electrical conductor. The power must then be removed as heat by means of a coolant and hence a large proportion of the problems encountered in developing these devices lie in the area of heat transfer at extreme rates. In common with most other laboratories water was chosen as the coolant.

References 1 and 2 describe the achievement of the first part of the goal, namely the building of a facility for cooling and monitoring large electromagnets and also for switching power to them. Since the development of the 30 T magnet was necessarily to be a research project in its own right the building of this facility turned out also to have a research content since the requirements it had to meet were not able to be met by any other existing facility. In essence the coolant system had to be capable of supplying coolant at flow rates and pressures whose range and general level exceeded those existing in other laboratories. The monitoring component of the facility was unusually extensive for it was required both to ensure the safe operation of the 30 T magnet and to provide the data upon which to base an understanding of the behaviour of a device built according to untried principles.

As well as the problem of heat transfer already mentioned the other great problem with resistive (and all) high field magnets is that of extreme mechanical stresses. The literature on both of these problem areas is fairly extensive beginning with Fabry in the last century and including such notables as Kapitza and Cockroft. However a review of the literature on relevant stress analysis revealed that it was inadequate for the extreme conditions that were to be attempted. I was mindful of the experience of Montgomery and co-workers at M.I.T. who in their attempt to achieve 25 T witnessed a number of seemingly inexplicable mechanical failures and burn-outs which in the end compelled them to settle for a lower field. Others too, including Kapitza, had experienced mechanical failures which they were unable to satisfactorily explain in terms of a reasonably exact and plausible theory. Ultimately I produced references 3 and 4 which were my attempt to fill in the gap that I detected, and upon this analysis was based a further survey of constructional techniques.

One of the most popular methods of construction is that due to Bitter - described in my reference 5. I found that a comprehensive analysis of the consequences of this method in relation to mechanical stresses was not available. I was especially interested in the effect of varying the interleaving pattern and also in the modes of friction failure since the Bitter technique relies on stress transfer through a friction bonded interface. All these things are examined in my reference 5 and the consequ-

sequent limitations of the Bitter technique delineated in reference 6.

It turned out that because of the limitations of the Bitter technique a new constructional method had to be devised for the inner parts of the magnet which experienced the most intense magnetic fields and mechanical stresses. This method and the underlying principles are described and explained in references 8 and 9. The outer part of the magnet was constructed generally in accordance with Bitter but the method had to be taken to extremes in order to extract a design of sufficient strength. The design of the outer solenoid is described in references 5 and 10 and the problems encountered in construction are related in part in ref 5.

The practicability of the new constructional technique chosen for the inner solenoid depended on the discovery of an alternative method of bonding the turns of the "subcoil" elements to replace the method of bonding by friction. This bond had to be mechanically strong at temperatures up to 150°C, electrically insulating, and unaffected by the presence of hot water. In addition the bonding method had to allow the turns to be spaced at a specific pitch. Epoxy resin was an obvious first choice but tests showed that in about six months water diffused inwards from the exposed edge and destroyed the epoxy-to-copper bond. Numerous experiments confirmed the nature of failure and the rate of diffusion and showed that the mechanism of bond failure was unrelated to any adverse effects of the water on the resin strength but rather that the diffused water molecules at the resin-to-metal interface competed with the resin to form chemical bonds with the surface molecules of the metal. Thus as a layer of hydroxide was formed on the metal the resin-to-metal bond was progressively destroyed. On the other hand resins which were effectively impervious to water were invariably enamel-like and had to be applied as a solution and subsequently baked to remove the solvent and cause polymerisation. Clearly these could not be used as bonding agents as there had always to be an escape path for the solvent during baking. In fact a simple experiment showed that the escaping solvent so honeycombed the resin with passages that the resin was left virtually without strength. Finally after a year's research a bonding method evolved which is essentially to precoat the metal with a baked phenol formaldehyde layer and to then bond the coated metal surfaces together with an epoxy resin the latter being applied in excess and allowed to exude as the turns are correctly spaced in a lathe-like machine. This method of bonding is described in the patent reference 14.

Besides the method of bonding the turns together described above, there are several other unique and previously untried features of the 30 T magnet particularly the method of distributing and applying the friction bonding force in the outer solenoid (normal to the bond interface) and the method in both solenoids for terminating the electrical connections so as to avoid assymmetry. The importance of this is discussed in refs 5,8,9 and 10.

The many novel features of the 30 T magnet necessitated careful instrumentation in order to ascertain whether the performance was safe and in accordance with expectations. The various aspects of the instrumentation system are discussed in reference 7. The results of testing the magnet are discussed in reference 11.

Following the success of the 30 T magnet which is now the largest and most powerful of its kind in the world and which has performed with unusually high reliability, I decided to explore the possibility of creating higher fields using the principles of the 30 T magnet which had now apparently been proved. This resulted in publication 12.

Finally I was invited to lead a team to design and construct the inner high field section of a hybrid magnet for the Clarendon laboratory, Oxford. A hybrid magnet is a combination of a low field superconducting outer solenoid and a resistive inner solenoid. Although this was in many respects merely the re-application of the principles of the 30 T magnet, there were nevertheless several novel features

High-field-magnet laboratory at Canberra

P. O. Carden, M.E., A.M.I.E.Aust., A.M.I.Mech.E.

Synopsis

Water-cooled electromagnets producing magnetic fields of hundreds of kilogauss and consuming many megawatts of power may be energised for periods as long as several minutes by the 500MJ Canberra homopolar generator and cooled by a unique cooling-water system employing compressed air. The system is automated and power is controlled by a variable-resistor circuit breaker and high-capacity isolators.

1 Introduction

In August 1966, Australia's first high-field-magnet laboratory began operating. There are several such laboratories elsewhere in the world, for example at Oxford and Cambridge in the UK, at Cambridge, Mass., USA, and at Leiden in the Netherlands. The magnets are used as experimental tools mainly in the study of solid-state physics. It is necessary to concentrate the magnets geographically because of the expensive common facilities they require, in particular motor–generators of up to 10MW continuous capacity and closed-loop cooling-water systems of several thousands of gallons per minute capacity.

The laboratory at Canberra is unique since it operates solely on a pulsed basis, the pulsing being, however, of many seconds or minutes duration and hence quasicontinuous for most experimental purposes. The reason for operating in this manner is to exploit the Engineering Physics Department's homopolar generator, which has repeatedly delivered powers of 300MW or more and pulse energies of 500MJ. In this way the economic barrier imposed by conventional continuous-power equipment, and the practical difficulties of absorbing large amounts of power from the national grid, are bypassed.

All the features described here are innovations designed to enable the generation of useful volumes of magnetic fields of as high an intensity as can be obtained with available materials. It is thought that this limit is about 500kGs.

2 Homopolar generators

Michael Faraday, towards the middle of the last century, constructed the forerunner of the homopolar machine. He rotated a disc, through which passed a magnetic field, and observed an e.m.f. between the disc axis and a stationary contact rubbing on the outer edge of the disc. Modern homopolar or unipolar generators (h.p.g.) make use of this principle. By preserving cylindrical symmetry in the exciting field and in the arrangement of electrical contacts and conductors, these machines can be made to convert mechanical (shaft-turning) energy into electrical energy in a highly efficient manner. A homopolar generator is also reversible; i.e. it will perform equally well as a motor or a generator. Thus, when no mechanical power is drawn from it or supplied, it possesses the characteristics of an electrical capacitor of capacitance $2E/V^2$, where E is the kinetic energy of the disc and V is the voltage.

The Canberra machine[3, 6, 11] has four rotating discs each weighing 20ton. At full storage capacity, the peripheral velocity of the discs is two thirds of the speed of sound, and this is the rubbing speed for the outer current-collecting solid brushes.[10] The electromagnet, which forms the exciting field through the discs, weighs 1500ton and stands 20ft high. The equivalent electrical capacitance is some 5000F, and discharge currents of up to $1{\cdot}8 \times 10^6$A have been obtained.

3 Electromagnets

High magnetic fields of the magnitude and duration we are considering here are generated exclusively by water-cooled 'air-cored' electromagnets. Iron-cored electromagnets are limited by saturation to about 40kGs. Superconducting electromagnets are limited to about 120kGs. Above this figure, the only means of generation is by copper or copper-alloy solenoids. For other than very short duration fields, water cooling is essential. Electric current densities up to 40kA/cm^2 and power densities up to 3kW/cm^3 are common. Field intensities, dimensions and powers of the largest available electromagnets are shown in Table 1.

Table 1

DISTRIBUTION OF HIGH-FIELD-MAGNET LABORATORIES

Country	Number of high-field-magnet laboratories	Highest available field	Highest available power	
			Continuous	Pulsed
		kGs	MW	MW
Australia . .	1	165		300 (1s) 5 (1min)
Europe (excluding USSR)	2	90	4	
Japan . . .	1	120	4	
UK . . .	3	130	3·5	
USA . . .	7	205	8	32 (4s)

Many different types of water-cooled magnets are described elsewhere.[4, 5, 7] A particularly successful design was developed by Francis Bitter[2] in 1936. This design is essentially of a single-layer solenoid. In its simplest form each turn consists of a set of thin copper discs, each with a central hole and a radial slit. The discs are interleaved with each other and with similar discs of insulation to form a continuous helix, the overlap between adjacent discs being up to 90°. Specially shaped end plates are used to make contact with the end discs, thus enabling connection to the power source and to provide a means of axially clamping the stack of discs together.

4 ANU facilities

The Australian National University Magnet Laboratory has at present one Bitter electromagnet producing

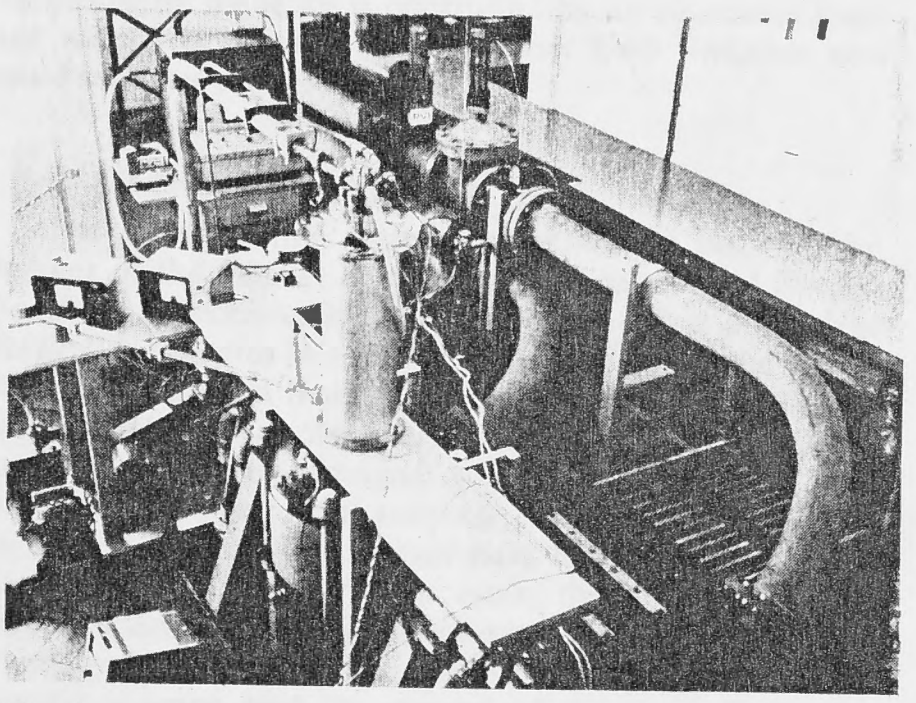

Fig. 1

View of magnet with cryostat above

Busbars and cables joining magnet and isolator can be seen and also the cooling-water pipes

Paper 5516 P, first received 1st August and in revised form 16th November 1967

Mr. Carden is with the Department of Engineering Physics, Australian National University, Canberra ACT, Australia

5kGs and requiring 5MW, 25000A and 1000gal/min of oling water (Fig. 1). A 300kGs magnet is presently being signed. This will require 200kA and 3000gal/min of cooling ter to remove the 30MW of heat generated. These magnets mpare favourably with what is available now in other parts the world, as can be seen from Table 1.

At the ANU, current is carried from the h.p.g. in minium busbars through an electrolytic variable resistor d a hydraulically operated isolator to the magnet.

Current control and circuit breaker

The primary purpose of the electrolytic variable resistor o act as a circuit breaker, but it also provides current trol to within a few per cent of any desired law, as can be n by the examples in Fig. 2. It was built in the first place

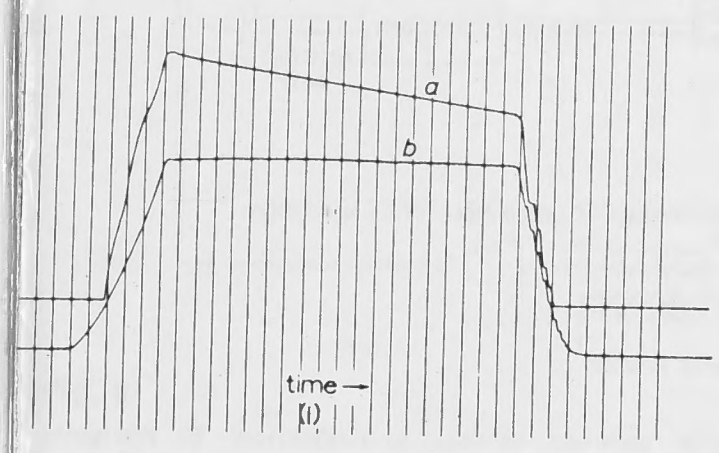

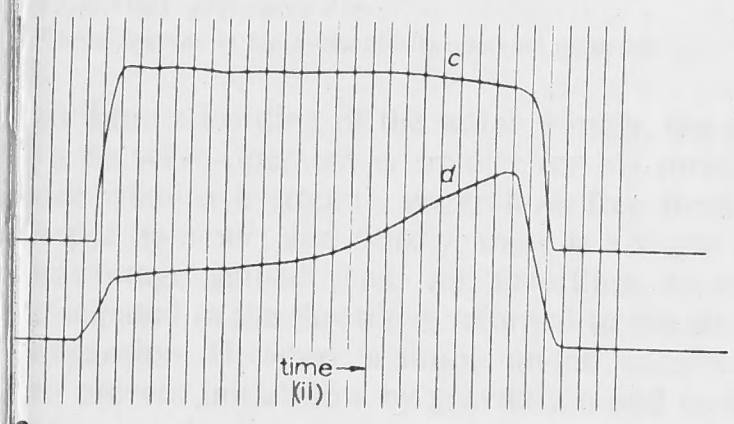

2

examples of field waveforms and associated depths of immersion e electrolytic variable resistor

ntervals of 1s are shown
5 on the 5th August 1966; curve (*a*) is an exponentially decaying field wave- of peak value 140kGs. The circuit resistance is maintained constant, as ed by the depth-of-immersion curve (*b*)
8 on the 5th April 1967; curve (*c*) shows one of the nearest approaches to nt field achieved. The peak value is 96kGs
(*d*) shows the corresponding depth of immersion

ovide a test load for the h.p.g.[3,9] Essentially a 7000lb of caustic soda is raised by a hydraulic servosystem to erge to varying degrees a set of steel electrode plates. servo input is by means of easily cut wooden cams,

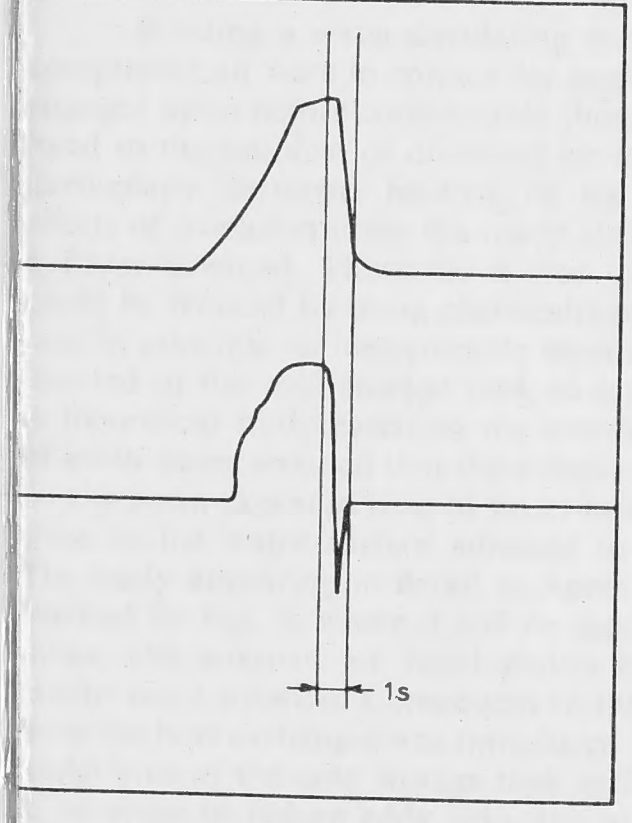

curve shows an actual recording of electrolytic-resistor tank against time during a trial circuit break, together with the onding record of high-field-magnet voltage showing acceptable voltage at break

except that there is a secondary servo input operative only at the extreme limits of travel of the tank to bring it to rest, and a latch mechanism to disengage the primary servosystem. The variable resistor acts as a circuit breaker whenever the latch is operated, the effect being to drop the tank away from the electrodes in a fraction of a second. Fig. 3 shows a recording of tank height against time during a trial circuit break. The device is known to break currents of over a million amperes effectively, and is expected to operate satisfactorily with the currents and magnet inductances anticipated in the future.

6 Electrical isolator

An isolator capable of carrying 200kA has been included in the circuit for reasons of safety and to facilitate circuit checking. It is, of course, an essential item when more than one magnet is available for connection to the h.p.g.

The ANU design is intended to be compact to match the geometry of the busbar system. The principle of operation is shown in Fig. 4. A single row of copper bars of alternate

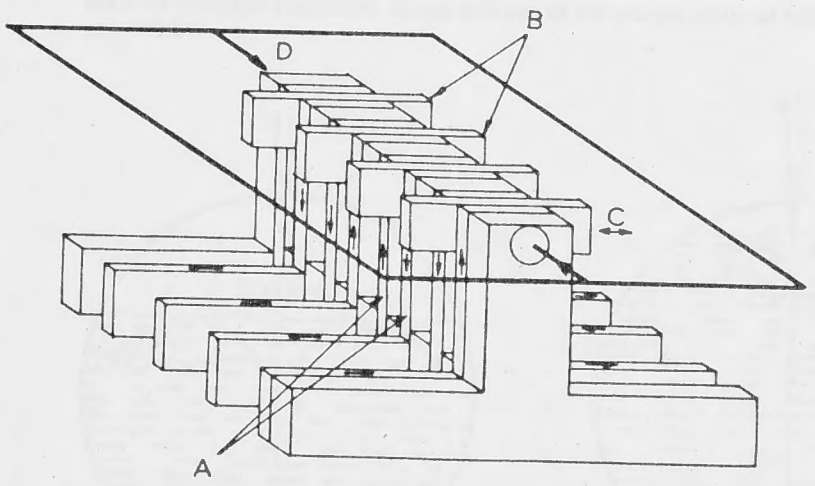

Fig. 4

Diagram of 200kA isolator (actual height about 2ft) showing principle of operation

A Vertical cantilever conductors clamped at lower end. B Bridging pieces capable of sliding in direction shown at C connect two adjacent verticals or separate them with insulation. D Heavy arrows and frame represent contact squeezing system operating at 'switching line'

polarity enter the isolator horizontally, turn at right angles and rise vertically to a 'switching line'. A similar set of separate bars drop vertically from the switching line to the level of the incoming bars, turn at right angles and continue horizontally out of the isolator. The two sets of vertical bars are interleaved and firmly clamped at their lower ends. The upper ends may be slightly sprung apart and are, in fact, interleaved yet again with a set of copper bridging bars at the switching line. When a hydraulic clamp acting along the switching line is pressurised, the circuit through both poles of the isolator is complete. On the other hand, when this clamp is relaxed and the bridging set is moved horizontally, Bakelite insulating sections are drawn between the contacts, thus effecting electrical isolation.

The bridging set is moved by hydraulic means, and the whole switching sequence is controlled by an electronic logic circuit which derives information from limit switches and pressure switches on the isolator.

7 Water-cooling system

The water-cooling system comprises the bulk of the equipment of the magnet laboratory. It is capable of forcing 4000gal/min of chemically pure water through a magnet at 200lbf/in^2. It operates in a pulsed manner to match the nature of the power received from the h.p.g. The water travels in a closed loop (Fig. 5) rapidly during a pulse, between a cold storage tank, through a magnet to a hot storage tank, and slowly during the period of recharge of the h.p.g., from hot storage, through a heat exchanger back to cold storage.

During the rapid part of this cycle, the flow is powered by means of compressed air stored in a 7ft-diameter spherical reservoir and released to the space above the water in the cold-water storage tank by means of an electrohydraulic servo-controlled 3in air valve. The servosystem is, in turn, controlled from an electronic variable-function generator, whose function may be tailored more or less by trial and

error to obtain the desired water-flow law. In this way, water may be conserved and matched to the magnet power law. Control of water flow by throttling air flow is to be preferred

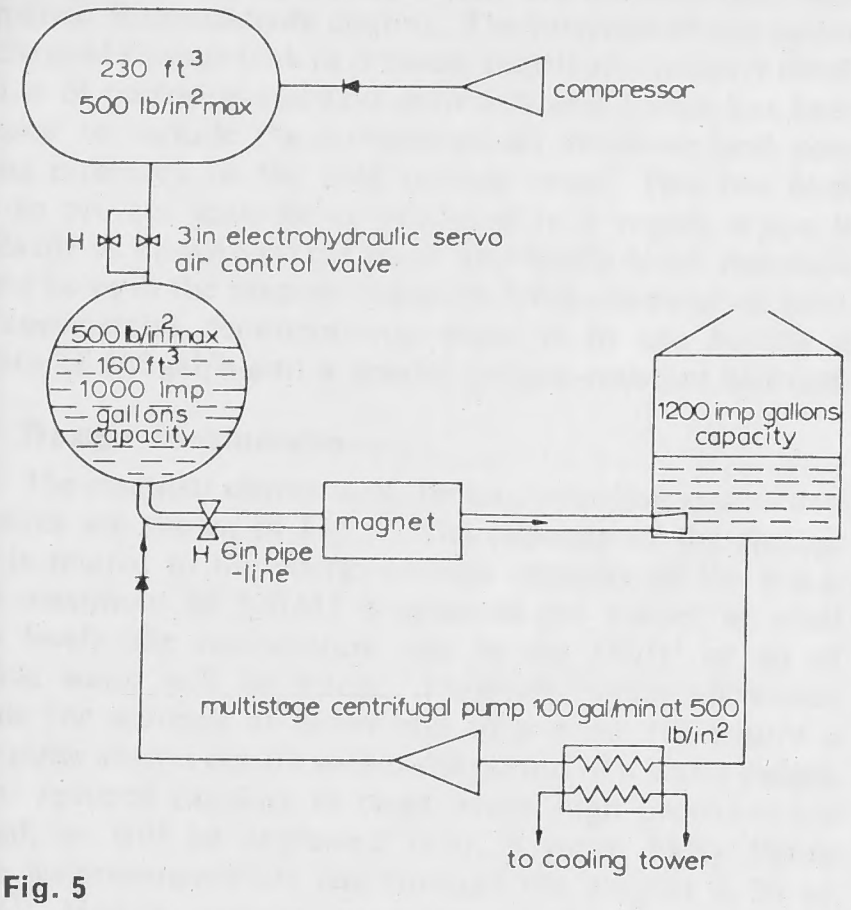

Fig. 5

Diagram of water-cooling system showing essential components capacities, pressures etc.

Valves marked H are hydraulically operated on or off

to direct throttling of the water. Firstly, the size of the valve to be servo-operated is smaller for air throttling; secondly, one obtains a smooth water flow free from the danger of water hammer; and thirdly, there is a slight thermodynamic advantage gained from air throttling, in that the energy dissipated in the throttle is returned to the air causing further expansion. However, a simple on–off water valve is required to prevent initial flow by gravitation and to finally halt flow after a pulse when compressed air still in the cold reservoir would otherwise maintain it. This valve is hydraulically operated and is equipped with a hydraulic device which limits the closing rate, thus preventing water hammer.

A feature of the ANU cooling system is the conservation of compressed air. After a pulse, a high-pressure multistage centrifugal pump is used to pump the water in 5 min or so from hot storage through a heat exchanger to cold storage. In so doing, compressed air is displaced through a bypass valve back into the compressed-air reservoir. This feature, besides being an economical way to compress air, ensures the minimum time between pulses.

7.1 Dissolved air

Building a water-circulating system where water and compressed air were in contact for appreciable times was not engaged upon before considerable thought was given beforehand to the problem of dissolved air in the water. This was particularly pertinent because of the possible deleterious effects of oxidation upon the many electrical contacts within a Bitter solenoid. However, it was clear that this danger could be reduced by using chemically pure water, and in any case in principle an impermeable membrane could always be inserted in the cold storage tank to separate air and water. A theoretical study based on the known diffusion properties of air in water revealed that the solution rate of air depended on the mean exposure time of water molecules to the regions close to the water surface adjacent to the compressed air. The study appearing in detail in Appendix 11 may be summarised by Fig. 6, where it will be seen that short exposure times, characteristic of rapid eddies of small dimensions, favour rapid solution. Consequent to this study, return water from the heat exchanger was introduced into the 6in-diameter outlet pipe of the cold storage tank rather than directly into it, in order to reduce eddy velocities at the surface. During the 'pumpback' part of the water cycle, we have measured solution rates corresponding to an exposure time of 1–2 min (A in Fig. 6). It is interesting to note that viscous effects at the cold-water storage-tank wall during refill would be expected to limit the eddy velocity to the same order of magnitude as the rate of rise of water level (Fig. 7), i.e. $\frac{1}{2}$ ft/min. Assuming a water-surface exposure distance of

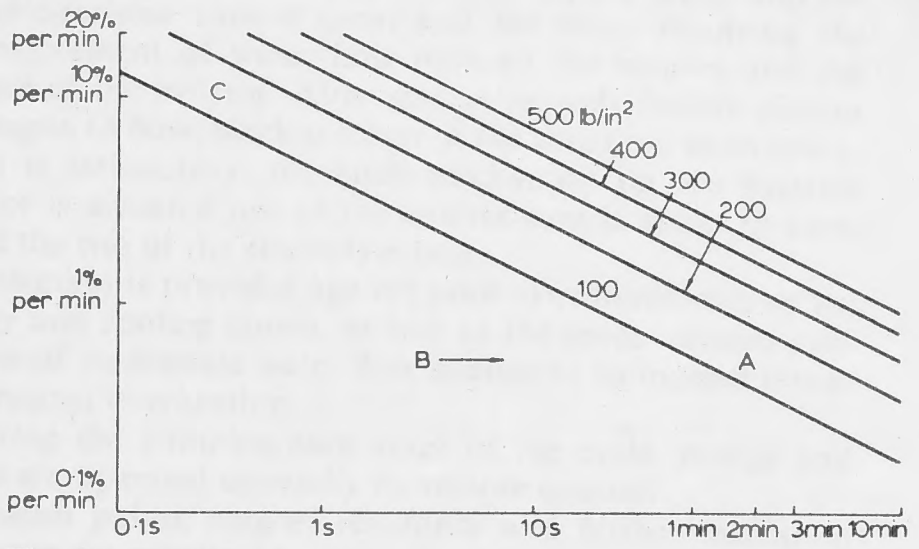

Fig. 6

Rate of solution of dissolved gas in water against mean exposure time of water molecules to surface layer

Rate of solution expressed as percentage of saturated value at atmospheric pressure per minute

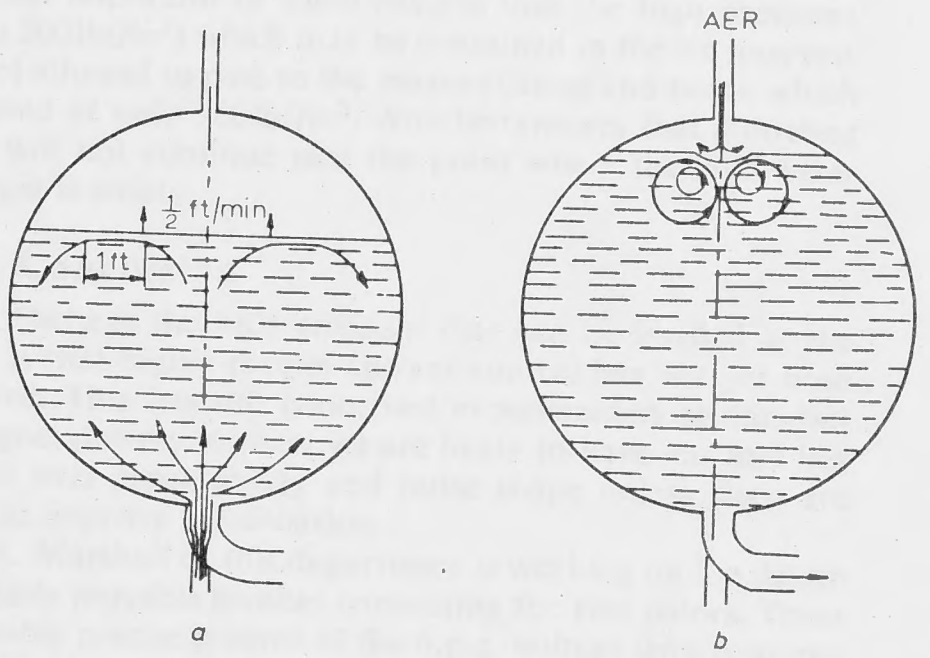

Fig. 7

Diagrams illustrating probable flow eddy currents in cold store

a During slow filling (pump back) *b* During pulsing
In (*a*), measured rates of solution are compatible with the assumptions that surface velocity = rate of rise of surface level ($\frac{1}{2}$ ft/min) and mean exposure distance = 1 ft

1 ft (vessel radius 3 ft), the expected maximum exposure time would therefore be 2 min. Hence it appears that we have reduced the solution of air to the lowest rate possible during this part of the cycle.

However, during the rapid-flow pulse through the magnet, conditions are quite different in the cold storage vessel. Apparently the rapid entry of compressed air induces surface turbulence, giving a twentyfold increase in rates of solution and a corresponding exposure time of only 1/4 s or so (C in Fig. 6). Despite this high rate of solution, the duration is comparatively short, and the total quantity of air introduced is, in fact, about the same as during the slower more docile part of the cycle.

Clearly the dissolved-air concentration would build up to saturation values and remain so if a deaerating plant were not included. We have built a vacuum deaerating unit which treats continuously 10 gal/min drawn from the hot-water storage tank and returned to it so as to promote mixing. In this way, the concentration in the hot storage tank is made to decay exponentially overnight to less than 1% of the equilibrium concentration at ambient temperature and atmospheric pressure. Thus we have ensured that the magnet will not be exposed unnecessarily during periods when it is not in use.

When more magnets are brought into service using the same cooling system, and it is shown that dissolved air is indeed harmful, it may be necessary to fix a plastic bag inside the cold storage vessel to separate the two media. Plans are well in hand for doing this when the occasion arises.

7.2 Water purity

Water purity is monitored by means of a conductivity cell and meter, and is generally below 1 μmho/cm. Materials

ed in contact with the water have been selected for their sistance to corrosion in the presence of oxygen. Thin-walled to 16s.w.g.) pipes and vessels are generally of stain- steel. Large pipes, 6in diameter, are of mild steel with internal formaldehyde coating. The interiors of 6in valves the cold storage tank (a pressure vessel) are similarly lined. e use of corrosion-resistant materials and linings has been nded to include the compressed-air reservoir and con- ting pipework to the cold storage vessel. This has been e to prevent scale being produced in a region where it easily be blown into the water and finally block the small ling holes in the magnet (typically 1/8in-diameter or less). commercial demineralising plant is in use having a acity of 100gal/h and a special oxygen-resistant element.

Design considerations

The essential elements of the water-cooling system and sizes are shown in Fig. 5. The capacity of the storage s is related to the energy-storage capacity of the h.p.g. he maximum of 500MJ is released (no matter at what er level), the temperature rise in the 160ft^3 or so of lable water will be 9degC. However, when allowance ade for margins at either end of a pulse (to ensure a er pulse always occurs within the period of a water pulse), for reduced capacity in cases where high pressures are ired, as will be explained later, a more likely figure he water-temperature rise through the magnet is 20 or gC. Higher average water-temperature rises are not sable, because hot spots in a magnet are always likely to ase local water-temperature rises considerably, because, economical heat transfer in the heat exchanger and iated heat sink, magnet inlet water temperatures may high as 30°C, and because boiling within the magnet be avoided owing to the possibility of an unstable heat- fer condition.[1,8]

e sizes in the pulse circuit have been selected as a promise between cost and friction drop over the length ved (dictated by the geometry of the building).

r constant-flow pulses, the air valve is throttled in such nner as to maintain constant pressure in the cold storage , despite the consequent drop in pressure in the air voir. Obviously the cold-storage-vessel pressure can only aintained as long as it is lower than the air-reservoir ure. The quantity of water Q transferred before equality essure occurs depends on the dimensions of the air voir (volume V), the initial pressure P_0 within it, and ressure being maintained in the cold storage vessel P_2. sis shows that, for adiabatic conditions in both vessels,

$$Q = \frac{V}{\gamma}\left(\frac{P_0}{P_2} - 1\right)$$

ng the ratio of specific heats of air at constant volume constant pressure. The capacity of the air reservoir, , has been chosen so that all the water may be expelled the cold storage when the pressure is maintained there f the initial air-reservoir pressure. Under these condi- a flow of 4000gal/min may be maintained at a pressure ntial of 125lbf/in^2 at the magnet. Higher pressures may ained for shorter pulse times.

System control

The safe, efficient control of the equipment described arily occupied a great deal of the designer's attention. ratifying, but at the same time sobering, to realise that first few months of operation most of the safety routines ed were at one time or another called upon to prevent erous situation developing.

tically all the logic circuitry consists of identical es, each of which may be made to perform the logic ns of AND or OR and which contain a driver stage o energise indicating lights and relays. The modules, t the ANU, use silicon transistors mounted on plug-in circuits.

ic displays are used extensively. An inexpensive, and flexible method for constructing mimic diagrams en developed which makes use of ink drawings on drawing material.

Operations immediately prior and during a pulse are completely automatic. The circuit checks that all is ready and allows initiation by a 'start' signal which commences two cycles of events in parallel: one involving the h.p.g. and the variable-resistor control cam; and the other involving the commencement of water flow through the magnet and the closure of the isolator. After several seconds, before current has begun to flow, stock is taken of the situation, so to speak. If all is satisfactory, the latch mechanism on the variable resistor is actuated just as the control cam is about to command the rise of the electrolyte tank.

Protection is provided against poor synchronisation of the energy and cooling pulses, as well as the more obvious conditions of inadequate water flow compared to magnet power and magnet overheating.

During the pumping-back stage of the cycle, pumps and valves are operated manually by remote control.

Between pulses, magnet resistance and busbar insulation resistance are monitored automatically.

Several permanent protective routines are built into the control system which operate at all times, whether the equipment is under automatic control or manual control, as it would be for instance during maintenance periods. One of the most important of these ensures that the high pressures (up to 500lbf/in^2) which may be contained in the air reservoir are not allowed to pass to the magnet casing and hoses, which are rated at only 200lbf/in^2. Another ensures that a cooling pulse will not continue past the point where the cold-water reservoir is empty.

9 Conclusion

Perhaps the only criticism that can be levelled at the h.p.g. is that highly precise current control has not yet been achieved. This has not concerned experimenters so far, but as magnet powers increase we are likely to have less and less control over repeatability and pulse shape unless steps are taken to improve the situation.

R. A. Marshall of this department is working on the design of radially movable brushes connecting the two rotors. These will enable precise control of the h.p.g. voltage with response times dependent only on the mechanism moving the brushes.

Considering this modification and the experience of over 500 pulses during the past year of operation of the 165kGs magnet, indications are that the combination of homopolar generator and air-driven cooling system is suitable for handling magnet powers of many tens of megawatts.

10 References

1 BERGLES, A. E., and ROHSENOW, W. M.: 'Forced-convection surface-boiling heat transfer and burnout in tubes of small diameter', Engineering projects laboratory report 8767–21, MIT, 25th May 1962

2 BITTER, F.: 'The design of powerful electromagnets', *Rev. Sci. Instrum.*, Pt. II, 1936, **7**, pp. 482–488, Pt. IV, 1939, **10**, pp. 373–381

3 BLAMEY, J. W., CARDEN, P. O., HIBBARD, L. U., INALL, E. K., MARSHALL, R. A., and OLIPHANT, SIR MARK: 'The large homopolar generator at Canberra', *Nature*, 1962, **195**, pp. 113–114

4 DE KLERK, D.: 'The construction of high field electro-magnets', Newport Instrument Co. Ltd., 1965

5 KOLM, H., LAX, B., BITTER, F., and MILLS, R. (Eds.): 'High magnetic fields', Proceedings of the international conference on high magnetic fields, MIT, 1961 (MIT Press and Wiley, 1962)

6 INALL, E. K.: 'Modifications to the Canberra homopolar generator', Atomic energy in Australia, Sydney, April 1965

7 KOLM, H., and FREEMAN, A.: 'Intense magnetic fields', *Sci. American*, 1965, **212**, pp. 66–78

8 MCADAMS, W. H.: 'Heat transmission' 'Boiling liquids' (McGraw-Hill, 1954, 3rd edn., chap. 14)

9 MARSHALL, R. A.: 'The electrolytic variable resistance test load/switch for the Canberra homopolar generator', Dept. Engineering Physics, Australian National University RR4, May 1964

10 MARSHALL, R. A.: 'The design of brush gear for high current pulses and high rubbing velocities', *IEEE Trans.* 1966, **PAS–85**, pp. 1177–1181

11 NEWSTEAD, G.: 'The homopolar generator', *Sci. J.*, 1967, **3**, pp. 55–60

11 Appendix

Mechanism of solution of air in the cold storage vessel

Consider first a vessel partially full of water containing no dissolved air and having absolutely no motion. If the rest of the vessel is now filled with compressed air, we may consider that the surface layer of the water instantaneously dissolves air up to the equilibrium concentration level given by Henry's law.

Henry's law applied to our case states that the equilibrium concentration of dissolved oxygen or nitrogen in water at a certain temperature is proportional to the partial pressure of the gas in contact with the water.

Migration of the dissolved gas beyond the surface layer is a process of diffusion, the basic equation of which is

$$J = -D\frac{\partial c}{\partial x}$$

where J = diffusion flux, e.g. grammes of dissolved gas crossing unit area per second (the area being parallel to the water surface);

c = local instantaneous concentration of dissolved gas, e.g. g/cm^3

x = distance co-ordinate normal to the surface, cm

D = diffusion coefficient whose value has been taken for the components of air as

$$D = 10^{-4}\text{cm}^2/\text{s}$$

The result of the diffusion process is that the saturated surface layer grows in depth, and one may gauge the rate of growth by defining a boundary depth Z so that, from the air–water interface to depth Z, the water is substantially saturated, i.e. it is at or close to the equilibrium concentration level, and beyond Z the concentration is substantially zero.

It can be simply shown that Z is of the order of magnitude

$$Z = \sqrt{(Dt_e)}$$

where t_e is the time for which the water surface has been exposed to the compressed air.

Substitution of representative values will show that, when there is no motion in the water, the relative amount of dissolved air entering the water is quite insignificant; e.g. if $t_e = 10\text{min}$ $Z \simeq \frac{1}{4}\text{cm}$, which must be compared with an average depth of remaining uncontaminated water of approximately 80cm.

Let us now consider the case where there is motion within the water of the form of nonturbulent eddy currents of a circulatory nature about horizontal axes (Fig. 8). There may be a number of these currents circulating in different directions. We are interested in those which have the air–water interface as a boundary. Each of these may be considered as disturbing the surface over a length y and width x, the characteristic surface velocity (in the y direction) being v.

The exposure time for a surface particle will therefore be

$$t_e = \frac{y}{v}$$

When a surface particle finally submerges after time t_e, we may consider that the water to a depth Z below it has reached saturation. We will assume that this saturated layer mixes thoroughly with the rest of the water before being exposed to the surface again.

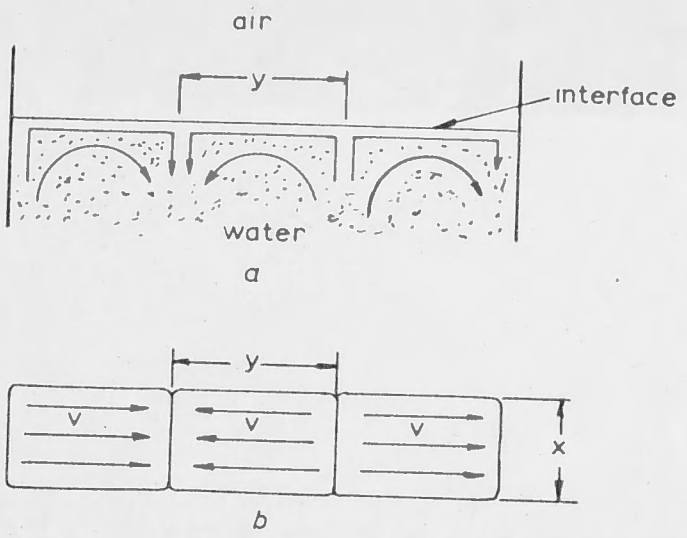

Fig. 8

Idealised eddy currents illustrating terms used in the analysis

a Side view
b Plan view

In time t, therefore, the total surface area exposed will be

$$A_e = vtx\left(\frac{A}{xy}\right)$$

where A is the area of the interface surface, A/xy being the number of eddy systems disturbing the surface.

The total volume of water reaching saturation is therefore

$$V_s = A_eZ = \frac{vtA}{y}\sqrt{(Dt_e)} = \sqrt{\left(\frac{D}{t_e}\right)}At$$

The average rate of increase in concentration over water volume V is

$$\frac{\Delta C_{av}}{t} = \frac{V_sC_s}{Vt} = \sqrt{\left(\frac{D}{t_e}\right)}\frac{C_s}{h}$$

where C_s is the equilibrium (saturated) concentration and h is the characteristic depth of water ($= V/A$).

Fig. 6 is a plot of this equation for various air pressures, the water temperature being about 20°C and $h \simeq 1\text{m}$. The ordinate dC_{av}/dt is for any component of air in terms of percentage of saturation at atmospheric pressure.

It will be seen that, during pumpback, measured values of dC_{av}/dt for oxygen imply $t_e \simeq 1$–2min, which, as explained in the text, is about as large as one can expect with ideal-flow re-entry geometry.

During pulsing, dC_{av}/dt was found to be very high, indicating short exposure times consistent with small rapid eddies

(2)

FEATURES OF THE HIGH FIELD MAGNET LABORATORY AT THE AUSTRALIAN NATIONAL UNIVERSITY, CANBERRA

EP-RR 19

P. O. CARDEN

January, 1967

Department of Engineering Physics

Research School of Physical Sciences

THE AUSTRALIAN NATIONAL UNIVERSITY

Canberra, A.C.T., Australia.

FEATURES OF THE HIGH FIELD MAGNET LABORATORY AT THE AUSTRALIAN NATIONAL UNIVERSITY, CANBERRA

by

P. O. CARDEN

January, 1967

Publication EP-RR 19

Department of Engineering Physics
Research School of Physical Sciences
THE AUSTRALIAN NATIONAL UNIVERSITY
Canberra, A.C.T. Australia

CONTENTS

SUMMARY

The High Field Magnet Laboratory at Canberra is described. High-field water-cooled electromagnets produce magnetic fields of hundreds of kilogauss, consume megawatts of power and require thousands of gallons of cooling water per minute.

Engineering details are given of the pulsed water cooling system, electrical and control systems, and instrumentation.

The paper is prefaced by a description of the Canberra homopolar generator used as energy store and power source for the Magnet Laboratory, and by a discussion of the scientific uses of high magnetic fields.

1. Introduction

The intention of this paper is to describe in some detail the equipment and facilities at Australia's first and only High Field Magnet Laboratory. However, since the Laboratory depends entirely for its power supply upon a unique energy storage device known as a homopolar generator, and since each electromagnet, together with its cooling equipment form with the homopolar generator an integrated system for the transformation and control of energy, some space will first be devoted to a brief description of the homopolar generator and its capabilities. A fuller description will be found in references 1, 2 and 3.

The electromagnets we are speaking of consume from 5 MW d.c. upwards to an easily conceivable 100 MW. The homopolar generator can meet these power requirements and has in fact repeatedly delivered powers of 300 MW or more. Further, the techniques are well established for increasing this threefold. However, being essentially a storage device, discharge times are a function of power, the product of the two being limited to 500 MW seconds (megajoules).

1.1 Homopolar Generators

It was Michael Faraday, towards the middle of the last century who constructed the forerunner of the homopolar machine. He rotated a disc through which passed a magnetic field and observed an e.m.f. between the disc axis and a stationary contact rubbing on the outer edge of the disc. By taking care to preserve cylindrical symmetry in the exciting field and in the arrangement of electrical contacts and conductors, such a device can be in fact converted into a highly efficient transformer of mechanical (shaft turning) energy into electric energy. Such a device is termed a homopolar (or unipolar) generator, h.p.g. for short. On the other hand if a large degree of asymmetry in magnetic field is introduced, and rubbing contacts are dispensed with, the generated currents will flow within the disc itself forming a useful braking device often used in watt hour meters, speedometers and the like.

The symmetrical device, the h.p.g., is in fact reversible, i.e. when fed with current in the reverse direction it will motor. The Canberra h.p.g. (see Figure 1) has no mechanical connections to its shaft at all, but has large massive discs which accelerate when fed with electrical energy, thus storing it in the form of kinetic energy. The energy is reconverted into an electrical output by merely connecting the load of appropriate impedance across the discs through special brush gear. The efficiency of conversion is normally 99%.

The Canberra machine has four rotating discs each weighing twenty tons. At full storage capacity, the peripheries of the discs are moving at two thirds the speed of sound, and this is the rubbing speed for the outer brushes. The electromagnet which forms the exciting field through the disc weighs 1500 tons and stands 25 feet high. The equivalent electrical capacity of the h.p.g. is some 5,000 farads and discharge currents of up to 1.8 million amperes, lasting for a second or so have been obtained. The electrical feature most essential for its application to the generation of high magnetic fields, however, is the maximum stored energy--500 megajoules.

It is this feature which enables the powering of electromagnets requiring tens of megawatts for periods of several seconds--long enough for the majority of experimental applications and longer than is possible anywhere else in the world.

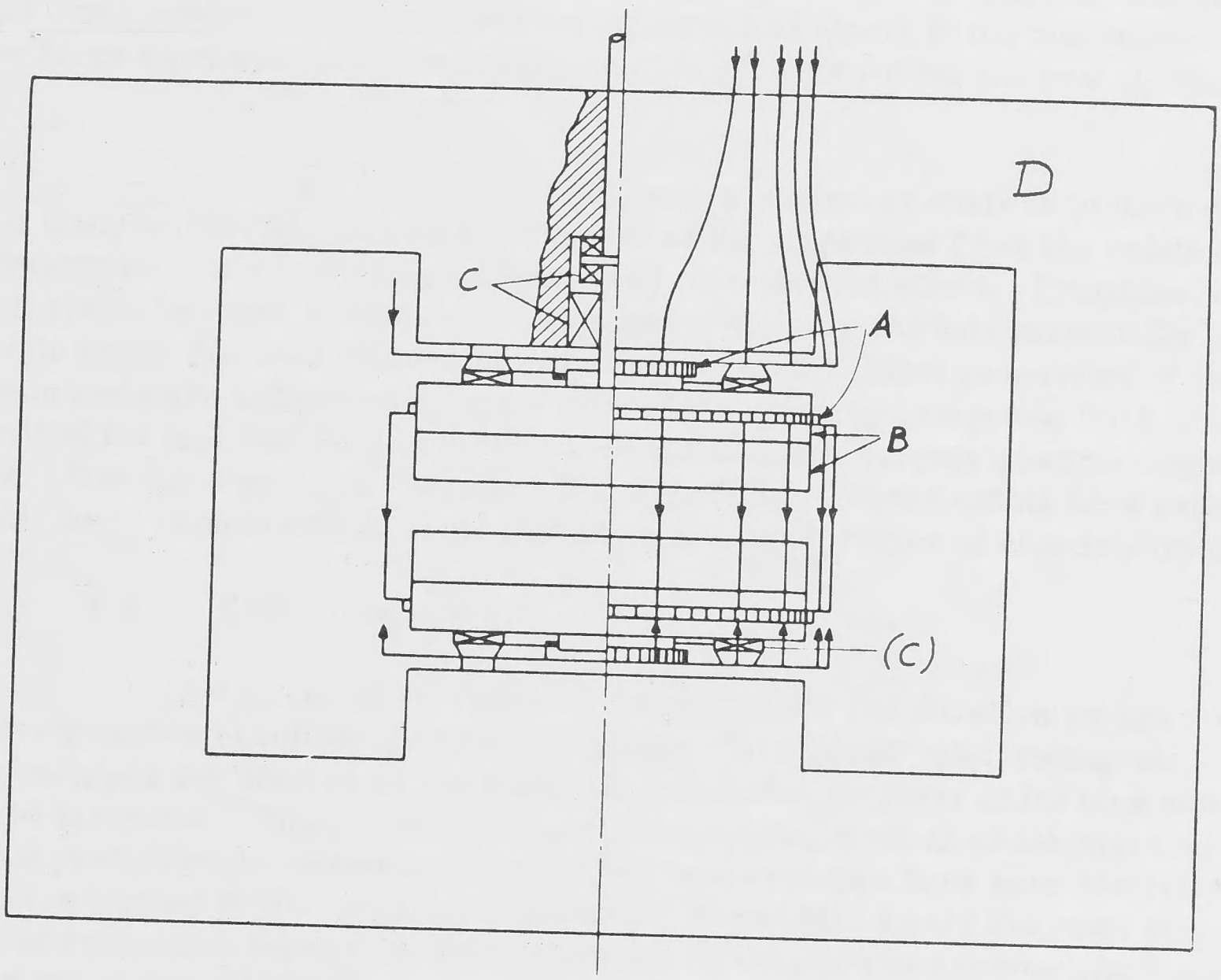

Figure 1. Diagram (half section) of the Canberra homopolar generator showing schematically the current paths (arrows), brush rings (A), rotors (B), bearings (C), and energising magnet steel yoke (D).

1.2 High Magnetic Fields and Solid State Physics

The chief experimental use of high magnetic fields is in the sphere of solid state physics. This branch of pure science has steadily grown in importance since World War II and received a tremendous boost with the invention of the transistor,

which grew directly from the results of research in this field. Since then, other semi-conductor and magnetic devices, lasers and the like have eventuated, showing the promise of this type of research.

In many respects, the physics of the solid state is complementary to atomic physics which for so long has outshone it in prestige. For it is in the solid state, where atoms and molecules crystalise and interact in orderly fashion, that one must change from considering the properties of individual atoms to the consideration rather of one large atom with millions of permissible electron orbits and new quantum properties.

In many branches of science, a method of study is to distort the object of study and try to build up a knowledge of its properties from the relation between the properties of the distorting influence and its observed effect. Examples of this approach are to be found in nuclear physics and chemistry and this essentially is how high magnetic fields are used in the study of the solid state. Most properties of matter in the solid state are influenced to some extent by an imposed magnetic field, this being a result of the fact that the interaction between atoms is largely electro-magnetic in nature. It is not surprising therefore that high field electromagnets have proved an invaluable tool, comparable to some degree to the accelerators of atomic physics.

1.3 Electromagnets

High magnetic fields of the magnitude and duration we are considering here are generated exclusively by water-cooled "air-cored" electromagnets. Iron cored electromagnets are limited by the magnetic saturation property of ferrous materials to about 40 kilogauss. Super-conducting electromagnets, devices which make use of the fact that certain exotic materials at very low temperatures have zero electrical resistance, are limited to just over 100 kilogauss. Above this figure the most economical means of generation appears to be with copper or copper alloy conducting material formed into a solenoid configuration. For other than very short duration fields, water cooling is essential. Electric current densities of up to 40 k amps/cm^2 and power densities of up to 3 kw/cm^3 are common. Field intensities, dimensions and powers of the largest available electromagnets are shown in Table I.

A particularly successful design of magnet has been developed by an American, Francis Bitter. The Bitter design is essentially of a single layer solenoid. In its simplest form, each turn consists of a set of thin copper discs, each with a central hole and a radial slit. The discs are interleaved with each other and with similar discs of insulation to form a continuous helix as illustrated in Figure 2, the overlap between adjacent discs being up to 90^o. Specially shaped end plates are used to make contact with the end discs, thus enabling connection to the power source and to provide a means of axially clamping the stack of discs together. On energising such a stack, an accessible magnetic field occurs in the central hole, largely in the axial direction.

TABLE I

Country	Number of high field magnet laboratories	Highest available field k.g.	Highest available power M.W.	
			continuous	pulsed
Australia	1	165		300 MW for 1 sec., 5 MW for 1 min.
Europe (excluding U.S.S.R.)	2	90	4	
Japan	1	120	4	
U.K.	3	130	3.5	
U.S.A.	7	205	8	32 for 4 sec.
U.S.S.R.	?	?	?	?

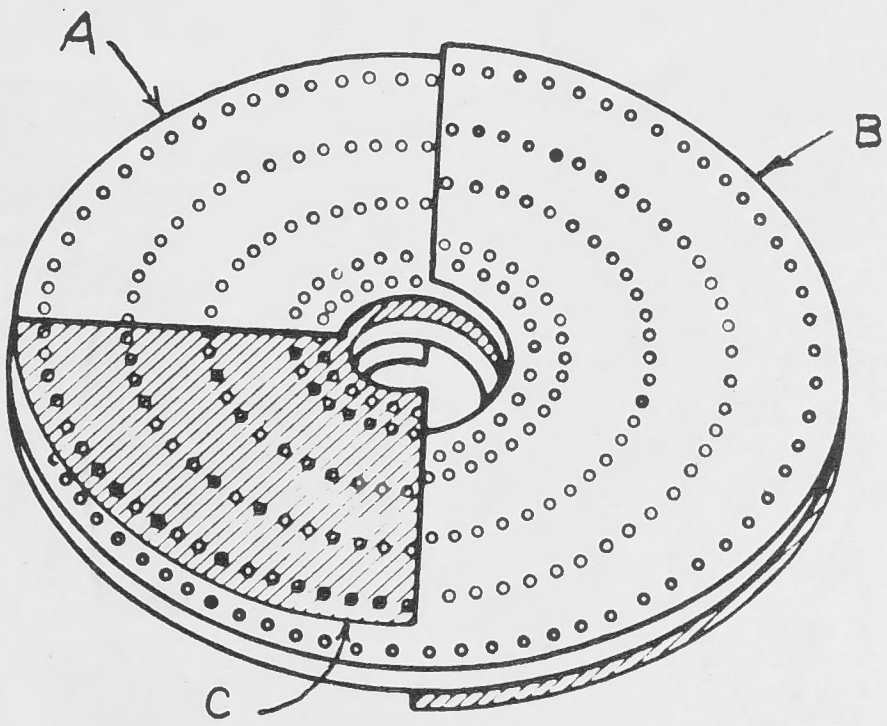

Figure 2. One turn of a typical Bitter disc comprising two copper discs A and B and one insulating disc C, all split and interleaved. Holes are for water cooling.

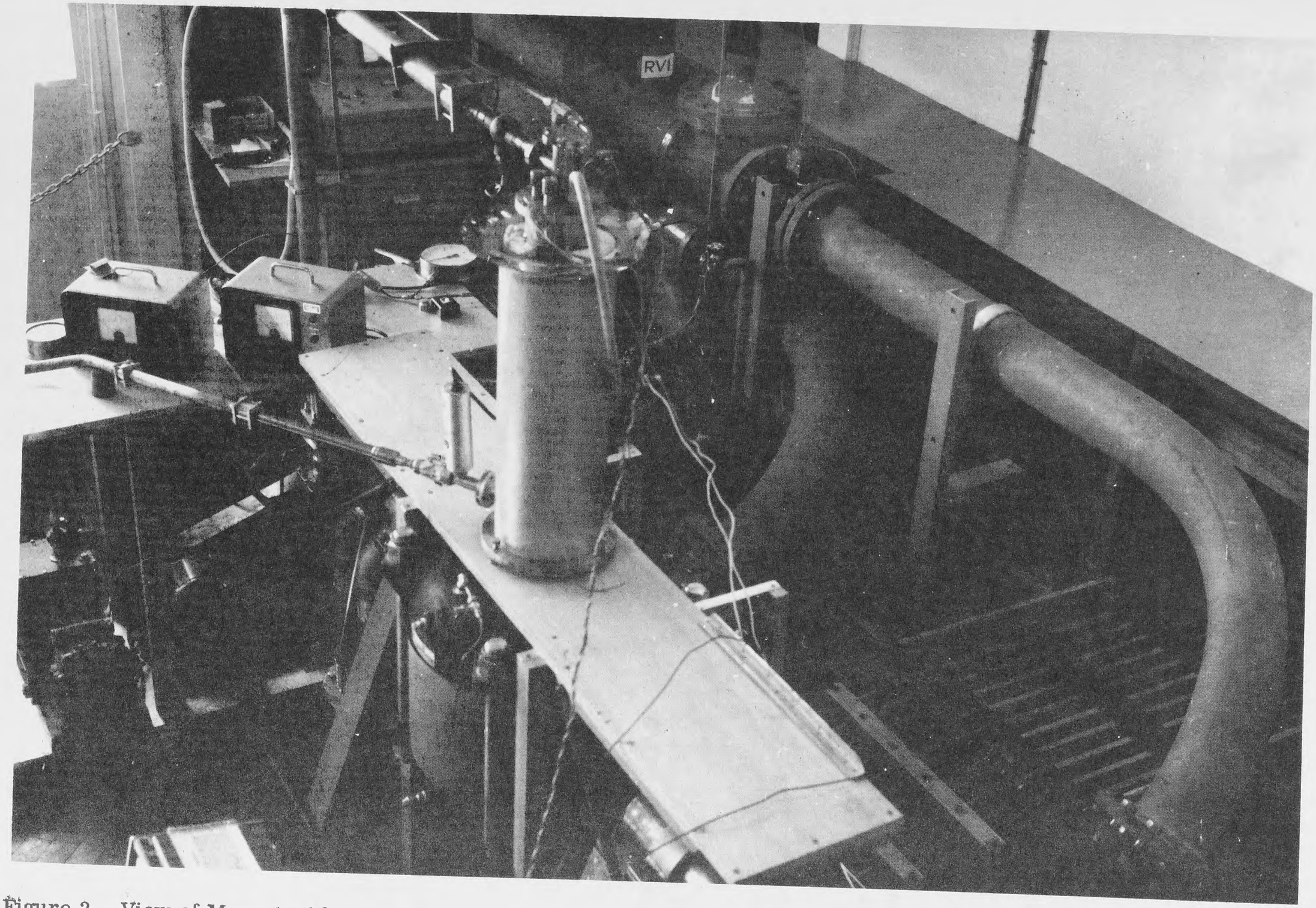

Figure 3. View of Magnet with cryostat above. Busbar and cables joining magnet and isolator can be seen, and also the cooling water pipes.

The interaction of the current with the magnetic field produces tremendous bursting forces and in fact the design of these magnets is in many respects similar to the design of thick-walled cylindrical pressure vessels. A magnetic field of 150 k.gauss is somewhat similar to a pressure acting in the central access hole of 13,000 p.s.i. The relationship is a square law, which points immediately to the limitation of unreinforced copper of about 52,000 p.s.i. for 300 k.gauss.

The situation is worsened by the fact that the copper discs have to be perforated with numerous cooling water holes (aligned in the axial direction) and are in any case operating at an appreciable temperature.

2. The A.N.U. Facilities

The Australian National University Magnet Laboratory has at present one Bitter electromagnet producing up to 165 kilogauss and requiring 5 MW, 25,000 amperes and 1000 g.p.m. of cooling water (see Figure 3). A 300 kilogauss magnet is being designed: this will require 200,000 amperes and require 3,000 g.p.m. of cooling water to remove the 30 MW of heat generated. These magnets compare favourably with what is available now in other parts of the world as can be seen from Table I.

At the A.N.U., current is carried from the h.p.g. in aluminium busbars through an electrolytic variable resistor and a hydraulically operated isolator to the magnet. The electrical circuit is shown in Figure 4.

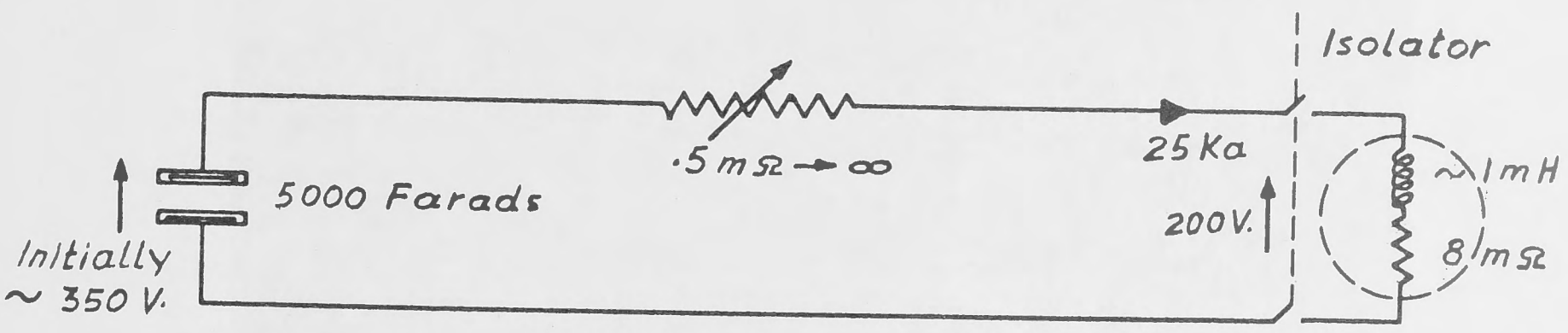

Figure 4. Equivalent electrical circuit diagram of homopolar generator (capacitor ≃ 5,000 farads), electrolytic variable resistor (and busbar resistance) ∞ to ≃ .5 m Ω , isolator and magnet inductance and resistance (approx. 1 mH and 8 m Ω). The variable resistor acts as current controller and circuit breaker.

2.1 Current Control and Circuit Breaker

The primary purpose of the electrolytic variable resistor is to act as a circuit breaker but it also provides current control to within a few percent of any desired law. It was built in the first place to provide a test load for the h. p. g. (see Blamey et al, reference 1). Essentially a 7,000 lb. tank of caustic soda is raised by a hydraulic servo system to submerge to varying degree a set of steel electrode plates.[5] The servo input is by means of easily-cut wooden cams, except that there is a secondary servo input operative only at the extreme limits of travel of the tank to bring it to rest, and a latch mechanism to disengage the primary servo system. The variable resistor acts as a circuit breaker whenever the latch is operated, the effect being to drop the tank away from the electrodes in a fraction of a second. Figure 5 shows a view of the variable resistor and Figure 6 shows an actual recording of tank height vs. time during a trial circuit break. The device is known to break currents of over a million amperes effectively and is expected to operate satisfactorily with the currents and magnet inductances anticipated.

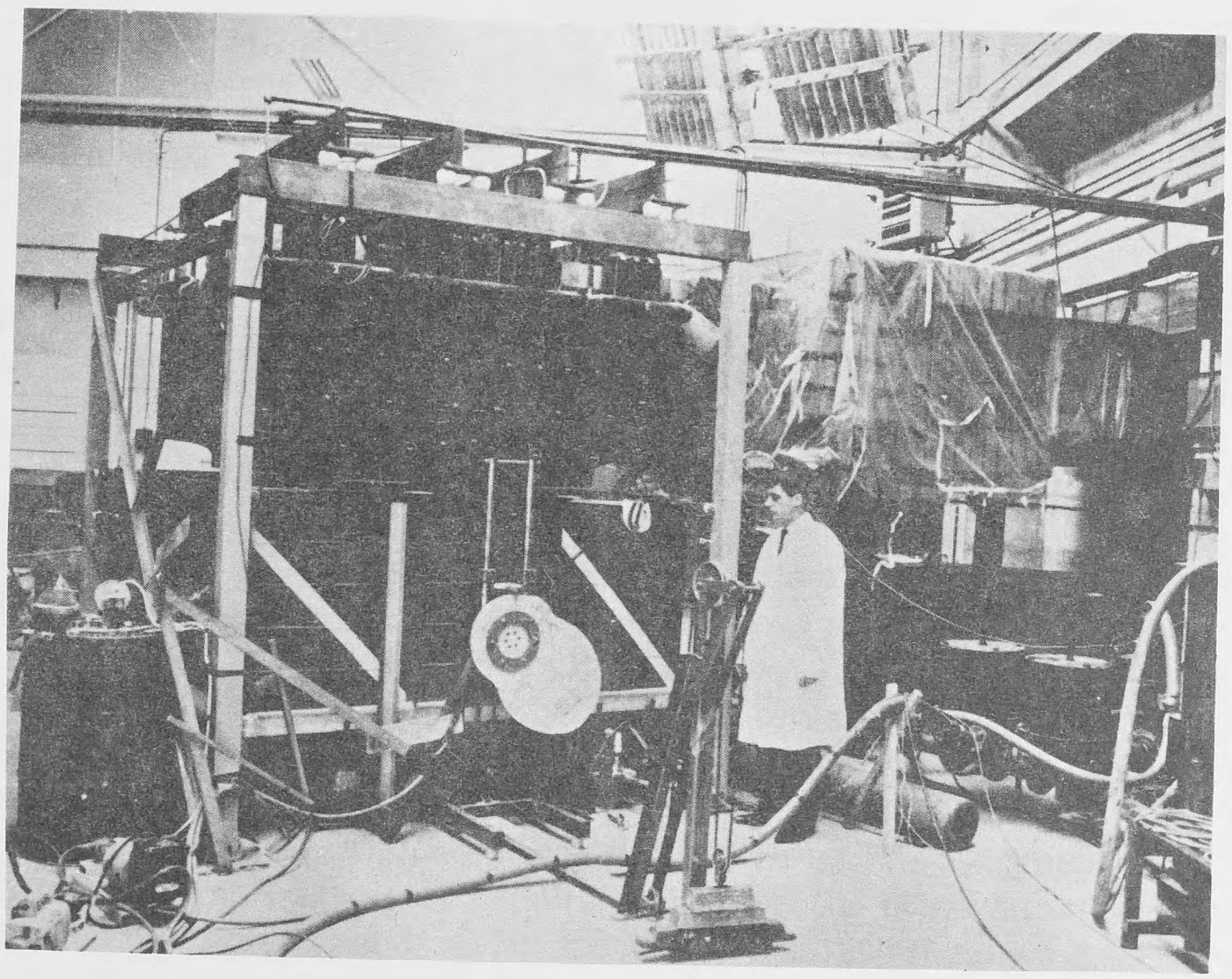

Figure 5. Photo of electrolytic variable resistor circuit breaker in open circuit position, i. e. tank lowered. The wooden cam which provides input information to the height-controlling hydraulic servo-mechanism can be seen clearly. The overhead busbar system is designed to take the full 1.6 million amperes capable of being delivered by the homopolar generator.

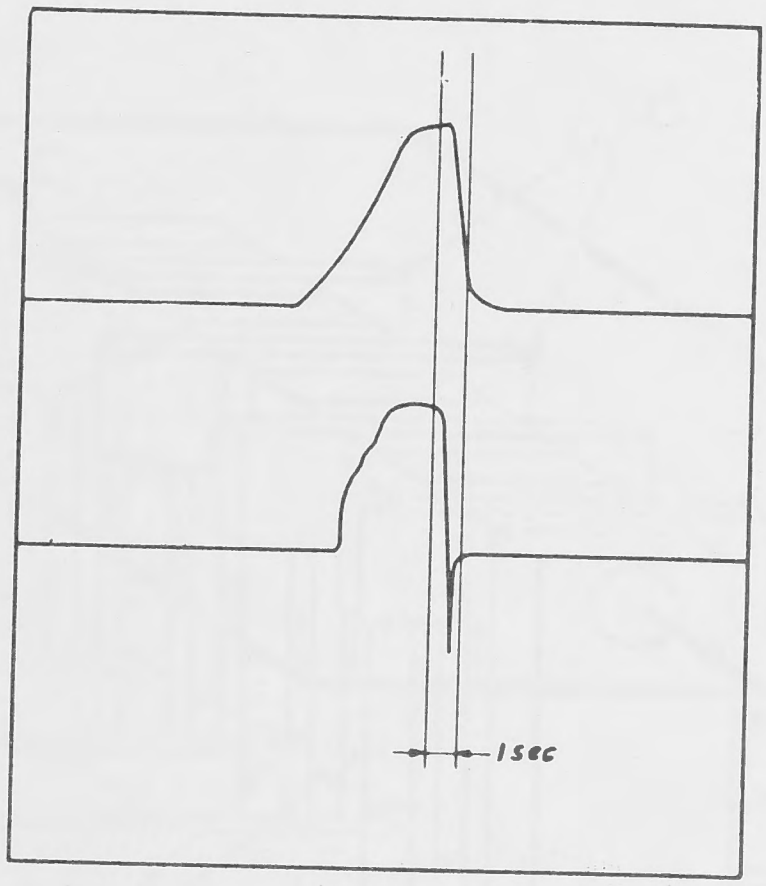

Figure 6. Upper curve shows an actual recording of electrolytic resistor tank height vs. time during a trial circuit break, together with the corresponding record of high field magnet voltage showing acceptable reverse voltage at break.

2. 2 Electrical Isolator

An isolator capable of carrying 200, 000 amperes has been included in the circuit for reasons of safety and to facilitate circuit checking. It is, of course, an essential item when more than one magnet is available for connection to the h. p. g.

The A. N. U. design is intended to be campact to match the geometry of thebusbar system. The principle of operation is shown in Figure 7. A single row of copper bars of alternate polarity enter the isolator horizontally, turn right angles and rise vertically to a "switching line". A similar set of separate bars drop vertically from the switching line to the level of the incoming bars, turn at right angles and continue horizontally out of the isolator. The two sets of vertical bars are interleaved and firmly clamped at their lower ends. The upper ends may be slightly sprung apart and are in fact interleaved yet again with a set of copper bridging bars at the switching line. When a hydraulic clamp acting along the switching line is pressurised, the circuit through both poles of the isolator is complete. On the other hand, when this clamp is relaxed and the bridging set moved horizontally, bakelite insulating sections are drawn between the contacts thus effecting electrical isolation.

The bridging set is moved by hydraulic means and the whole switching sequence is controlled by an electronic logic circuit which derives information from limit switches and pressure switches on the isolator. Figure 8 is a logic diagram showing the connection between operations involved in opening and closing the isolator.

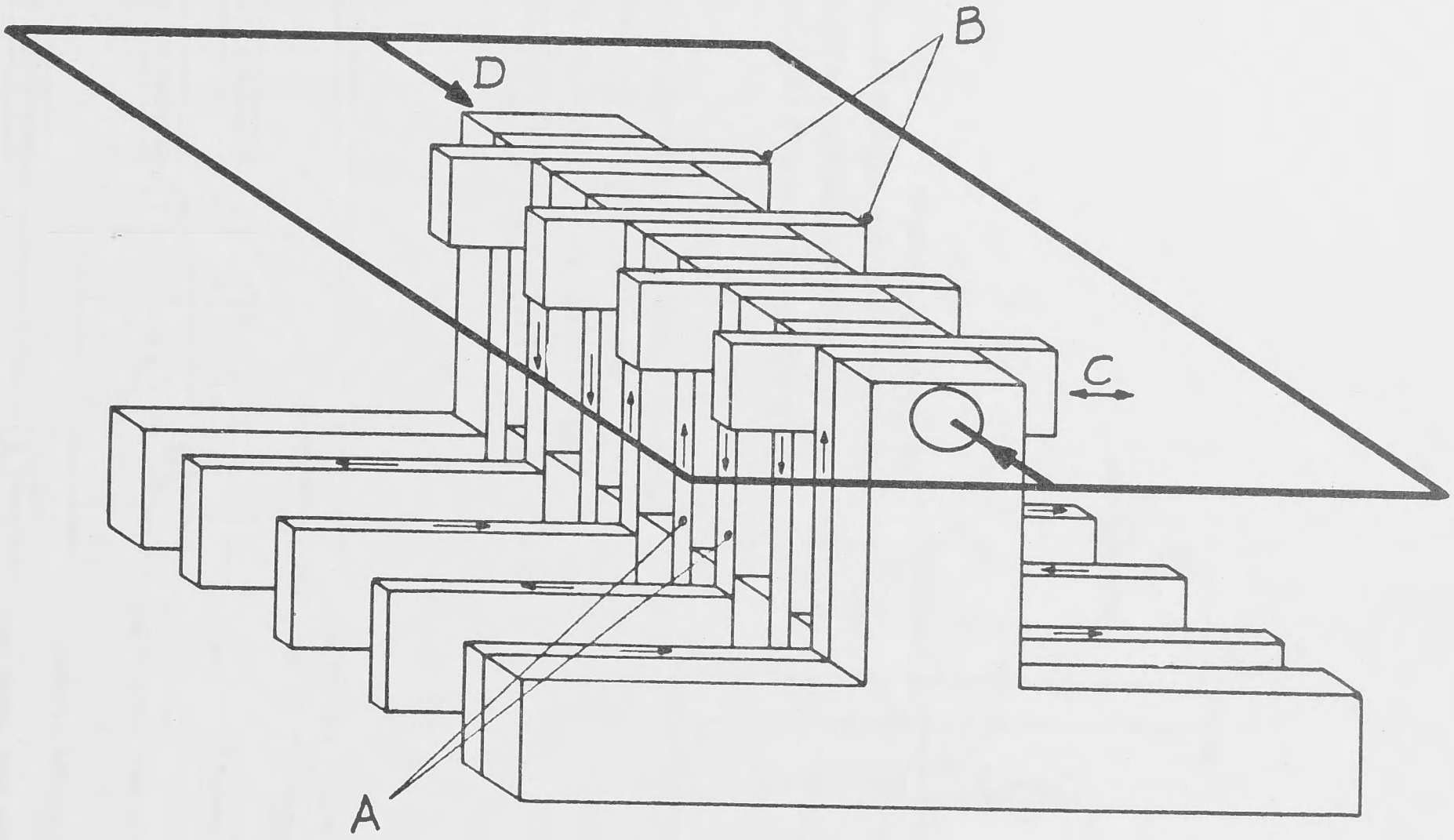

Figure 7. Diagram of 200 kiloamp isolator (actual height about 2 ft) showing principle of operation. (A) Vertical cantilever conductors clamped at lower end. (B) Bridging pieces capable of sliding in direction shown at (C) connect two adjacent verticals or separate them with insulation. (D) Heavy arrows and frame represent contact squeezing system operating at "switching line".

2.3 Water Cooling System

The water cooling system comprises the bulk of the equipment of the Magnet Laboratory. This system is capable of forcing 4,000 gallons per minute of chemically pure water through a magnet at 200 p.s.i. It operates in a pulsed manner to match the nature of the power received from the h.p.g. The water travels in a closed loop, rapidly during a pulse, between a cold storage tank, through a magnet to a hot storage tank (see Figure 9); and slowly during the period of recharging the h.p.g., from hot storage, through a heat exchanger back to cold storage.

During the rapid part of this cycle, the flow is powered by means of compressed air stored in a 7-foot diameter spherical reservoir and released to the space above the water in the cold water storage tank by means of an electrohydraulic servo controlled 3 in. air valve. The servo system is in turn controlled from an electronic variable function generator whose function may be tailored more or less by trial and error to obtain the desired water flow law. In this way water may be conserved and matched to the magnet power law. Control of water flow by throttling

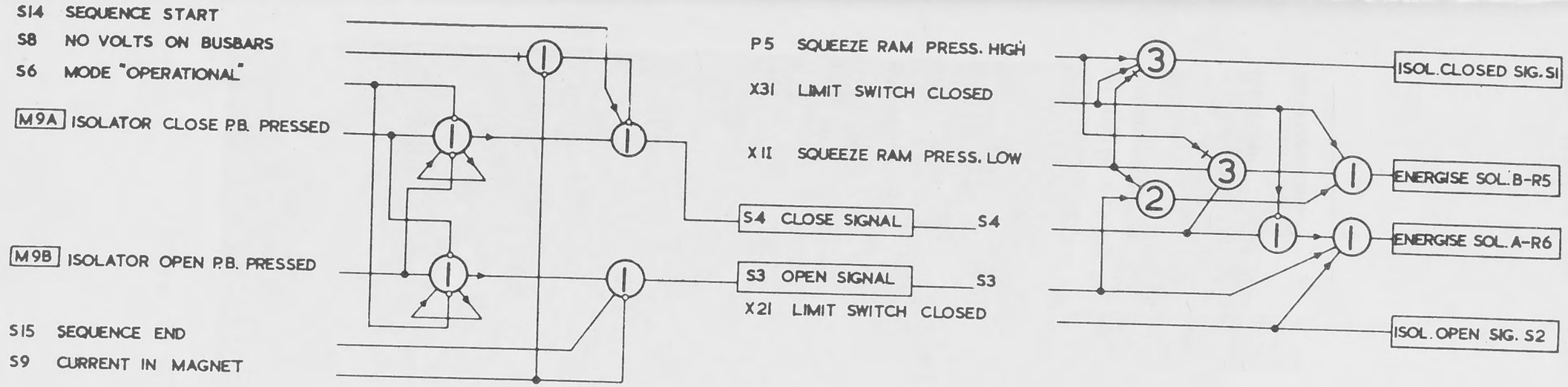

The lower diagram is a schematic of the isolator. The heavy lines represent the incoming and outgoing current paths. The isolator may be closed by insertion of bridging bars (shown as an "H" sideways) and application of squeeze pressure shown diagrammatically as a small ram above the upper current lead. X2I and X3I are limit switches which send a "1" when activated by the bridging bars. X1I is a switch which sends a "1" when the squeeze ram is released.

Solenoids A and B operate the hydraulic control valves in the direction shown when signals R6 and R5 respectively are "1".

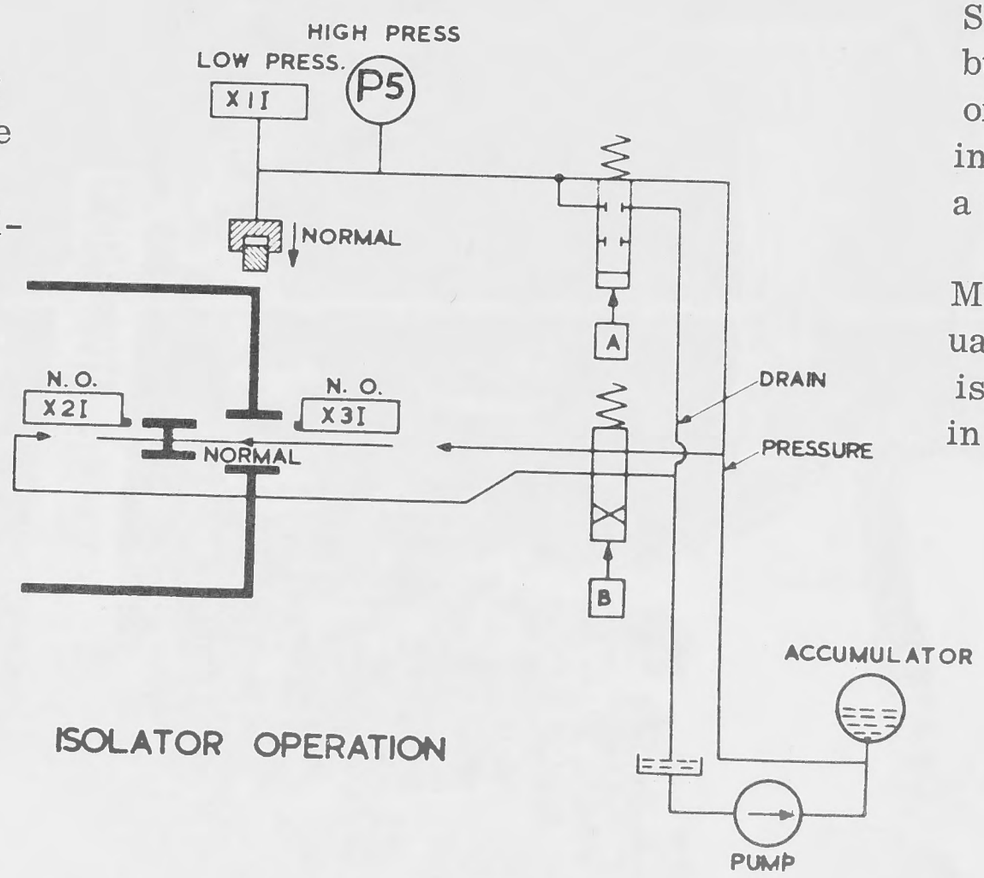

ISOLATOR OPERATION

S14 and S15 are normally "0", but change to "1" for a period of about 3 seconds at the beginning and end respectively of a current pulse.

M9A and M9B are the only manual controls associated with the isolator and are effective only in "non op" mode.

Figure 8. Isolator Logic Diagram

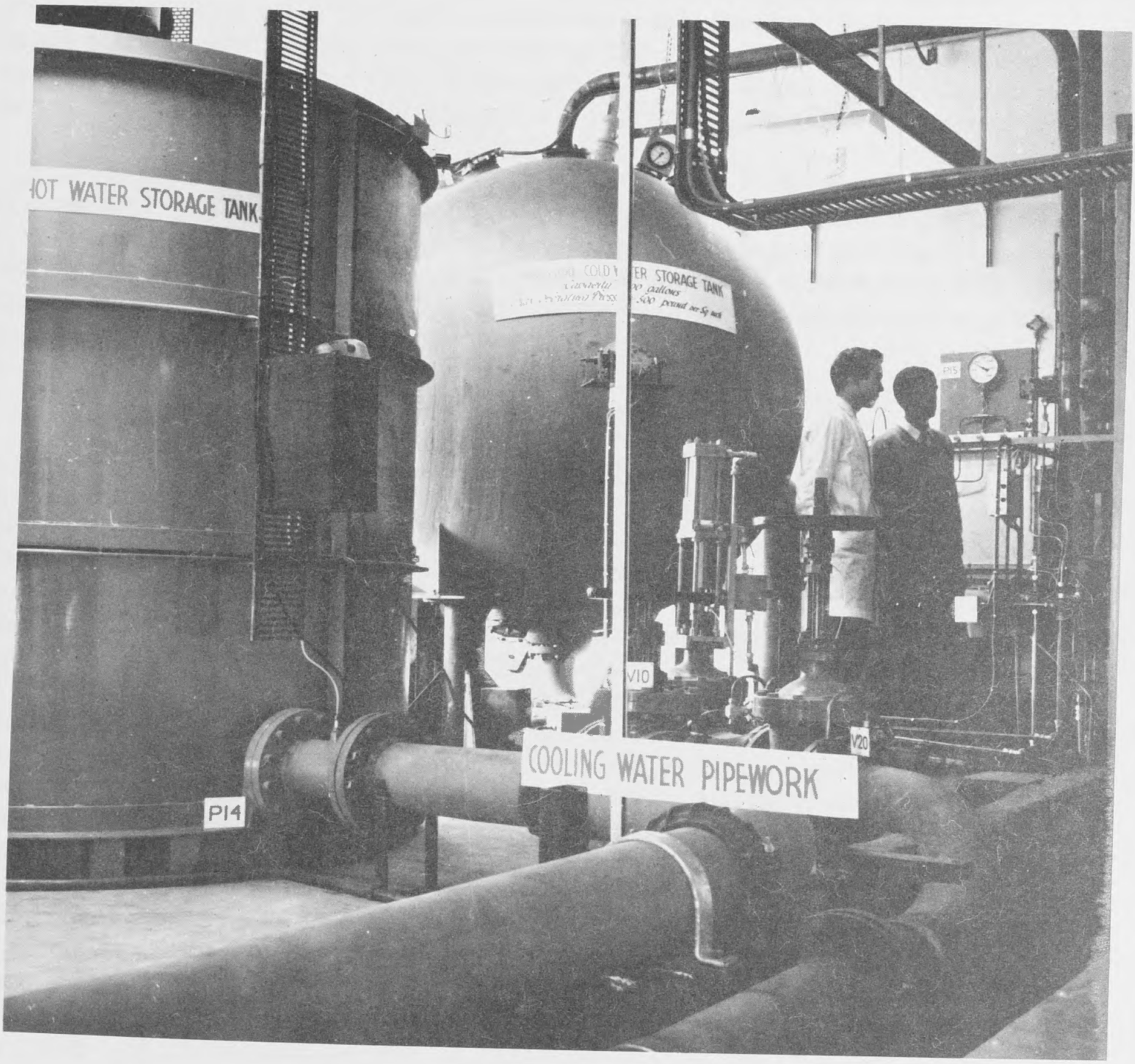

Figure 9. The cold storage tank (spherical), hot storage tank and some of the piping and valves.

air flow is to be preferred to direct throttling of the water. Firstly, the size of the valve to be servo operated is smaller for air throttling. Secondly, one obtains a smooth water flow free from the danger of water hammer, and thirdly, there is a slight thermodynamic advantage gained from air throttling in that the energy dissipated in the throttle is returned to the air causing further expansion. However, a simple on-off water valve is required to prevent initial flow by gravitation and to finally halt flow after a pulse when compressed air still in the cold reservoir would otherwise maintain it. This valve is hydraulically operated and is equipped with a hydraulic device which limits the closing rate thus preventing water hammer.

A feature of the A. N. U. cooling system is the conservation of compressed air. After a pulse, a high pressure multistage centrifugal pump is used to pump the water in 5 minutes or so from hot storage through heat exchanger to cold storage. In so doing, compressed air is displaced through a bypass valve back into the compressed air reservoir. This feature, besides being an economical way to compress air, ensures the minimum time between pulses.

2.3.1 Dissolved air

Building a water circulating system where water and compressed air were in contact for appreciable times was not engaged upon before considerable thought was given beforehand to the problem of dissolved air in the water. This was particularly pertinent because of the possible deleterious effects of oxidation upon the many electrical contacts within a Bitter solenoid. However, it was clear that this danger could be reduced by ensuring chemically pure water and in any case in principle an impermeable membrane could always be inserted in the cold storage tank to separate air and water. A theoretical study based on the known diffusion properties of air in water revealed that there was a great dependence on the mean exposure time of water molecules to the regions close to the water surface adjacent to the compressed air. The study, appearing in detail in Appendix I, may be summarised by Figure 10, where it will be seen that short exposure times, characteristic of rapid eddies of small dimensions, favour rapid solution. Consequent to this study, return water from the heat exchanger was introduced into the 6 in. diameter outlet pipe of the cold storage tank rather than directly into it in order to reduce eddy velocities at the surface. Ideally, by means of flow dispersing vanes, it should be possible to reduce surface velocities to the order of magnitude of the rate of change of water level, but because such devices are bound to interfere with the rapid efflux of water from the cold storage vessel, they have not been considered. It is thought that the rate of change of level has a limiting effect because of viscous effects at the tank walls (see Figure 11). It was thought that surface velocities during the slow refilling of the cold store would be somewhere between the efflux velocity from the 6 in. pipe and the rate of rise of level, i. e. somewhere between 45 ft/min and 1/2 ft/min. Assuming a surface exposure distance of 1 ft (vessel radius 3 ft), it was therefore concluded that exposure times should be between one or two seconds and 2 min. Recent measurements (Figure 10) on the system indicate that actual values of exposure time are between 1 and 2 min.

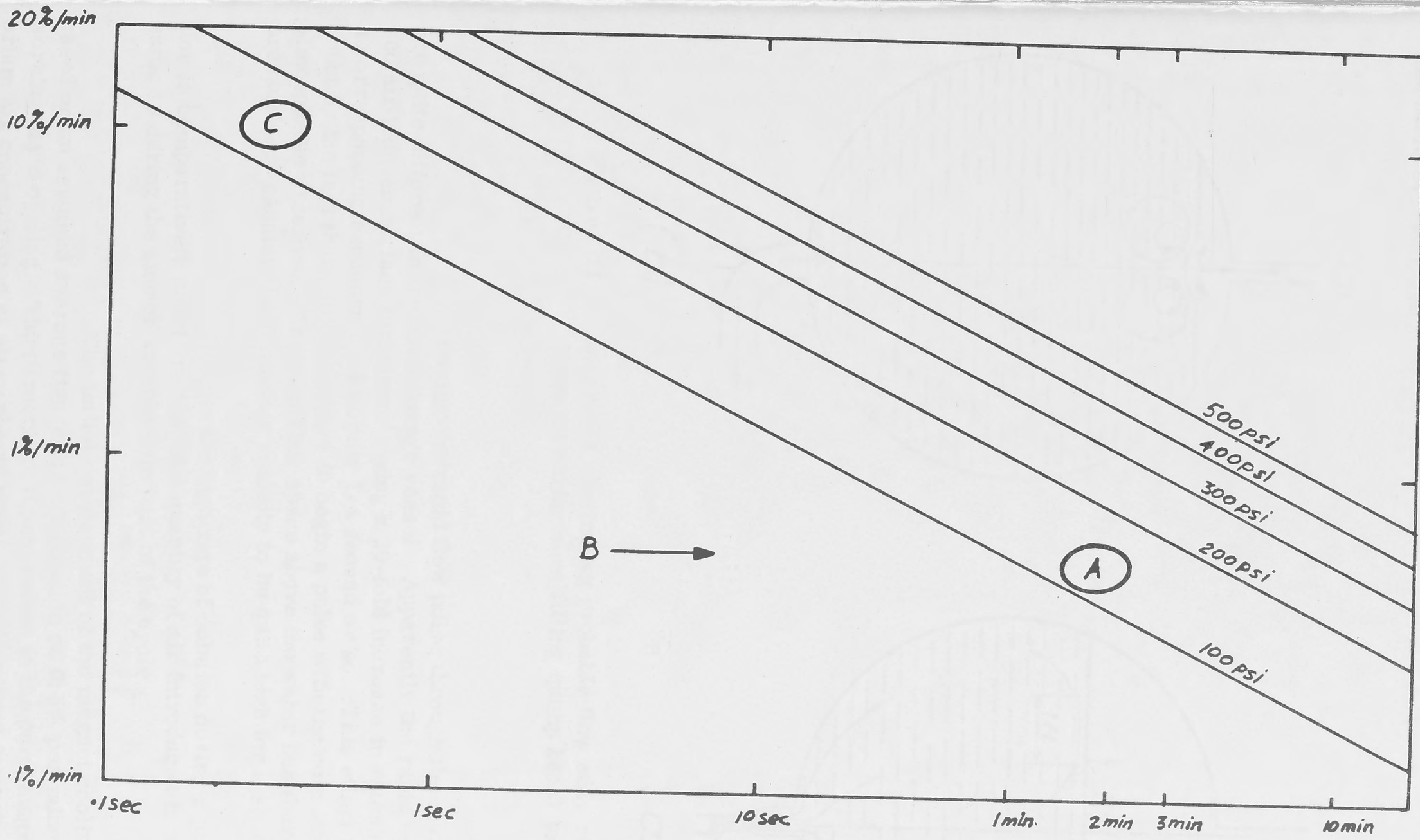

Figure 10. Rate of solution of dissolved gas in water vs. mean exposure time of water molecules to surface layer. Rate of solution is expressed as percentage of saturated value at atmospheric pressure per minute.

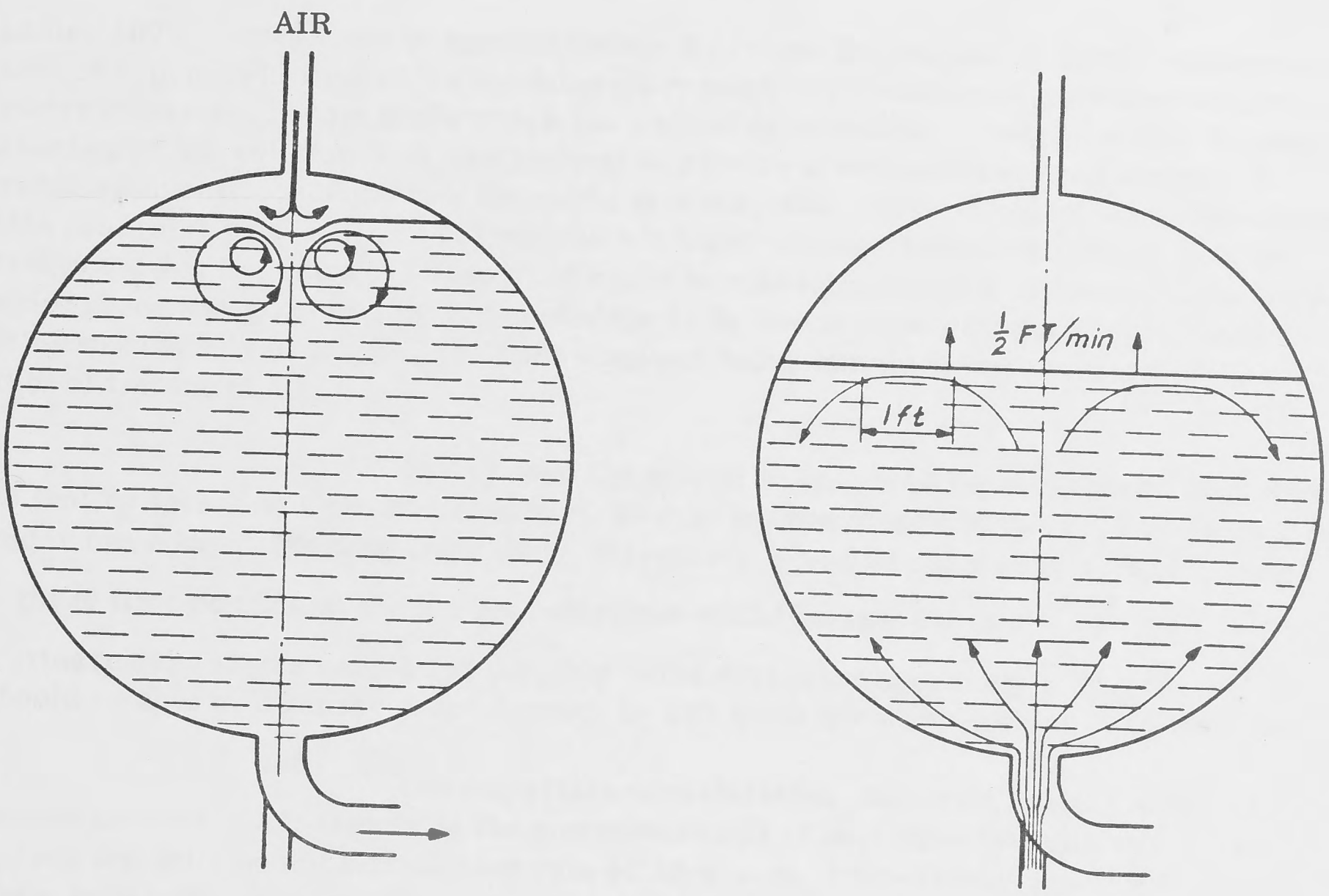

Figure 11. Diagrams illustrating probable flow eddy currents in cold store (a) during slow filling (pump back) and (b) during pulsing.

During the rapid flow pulse through the magnet, conditions are quite different in the cold storage vessel. Apparently the rapid entry of compressed air induces surface turbulence giving a 20-fold increase in rates of solution and a corresponding exposure time of only 1/4 second or so. This effect is worsened no doubt by the fact that it is customary to begin a pulse with the cold stored water at atmospheric pressure. The small air space above the water has therefore first to be pressurised, causing the initial air velocity to be quite high for a short time.

Despite the high rate of solution during a pulse, the duration is comparatively short and the total quantity of air introduced is in fact about the same as during the slower more docile part of the cycle.

The initial development of the magnet cooling system was based on an assumed average figure for air solution of 0.5% per minute during a working day's cycling. The percentage figure refers to the percentage of the equilibrium air concentration at atmospheric pressure and ambient temperature. On this

basis, 100% corresponds to approximately 8 p.p.m. (by weight) of dissolved oxygen and 16 p.p.m. of nitrogen. (The laboratory acquired a biological dissolved oxygen meter calibrated to this scale which has proved most useful in understanding the mechanism of air solution.) It was planned to provide a vacuum deaerator capable of reducing the air concentration overnight to a low value. The simplest way of operating this deaerator was to draw off from the hot water storage tank a continuous flow for treatment and to return the deaerated water to a different part of the same tank. Provided there was good mixing in the storage tank, the air concentration there should fall exponentially overnight, the time constant being simply volume of water stored/ rate of treatment.

In our case the stored volume was approximately 1000 galls so that by selecting a treatment rate of 10 g.p.m. one should obtain a time constant of under two hours. Starting from 100% therefore, it was hoped that in 12 hours overnight (6 time constants) the air concentration would be reduced to $(\frac{1}{e})^6$ or $\frac{1}{4}$ %. Furthermore, it was calculated that this same deaerator operating during the day should be able to limit the concentration to 50% (with air dissolving at 0.5% per min).

The important consideration, however, was to be able to reduce concentration rapidly at the commencement of shut down periods and in this regard the selection of a treatment rate of 10 g.p.m. seemed adequate. Without adequate knowledge of the mechanism and rate of air solution and its effects, it seemed imprudent to outlay any more money on this or any alternative method of lowering air concentration.

In practice we have measured average air solution rates of over twice the assumed figure of 0.5% per minute. This we believe is partly due to turbulence introduced during pulsing as already explained. Over 400 pulses have been taken by the magnet since August 1966 and so far no ill effect has been noticed on the electrical or cooling characteristics of the magnet. We are, however, designing a plastic membrane and hope to introduce it at a later date.

2.3.2 Water purity

Water purity is monitored by means of a conductivity cell and meter and is generally below 1 micro mho per cm. Materials used in contact with the water have been selected for their resistance to corrosion in the presence of oxygen. Thin-walled (up to 16 s.w.g.) pipes and vessels are generally stainless steel. Large pipes 6 in. diameter are mild steel with an internal formaldehyde coating. The interiors of 6 in. valves and the cold storage tank (a pressure vessel) are similarly lined. The use of corrosion resistant materials and linings has been extended to include the compressed air reservoir and connecting pipe work to the cold storage vessel. This has been done to prevent scale being produced in a region where it may easily be blown into the water and finally block the small cooling holes in the magnet (typically 1/8 in. diameter or less).

A commercial demineralizing plant is in use having a capacity of 100 gals per-hour and a special oxygen resistant element.

2.3.3 Design considerations

The essential elements of the water cooling system and their sizes are shown in Figure 12. The capacities of the storage tanks are related to the energy storage capacity of the h.p.g. If the maximum of 500 megajoules is released (no matter at what power level), the temperature rise in the 160 or so cubic feet of available water will be $9^{o}C$. However, when allowance is made for margins at either end of a pulse (to ensure a power pulse always occurs within the period of a water pulse), and for reduced capacity in cases where high pressures are required, as will be explained later, a more likely figure for the water temperature rise through the magnet is $20^{o}C$ or $30^{o}C$. Higher average water temperature rises are not advisable because hot spots in a magnet are always likely to increase local water temperature rises considerably; because for economical heat transfer in the heat exchanger and associated heat sink, magnet inlet water temperatures may be as high as $30^{o}C$; and because boiling within the magnet is to be avoided due to the resulting unstable heat transfer coefficient.

Pipe sizes in the pulse circuit have been selected as a compromise between cost and friction drop over the length involved (dictated by the geometry of the building).

The design performance is given in Figure 13. Here, available pressure at a magnet is plotted against flow for two particular values of pressure in the cold storage vessel. Constant flow pulses are visualised during which the air valve is throttled in such a manner as to maintain constant pressure in the cold storage vessel despite the consequent drop in pressure in the air reservoir. Obviously the cold storage vessel's pressure can be maintained only as long as it is lower than the air reservoir pressure. The quantity of water (Q) transferred before equality of pressure occurs depends on the dimensions of the air reservoir (volume V), the initial pressure (Po) within it, and the pressure being maintained in the cold storage vessel (P2). Analysis shows that for adiabatic conditions in both vessels, $Q = \frac{V}{\gamma}\left(\frac{Po}{P2} - 1\right)$. ($\gamma$ being the ratio of specific heats of air at constant volume and constant pressure.) The capacity of the air reservoir, 230 cubic feet, has been chosen so that all the water may be expelled from the cold store when the pressure is maintained there at half the initial air reservoir pressure. The lower curve on Figure 13 refers to this condition when Po is at its design maximum of 500 p.s.i. The upper curve is for a higher P2 in which case the quantity of water transferred is reduced to half.

2.4 System Control

The safe, efficient control of the equipment described necessarily occupied a great deal of the designer's attention. It is gratifying, but at the same

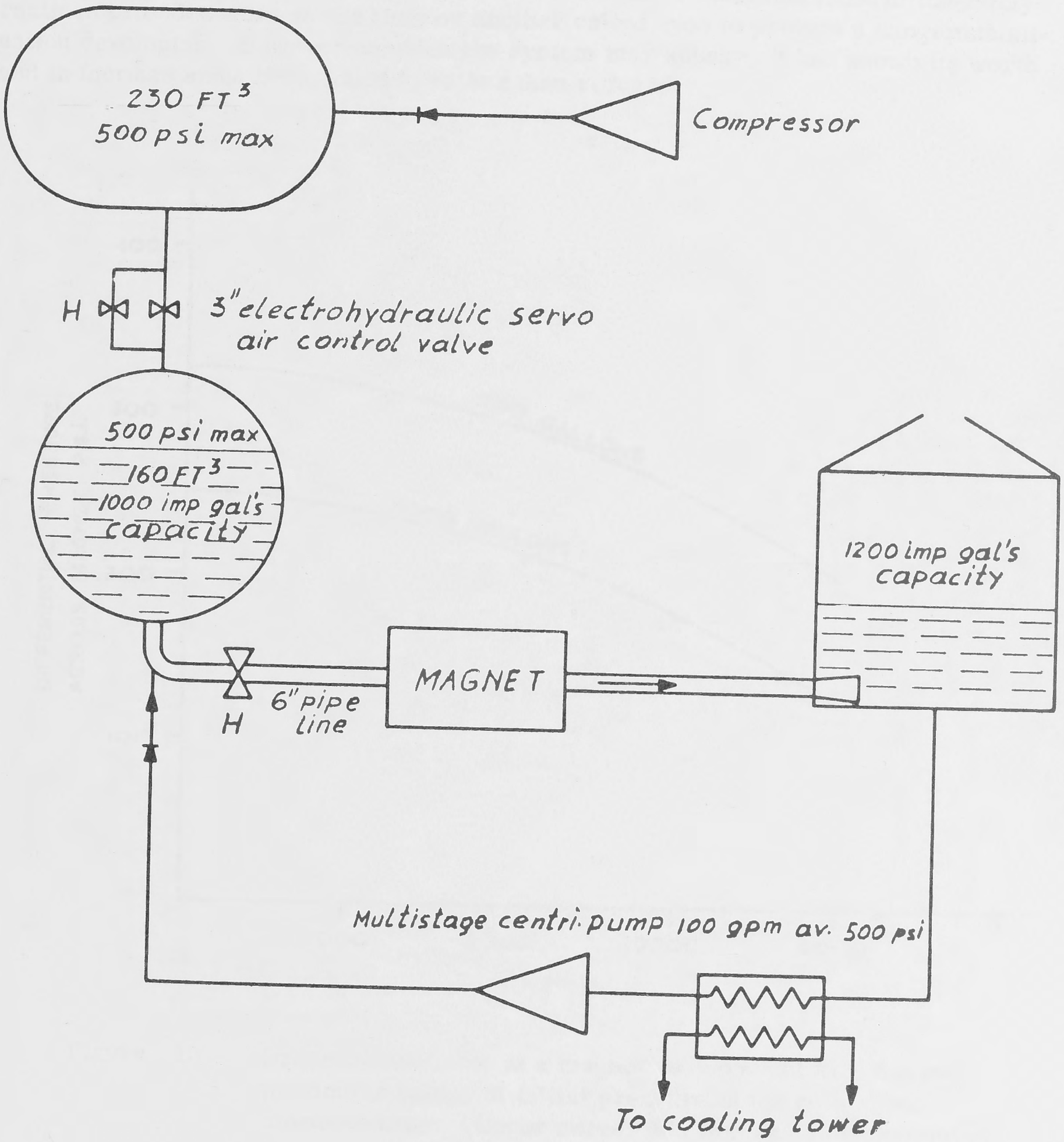

Figure 12. Diagram of water cooling system showing essential components, capacities, pressures. Valves marked "H" are operated on and off hydraulically.

time sobering, to realize that in the first few months of operation most of the safety routines provided were at one time or another called upon to prevent a dangerous situation developing. However complex the system may appear, it has shown its worth and in fact has since been added to rather than reduced.

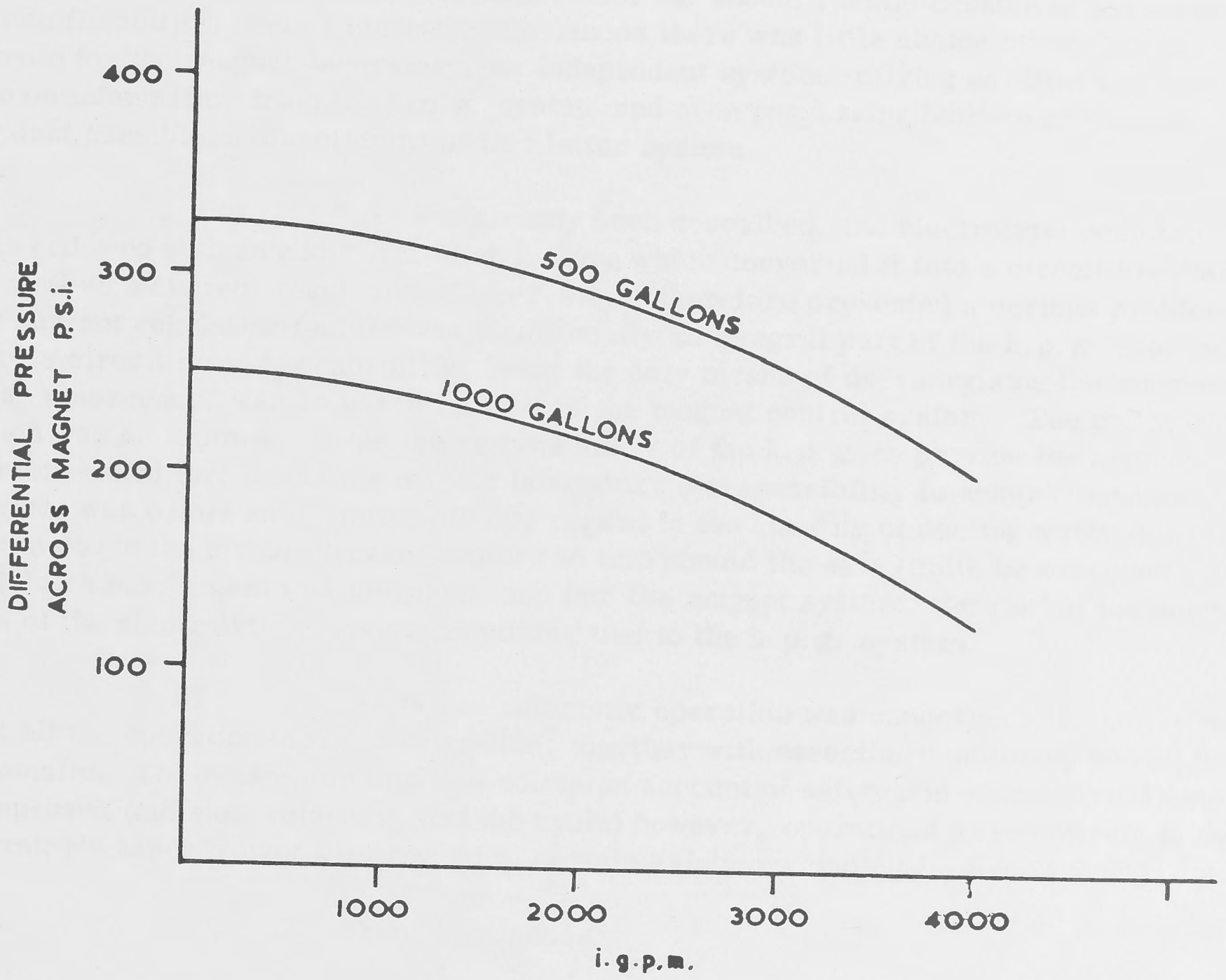

Figure 13. Pressure available at a magnet vs. constant flow for two particular values of initial pressure in the cold water storage vessel. Upper curve, 500 imp. gals. transferred; lower curve 1000 imp. gals. transferred.

The control problem may be divided into two broad sections: the policy of control; and the technical means of achieving it. It will be mainly the former that will be discussed here since it is this that lends purpose and consistency to the latter.

2.4.1 Policy

At the time of conception of the Magnet Laboratory, the h.p.g. and electrolytic variable resistor were going concerns. It was imperative that the magnet laboratory control system interfere as little as possible with the existing h.p.g. system and it was just as imperative that the h.p.g. system should not be orientated towards any particular user but should remain capable of the maximum flexibility. Under these circumstances there was little choice other than to create for the magnet laboratory, an independent system, relying as little as possible on information from the h.p.g. system and even possessing built-in protection against possible malfunctioning of that latter system.

As has already been described, the electrolytic resistor was endowed with an additional latch feature which converted it into a circuit breaker as well as a current regulator. This resistor therefore presented a curious problem: its current regulating feature was traditionally an integral part of the h.p.g. system but its circuit breaking capability, being the only means of de-energising the magnet in an emergency, was an essential part of the magnet control system. The policy solution was as follows: it was the responsibility of the h.p.g. to provide the magnet current asked for; it was the magnet laboratory's responsibility to ensure that this current was within safe limits with due regard to the quantity of cooling water flowing, and to cause the circuit breaker feature to trip should the safe limits be exceeded. The latch mechanism was therefore tied into the magnet system, the rest of the operation of the electrolytic resistor remaining tied to the h.p.g. system.

As far as automatic operation was concerned, the policy was that all the operations for a water pulse, together with essential monitoring should be automatic. The reason for this was solely on account of safety and efficiency. During pump-back (the slow return part of the cycle) however, operations were entirely in the operator's hands except with regard to certain safety overriding features.

2.4.2 Operating modes

It was recognised that on many occasions water pulses alone would be required, without necessarily involving the h.p.g. control system. There would also be occasions when individual components would be required to operate without involving the full sequence of events of a water pulse. These occasions would occur during testing and maintenance. To make provision for this need, the policy was expanded to include two modes of operation: "mode op" and "mode non-op". The later was a non restrictive mode where every item could be individually operated provided such operations were basically "safe". For example in "mode non-op" the isolator could be opened or closed at will, the only restrictions being that it could not be closed on live busbars or opened when carrying current.

Another example was the water valve, which could be operated at will except that it automatically closed when the water level in the cold storage

vessel was very low. This was to prevent compressed air being blown through the water system and into the hot storage vessel. An additional back up protection was that concurrently the hot storage vessel was opened to atmosphere. These restrictions were quite basic and always in force in either mode. Each operable item had a set of similar basic restrictions which were always in force.

In contrast "mode op" was quite restrictive. In this mode, items operable in a pulse were under automatic control only. The term "safe" now had a wider scope because in this mode it was possible to receive electric power from the h.p.g.

The idea of two modes could only be pursued, of course, if it were made impossible to receive h.p.g. power while in "mode non-op". Provision against this happening was incorporated in the policy of pulse initiation. The view was taken that the h.p.g. could initiate a pulse at will but it was the magnet laboratory control system's responsibility to accept the power only when it was safe to do so and when it was required. (In practice of course power is delivered when required, but the safety of the magnet should not be dependent on this being always so.) The magnet laboratory's control system does this by compiling automatically a check list of all essential conditions to be fulfilled prior to a pulse. It requires then a warning signal from the h.p.g. two seconds before the h.p.g. initiates a power pulse. This signal is used to initiate water flow and to close the isolator switch. When the system has established that the isolator is closed and that water flow is adequate, the latch mechanism is primed, thus allowing the electrolytic resistor to be raised to the conducting condition. An essential item on the check list is that the mode must be "mode op". Only when all items on the check list are fulfilled will the control system accept the warning signal from the h.p.g. To aid communication, a "ready" signal is sent to h.p.g. control at this time also.

2.4.3 Normal sequence

During normal current pulsing, the mode is, of course, set "mode op" and the following sequence of events occurs. We will assume a current pulse has just occurred and we shall follow events up to the initiation and through the execution of the next current pulse. The operator, by push button control, starts the high pressure pump and opens the "bypass valve" which allows displaced compressed air to return to the air reservoir. The pump is automatically switched off by a float switch in the cold water storage reservoir. At the same time a "level correct" signal is registered in the automatic check list.

Sometime during this "pump back" stage another "level correct" check list signal will have been registered indicating that there is sufficient room available in the hot storage tank to receive a full pulse of water.

The operator will close the bypass valve by push button and open a vent valve allowing the small quantity of compressed air left in the cold store

to escape to atmosphere. The equipment is now in a "standby" condition. Only two items will normally be required to complete the check list, and the water, not being in contact with compressed air, will remain at a steady level of air concentration (or slightly decreasing with time due to the evolution of small air bubbles in regions rendered supersaturated after the reduction in pressure to one atmosphere).

Items not yet mentioned which will by now have been registered on the checklist are:

--gauge pressure in cold store zero (necessary to eliminate excessive side loads on the gate water control valve while opening, a situation which might cause excessive and variable delay).

--air valve ready--indicating the function generator is ready to begin its cycle.

--hydraulic pressure okay--essential because of the dependence of operations on hydraulic power.

--three manually-operated valves in correct position.

--air pressure in reservoir satisfactory

--water temperature satisfactory

--isolator switch open

--busbar and circuit breaker insulation satisfactory

--magnet resistance satisfactory

The last two items are included to check that odd items such as tools or wires have not been left in dangerous positions, and to check the state of the insulators in the electrolytic resistor which are subject to immersion in caustic soda.

The remaining two items on the checklist are:

--vent valve closed

--operator's confirmation that all is ready including the experimenter--indicated by pressing a "ready" push button (this confirmation is automatically lost should any item on the check list subsequently disappear prior to the initiation of a pulse).

Once an operator has completed the list, a "ready" signal is sent to the h.p.g. control and the magnet laboratory's control system will now accept

an initiating signal from the h. p. g. When this arrives, the following events occur automatically:

--the function generator commences cycling, in a half second or so opening the air valve and pressurising the cold storage reservoir.

--the water valve opens

--the isolator closes

Normally in two or three seconds all these operations have been completed and a substantial quantity of cooling water is flowing. The control system checks that this is so and then inserts the latch in the circuit breaker mechanism just prior to the rising of the tank of electrolyte.

2.4.4 Protection against faults

Should the latch be inserted too late, the tank will not follow the cam and the circuit breaker will remair open throughout the time of the pulse.

On the other hand should the latch be inserted, but for some reason the tank be considerably late in rising, the latch will again be withdrawn. These two features prevent serious lack of synchronism between the current and water pulses.

The occurrence of any of the following during a pulse will cause the circuit breaker to trip:

--magnet temperature too high

--water flow too low compared with electrical power input

At the end of a pulse, the completion of the electrolytic resistor control cam cycle initiates an "end of cycle" signal which opens the isolator and closes the water valve (the function generator controlling the air valve by this time having completed its cycle). At the same time the circuit breaker latch is withdrawn and the system is ready for "pump back".

2.4.5 Control hardware

Practically all the logic circuitry for the magnet laboratory system is comprised of identical modules each of which may be made to perform the logic functions of "and" or "or" and which contain a driver stage used to energise indicating lights and relays. The modules, made at the A. N. U., use silicon transistors mounted on plug-in printed circuits.

Mimic displays are used extensively. An inexpensive, reliable and flexible method for constructing mimic diagrams has been developed at the Magnet Laboratory which makes use of ink drawings on special drawing material. Figure 14 shows the control panels and instruments.

2.5 Instrumentation

Instrumentation provided in the laboratory (apart from experimenters' instrumentation) includes a float driven potentiometric contents gauge in each reservoir and a back-up pressure-operated contents gauge in the hot water reservoir; a propeller driven water flow meter (the propeller producing electrical pulses at a rate proportional to flow); a multichannel temperature indicator using thermistors; insulation and magnet resistance meters, various pressure gauges, magnet voltmeter, a magnetic field meter employing a field pick-up coil and an electronic integrator, and a multichannel galvanometer recorder.

3. The Future

Undoubtedly the main work of the laboratory at this stage must be oriented towards building and putting into operation as soon as possible the 300 kilogauss magnet. Many physicists from Australia and overseas have indicated that they would wish to experiment in such a field and have expressed the opinion that this venture is of great value to science.

The main purpose of the existing 165 k. g. magnet is therefore to establish a working laboratory as soon as possible and to give us experience with the sort of problems likely to be met with the larger magnet.

Experiments in solid state physics have been carried out with the present magnet by Monash University's Physics Department under the direction of Professor Street. The results of these experiments will be published in the scientific literature in due course. Other experiments are planned for the near future and it is anticipated that as facilities increase the 165 k. g. magnet will come into almost full time operation.

Design of the 300 kilogauss magnet has not yet been finalized. It is expected that this magnet will weigh about 3 tons and require a total power of some 30 MW., divided approximately in the ratio of 2:1 between outer and inner solenoid respectively. The solenoids will be connected electrically in parallel, requiring 200, 000 amperes at 150 volts. It is hoped to have the magnet operational towards the middle of 1968.

Some effort is being channelled into solving the problem of more precise magnet current control. It is anticipated that eventually magnetic field stability of 0. 1% will be required. There are three ways this might be practically achieved: by controlling the h. p. g. field; by providing a set of radially moveable inner brushes on the h. p. g. which would convert the h. p. g. into a variable voltage machine; or by a series resistor.

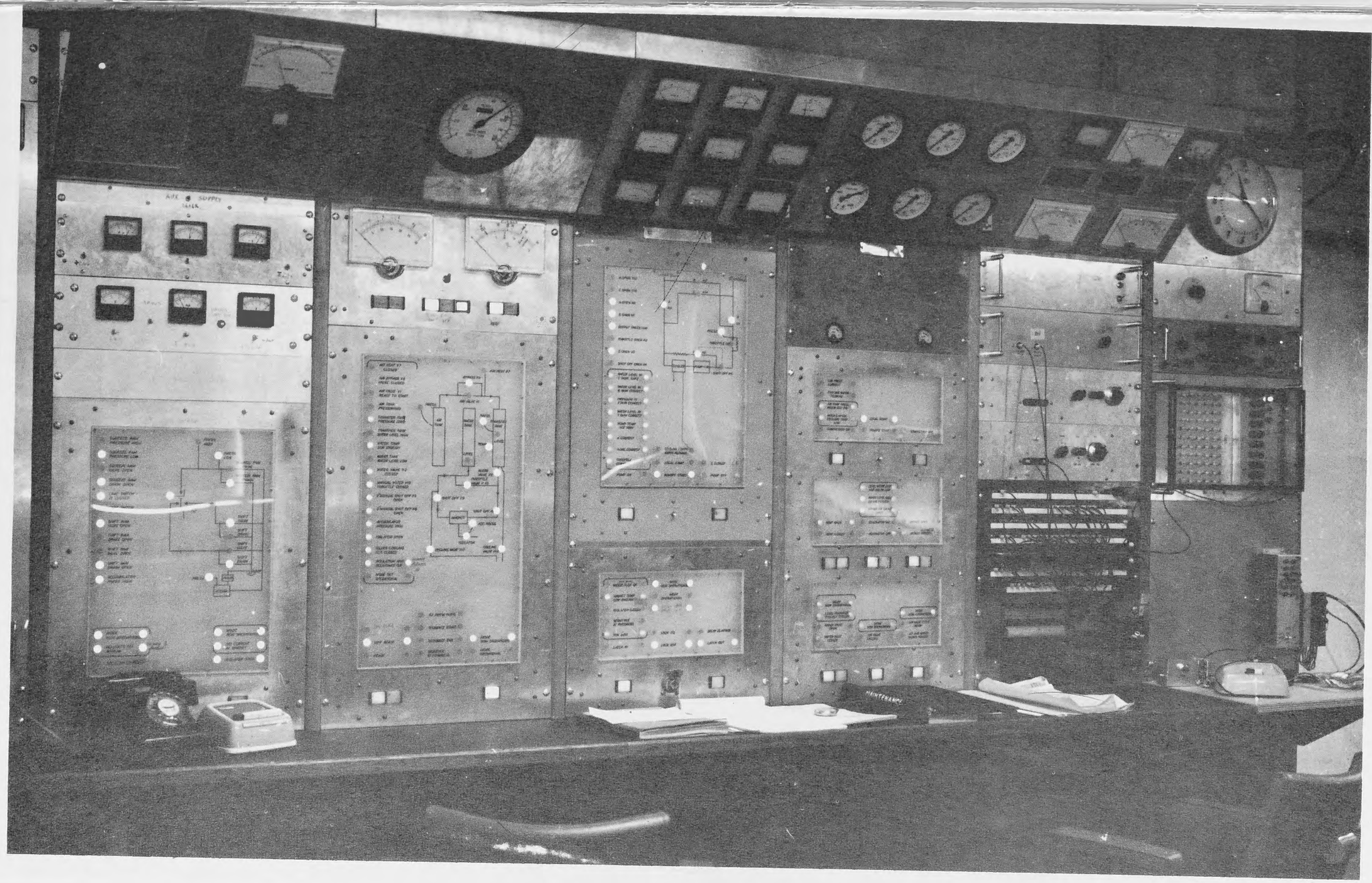

Figure 14. Control panels and instruments, showing mimic diagrams, ultra-violet galvanometer recorder (5th panel from right), air valve function generator (6th panel), meters and gauges overhead.

The last method is now being used, but a h.p.g. current feed back would have to be employed to obtain the accuracy called for. The first method is not applicable when powers exceed 40 MW or so because the inductance of the h.p.g. field windings will not allow a rapid enough increase in field to compensate decreased rotor speed without seriously exceeding their voltage rating. The second method is the most promising offering as it does fast response and high efficiency. R. A. Marshall of this department, who developed the original brush gear for the h.p.g., is at present working on this solution.

4. Conclusion

Although the A.N.U. Magnet Laboratory is in its infancy, it holds promise, given the chance, of making significant contribution to science. If it is successful, it will be by virtue of the present monopoly it holds on large power sources and by the calibre of the researchers it is able to attract in this present developing stage. It is therefore, like most scientific ventures, a gamble and being just that, is prone to falling victim to the attitude which questions its worth in favour of ventures having more recognisable returns. It is hoped that this attitude will not prevail and that the project will meet with the support it needs to become a resounding success.

5. References

1. BLAMEY, J.W., P.O. CARDEN, L.U. HIBBARD, E.K. INALL, R.A. MARSHALL and Sir Mark OLIPHANT: "The Large Homopolar Generator at Canberra," Nature, London 195, 113-114, 1962.

2. INALL, E.K.: "Modifications to the Canberra Homopolar Generator," Atomic Energy in Australia, Sydney, April, 1965.

3. NEWSTEAD, G.: "The Homopolar Generator," Science Journal, London, February, 1967.

4. MARSHALL, R.A.: "The Design of Brush Gear for High Current Pulses and High Rubbing Velocities," IEEE Trans. Power Apparatus, Systems, 1966 Winter Power Meeting. Vol. PAS 85, No. 11, pp 1177-1188, November, 1966.

5. MARSHALL, R. A.: "The Electrolytic Variable Resistance Test Load/Switch for the Canberra Homopolar Generator". The Australian National University, Department of Engineering Physics Publication EP-RR 4, First published May 1964, reissued April 1967.

APPENDIX I

The Mechanism of Solution of Air in the Cold Storage Vessel

Consider first a vessel partially full of water containing no dissolved air and having absolutely no motion. If the rest of the vessel is now filled with compressed air we may consider that the surface layer of the water instantaneously dissolves air up to the equilibrium concentration level given by Henry's Law.

Henry's law applied to our case states that the equilibrium concentration of dissolved oxygen or nitrogen in water at a certain temperature is proportional to the partial pressure of the gas in contact with the water.

Migration of the dissolved gas beyond the surface layer is a process of diffusion, the basic equation of which is

$$J = -D \frac{\partial c}{\partial x}$$

where J is the diffusion flux, for example, gms of dissolved gas crossing unit area per second (the area being parallel to the water surface);

c is the local instantaneous concentration of dissolved gas, for example, in gms per c.c.

x is the distance co-ordinate normal to the surface (in cms) and

D is the diffusion coefficient whose value has been taken for the components of air as

$$D = 10^{-4} \text{ cm.}^2/\text{sec}$$

The result of the diffusion process is that the saturated surface layer grows in depth and one may gauge the rate of growth by defining a boundary depth Z such that from the air-water interface to depth Z the water is substantially saturated, for example it is at or close to the equilibrium concentration level, and beyond Z the concentration is substantially zero.

It can be simply shown that Z is of the order of magnitude

$$Z = \sqrt{D t_e}$$

where t_e is the time the water surface has been exposed to the compressed air.

Substitution of representative values will show that when there is no motion in the water the relative amount of dissolved air entering the water is insignificant.

$$\text{e.g. if } t_e = 10 \text{ mins}$$

$$Z \simeq 1/4 \text{ cm},$$

which must be compared with an average depth of remaining uncontaminated water of approximately 80 cms.

Let us now consider the case where there is motion within the water of the form of non turbulent eddy currents of a circulatory nature about horizontal axes. There may be a number of these currents circulating in different directions. We are interested in those which have the air-water interface as a boundary. Each of these may be considered as disturbing the surface over a length y and width x, the characteristic surface velocity (in the y direction) being v (see Figure 15).

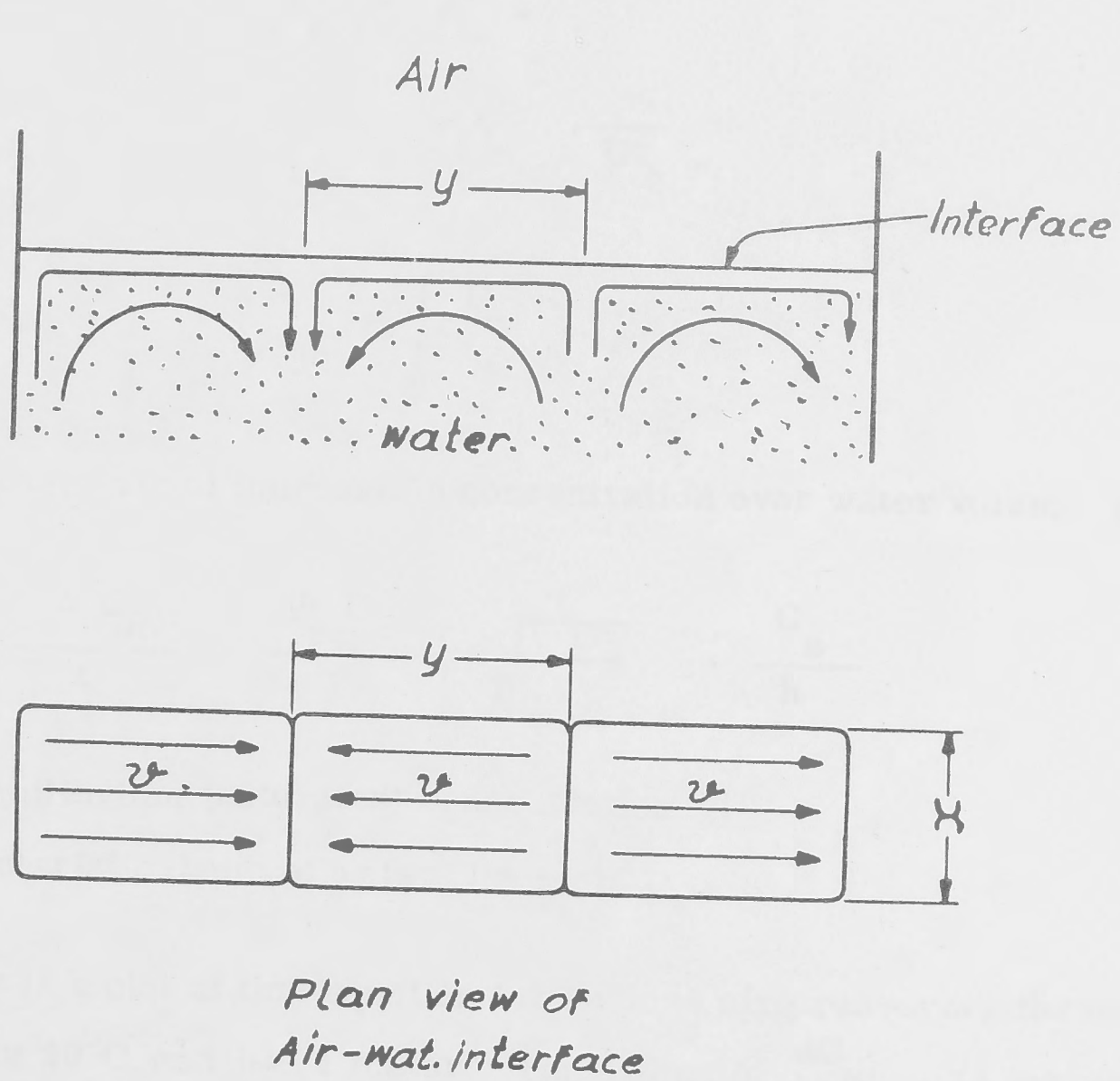

Figure 15. Idealized eddy currents illustrating terms used in the analysis.

The exposure time for a surface particle will therefore be

$$t_e = \frac{y}{v}$$

When a surface particle finally submerges after time t_e, we may consider that the water to a depth Z below it has reached saturation. We will assume that this saturated layer mixes thoroughly with the rest of the water before being exposed to the surface again.

In time t therefore the total surface area exposed will be

$$A_e = vt \times \left(\frac{A}{xy}\right)$$

where A is the area of the interface surface, $\frac{A}{xy}$ being the number of eddy systems disturbing the surface.

The total volume of water reaching saturation is therefore

$$V_s = A_e \, z$$

$$= \frac{vtA}{y} \sqrt{Dt_e}$$

$$= \sqrt{\frac{D}{t_e}} \cdot At$$

The average rate of increase in concentration over water volume V is

$$\frac{\Delta C_{av}}{t} = \frac{V_s C_s}{v} = \sqrt{\frac{D}{t_e}} \cdot \frac{C_s}{h}$$

where C_s is the equilibrium (saturated) concentration
and h is the characteristic depth of water $\left(= \frac{V}{A}\right)$

Figure 10 is a plot of this equation for various air pressures, the water temperature being about $20^{\circ}C$ and $h \approx 1$ meter. The ordinate $\frac{dC_{av}}{dt}$ is for any component of air in terms of percentage of saturation at atmospheric pressure.

It will be seen that during pump-back, measured values of $\frac{dC_{av}}{dt}$ for oxygen imply te $\backsimeq$ 1-2 min. which as explained in the text is about as large as one can expect with ideal flow re-entry geometry.

During pulsing $\frac{dC_{av}}{dt}$ was found to be very high indicating short exposure times consistent with small rapid eddies.

Publications by Department of Engineering Physics

No.	Author	Title	First Published	Re-issued
EP-RR 1	Hibbard, L. U.	Cementing Rotors for the Canberra Homopolar Generator	May, 1959	April, 1967
EP-RR 2	Carden, P. O.	Limitations of Rate of Rise of Pulse Current Imposed by Skin Effect in Rotors	Sept., 1962	April, 1967
EP-RR 3	Marshall, R. A.	The Design of Brushes for the Canberra Homopolar Generator	Jan., 1964	April, 1967
EP-RR 4	Marshall, R. A.	The Electrolytic Variable Resistance Test Load/Switch for the Canberra Homopolar Generator	May, 1964	April, 1967
EP-RR 5	Inall, E. K.	The Mark II Coupling and Rotor Centering Registers for the Canberra Homopolar Generator	Oct., 1964	April, 1967
EP-RR 6	Inall, E. K.	A Review of the Specifications and Design of the Mark II Oil Lubricated Thrust and Centering Bearings of the Canberra Homopolar Generator	Nov., 1964	April, 1967
EP-RR 7	Inall, E. K.	Proving Tests on the Canberra Homopolar Generator with the Two Rotors Connected in Series	Feb., 1966	April, 1967
EP-RR 8	Brady, T. W.	Notes on Speed Balance Controls on the Canberra Homopolar Generator	Mar., 1966	April, 1967
EP-RR 9	Inall, E. K.	Tests on the Canberra Homopolar Generator Arranged to Supply the 5 Megawatt Magnet	May, 1966	April, 1967

No.	Author	Title	First Published	Re-issued
EP-RR 10	Brady, T.W.	A Study of the Performance of the 1000 kW Motor Generator Set Supplying the Canberra Homopolar Generator Field	June, 1966	April, 1967
EP-RR 11	Macleod, I.D.G.	Instrumentation and Control of the Canberra Homopolar Generator by On-Line Computer	Oct., 1966	April, 1967
EP-RR 12	Carden, P.O.	Mechanical Stresses in an Infinitely Long Homogeneous Bitter Solenoid with Finite External Field	Jan., 1967	
EP-RR 13	Macleod, I.D.G.	A Survey of Isolation Amplifier Circuits	Feb., 1967	
EP-RR 14	Inall, E.K.	The Mark III Coupling for the Rotors of the Canberra Homopolar Generator	Feb., 1967	
EP-RR 15	Bydder, E.L. Liley, B.S.	On the Integration of "Boltzmann-Like" Collision Integrals	Mar.,1967	
EP-RR 16	Vance, C.F.	Simple Thyristor Circuits to Pulse-Fire Ignitrons for Capacitor Discharge	Mar.,1967	
EP-RR 17	Bydder, E.L.	On the Evaluation of Elastic and Inelastic Collision Frequencies for Hydrogenic-Like Plasmas	Sept.,1967	
EP-RR 18	Stebbens, A. Ward, H.	The Design of Brushes for the Homopolar Generator at The Australian National University	Mar.,1964	Sept., 1967

Copies of this and other Publications (see list inside) of the Department of Engineering Physics may be obtained from:

The Australian National University Press,
P.O. Box 4, Canberra, A.C.T., 2600.
Australia.

Price: $A1.00

hanical stresses in bonded e helical solenoids with trary external field

en
nt of Engineering Physics, Research School of cience, The Australian National University, Australia

d 24 April 1967, in revised form 19 October 1967

The paper deals primarily with the elastic stresses eneous (bonded) plane helical solenoids which are bers of multicoil systems. The terms 'bonded' nded' are defined with regard to solenoid types and conditions under which they operate. Distinction is made between the treatment required for bonded and unbonded solenoids, the work of other authors being clarified in this respect. The case of an infinitely long homogeneous solenoid with non-zero external field is analysed and expressions for the stresses are derived. These formulae are sufficiently manageable to be used in the preliminary design study of real solenoid systems with some loss in accuracy. They are directly applicable under certain conditions for the stress analysis of real solenoids. A set of computed stress curves are included in an appendix.

mbols

$\bar{E}\ \bar{F}\ \bar{G}\ \bar{H}$ constants in stress equations
ial co-ordinate
er radius of solenoid
er radius of solenoid
gnetic induction
t radius a
nponent of B in radial direction
t solenoid centre
nponent of B due to infinite solenoid alone
nponent of B_m due to infinite solenoid alone
xternal to infinite solenoid
in in direction 1
dulus of elasticity
y force, force per unit volume
l average current density
a_1
ding moment
procal of Poisson's ratio
al principal stress, compressive
gnetic pressure'
ltant axial compressive stress.
stant
r stress in the a–z plane
ensionless factor expressing relative magnitude of xternal field
cipal stress, azimuthal direction, tensile
l tension with no external axial force applied to olenoid
al displacement of point in solenoid due to strain
r disk thickness
meter in stress equation
l coordinate
a_2/a_1
of half solenoid length to a_1
ficient of friction
e
eability of free space
a_1

$\Delta\beta$ ratio of half 'correlation distance' to a_1
* average or mean value, e.g. u^*, t^*.

1 Introduction

Single-layer plane helical solenoids are particularly suited for the generation of high intensity magnetic fields because of the robust construction they allow. The essential feature of these solenoids that each turn is small in the axial direction but large in the radial direction. The azimuthal current density therefore bears a reciprocal relation to radius. As examples of this type of solenoid, mention should be made of those developed by Bitter (1936, 1937, 1938, 1939) in which the plane helix is made up of disks, cut along a radius, interleaved with insulation and clamped to form, effectively, a continuous helix (figure 1). If the clamping force is sufficiently large, these solenoids may be regarded as completely bonded plane helices.

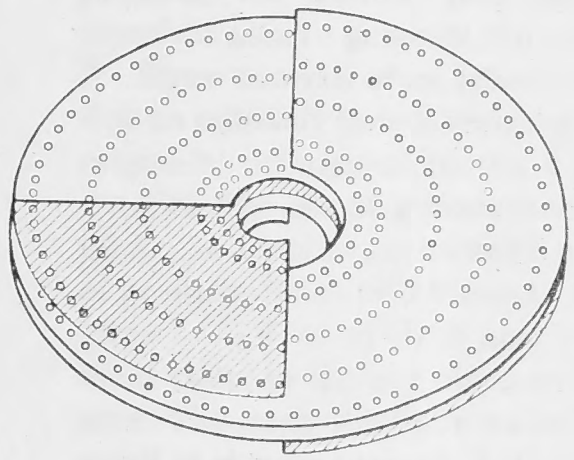

Figure 1 Typical single turn of a Bitter solenoid consisting of two conducting disks and one insulating disk. Holes are for water cooling

Solenoids are also constructed from physically continuous helices in which case it is more attractive to bond the turns together using a synthetic resin and insulating material. To meet the requirement for more intense fields it is found

ble, for stress reasons, to turn to multicoil systems of ntric solenoids. This paper is concerned primarily with embers of such multicoil systems which are bonded helical solenoids.

sses in plane helical solenoids have been investigated by , most notably Kuznetsov (1961) and Léon (1964). tsov analyses a single long unbonded helix using a stress system and an exact relationship for the axial nent of field intensity in the central region. The is is not applicable to bonded solenoids because a stress system is not a suitable model, being one where tress is everywhere zero and axial strain varies with n. Léon makes use of a precomputed field profile along edian plane of a solenoid. His method is therefore ble to members of multicoil systems. Léon claims analysed a homogeneous, isotropic solenoid (regarded synonomous with 'bonded solenoid') and makes two otions about shear stress s in the a–z plane: $s = 0$ and $= 0$.

first assumption is correct but the second is generally ct, as can be seen by the general shear stress distri- in figure 2. As shown in appendix 1, the derivative of

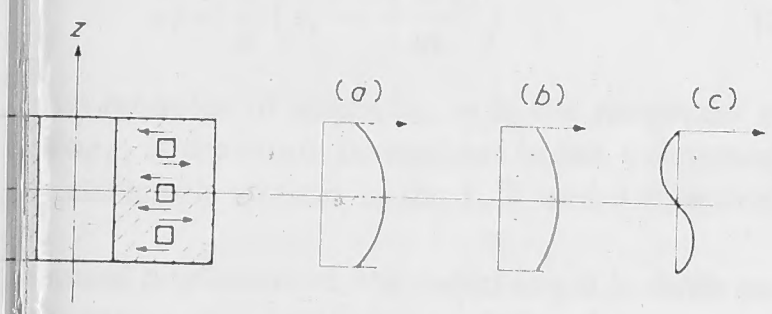

2 Section of a bonded solenoid showing the ive of shear stress with respect to z to be generally o at the median plane. (*a*) Mean body force per ial length, (*b*) radial displacement u, (*c*) shear x du/dz.

ar stress in the a–z plane is the agent for effectively puting the body forces over a length $2a_1\Delta\beta$, defined 'correlation' distance so that, within this length, the al stress is practically constant and a function of the ody force $(f)_a$*. In addition to this, Léon has based his on a plane stress system. On two counts therefore, hod is not strictly applicable to bonded solenoids. uznetsov and Léon have analysed what is in effect a clamped unbonded solenoid, i.e. one where turn-to- ative motion is allowed. The stability of such solenoids er question.

uld be mentioned at this stage that there is great need nize the parameters of solenoid systems because of the on of the strength of materials, the size of existing ources and the cost of new ones. In the development work comparative studies have to be made rather than determinations of stress, and for this work manage- xact formulae are of more use than exact unwieldy his attitude appears justified because of the dearth rimental evidence to support any set of formulae ause, in any case, formulae based on the assumption lastic material should not be expected to predict hanical failure of a ductile solenoid which will occur in the plastic state, except where fatigue is .

resent work was undertaken to satisfy this need in to the development of a 30 Wb m^{-2} (300 kG), 30 MW pulsed system (pulses of many seconds duration limited by the power source). Here, initial local yielding was considered permissible provided subsequent stress changes were elastic within limits based on fatigue considerations for the expected life of the solenoid.

This implies that after the first pulse, stresses would not be zero. There would for instance be a zone of compression around the inner boundary of each solenoid and tension near the outer boundary. Provided stresses in this non-energized state are less than the yield stress, subsequent pulses should cause no more yielding, merely changing the compression zone to tension and raising the stress in the tension zone. The stress changes during pulses other than the first would therefore be elastic and an elastic analysis is applicable. Such an analysis of course can give no idea of how close to rupture the solenoid is during any particular pulse, i.e. to what degree the device can be over energized before rupture occurs. This can only be determined through a study in the plastic state.

2 Bonded and unbonded solenoids

The terms 'bonded' and 'unbonded' have already been referred to and will be used elsewhere in this paper. It will therefore be useful to dwell a little on the meaning of these terms. A bonded solenoid will be defined as one which is essentially homogeneous and isotropic. An example would be a continuous plane helix having its turns glued together with a thin layer of insulation. The insulation must be relatively thin so that its differing elastic properties have negligible effect on the homogeneity and isotropy of the structure. A continuous plane helix could also be bonded effectively by friction, resulting from electromagnetic and applied axial compression. In this case the test to show that the solenoid is bonded is to assume that it is and examine both the resultant axial stress everywhere and the shear stress along planes orthogonal to the axis. The axial stress must be compressive and the shear stress less than the axial stress multiplied by the coefficient of friction.

For Bitter disk solenoids a third criterion applies with regard to the effect of the disk slits. This is discussed further in § 5.2.

The term 'unbonded' covers all plane helical solenoids which are not 'bonded'. It is applicable to all cases where there is no effective turn-to-turn mechanical interaction, or where the plane helix cannot be regarded as physically continuous. An example of the latter would be a Bitter disk solenoid having relatively few disks so that the azimuthal force requires, for transfer past the slits, an appreciable disk interface area to generate the required friction.

3 Stress analysis of an infinitely long bonded solenoid

For an infinitely long homogeneous isotropic solenoid, planes originally orthogonal to the z axis must remain plane and parallel. The use of a plane strain system is therefore appropriate, i.e. axial strain is considered constant and independent of position. Since field intensity is independent of z, the body force $f = jB_z$ (N m^{-3}) is also independent of z and hence shear stress in the a–z plane and orthogonal to the z axis is zero. The basic relations outlined in § 3.1 are developed in detail in standard texts (e.g. Case 1940).

3.1 *Basic relations*

Consider an elemental ring (figure 3) radius a, radial width da, and axial length unity. The radial compressive stress acting on the ring is p and the azimuthal or 'hoop' tension is t. The difference in compressive stress acting on the two sides of the ring is dp. Consideration of force balance on a section of the ring gives

$$p + t = fa - a\frac{dp}{da} \qquad (1)$$

where f is the radial body force acting within the ring due to the interaction of current (azimuthal) and field (axial).

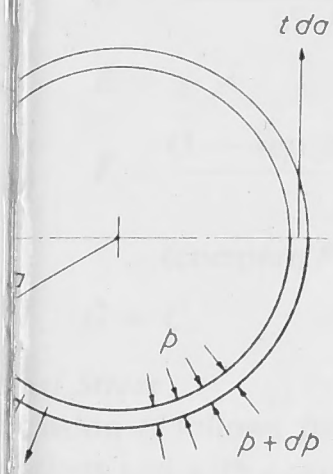

Elemental ring for stress analysis

B are local average values of current density and y respectively, then

$$f = jB.$$

omogeneous elastic material the basic stress–strain p is

$$e_1 = \frac{1}{E}\left(t_1 - \frac{t_2 + t_3}{m}\right) \tag{2}$$

the modulus of elasticity, m is the reciprocal of atio, e_1 is the strain (extension) in the 1 direction, t_3 are tensile stresses in the 1, 2, and 3 directions y.

e radial displacement, the radial strain is du/da and hal strain u/a. Application of the above general tion gives

$$\frac{du}{da} = -\frac{1}{E}\left(p + \frac{t_z + t}{m}\right)$$

$$\frac{u}{a} = \frac{1}{E}\left(t - \frac{t_z - p}{m}\right)$$

the axial tensile stress. These may be combined to

$$+ t)\left(1 + \frac{1}{m}\right) + \frac{a}{m}\frac{dp}{da} + a\frac{dt}{da} = \frac{a}{m}\frac{dt_z}{da}. \tag{3}$$

xial direction we assume strain is constant with z. Hence, using equation (2)

$$\frac{dt_z}{da} = -\frac{1}{m}\frac{d}{dz}(p - t)$$

uting this in equation (3):

$$\left(1 + \frac{1}{m}\right) + \frac{a}{m}\frac{dp}{dz} + a\frac{dt}{da} = -\frac{a}{m^2}\frac{d}{da}(p - t).$$

be combined with equation (1) and simplified

$$\frac{d}{da}(p - t) = \frac{f}{1 - 1/m}. \tag{4}$$

rce f

is made between the component B_B of mag- tion due to the solenoid being analysed and the lue of field B, the relation between the two being

$$B = B_B + B_c$$

the field external to the solenoid. The inclusion of d enables the results to be applied to the case of centric solenoids. The value of B_B in the bore of the solenoid is defined as B_{Bm}. The value of B in the bore is defined as B_m, i.e. $B_m = B_c + B_{Bm}$. The ratio of the field components at the bore is defined as S, i.e. $B_c = SB_{Bm}$. Hence $B_m = (S + 1)B_{Bm}$ and $B_c = SB_m/(S + 1)$.

The field components defined above are shown in figure 4.

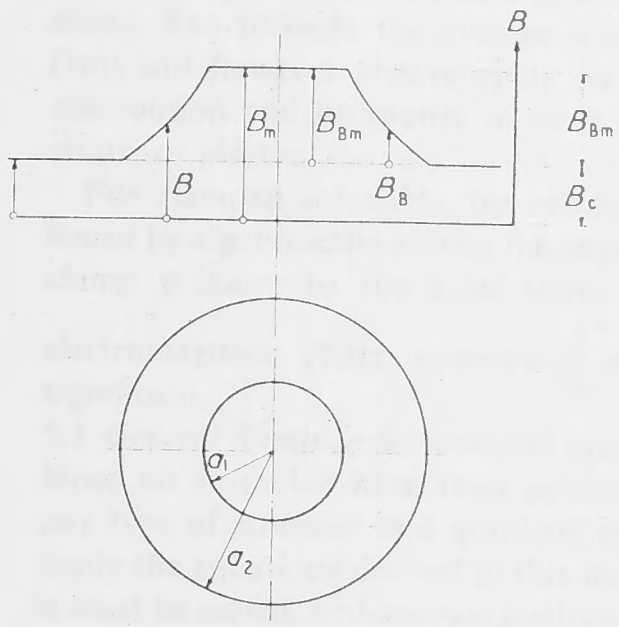

Figure 4 Illustration of terms used in text

Current density is inversely proportional to radius, i.e. $j = q/a$.

This current density is the local average value which can be regarded as varying monotonically through conductor, insulation and coolant alike and which will produce the same magnetic field as the actual current distribution. We find, therefore, $B_B = \mu_0 q \ln a_2/a$. It follows that

$$B = \mu_0 q\{\ln(\alpha/\delta) + S \ln \alpha\}$$

and $B_m = (S + 1)\mu_0 q \ln \alpha$ where $\alpha = a_2/a_1$ and $\delta = a/a_1$.

'Magnetic pressure' p_m is defined as $p_m = B_m^2/2\mu_0$. Hence $p_m = \frac{1}{2}(S + 1)^2\mu_0 q^2 (\ln \alpha)^2$.

Body force f is given by

$$f = jB = \frac{2p_m}{a}\frac{\ln(\alpha/\delta) + S \ln \alpha}{(S + 1)^2(\ln \alpha)^2}$$

and $$\int f da = p_m(2X - X^2) + \text{constant} \tag{5}$$

where $$X = (\ln \delta)/(S + 1) \ln \alpha.$$

Also, $$fa = \frac{2p_m}{\ln \delta}(X - X^2). \tag{6}$$

3.3 *Azimuthal and radial stresses*

Equations (1), (4), (5) and (6) may be combined and solved for the stresses p and t using the boundary conditions $p = 0$ for $\delta = 1, \alpha$.

The solutions are:

$$\frac{t}{p_m} = \bar{A}X^2 + \bar{B}X + \bar{C}(\delta^{-2} + 1) + \bar{D} \tag{7}$$

$$\frac{p}{p_m} = \bar{E}X^2 + \bar{F}X + \bar{G}(\delta^{-2} - 1)$$

where $$\bar{A} = m/2(m - 1)$$

$$\bar{B} = \frac{(1 - \frac{1}{2}m)\{(S + 1) \ln \alpha\}^{-1} - m}{(m - 1)}$$

$$\bar{C} = \frac{-\alpha^2}{1 - \alpha^2}\frac{m(S + \frac{1}{2}) + (1 - \frac{1}{2}m)/(\ln \alpha)}{(S + 1)^2(m - 1)}$$

$$\bar{D} = \frac{(m-2)(S+1) - (1-\frac{1}{2}m)/\ln\alpha}{(S+1)^2(m-1)\ln\alpha}$$

$$\bar{E} = -\bar{A}$$

$$\bar{F} = \frac{(1-\frac{1}{2}m)\{(S+1)\ln\alpha\}^{-1} + m}{(m-1)}$$

(compare $\bar{F}$ with $\bar{B}$)

$$\bar{G} = \bar{C}.$$

xial Stress

tension t_z follows from equation (2) with appropriate utions and with e_z constant

$$\frac{t_z}{p_m} = \frac{2}{m}(\bar{A}X^2 - 2\bar{A}X + \bar{H}). \qquad (9)$$

here is no externally applied force then the condition hat

$$\int_{a_1}^{a_2} at_z da = 0.$$

then found to be

$$\frac{\alpha^2\{\ln\alpha + (2S+1)(\ln\alpha)^2\}/(\alpha^2-1) - \frac{1}{2} - (S+1)\ln\alpha}{(S+1)^2(\ln\alpha)^2}.$$

erage azimuthal stress

erage azimuthal stress t^* may be found by integrating on (7) across a radius or by integration of the body in a sector and considering the resultant of the hal stresses necessary to provide equilibrium. latter gives

$$t^* = \frac{1}{a_2 - a_1}\int_{a_1}^{a_2} f a da.$$

g equation (6) it is found that

$$\frac{t^*}{p_m} = \frac{2\{(\alpha-1)(1+S\ln\alpha) - \ln\alpha\}}{(\alpha-1)(S+1)^2(\ln\alpha)^2}. \qquad (10)$$

sentation of formulae in graphical form

tion of curves for the two normalized principle stresses nd p/p_m appears in the appendix 2, these being the ost tedious to evaluate. These curves were plotted ne computing facilities of the Commonwealth Scientific dustrial Research Organization Computing Research at Canberra.

ch case m is taken as 3·3 for a representative range of S.

licability of formulae

ite length solenoids

rmulae for infinite solenoids may be applied to any ngth solenoid in which $(B)_a$ may be considered constant e correlation distance $2a_1\,\Delta\beta$ (appendix 1) and where s logarithmically with radius as for an infinite solenoid. ld be noted that the second condition must follow if independent of z. Hence generally either condition is nt. In multicoil systems the above conditions do not rily apply only to 'long' solenoids.

ongly clamped friction bonded solenoids

ious helices satisfying the conditions in § 5.1 and with g stresses equal to or exceeding t_z (equation (9)) at dius are effectively bonded.

r disk solenoids, however, are not effectively bonded he above proviso holds and the volume of under- (azimuthally) material in the vicinity of the radial elatively small. Consideration of strain shows that is effective over a region of azimuthal dimensions mately $wt/2\gamma p_z$ either side of a slit, where t is the azimuthal stress away from the slit, w the disk thickness, γ the coefficient of friction and p_z the axial compressive stress.

The second proviso may be restated therefore as

$$\frac{wt}{\gamma p_z} \ll 2\pi a \text{ for } a_1 < a < a_2.$$

If this proviso is not met, considerable slip must occur leading to gross redistribution of stress, especially azimuthal stress. The formula for average azimuthal stress (equation (10)) will however always apply no matter what the stress distribution and no matter in what state the material is in, elastic or plastic.

For clamped solenoids, the resultant local axial stress is found by algebraically adding the applied and electromagnetic clamp pressure to the axial stress t_z (equation (9)). The electromagnetic clamp pressure $j\int_z^{a_1\beta} B_a dz$ is generally quite significant.

5.3 *General formulae for multicoil systems*

Since no formulae have been published for the stresses in any type of solenoid in a multicoil system, it is tempting to apply the equations derived in this paper to fill the need but, it must be added, with no real justification. However, in some cases it does appear that errors cancel sufficiently for the azimuthal stress formulae at least to provide a reasonable approximation. The importance of this is that it enables one to investigate with ease the effect of simultaneous small excursions in parameters – a process necessary in design optimization.

As an example, the inner solenoid of the duplex system, whose parameters are shown in the table for the median plane,

	α	β
Inner solenoid	4·15	2·67
Outer solenoid	2·56	1·55

$s = 0{\cdot}705$

was analysed by Léon's technique and by the infinite solenoid stress equations. It was found that the field distribution differed only 2½% from an equivalent infinite solenoid field distribution (with identical α) which was chosen to match at the inner and outer radii of the solenoid. However there was appreciable axial gradient which was manifest by the fact that the current density distribution for the solenoid was everywhere 1·29 times that in the equivalent infinite solenoid. Since this factor represented a universal proportionate increase in body force it was appropriate to multiply the stresses derived from the infinite stress equations by this factor also. The result was an azimuthal stress distribution which was 13% higher than that given by Léon's method at the inner radius and about 6% higher for the average stress. Comparison of the radial stress was not so good and of course there was no agreement for axial stress.

6 Summary and conclusion

This paper endeavours to point out the significance of correct classification of solenoids before applying an analytical solution for the mechanical stresses. Broadly speaking the realm of plane helical solenoids may be divided into the bonded group and the unbonded group.

The bonded group can be further divided on the basis of the magnitude of the axial field gradient: where the axial field does not vary appreciably over the correlation distance, we may say we have 'quasi-infinite' conditions; where there is appreciable gradient we may refer to this situation as a complex stress condition.

ed solenoids, on the other hand, may be classified as inuous or discontinuous. As an example, a lightly itter disk solenoid would be discontinuous un- ereas a solenoid of similar construction forming the of a multicoil system might easily be classed as onded because of the unusually high electro- amping resulting from the radial field components ner coils.

four classifications only one has been examined by uthors, viz. the continuous unbonded, while the k covers the case of the 'quasi-infinite' bonded.

trict ourselves to solenoid members of multicoil e find again only one of the four classifications has usly dealt with but in a manner more suitable for a particular problem rather than generalization. work again covers the quasi-infinite bonded case. concluded therefore that the study of the infinitely d solenoid system extends the range of analytical a significant portion of the plane helical solenoid urther it provides the only available set of multi- quations in manageable form and may prove there- daptable throughout the spectrum until the body ntal evidence grows sufficiently to warrant further sophistication.

onded solenoids with appreciable axial field gradient

ng treatment is an approximate one pursued to relative importance of various effects. Various es are referred to but no attempt will be made to rigorously.

e a general approach, consider first the effect of in a long solenoid confined to a disk-like region lth $dz \to 0$) centred at $z = 0$ (a Dirac function of z)

$$f \neq 0 \text{ for } \frac{-dz}{2} < z < \frac{dz}{2}$$

$$f = 0 \text{ for all other } z.$$

letermine the extent of the resulting deformation β and hence conclude that the stresses at any eal solenoid are a function of the body forces in bounded by the inner and outer surfaces of the d planes orthogonal to the axis spaced $a_1\Delta\beta$ f the point in question.

nce $2a_1\beta\Delta$ will be called the correlation distance. ental sector (figure 5) of angle $d\theta$ and axial thick- upported in general by the radial resultant dH thal stresses, and the radial resultant shear force its two major surfaces.

$$dH = t^*\Delta a\, dz\, d\theta$$

$$\Delta a = a_2 - a_1.$$

rst order t^* is related to radial displacement thus

$$t^* = Eu^*/a^* \qquad (1)$$

the mean radial displacement of the section and erage radius $\frac{1}{2}(a_1 + a_2)$.

her hand

$$dS = -\frac{ds^*}{dz}\, a^*\Delta a\, d\theta\, dz \qquad (2)$$

average shear stress.

mental sector is also regarded as part of a long ding in the axial direction, then displacement u_b ending of the beam is related to S by

$$\frac{d^4u_b}{dz^4} = \frac{1}{EI}\frac{dS}{dz} \qquad (3)$$

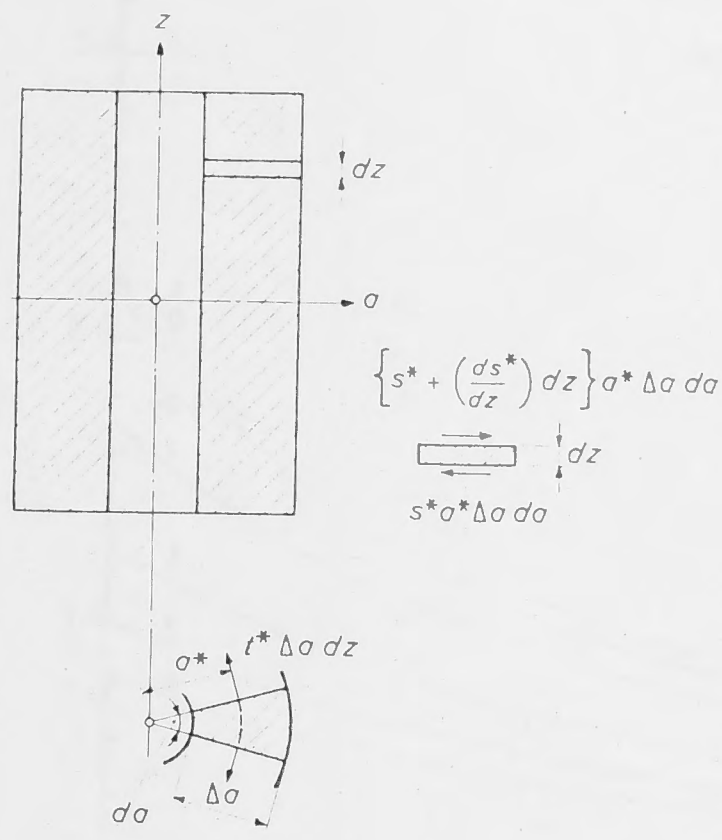

Figure 5 Section of a bonded solenoid showing elemental sector

where I is the moment of inertia of the section, and the displacement u_s due to shear is related by

$$\frac{d^2u_s}{dz^2} = -\frac{1}{E}\frac{dS}{dz}.$$

u_b is found to be always more significant than u_s; hence we will consider only u_b.

In general a resultant radial body force dF acts on the elemental section of magnitude

$$dF = f^*a^*\Delta a\, d\theta\, dz$$

f^* being the average body force.

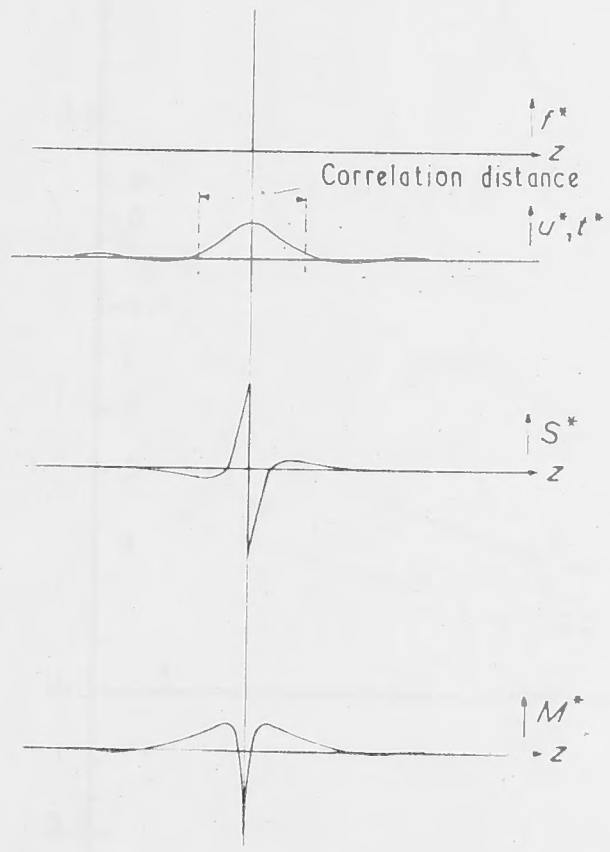

Figure 6 An impulse or Dirac function of mean body force f^* and resulting mean radial displacement u^*, azimuthal stress t^*, shear stress s^* and bending moment M^*

cause of equilibrium it follows that

$$f = \frac{E}{a^{*2}}\left(u^* + \frac{(\Delta a)^2 a^{*2}}{12}\frac{d^4u^*}{dz^4}\right) \qquad (4)$$

$a^* d\theta(\Delta z)^3/12$ has been substituted for I.

uation (4) is identical with that for an elastically supported which is dealt with in standard texts (e.g. Karman and 1940). The solution for the concentrated load we are dering is $u^* = u_0 e^{-bz}(\cos bz + \sin bz)$ for $z > 0$ and $u_0 e^{bz}(\cos bz - \sin bz)$ for $z < 0$

$b = 3^{1/4}(a\,\Delta a)^{-1/2}$

ure 6 shows the form of this solution and also the form various resulting stress distributions.

distance between the first zeros of u^* either side of is found to be approximately $3{\cdot}6\,(a^*\,\Delta a)^{1/2}$, i.e. $\Delta\beta$ is order of $(\alpha^2 - 1)^{1/2}$.

ce every real body force function can be considered as inite number of Dirac functions displaced in z we may the following conclusions.

*, t^*, s^* and M^* at any point depend on f^* over the orrelation distance centred on the point in question.

f f^* is constant over the correlation distance then s^* nd M^* will be zero at the point in question since, as unctions of the Dirac body force, their average is zero.

f f^* is not constant over the correlation distance, then * and t^* are functions of the weighted average of f^* ver the correlation distance, and s^* and M^* are functons of the difference between this weighted average and he actual f^*.

dix 2

uted normalized stress curves

ordinates are normalized stress and the absciscae a/a,

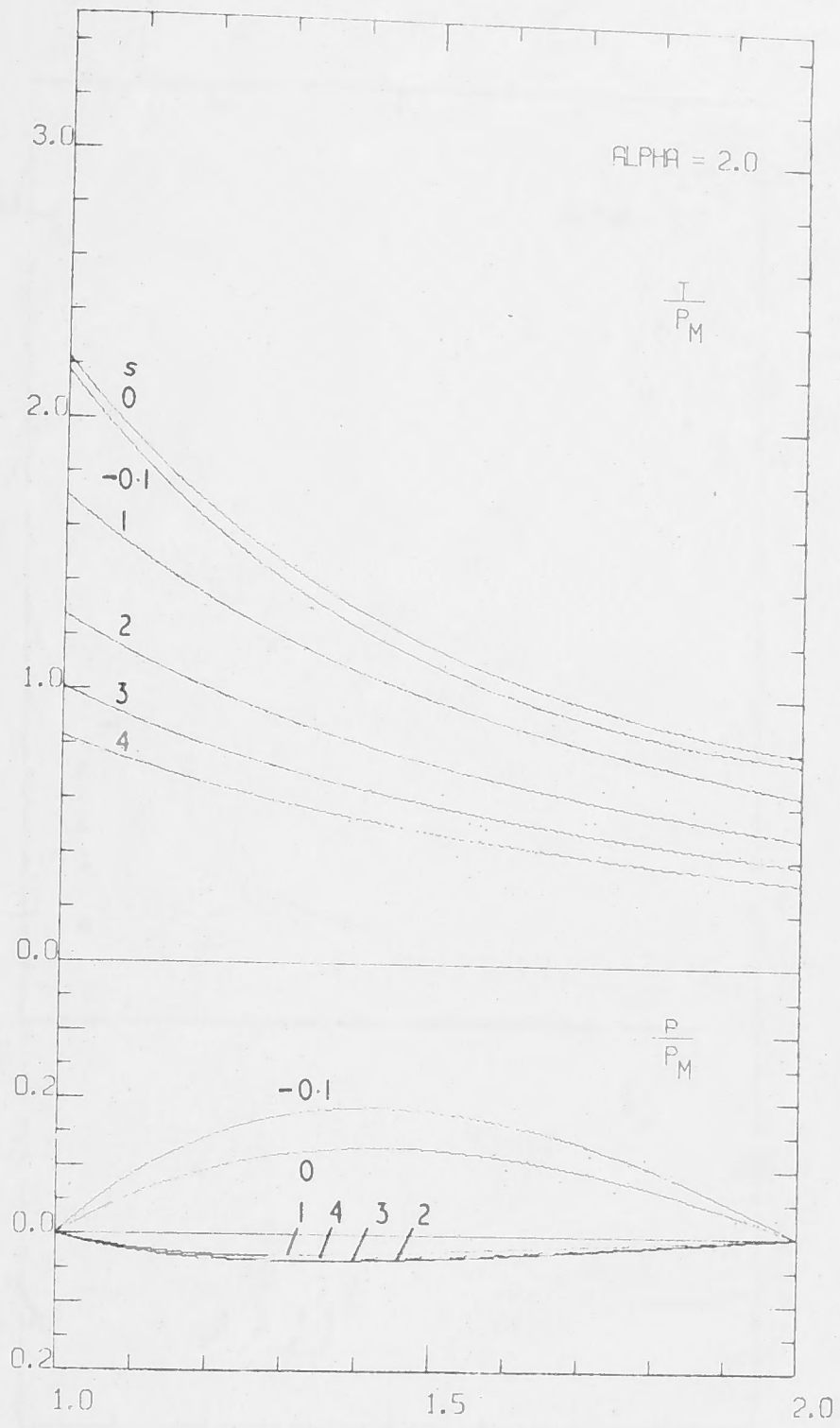

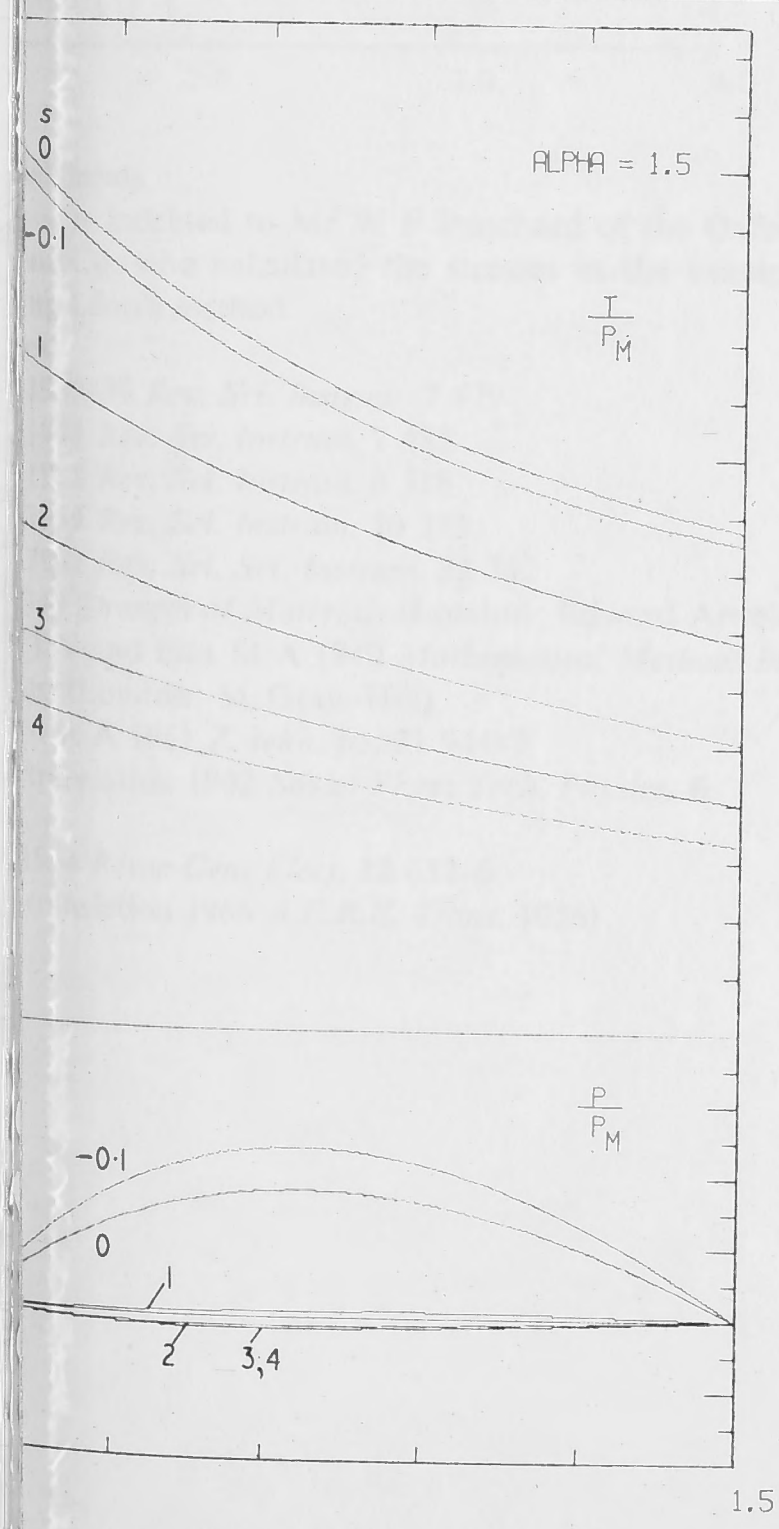

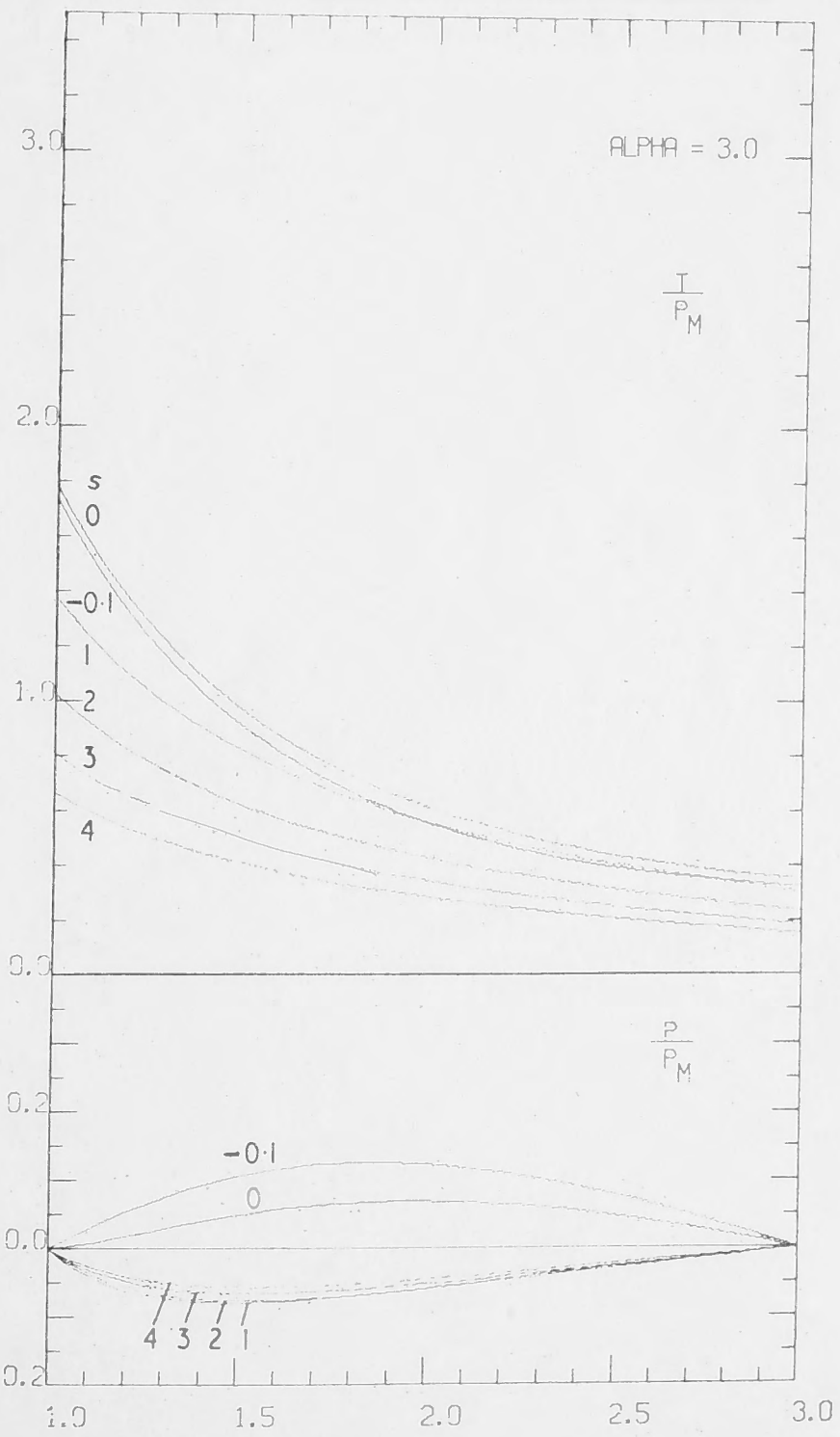

(4)

EP-RR 12

MECHANICAL STRESSES IN AN INFINITELY LONG HOMOGENEOUS BITTER SOLENOID WITH FINITE EXTERNAL FIELD

P. O. CARDEN

January, 1967

Department of Engineering Physics

Research School of Physical Sciences

THE AUSTRALIAN NATIONAL UNIVERSITY

Canberra, A.C.T., Australia.

MECHANICAL STRESSES IN AN INFINITELY LONG HOMOGENEOUS BITTER SOLENOID WITH FINITE EXTERNAL FIELD

by

P. O. CARDEN

First Published, January, 1967

Publication EP-RR 12

Department of Engineering Physics
Research School of Physical Sciences
THE AUSTRALIAN NATIONAL UNIVERSITY
Canberra, A.C.T. Australia

SUMMARY

Equations for the radial and azimuthal principal stresses are derived for the case of an infinitely long solenoid immersed in an externally applied parallel field, the solenoid having a 1/radius or "Bitter" current density distribution and being constructed of homogeneous, isotropic material.

A series of computed normalized stress curves is appended.

Application to real solenoids of finite length is briefly discussed.

LIST OF SYMBOLS

$\underline{A}$	Constant in final stress equation
a	Radial coordinate
a_1	Inner radius of solenoid
a_2	Outer radius of solenoid
$\underline{B}$	Constant in final stress equation
B (B_m)	Magnetic induction (maximum value)
b	Constant
$\underline{C}$	Constant in final stress equation
c	Constant
$\underline{D}$	Constant in final stress equation
$\underline{E}$	Constant in final stress equation
E	Modulus of elasticity of solenoid material
e (e_1)	Strain (in direction 1)
$\underline{F}$	Constant in final stress equation
f	Body force--force units per volume unit
$\underline{G}$	Constant in final stress equation
g	Constant
H (H_m)	Field intensity (maximum value)
H_B (H_{Bm})	Field intensity--component due to solenoid (maximum value)
H_C	Field intensity--constant component
j	Current density
K	Constant in defining equation for j
k	Constant
m	Reciprocal of Poisson's ratio for solenoid material
p	Radial stress-compressive
p_m	Magnetic pressure
p'	p normalized with respect to p_m

LIST OF SYMBOLS (Cont.)

Q	Constant
S	Parameter describing relative value of H_C
t	Azimuthal ("hoop") stress--tensile
t_1, t_2, t_3	Generalized tensile stress in directions 1, 2, 3
t'	t normalized with respect to p_m
u	Radial displacement
X	Parameter in stress equations
Z	Axial coordinate
α	ratio $\frac{a_2}{a_1}$
δ	ratio $\frac{a}{a_1}$

INTRODUCTION

In the generation of high intensity magnetic fields, the Bitter solenoid[1] has proved its importance due mainly to its robust construction.

Essentially each turn of a Bitter solenoid is thin (in the axial direction) and wide (in the radial direction) giving rise to a current density distribution inversely proportioned to the radius.

As magnetic fields generated by such solenoids become more intense, mechanical stresses increase towards the limits of available materials. A knowledge of stresses within the solenoid is of primary importance in design and it is as a contribution to this knowledge that the calculations and graphs in this report are given.

The calculations are based on the assumption of a mechanically elastic homogeneous material. All stresses are normalised by dividing by the magnetic pressure p_m i.e. $\frac{B_m^2}{8\pi}$ (gauss) in the C.G.S. system or $\frac{B_m^2 \ (w/m^2)}{2\mu_o}$ in the M.K.S. system.

STRESSES - BASIC RELATIONS

Consider an elemental ring radius a, radial width δ a, and axial length unity. The radial compressive stress acting on the ring is p and the azimuthal or "hoop" tension is t.

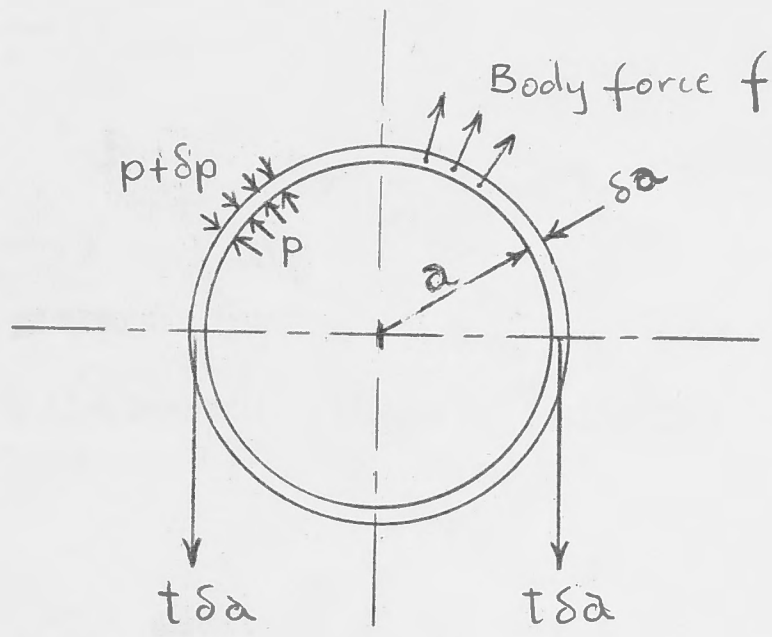

The difference in compressive stress acting on the two sides of the ring is δ p.

Consideration of force balance on a section of the ring gives

$$p + t = fa - a\frac{dp}{da} \qquad (1)$$

where f is the radial body force acting within the ring due to the interaction of current (azimuthal) and field (axial).

If j and B are local values of current density and flux density respectively, then f = jB.

For a homogeneous elastic material the basic stress-strain relationship is (e.g. case 2)

$$e_1 = \frac{1}{E} \left(t_1 - \frac{t_2 + t_3}{m} \right) \qquad (2)$$

where E is the modulus of elasticity
m is the reciprocal of Poisson's ratio
e_1 is the strain (extension) in direction "1"
t_1, t_2, t_3 are tensile stresses in the 1, 2, and 3 directions respectively

If u is the radial displacement, the radial strain is $\frac{du}{da}$ and the azimuthal strain $\frac{u}{a}$. Application of the above general strain equation gives

$$\frac{du}{da} = -\frac{1}{E} \left(p + \frac{t_Z + t}{m} \right)$$

$$\frac{u}{a} = \frac{1}{E} \left(t - \frac{t_Z - p}{m} \right)$$

where t_Z is the axial tensile stress. Multiplying the second of these by a, differentiating and substituting in the first for $\frac{du}{da}$ gives

$$(p + t) \left(1 + \frac{1}{m} \right) + \frac{a}{m} \frac{dp}{da} + a \frac{dt}{da} = \frac{a}{m} \frac{dt_Z}{da} \qquad (3)$$

In the axial direction we assume strain is constant with respect to a.

Hence, using (2)

$$\frac{dt_Z}{da} = -\frac{1}{m} \frac{d}{da} (p - t)$$

and substituting this in (3) gives

$$(p + t) \left(1 + \frac{1}{m} \right) + \frac{a}{m} \frac{dp}{da} + a \frac{dt}{da} = -\frac{a}{m^2} \frac{d}{da} (p - t)$$

This may be combined with (1) and simplified yielding

$$\frac{d}{da}(p - t) = \frac{f}{1 - \frac{1}{m}} \qquad (4)$$

BODY FORCE f.

$$\frac{a_2}{a_1} = \alpha$$

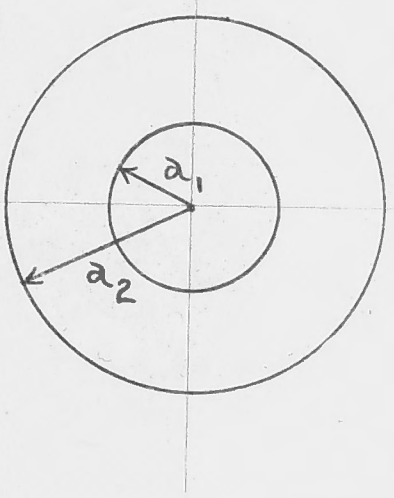

Distinction is made between the field component due to the Bitter solenoid H_B and the absolute value of field H, the relation between the two being $H = H_B + H_c$ where H_c is the field external to the solenoid. The inclusion of external field enables the results of this report to be applied to the case of several concentric solenoids.

The value of H_B in the bore of the solenoid is defined as H_{Bm}.

The value of H in the bore is defined as H_m. $H_m = H_c + H_{Bm}$.

The ratio of the field components at the bore is defined as S, i.e. $H_c = S H_{Bm}$.

Hence $H_m = (S + 1) H_{Bm}$

and $H_c = \frac{S H_m}{S+1}$

Current density is inversely proportional to radius

i.e. $j = \frac{K}{a}$

BODY FORCE f.

Hence $H_B = \frac{4\pi K}{10} \ln \frac{a_2}{a}$ in the C.G.S. system.

It follows that $H = \frac{4\pi K}{10} \left(\ln \frac{\alpha}{\delta} + S \ln \alpha \right)$

and $H_m = (S+1) \times \frac{4\pi K}{10} \ln \alpha$

where $\alpha = \frac{a_2}{a_1}$

and $\delta = \frac{a}{a_1}$

Magnetic Pressure $p_m = \frac{B_m^2}{8\pi}$ in C.G.S. system

$$= \frac{H_m^2}{\left(\frac{8\pi}{}\right)}$$

Hence $p_m = \frac{(S+1)^2}{8\pi} \left(\frac{4\pi K}{10} \right)^2 (\ln \alpha)^2$

Body force f.

$$f = \frac{j H}{10} = \frac{2 p_m}{a} \frac{\left[\ln \frac{\alpha}{\delta} + S \ln \alpha \right]}{(S+1)^2 (\ln \alpha)^2}$$

and $\int f \, da = p_m [2X - X^2] + \text{constant}$ (5)

where $X = \frac{\ln \delta}{(S+1) \ln \alpha}$

Also $f a = \frac{2 p_m}{\ln \delta} [X - X^2]$ (6)

Integration of equation (4) and substitution of (5) yields

$$\frac{p - t}{p_m} = \frac{1}{\left(1 - \frac{1}{m}\right)} \left[2X - X^2 \right] + A \qquad (7)$$

where A is a constant of integration. Also substitution of (6) in (1) yields

$$\frac{p + t}{p_m} = \frac{2}{\ln \delta} \left[X - X^2 \right] - Q \frac{dp}{dX} \qquad (8)$$

where $Q = \frac{X}{\ln \delta}$ which is constant.

Elimination of t from (7) and (8) gives

$$p' + \tfrac{1}{2} Q \frac{dp'}{dX} = \left[\frac{-1}{2 \left(1 - \frac{1}{m}\right)} \right] X^2 + \left[\frac{1}{1 - \frac{1}{m}} - Q \right] X + \text{constant} \qquad (9)$$

where $p' = \frac{p}{p_m}$

The solution of (9) is

$$p' = g X^2 + bX + c + k e^{\frac{-2X}{Q}} \qquad (10)$$

with $g = - \frac{1}{2 \left(1 - \frac{1}{m}\right)}$

$$b = \frac{1 + Q \left(\frac{1}{m} - \frac{1}{2}\right)}{1 - \frac{1}{m}}$$

BODY FORCE f.

From (8)

$$t' = \frac{2}{\ln \delta} \left[X - X^2 \right] - Q \frac{dp'}{dX} - p'$$

where $$t' = \frac{t}{p_m}$$

Differentiating (10) to obtain $\frac{dp}{dX}$ and substituting this and (10) in the above gives

$$t' = -g X^2 - \left[b + 2Q + 2gQ \right] X + ke^{\frac{-2X}{Q}} + 2Q - bQ - c \qquad (11)$$

c is evaluated by considering boundary conditions:

when $\delta = 1$, $p' = 0$ also $X = 0$

when $\delta = \alpha$, $p' = 0$ and $X = \frac{1}{S+1} = Q \ln \alpha$

Applying these conditions to (10) it is found that

$$c = -k = \frac{\alpha^2}{(1 - \alpha^2)(S+1)^2} \left[g + b(S+1) \right]$$

Using these values for g, b, c and k, equations (10) and (11) may then be written

$$\frac{t}{p_m} = \underline{A} X^2 + \underline{B} X + \underline{C} (\delta^{-2} + 1) + \underline{D} \qquad (12)$$

$$\frac{p}{p_m} = \underline{E} X^2 + \underline{F} X + \underline{G} (\delta^{-2} - 1) \qquad (13)$$

where $$\underline{A} = \frac{1}{2 (1 - \frac{1}{m})}$$

BODY FORCE f.

$$\underline{B} = \frac{\frac{1}{(S+1)\ln\alpha}\left(\frac{1}{m} - \frac{1}{2}\right) - 1}{1 - \frac{1}{m}}$$

$$\underline{C} = \frac{-\alpha^{2}}{(1-\alpha^{2})} \cdot \frac{\left[\frac{S+\frac{1}{2}}{S+1} + \frac{1}{(S+1)\ln\alpha}\left(\frac{1}{m} - \frac{1}{2}\right)\right]}{(S+1)\left(1 - \frac{1}{m}\right)}$$

$$\underline{D} = \frac{1 - \frac{2}{m} - \frac{1}{(S+1)\ln\alpha}\left(\frac{1}{m} - \frac{1}{2}\right)}{(S+1)\ln\alpha\left(1 - \frac{1}{m}\right)}$$

$$\underline{E} = -\underline{A}$$

$$\underline{F} = \frac{\frac{1}{(S+1)\ln\alpha}\left(\frac{1}{m} - \frac{1}{2}\right) + 1}{1 - \frac{1}{m}}$$

(compare with $\underline{B}$)

$$\underline{G} = \underline{C}$$

GRAPHICAL RELATIONS

In the following computed graphs, the equations (12) and (13) are plotted as functions of δ for values of α between 1.5 and 5 and values of S from -0.1 to 5 inclusive.

In every case $m = 3.3$

The curve for $S = -0.1$ has been included since solenoids of finite length produce negative fields on the median plane at their outer surface with S values of this order.

Stresses in a finite length solenoid may be approximated by considering it to be of infinite length provided

a. actual field values occurring at inner and outer surfaces of the solenoid are used in calculating the appropriate S

b. infinite solenoid stresses (eqns. 12, 13 or graphs) are increased by a factor which takes into account the fact that finite length solenoids require higher current densities to produce a given field (and Pm) than infinite length solenoids. This factor is

$$\frac{j_1}{j_{1\infty}}$$

where j_1 is the current density at the inner radius of the finite solenoid.

and $j_{1\infty}$ is the current density which would be required were the solenoid to be lengthened to infinity and still retain the field difference between inner and outer surfaces.

Experience so far has indicated that this approximate method gives azimuthal stress values at the inner surface which are of the order of 7% greater than values calculated by more exact methods, e.g. Léon[3]. Average azimuthal stress is about 4% greater.

The accuracy of the curves are limited by the accuracy of the plotter which plots in increments of .01 in., and by linear interpolation between 51 points for each curve.

REFERENCES

1. BITTER, F.: Rev. Sci. Instruments, Part I, 7, 479; Part II, 7, 482; Part III, 8, 318; Part IV, 10, 373, 1936-39.

_____: Rev. Sci. Instruments, 33, 342, 1962.

2. CASE, J.: Strength of Materials (Edward Arnold and Company, 1940).

3. LÉON, B.: "Calculation of mechanical stress in coils of revolution used for the production of intense magnetic fields," Révue Générale de l'Eletricité, Vol. 73, No. 12 pp 632-636, 1964. UKAE translation by W. G. Stripp, 1966.

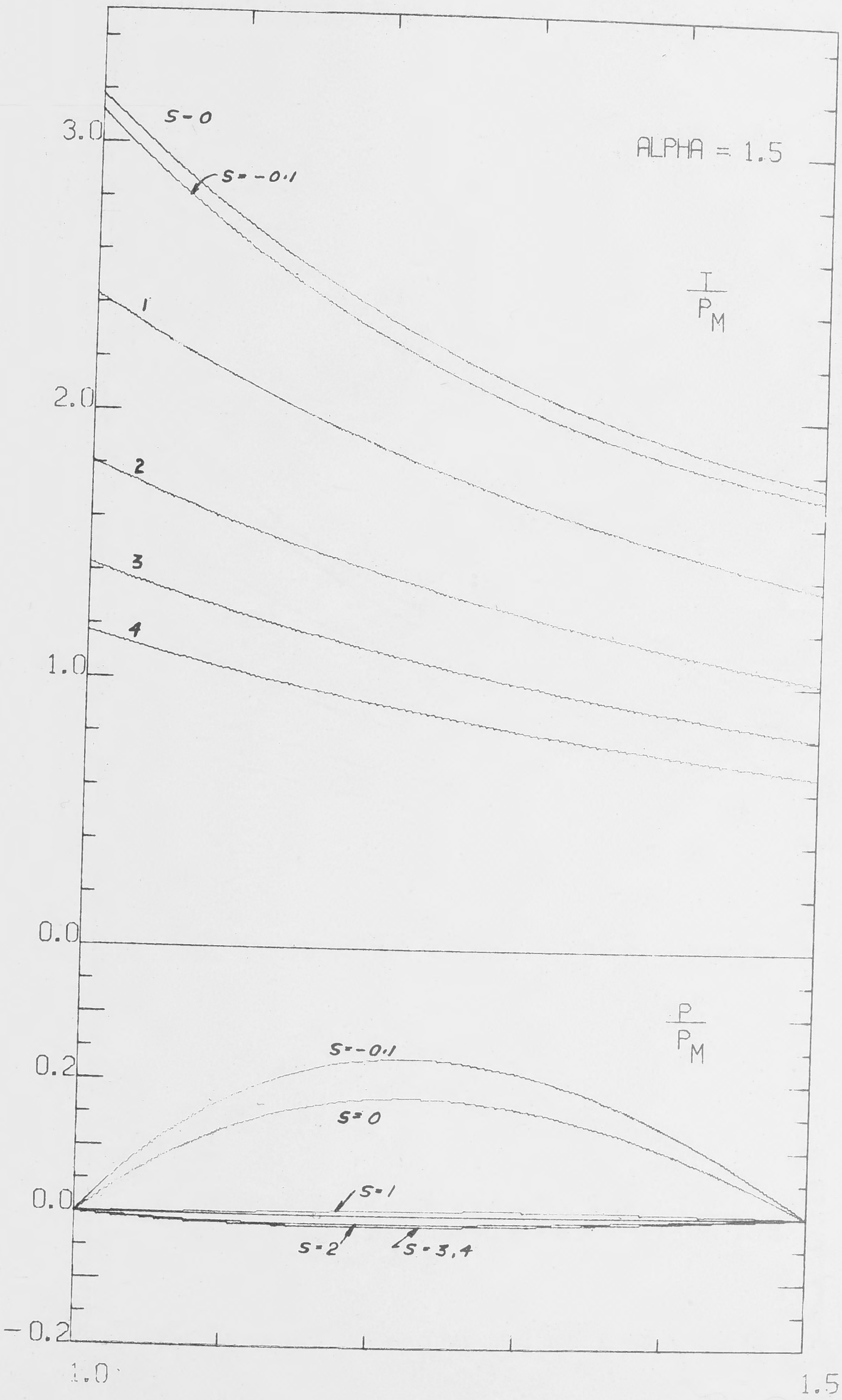
ALPHA = 1.5
I/P_M
S=0
S=-0.1
1
2
3
4
3.0
2.0
1.0
0.0
P/P_M
S=-0.1
S=0
S=1
S=2
S=3,4
0.2
0.0
-0.2
1.0
1.5
δ

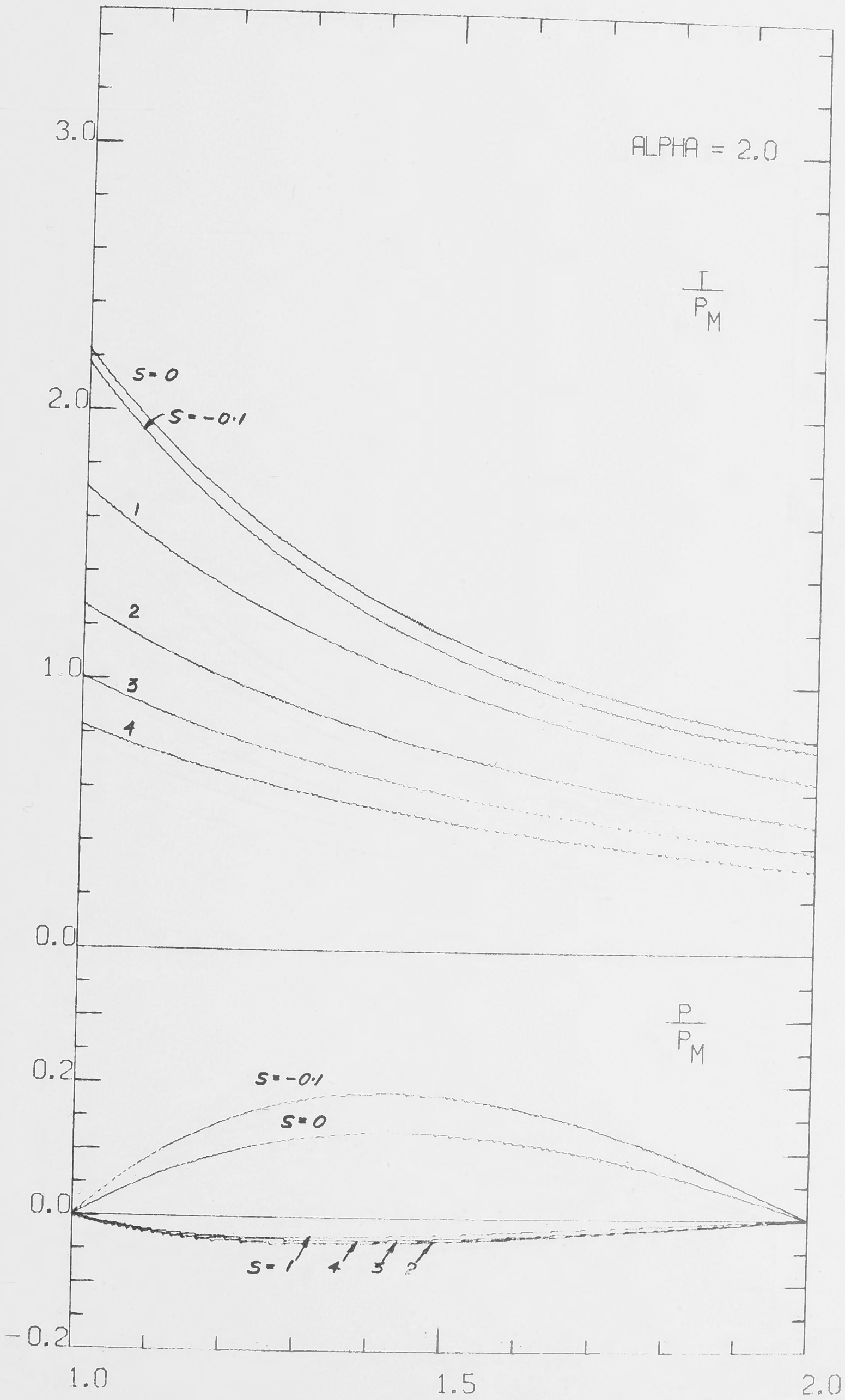
ALPHA = 2.0
I/P_M
3.0
2.0
1.0
0.0
S=0
S=-0.1
1
2
3
4
P/P_M
0.2
0.0
-0.2
S=-0.1
S=0
S=1
4
3
2
1.0
1.5
2.0
δ

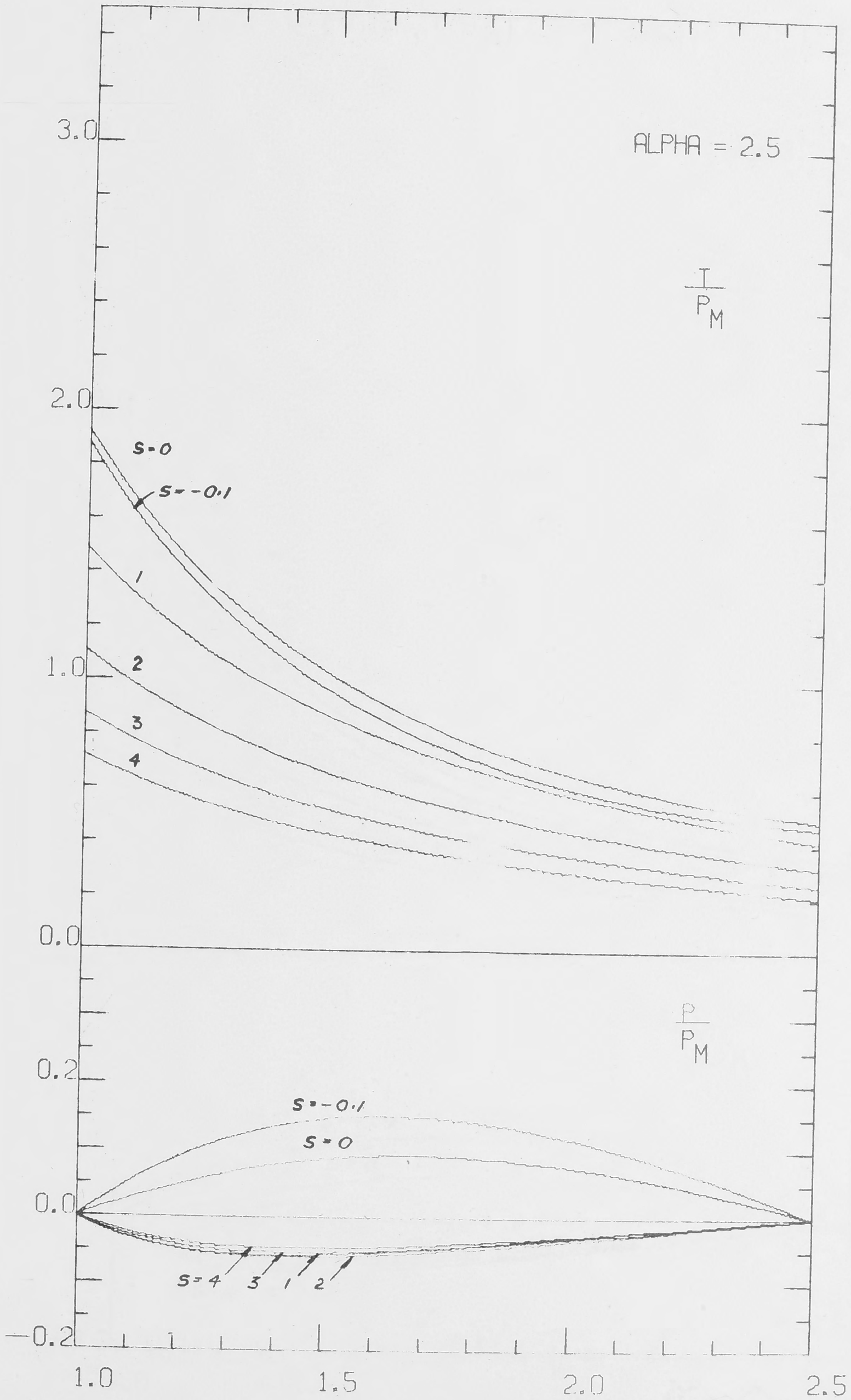
ALPHA = 2.5
I / P_M
3.0
2.0
1.0
0.0
S=0
S=-0.1
1
2
3
4
P / P_M
0.2
0.0
-0.2
S=-0.1
S=0
S=4
3
1
2
1.0
1.5
2.0
2.5
δ

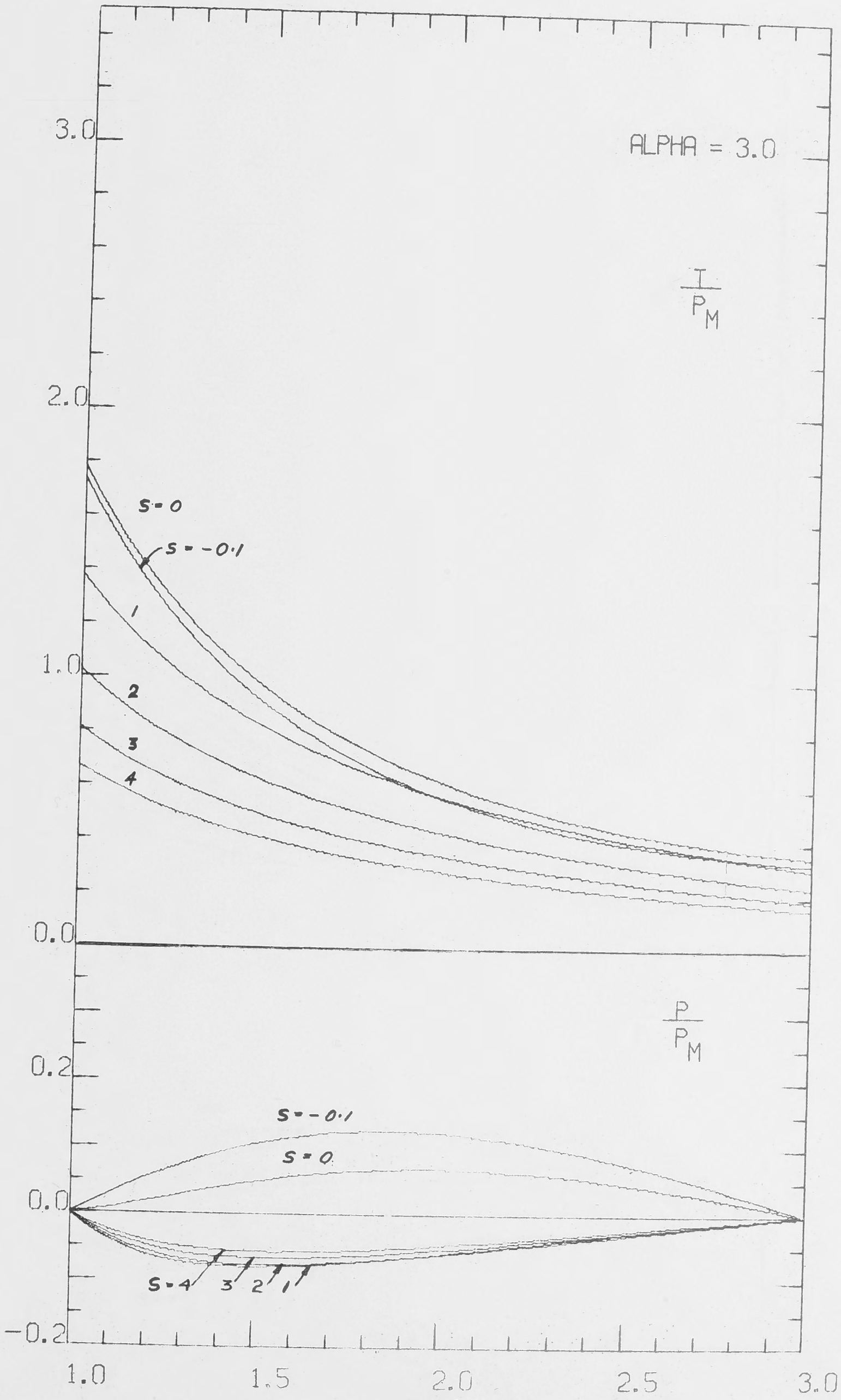
ALPHA = 3.0
I/P_M
3.0
2.0
1.0
0.0
S = 0
S = -0.1
1
2
3
4
P/P_M
0.2
0.0
-0.2
S = -0.1
S = 0
S = 4
3
2
1
1.0
1.5
2.0
2.5
3.0
δ

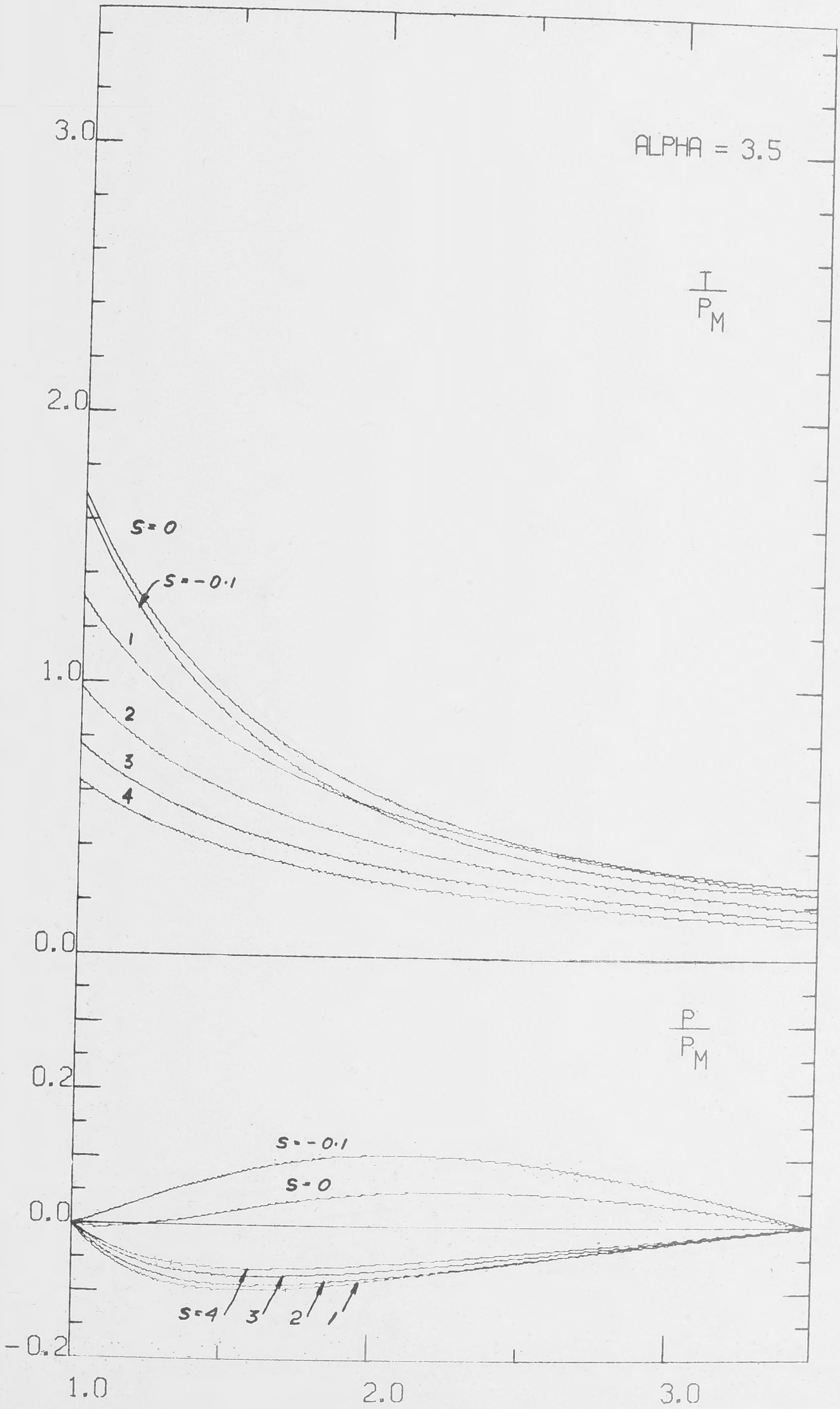
ALPHA = 3.5
I / P_M
3.0
2.0
1.0
0.0
S = 0
S = -0.1
1
2
3
4
P / P_M
0.2
0.0
-0.2
S = -0.1
S = 0
S=4
3
2
1
1.0
2.0
3.0
δ

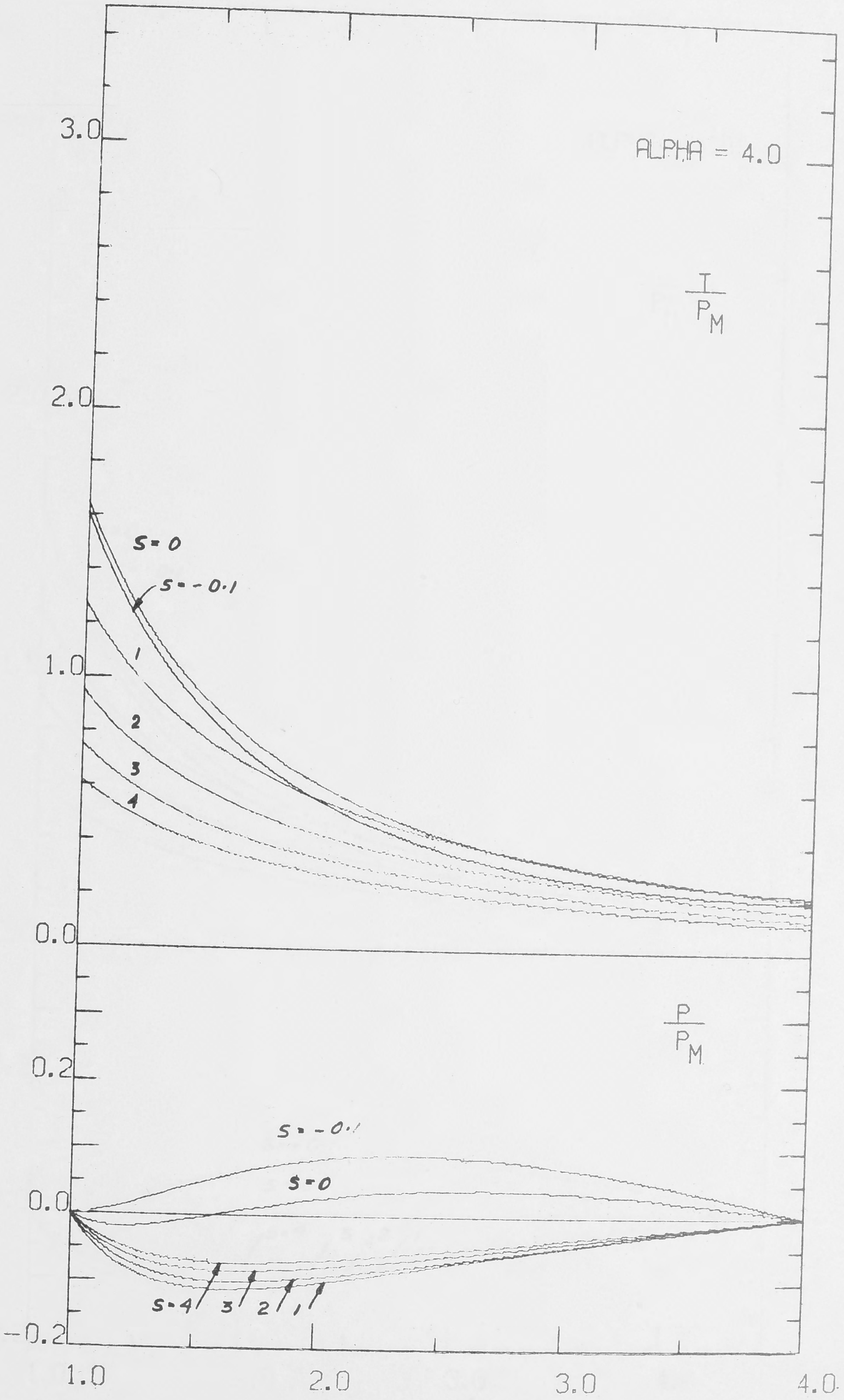
ALPHA = 4.0
I/P_M
3.0
2.0
1.0
0.0
S = 0
S = -0.1
1
2
3
4
P/P_M
0.2
0.0
-0.2
S = -0.1
S = 0
S = -4
3
2
1
1.0
2.0
3.0
4.0
δ

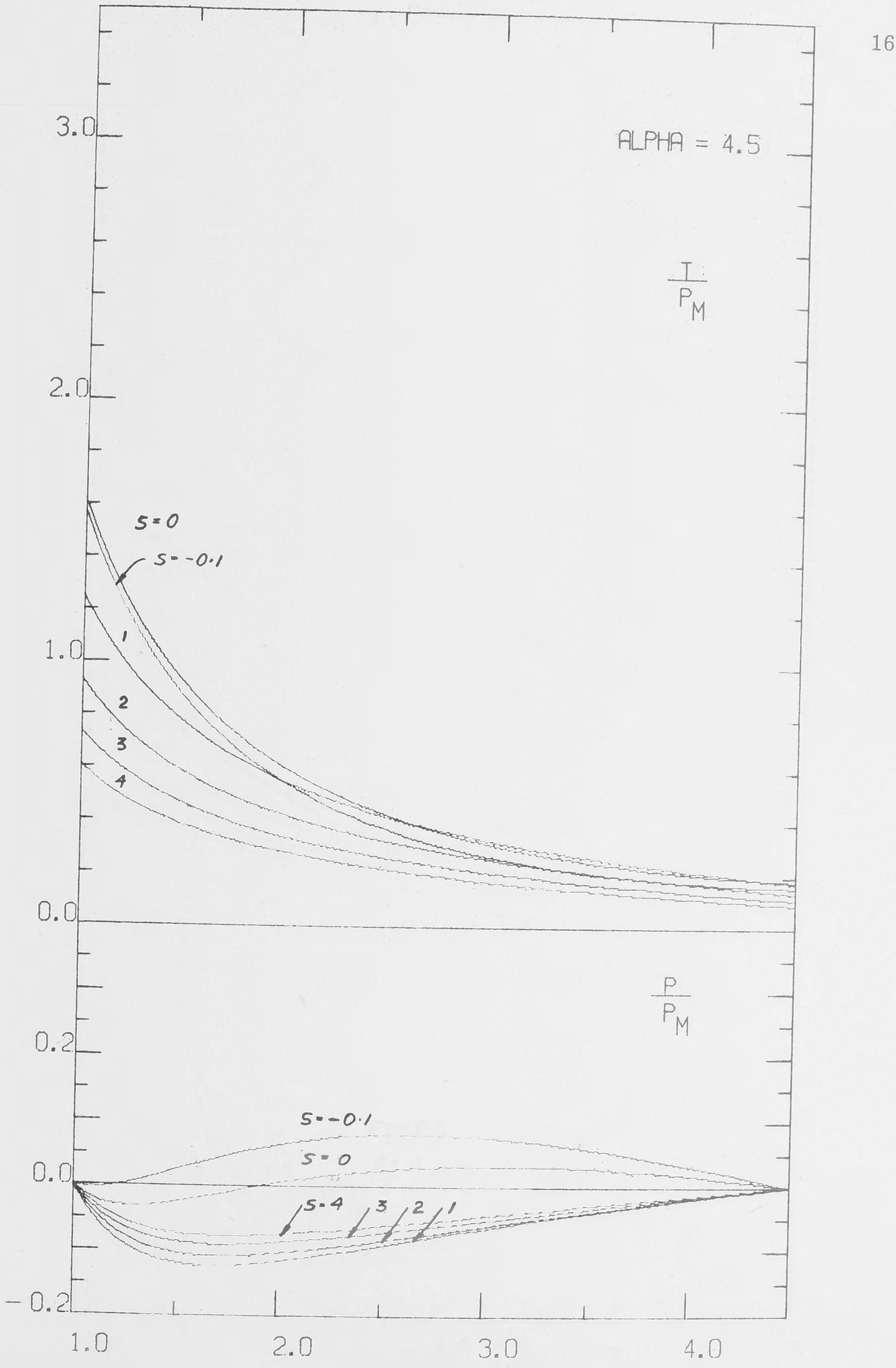
ALPHA = 4.5
I/P_M
3.0
2.0
1.0
0.0
S=0
S=-0.1
1
2
3
4
P/P_M
0.2
0.0
-0.2
S=-0.1
S=0
S=4
3
2
1
1.0
2.0
3.0
4.0
δ

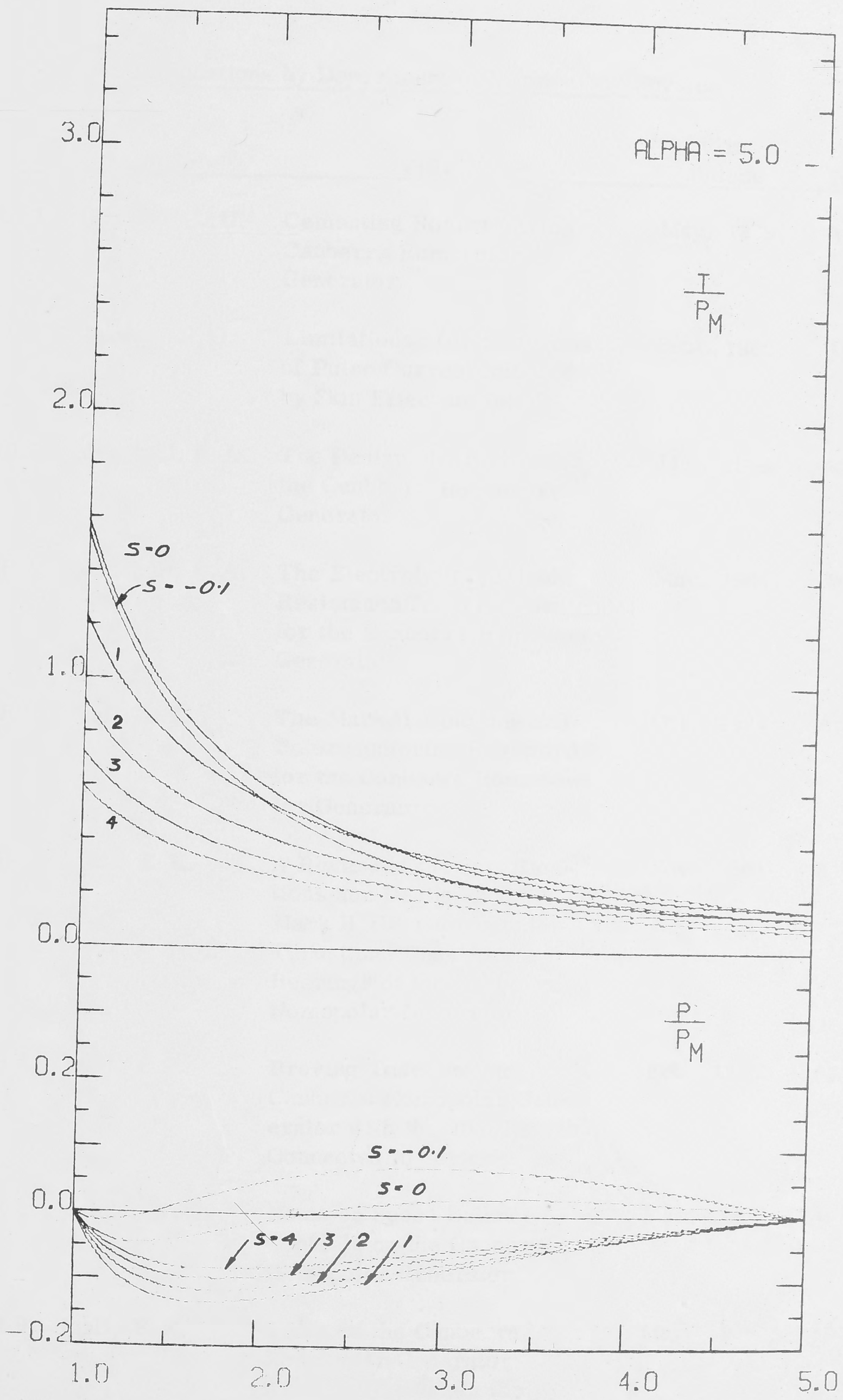
ALPHA = 5.0
I / P_M
P / P_M
S=0
S=-0.1
1
2
3
4
S=-0.1
S=0
S=4
3
2
1
3.0
2.0
1.0
0.0
0.2
0.0
-0.2
1.0
2.0
3.0
4.0
5.0
δ

Publications by Department of Engineering Physics

No.	Author	Title	First Published	Re-issued
EP-RR 1	Hibbard, L. U.	Cementing Rotors for the Canberra Homopolar Generator	May, 1959	April, 1967
EP-RR 2	Carden, P. O.	Limitations of Rate of Rise of Pulse Current Imposed by Skin Effect in Rotors	Sept., 1962	April, 1967
EP-RR 3	Marshall, R. A.	The Design of Brushes for the Canberra Homopolar Generator	Jan., 1964	April, 1967
EP-RR 4	Marshall, R. A.	The Electrolytic Variable Resistance Test Load/Switch for the Canberra Homopolar Generator	May, 1964	April, 1967
EP-RR 5	Inall, E. K.	The Mark II Coupling and Rotor Centering Registers for the Canberra Homopolar Generator	Oct., 1964	April, 1967
EP-RR 6	Inall, E. K.	A Review of the Specifications and Design of the Mark II Oil Lubricated Thrust and Centering Bearings of the Canberra Homopolar Generator	Nov., 1964	April, 1967
EP-RR 7	Inall, E. K.	Proving Tests on the Canberra Homopolar Generator with the Two Rotors Connected in Series	Feb., 1966	April, 1967
EP-RR 8	Brady, T. W.	Notes on Speed Balance Controls on the Canberra Homopolar Generator	Mar., 1966	April, 1967
EP-RR 9	Inall, E. K.	Tests on the Canberra Homopolar Generator Arranged to Supply the 5 Megawatt Magnet	May, 1966	April, 1967

No.	Author	Title	First Published	Re-issued
EP-RR 10	Brady, T.W.	A Study of the Performance of the 1000 kW Motor Generator Set Supplying the Canberra Homopolar Generator Field	June, 1966	April, 1967
EP-RR 11	Macleod, I.D.G.	Instrumentation and Control of the Canberra Homopolar Generator by On-Line Computer	Oct., 1966	April, 1967
EP-RR 12	Carden, P.O.	Mechanical Stresses in an Infinitely Long Homogeneous Bitter Solenoid with Finite External Field	Jan., 1967	
EP-RR 13	Macleod, I.D.G.	A Survey of Isolation Amplifier Circuits	Feb., 1967	
EP-RR 14	Inall, E.K.	The Mark III Coupling for the Rotors of the Canberra Homopolar Generator	Feb., 1967	
EP-RR 15	Bydder, E.L. Liley, B.S.	On the Integration of "Boltzmann-Like" Collision Integrals	Mar.,1967	
EP-RR 16	Vance, C.F.	Simple Thyristor Circuits to Pulse-Fire Ignitrons for Capacitor Discharge	Mar.,1967	
EP-RR 17	Bydder, E.L.	On the Evaluation of Elastic and Inelastic Collision Frequencies for Hydrogenic-Like Plasmas	Sept.,1967	
EP-RR 18	Stebbens, A. Ward, H.	The Design of Brushes for the Homopolar Generator at The Australian National University	Mar.,1964	Sept., 1967

Copies of this and other Publications (see list inside) of the Department of Engineering Physics may be obtained from:

The Australian National University Press,
P.O. Box 4, Canberra, A.C.T., 2600.
Australia.

Price: $A1.00

 Proc Int Conf. Magnet Tech. Hamburg 1970

(5)

THE DESIGN AND CONSTRUCTION OF A BITTER SOLENOID HAVING A 26 cm DIAMETER BORE AND GENERATING 16.5 TESLA WITH 26 M.W. OF POWER

P.O. CARDEN

Australian National University,
Department of Engineering Physics,
CANBERRA.

ABSTRACT

The Bitter solenoid described here is the outer coil of a two coil system for generating 30 Tesla.

Analysis showed that a homogeneous plane helix would be adequately strong. The Bitter principle of constructing a plane helix was chosen for practical reasons but difficulties arose due to loss of strength from the slits in the discs and the fact that circumferential strength had to be developed through friction between the discs. The problems were overcome by adopting a design where each turn was made up of 16 discs interwound in a staggered pattern which dispersed the slits and provided adequate friction bonding. The effect of the slits is small reducing the strength to 15/16ths of an ideal continuous plane helix.

It is shown that such a Bitter solenoid may fail either by expansion or by unwinding. The relevant factors involved in both modes are discussed and it is shown that unwinding is the most serious mode and cannot be remedied by increasing the number of discs per turn. A system of keying the end turns via tortion cylinders is described and illustrated.

The solenoid is in fact a two-start helix with one turn each end four-start. Reasons for these features are described associated with current distribution and ease of insulation checking.

The unusual construction technique is described and illustrated.

INTRODUCTION

About three years ago work was begun at the Australian National University on the design of a water cooled 30 Tesla experimental electromagnet which was to be used for research in solid state physics. The design evolved into basically two concentric plane helical solenoids, electrically in parallel, the outer one of which is the subject of this paper.

This solenoid has a 26 cm diameter bore into which the inner coil with a 5 cm bore may be inserted or which may be used by experimenters wanting a large volume of 16.5 Tesla. The outer solenoid will require 26 M.W. of power from the Department's homopolar generator delivered at 150 volts and 173 k.a. whereas the two coils together will require 30 MW at the same voltage and 200 k.a.

The outer solenoid, which will henceforth be called the A.N.U. solenoid, will require cooling water at the rate of 6.5 cubic feet per second at approximately 100 p.s.i. pressure. The major dimensions of this solenoid are shown in Table I.

STRESSES

Stresses have been calculated using formulae and methods derived by several authors[1, 2, 3] for the case of a bonded plane helix in which the mechanical properties of the solenoid material are homogeneous, elastic, and isotropic everywhere including the interface between turns. Although the design chosen is neither homogeneous, elastic, or isotropic, this model is nevertheless the best available that has been mathematically analysed.

The calculated azimuthal or hoop stress is shown in fig. 1. It will be seen that the maximum stress is high, this being the result of compactness which is favoured because of the economies it brings in material, power and water consumption.

Axial compressive stress results from electromagnetic forces and externally applied axial forces. The electromagnetic component is zero at the ends but builds up to as high as 12,000 p.s.i. at the median plane of the solenoid.

SIGN AND CONSTRUCTION

The construction method invented by the late Francis Bitter[4] was chosen the ANU solenoid as the most practical way of achieving a bonded plane helix he size required. This method involves making a large number of thin discs h perforated with cooling holes and each having a radial cut or slit right through. discs are interleaved in a pattern to form a helix, the holes aligning to form al cooling channels.

A solenoid constructed this way requires axial compression to provide friction which effectively bonds the discs together. The magnitude of the axial pression required depnds on the number of interleaved discs and the pattern of rleaving. In general the greater the number of discs and the greater the extent nterleaving, the less axial compression will be required.

Usually adequate axial compression resulting from electromagnetic es prevails throughout most of the solenoid except near the ends. An external ns of applying axial force is therefore necessary.

The pattern in which the discs are interleaved is best represented in a ram obtained by projecting the solenoid radially outwards upon any cylindrical face and developing the projection so formed. Vertical dimensions are exaggerfor clarity. Fig. 2(a) is such a representation of the ANU solenoid. The pattern lf is believed to be unique and the number of discs per turn-16 is, to the author's wledge, greater than anything attempted previously.

The pattern, identified henceforth as the ANU pattern, may be generalised any number of discs per turn n. Its special features are that n must be even; the slits of alternate discs appear in planes perpendicular to the axis, the planes g $\frac{n}{2}$ disc thicknesses apart; that the slits in each plane are spaced $\frac{4\pi}{n}$ radians rt; and that the slits in one plane are angularly displaced $\frac{2\pi}{n}$ radians from the s in the neighbouring planes.

The discs are made from hard rolled silver-copper (.07% Ag) of nominal kness 0.0204 inch. They arrived at the ANU workshop as full discs of approxiely the finished outside diameter. All subsequent processes were carried out in the University. Cooling holes and the central hole were punched out, the outdiameters turned and the radial slits guillotined. Some of the discs were found pen or close at the slit when placed on a flat surface due to the fact that they had inally been slightly conical or buckled. This fault was corrected by pressing the full length of selected radii using a press tool in the shape of a narrow gated triangle. Depending on the orientation of the triangle with respect to the (point directed inwards or outwards) a gap or an overlap at the slit could be rected.

Other difficulties arose because of the variation in thickness both from sc to disc and within each disc. The average thickness was found to vary between 0190" and 0.0225" , whereas, typically, the variation within discs was $\pm$ 0.00035". he former variation necessitated sorting (by weight) into sixteen groups. Members each group butted together in the solenoid thus preventing steps and voids which uld otherwise occur if discs of unequal thickness were butted.

The latter variation-within discos was unfortunately systematic which, uncorrected, would have caused a hump in the middle of the solenoid greater than e 1/8 inch each end which could be tolerated. It was corrected by grinding the ddle of each eighth disc of the solenoid.

Insulation consists of 0.003 inch "Pyre ML" bonded glass fabric supplied Dupont Corp. The original plan was to divide the solenoid into four starts, ad- ent starts being separated by one layer of fabric, but it was soon found that, spite precautions in cleanliness, occasional metal particles had become lodged ween the glass threads of the open weave. Some of these were discovered to be ide globules of resin and became evident as a short circuit only after pressure s applied. This difficulty was overcome by inspecting every sheet on a metal le using a weighted roller electrically connected to the table through a circuit ch registered continuity. Once a short circuit was discovered a bearing could drawn along the line-of-contact of the roller and the fabric. The intersection of such bearings located the metal particle which was then isolated and removed ng a microscope and another electrically connected needle-like probe. In addition his inspection, the design was altered to two starts with double insulation for most he solenoid.

Assembly was performed on a special table fitted with various aids. method was to slide each disc in turn into place usually under some discs already embled. To perform this operation accurately and without disturbing discs already embled, it was necessary to clear a passage for the next disc by inserting small ms which supported the assembled discs above the passage. A routine for moving se supports appropriately for each new disc was soon worked out. Fig. 3 shows solenoid part way through the assembly and Fig. 4 shows the completed solenoid.

The main disadvantage of the design is the large number of individual s which have to be made and handled, and the fact that, with techniques developed ar, assembly must proceed one disc at a time.

The advantage of strength however is outstanding as will become apparent e next section.

DES OF FAILURE

As far as the author is aware, there are three possible modes of failure e ANU solenoid. These have been named here unwinding, expansion and tensile they will now be discussed in turn.

inding . The unwinding mode of failure may be defined as failure along a helical path . Unwinding results in radial growth and twisting about the axis of the noid. In Appendix I helical fault paths involving friction bond failure are analysed. shown that the relation between azimuthal stress f_θ , axial compressive stress

nd coefficient of friction μ, for a helix angle ϕ is :

$$\frac{p_z}{f_\theta} = \frac{\phi}{\mu - \phi}$$

The most obvious unwinding fault path is the plane helical interface een turns. Making appropriate substitutions for the ANU solenoid viz.

f_θ = 40,000 p.s.i.

μ = 0.2 at inner radius

ϕ = 0.01 radians

found that p_z must be of the order of 2,000 p.s.i. In fact even higher values are indicated because the interface between turns is not apparently the fault with the steepest helix angle. Fig. 5(a) illustrates what is believed to be the est unwinding fault path for the ANU pattern. It requires approximately $\frac{n+2}{n}$ s greater p_z than that calculated above.

To provide such high values of p_z for the critical end turns would be impracticable requiring immense compression mechanisms and super structure.

The problem was overcome by attaching radial key bars to the discs at end of the solenoid which keyed into appropriate slots in two stainless steel s. These discs were welded to two locked cylinders which encased the solenoid. discs and cylinders, forming what are known as tortion jackets, resist twisting therefore are effective in preventing failure by unwinding.

These tortion jackets are shown in fig. 4.

The remaining possible modes of failure are ones having axially orient- fault paths. These are the expansion and tensile modes of failure.

nsion. Failure by expansion is characterised by growth in a generally radial ction without twisting about the solenoid axis. It results from failure of the ion bond between interleaved discs resulting in slipping as illustrated in fig. 5(b) he ANU pattern. As explained in Appendix I, where end constraints are oyed to prevent unwinding, the expansion mode of failure may be treated without rd to unwinding or the moments generated by the end constraints. The tensile ngth of interleaved discs is proportional to the area of the slip planes along the surface and therefore the path of the fault surface will be the path of minimum h which has no nett angular displacement (if the fault surface has nett angular acement, the failure is a form of unwinding which is prevented by the key-bars).

By inspection, the minimum possible path length per turn for the ANU rn is found to be $\frac{(n^2 - 4)\pi}{n}$ radians where, as before, n is the number of discs urn. It follows that if: p_y is the compressive stress perpendicular to the slip s at radius r, f_x the tensile stress at radius r parallel to the slip planes when e by expansion is about to occur, μ the coefficient of friction, t the turn thickness,

$$\frac{p_y}{f_x} = \frac{n\,t}{(n^2 - 4)\ \pi\, r\, \mu} \qquad (1)$$

The only pattern known to have a lower ratio than this is the 180^o alternate overlap pattern shown in fig. 6 where the ratio is

$$\frac{p_y}{f_x} = \frac{t}{n\,\pi\, r\, \mu}$$

However, as will be shown, there are serious weaknesses with this pattern and in any case, for high n, the two ratios approach one another.

The appropriate substitutions in (1) for the ANU solenoid are :

n	=	16
t	=	0.34 inch
r	=	5.25 inch (inner radius)
μ	=	.2
f_x	=	40,000 p.s.i.

hence p_y 260 p.s.i.

An axial compression of 500 p.s.i. has been provided in this region ithout an excessive structure thus allowing a margin of safety of almost 2.

ensile failure. The pattern shown in fig. 6 has the slits grouped in two columns. will be obvious that in this case the strength of the solenoid cannot exceed half of hat it would be if it were homogeneous. Most known patterns suffer in this way, 0% or 25% reduction being quite common. On the other hand in fig. 2(a), the slits re dispersed to the extent that no two slits are closer than 15 disc thicknesses i.e. e reduction in strength is only 1/16 or 6%. The wide dispersion of the slits is ore apparent in the full scale developed view of the bore of the solenoid - fig. 2(b).

HE END TREATMENT

One more feature of the ANU solenoid is worthy of note, viz. the end eatment. Stresses are normally calculated in a plane helical solenoid on the esupposition that current density is a function of radius only. It follows that any ane cutting the solenoid and perpendicular to its axis is not an equipotential surface e to the insulation between turns and the fact that current passes obliquely through e plane at the helix angle. In fact, following around any circle in the cutting plane e would find a uniform potential gradient everywhere except at the cut insulation e where there would be a compensating potential discontinuity equal to the turn--turn voltage.

If these conditions are not reproduced at the end of the solenoid, which e essentially planes perpendicular to the solenoid axis also, then one cannot

ct the end stresses to be similar in nature to those in the body of the solenoid.

In most previous solenoids known to the author, the ends are simply in contact with an equipotential electrode. Fig. 7 illustrates what must happen s is done with a simple one "start" helix. Symmetry is destroyed in the end rodes and current enters the solenoid along a narrow radial zone. What is ly more important, symmetry is destroyed in the end turn also, resulting in shear stresses instead of hoop stresses.

If the hoop force per turn is H i.e.

$$H = \int f_\theta \, d A$$

e f_θ is hoop stress , and the integral is taken over the area of the radial section e turn, then it is easily shown that the unbalanced force on the end turn is H.

The difficulty was alleviated for our solenoid by giving it four "starts" ch end for about 1 turn. This provided four entry and four exit points of almost current, and the degree of balancing which resulted was found to be satisfactory. from the ends the number of starts was reduced to two, the insulation between being doubled. By maintaining two starts we were able to check on the insulation g assembly.

For the inner coil of our 30 Tesla magnet a different end treatment is Here, twelve entry zones are formed equally spread around each end of the e start coil. Each zone is fed from a resistor of such a value as to ensure that passes one twelfth of the total current.

CLUSION

The unwinding failure mode is one to watch when designing high perform- Bitter solenoids. End constraints which will resist axial twisting appear to be ctical alternative to providing large axial compression otherwise necessary to op the friction bond strength required at the end turns.

It would appear that there might be some advantage in raising voltage he number of turns wherever possible thus reducing current and the helix angle is must be weighed against the increased number of discs required.

The unexpectedly high axial compression that would be necessary to nt unwinding in the ANU solenoid makes the author suspect that some existing r solenoids whose end compression appears to be rather emperically derived here end turn displacement has been reported, may be suffering from a type of re by unwinding.

APPENDIX I

Homogeneity

The analysis in this appendix requires a firm concept of homogeneity which may be defined as follows. If a structure can be divided into cells of equal magnitude such that all cells are identical in the number, size and magnitude of any anomalies they may contain, then the structure is homogeneous down to the scale of the cell size. This means that stress analysis carried out on the basis of a homogeneous model will give the averages of the actual stresses in the cells. To obtain the finer structure of the stress distribution a study of the effect of the anomalies within the cells must be made. This will result in a "fine structure" stress distribution which may be superimposed upon the previous "homogeneous" stress to obtain the actual stress, and which by itself averages to zero throughout a cell.

In the light of this concept a plane helical solenoid is now analysed. For the ANU solenoid cell size should be of the order of magnitude of the distance between slits in the θ direction, the helix pitch in the z direction and probably the entire width in the r direction.

We consider first the electromagnetic forces acting on the solenoid viz. the radially acting $j_\theta \times B_z$ and the axially acting $j_\theta \times B_r$ body forces. These forces result in principle stresses f_θ, and p_z (f tensile, p compressive).

Secondly we consider twisting moments applied to the end faces of the solenoid which result in shear stress s_o in planes at right angles to the solenoid axis and in orthogonal planes containing the solenoid axis).

These stresses are shown in fig. 8. They may be combined using Mohr's relationships which require for their validity only that the material be homogeneous. The same relationships may be used to derive the stresses related to planes inclined in any direction, in particular the interfaces between the discs. These stresses, also shown in fig. 8, are s_y the shear stress along the plane, p_y the compressive stress across the plane, and f_x the tensile stress in the direction of the plane (i.e. in the direction of the helix).

The components of f_x, p_y and s_y derived respectively from the principle stresses f_θ and p_z and the applied shear stress s_o are shown in the following table where ϕ is the helix angle.

Principal or applied stress	f_x	p_y	s_y
f_θ	$f_\theta \cos^2 \phi$	$- f_\theta \sin^2 \phi$	$f_\theta \sin \phi \cos \phi$
p_z	$- p_z \sin^2 \phi$	$p_z \cos^2 \phi$	$p_z \sin \phi \cos \phi$
s_o	$s_o \sin 2\phi$	$s_o \sin 2\phi$	$- s_o \cos 2\phi$

Hence, making approximations for small angles

$$p_y = 2\phi\, s_o + p_z \qquad \text{(neglecting terms in } \phi^2\text{)} \qquad (1)$$

$$s_y = \phi\, f_\theta + \phi\, p_z - s_o \qquad (2)$$

$$f_x = f_\theta + 2\phi\, s_o \qquad (3)$$

So far we have explored the average stresses in the cells previously efined. We may now examine the effects of anomalies within the cells.

The stresses whose average is f_x are subject to gross redistribution ithin the cell because of the presence of the slits. This redistribution involves ear stress components in the friction bond of magnitude $k f_x$ where k is a factor hich depends on the geometry of disc interleaving. These stresses are part of e fine structure previously referred to and are illustrated in Fig. 9 where, it ill be seen, they alternate in sign (the sign convention is also shown in Fig. 9).

k is defined by assuming that the strength of the turns of the solenoid the direction of f_x is solely dependent upon the interleaving geometry and the rmal force p_y. It is governed by the friction relation

$$k f_x = \mu p_y \qquad (4)$$

and implies that $s_y = 0$

hus

$$k = \frac{\text{turn thickness}}{\text{minimum expansion mode slip path length}}$$

$$= \frac{n t}{(n^2 - 4)\pi r}$$

for the ANU solenoid

It remains to be seen what effect the inclusion of s_y has on the estim- tion of turn strength.

Contrary to what has been said about f_x, the average shear stress s_y, efined by equation (2), is not affected significantly by the slits and is uniform in ign throughout the cell although, it must be noted, this sign may be positive or egative. The addition of the s_y and $k f_x$ components results in the formation of wo possible types of continuous high stress paths depending on the sign of s_y. hese are illustrated in figs. 10(a) (s_y positive) and 10(b)(s_y negative). Failure long the former type of path results in strains which lengthen the circumference of e solenoid and is therefore referred to here as failure by "unwinding". For the atter type, strains shorten the circumference and the failure is said to be by winding". An alternative set of definitions can be made in terms of the twisting train experienced by the solenoid. For a right hand helix, unwinding results in the lockwise rotation of the near end relative to the far end, while the opposite rotation ccurs with winding. Both of these types of failure cause widening of the slits.

For the special case $s_y = 0$, both types of failure may occur simul- aneously resulting in the widening of the slits but not necessarily resulting in any et twisting strain. This is the "expansion" mode of failure referred to in the paper.

quation for unwinding failure

The necessary condition resulting from failure of the friction bond is $y + k f_x = \mu p_y$. Substitution of equations 1, 2 and 3 give

$$s_o\left[\frac{1}{\phi + k} + \frac{2\phi}{\phi + k}(\mu - k)\right] + p_z\left[\frac{\mu}{\phi + k} - \frac{\phi}{\phi + k}\right] = f_\theta \qquad (5)$$

For relative small k and $s_o = 0$, (5) simplifies to

$$\frac{p_z}{f_\theta} = \frac{\phi}{\mu - \phi} \tag{6}$$

which is a simple criterion for determining maximum unwinding strength in the absence of end face anchoring.

Equation for expansion failure

Failure by winding depends on the strength of the friction bond in the opposite direction to unwinding, the necessary condition being

$$-s_y + k f_x = \mu p_y$$

Substitution as before results in

$$s_o \left[\frac{1}{\phi - k} - \frac{2\phi}{\phi - k} (\mu - k) \right] - p_z \left[\frac{\mu}{\phi - k} + \frac{\phi}{\phi - k} \right] = f_\theta \tag{7}$$

(5) and (7) may be thought of as defining the safe limits of s_o as a function of f_θ (taking p_z as constant). Fig. 11 shows both equations plotted in this way.

Combinations of s_o and f_θ lying in the shaded regions will lead to failure either by winding or unwinding. The intersection of the two bounding curves (if it occurs) will correspond, as explained, to $s_y = 0$ and failure by expansion. The strength of the solenoid with regard to the expansion mode is therefore determined from $s_y = 0$ and $k f_x = p_y$ which are the simple assumptions made when defining k (equations 4).

Reference

W. Prager. Introduction to Mechanics of Continua - Ginn and Co., Boston, 1961, pp. 50 - 55.

ERENCES

Léon B 1964 Revue Gen. Elect. 12 632-6 (English translation 1966 A.E.R.E. Trans. 1056)

uznetsov A A 1961 Z. tekh. fiz. 31 944-7 (English translation 1962 Soviet Phys: Tech. Physics. 6 687-90

arden P O Journal of Scientific Instruments (Journal of Physics E) 1968 Series 2 Volume 1

itter F 1936-39 Rev. Sci. Instrum. 7 479

Bitter F 1937 Rev. Sci. Instrum. 7 482

Bitter F 1938 Rev. Sci. Instrum. 8 318

Bitter F 1939 Rev. Sci. Instrum. 10 373

Bitter F 1962 Rev. Sci. Instrum. 33 342

TABLE 1

Outside diameter	26.8 inch
Inside diameter	10.5 inch
Length	16.25 inch
Number of turns	48.2
Pitch	0.338 inch

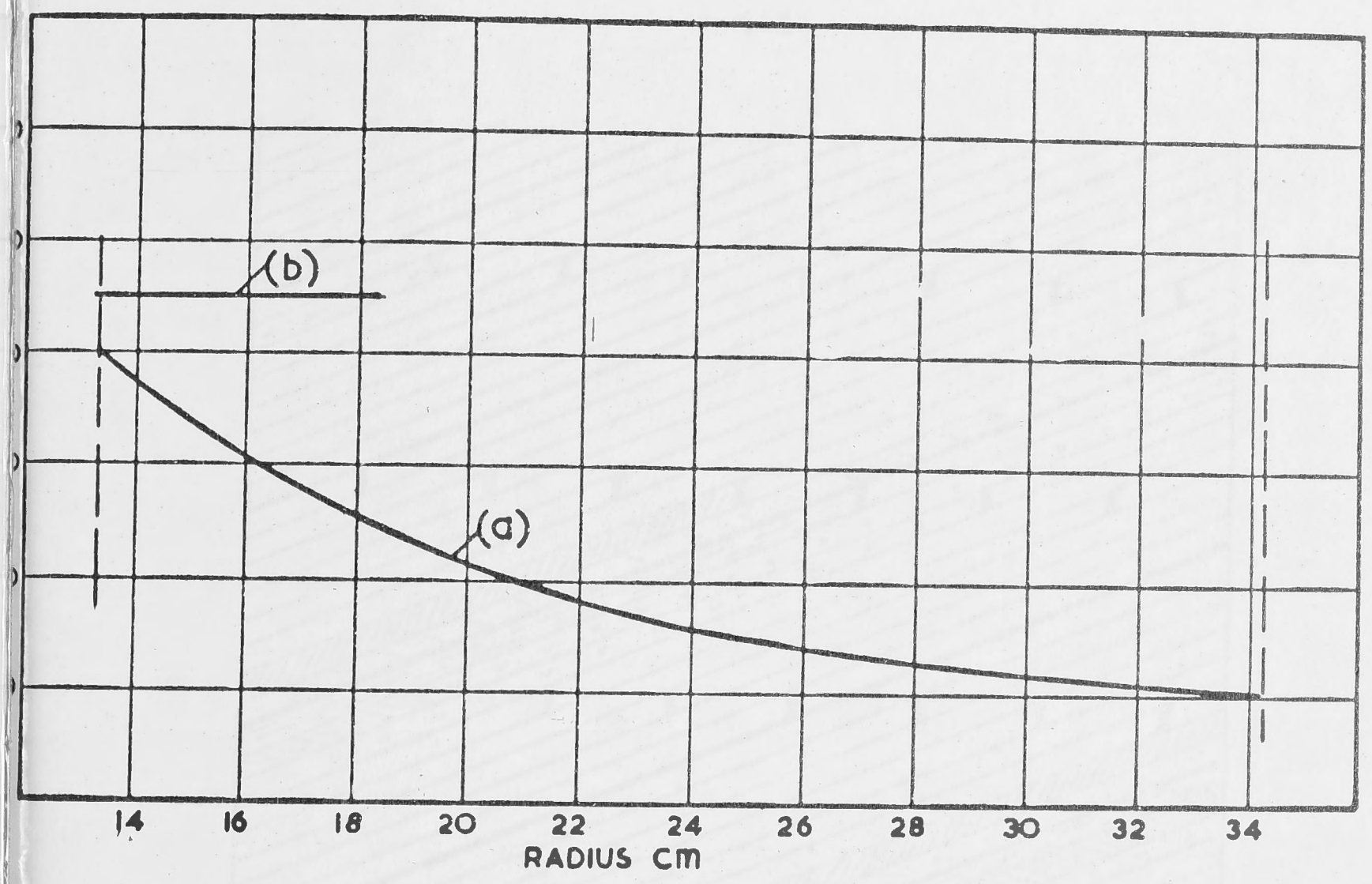

Figure 1. Stresses in outer coil. Material is .07% Ag-Cu hard temper.
(a) expected azimuthal stress.
(b) expected 0.1% proof stress.

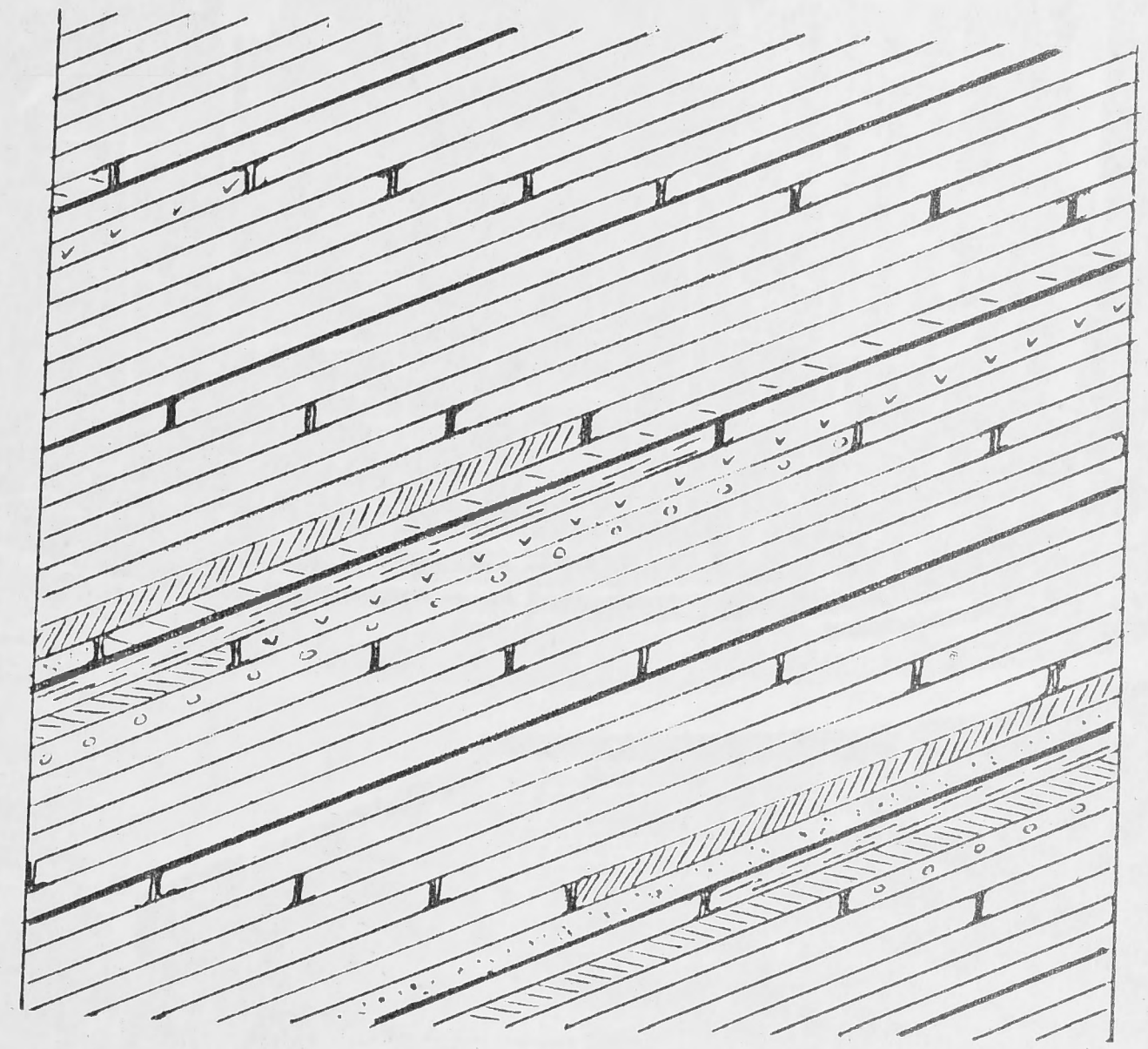

Fig. 2(a)

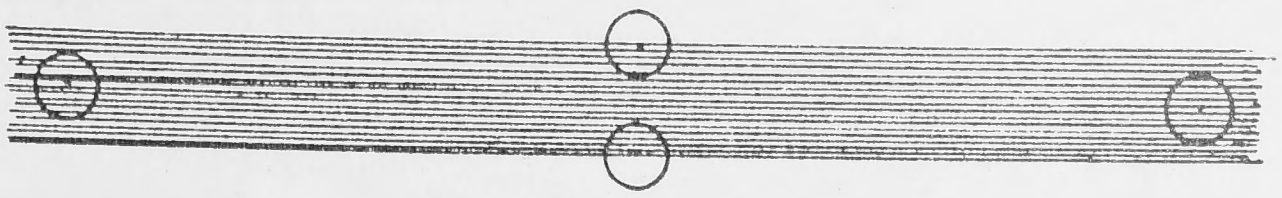

Slits encircled

Fig. 2(b)

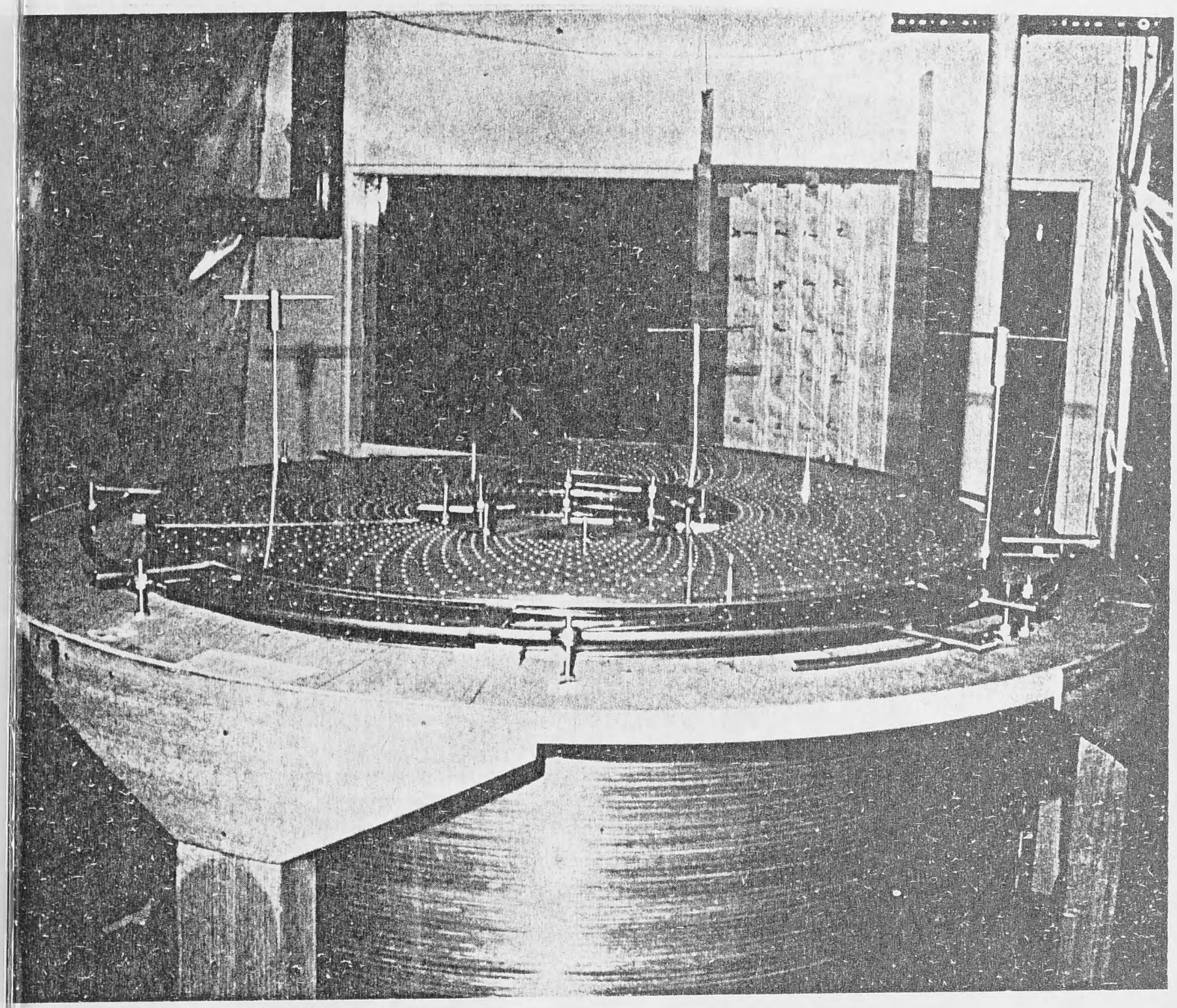

3 The ANU solenoid during assembly showing small beams supporting some discs to allow entry of the next, and three rods (with handles) in cooling holes to aid location. Three other locating rods are inserted from the bottom of the solenoid and are shown protruding. The circular platform surrounding the solenoid and one in the centre are vertically adjustable.

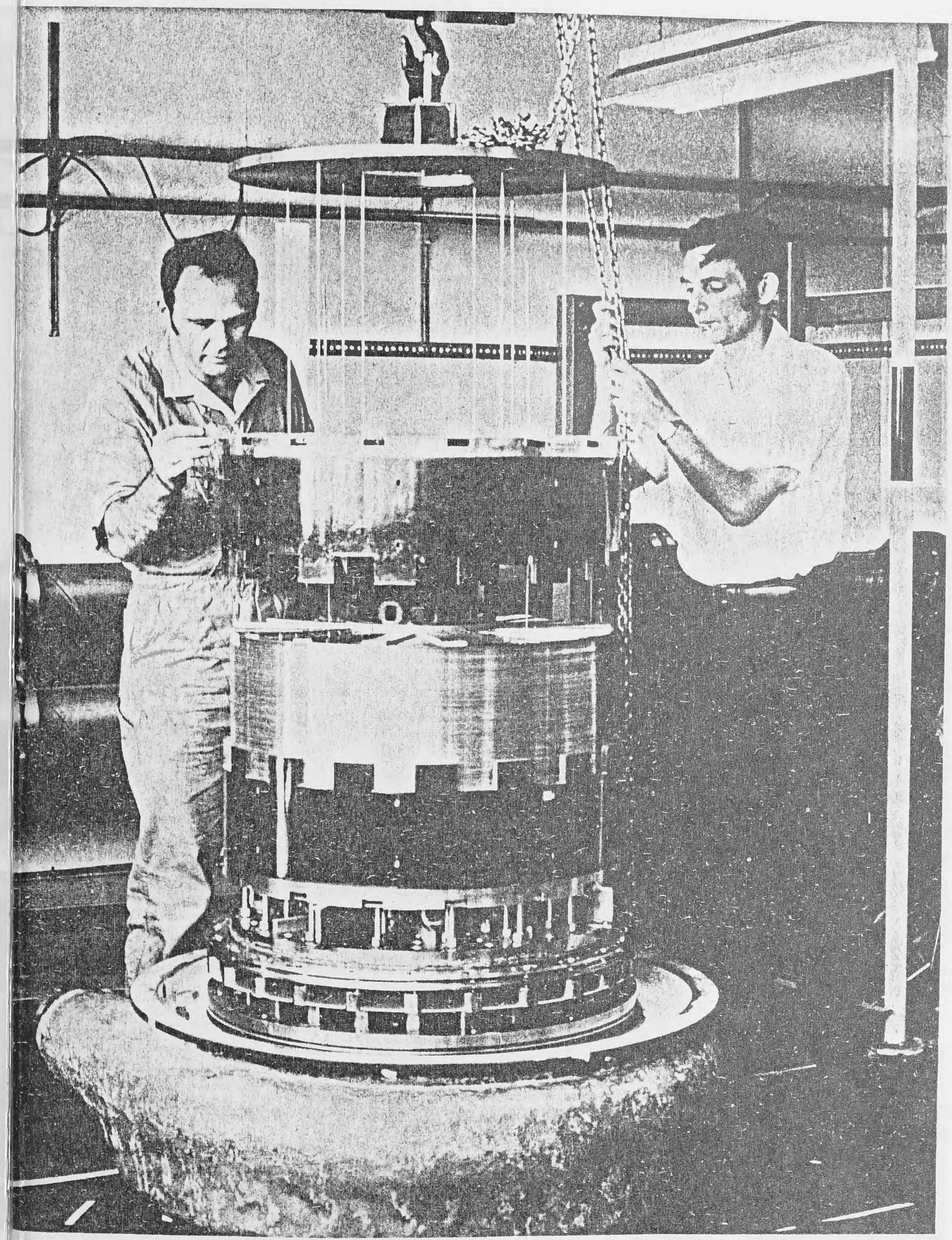

The solenoid in position in one tortion jacket while the other is being lowered. Key bars on top of the solenoid are visible.

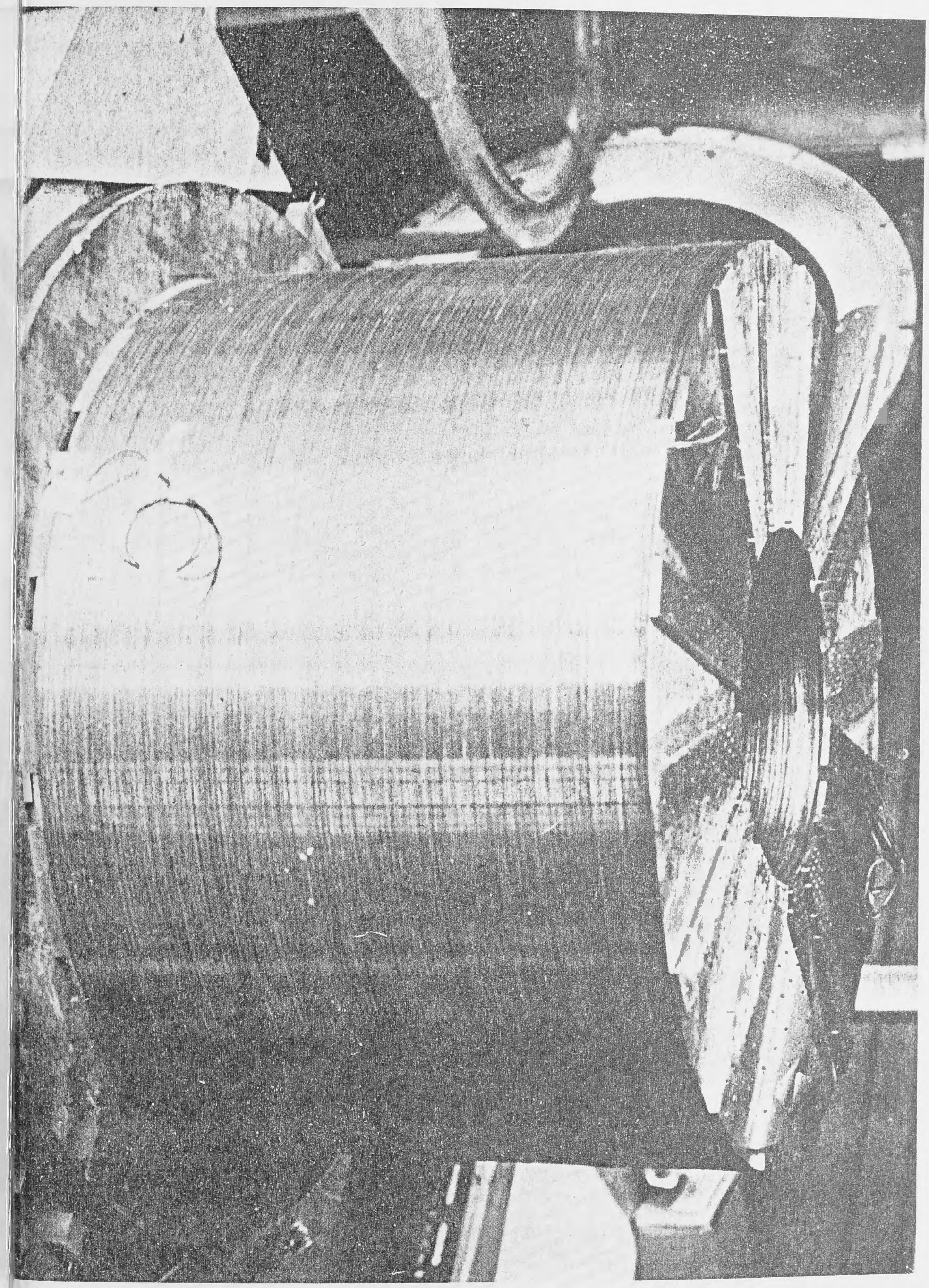

The outer coil.

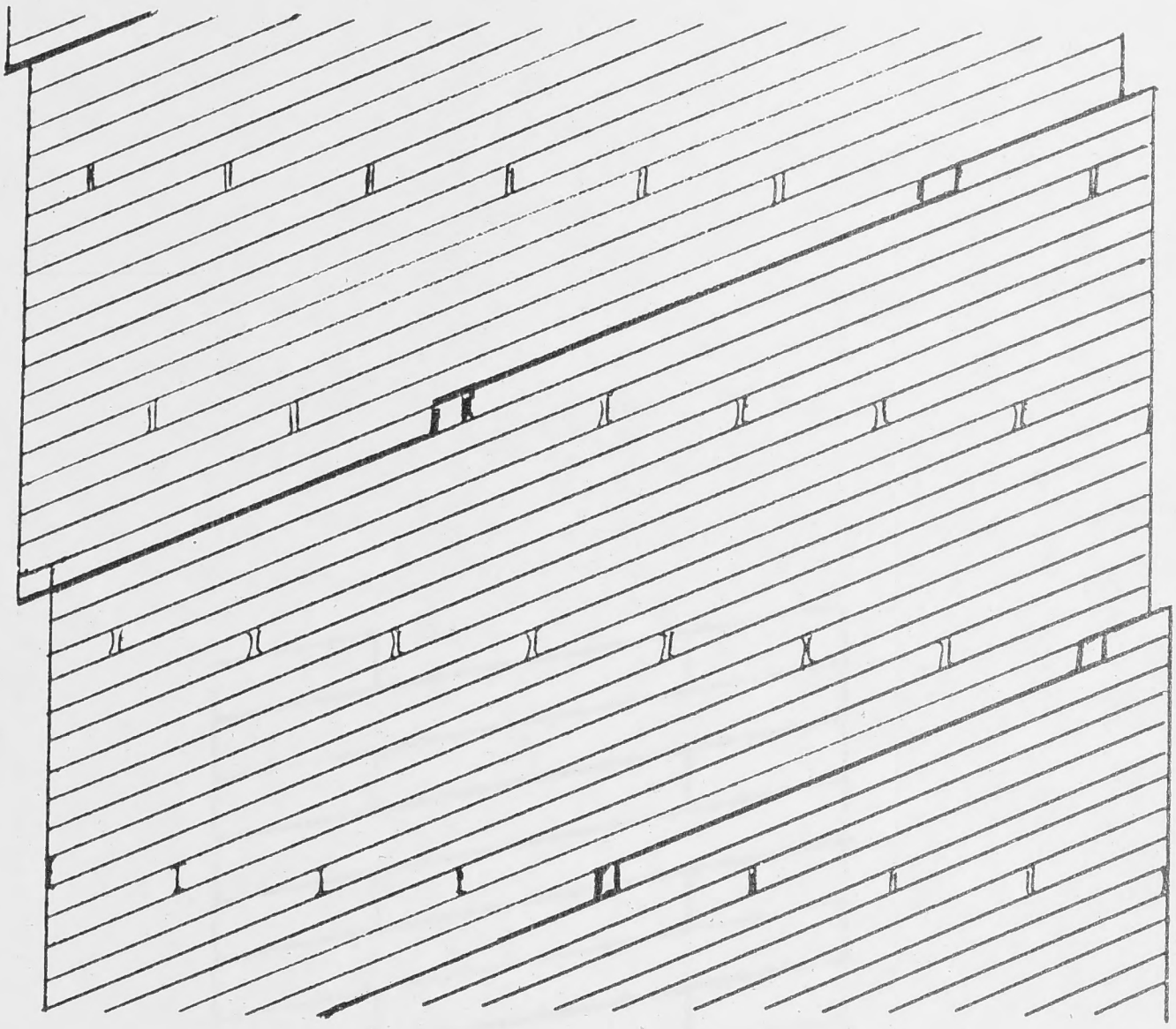

Fig.5(a)

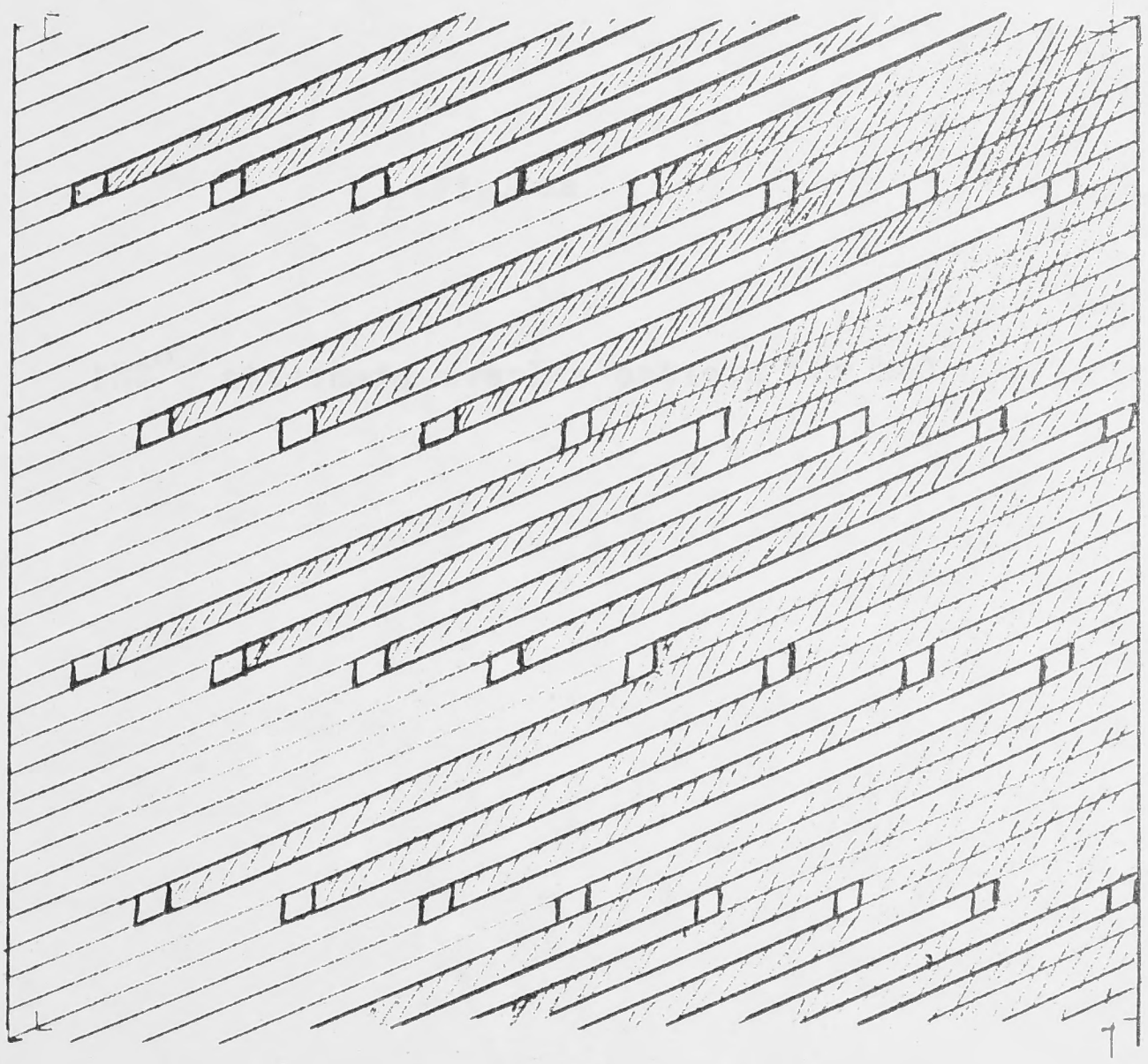

Fig. 5(b)

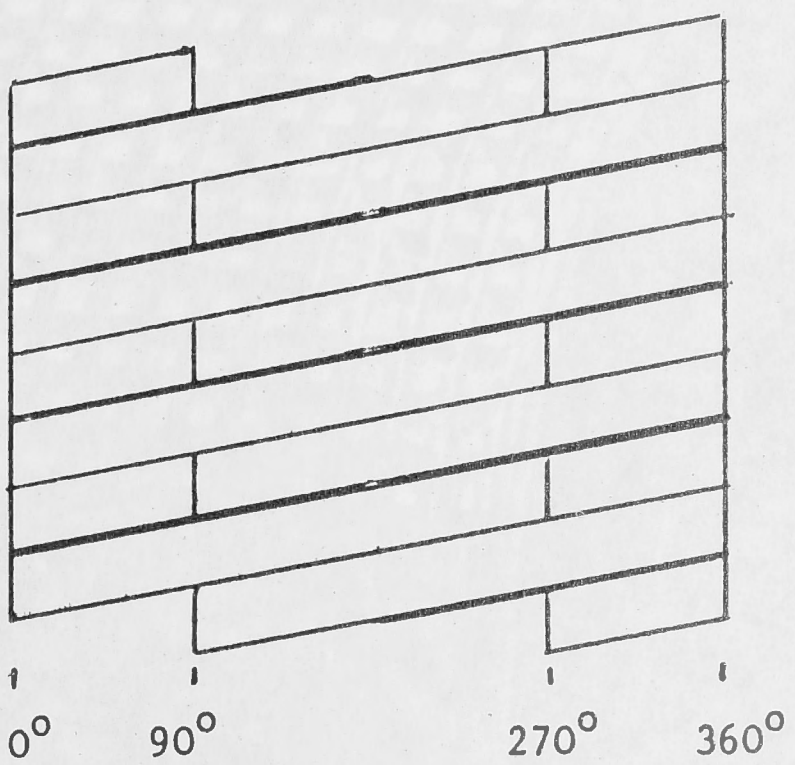

Fig. 6a

180° alternate overlap pattern for n=2

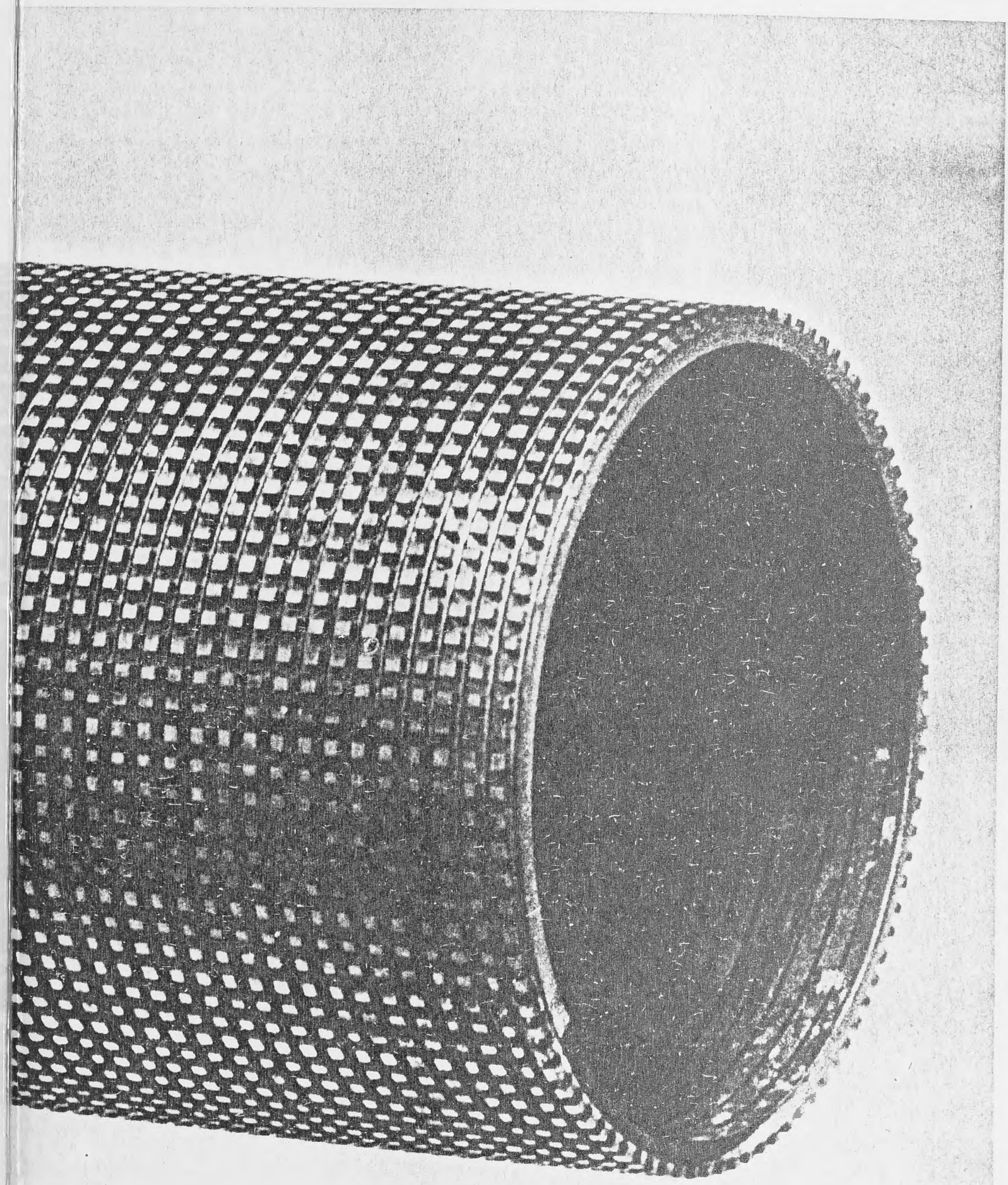

The innermost nesting sub-coil of the inner coil. Inside diameter 2.22 inches.

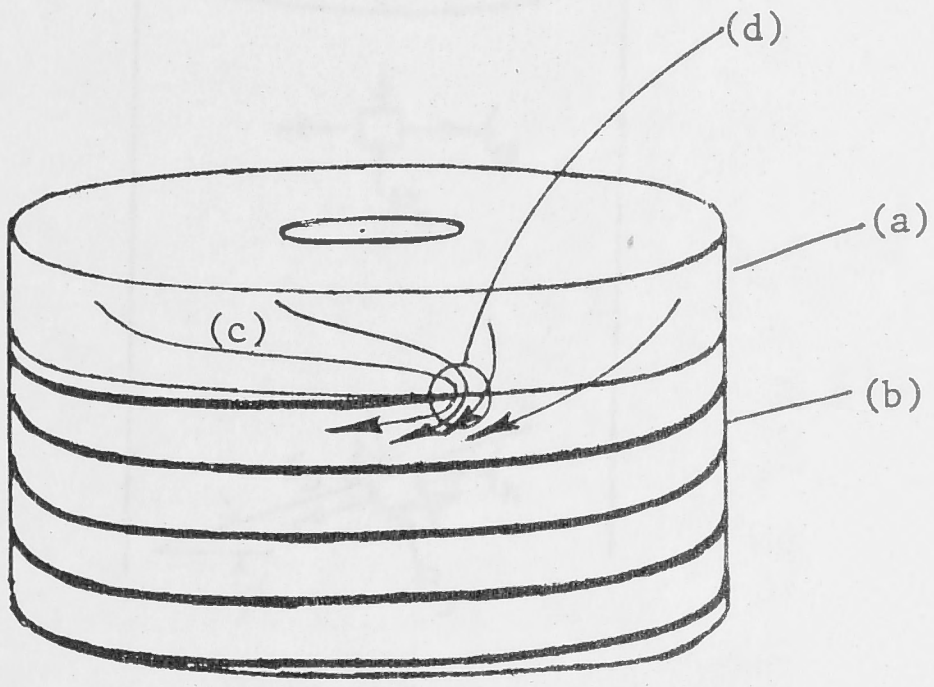

Fig. 7

(a) Equipotential electrode
(b) Plane helical solenoid
(c) Arrows showing current path
(d) Current concentration and hot spot

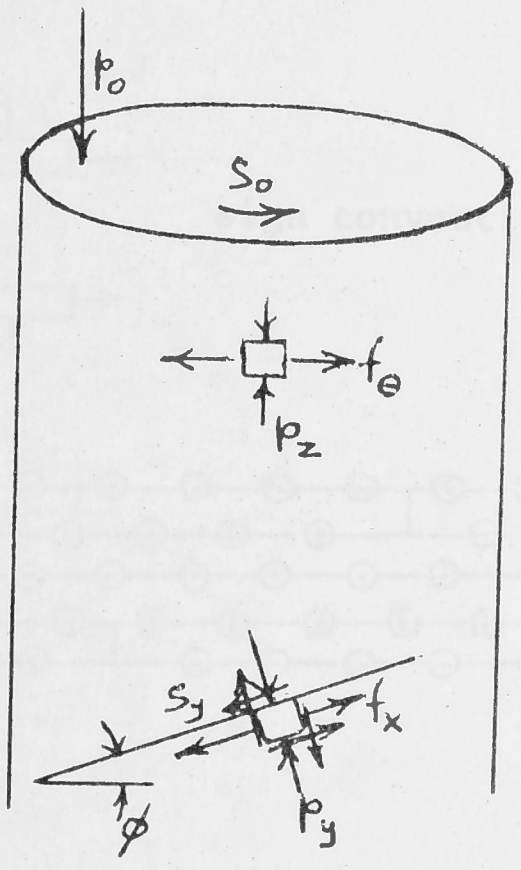

Fig. 8

sign convention

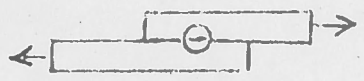

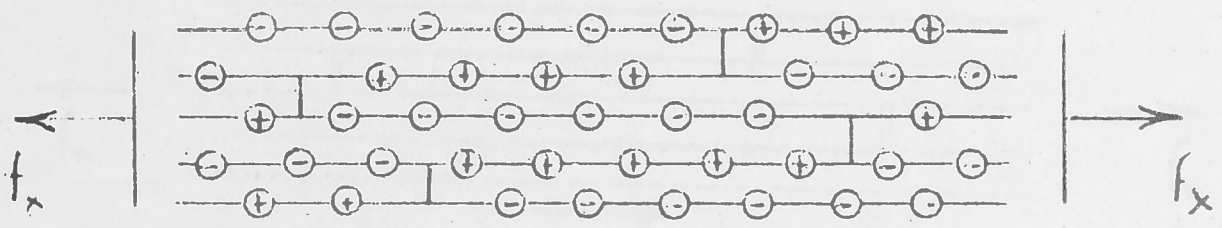

Fig. 9

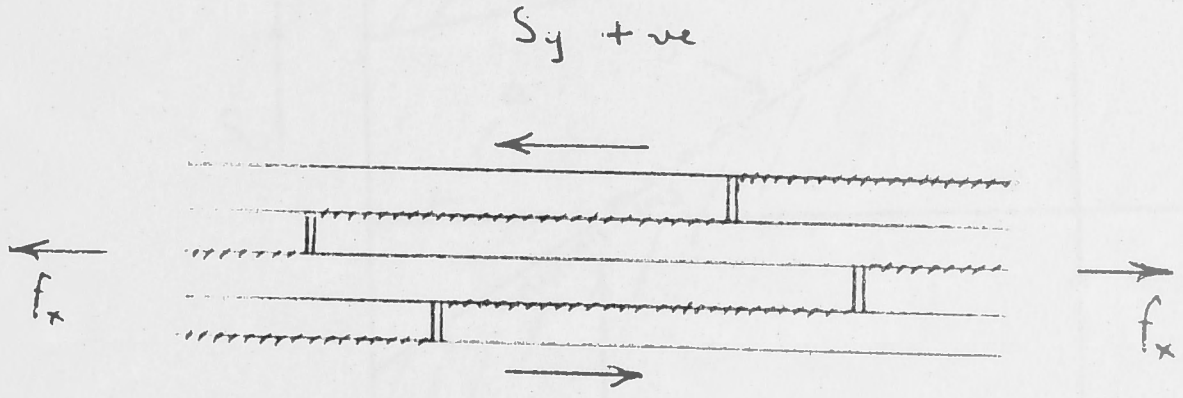

Fig. 10(a)

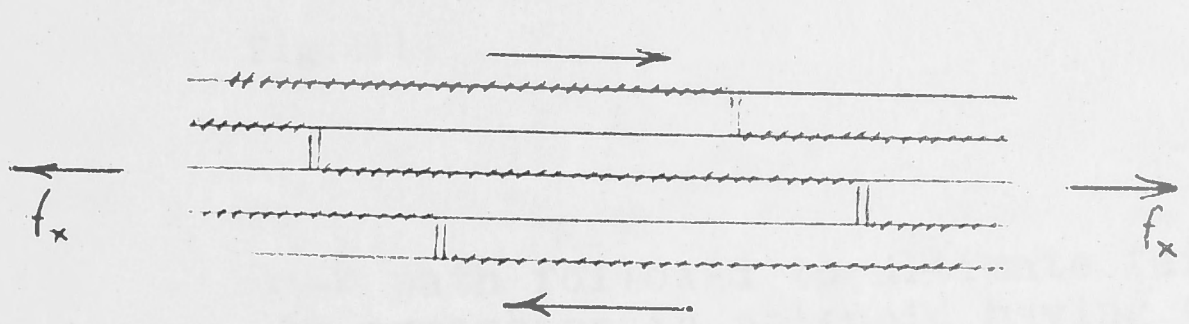

Fig. 10(b)

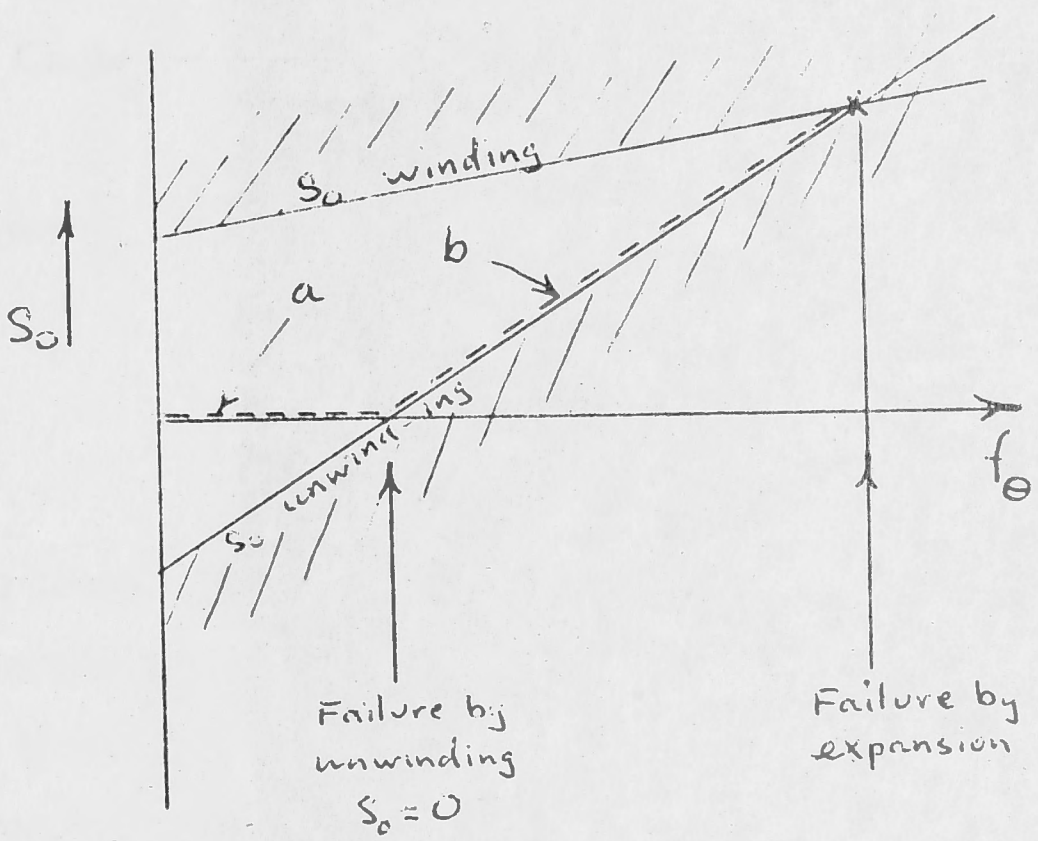

Fig. 11

a-b path followed to ultimate failure by expansion in solenoid having end face anchoring, as magnet field is increased.

b incipient failure by unwinding which causes compensating loading of the end face anchoring.

Proc Int Conf. Magnet Tech
Hamburg 1970

(6)

THE LIMITATIONS OF HOMOGENEOUS PLANE HELICAL SOLENOIDS IN HIGH FIELD APPLICATIONS

P.O. CARDEN

Department of Engineering Physics

Research School of Physical Sciences

THE AUSTRALIAN NATIONAL UNIVERSITY

Canberra, A.C.T., Australia

INTRODUCTION

In order to generate continuous magnetic fields above about 15 Tesla one must still resort to finite resistance conducting materials. In these materials, current density is limited by the practical difficulty of removing the heat generated. One is usually forced then into using very wide turns in order to obtain the required ampers per meter of coil axis. The result is a solenoid with a high ratio of outside diameter to inside diameter - the ratio known as alpha.

Plane helical solenoids are single layer solenoids with wide plate-like turns. They are characterised by the current density being inversely proportional to radius. A homogeneous plane helix is one made of materials whose mechanical properties are homogeneous. The term is used here however to cover the additional properties of elasticity and isotropy, the latter being of prime significance in this paper. The homogeneity must extend across the bond between turns.

STRESSES

The stresses in a long homogeneous plane helical solenoid have been treated by several authors[1, 2, 3]. The results of the present author's treatment described elsewhere[3] are reproduced here. The formulae include a superimposed field from another solenoid surrounding the one under consideration, the magnitude of which is characterised by S.

Assembly and replacement of damaged parts are easier in a system of sub coils than in a Bitter construction of similar strength.

OUTER REGION

So far it has been shown that the stress distribution in the inner region of a high alpha homogeneous solenoid can be improved upon by removing the homogeneity. What of the outer region? Here, when homogeneity is preserved, the radial stress is compressive which, being the reverse of the situation in the inner region, helps reduce the hoop stress at the inner radius of the region at the expense of the hoop stress at the outer radius which is in any case lower. A homogeneous structure is therefore beneficial in helping to distribute stress uniformly.

MULTICOIL MAGNETS

What has been said so far about a single homogeneous solenoid applies also to the outer solenoid of a multi coil magnet since the stray fields from the inner coils are relatively small in the body of the outer solenoid.

The two physically separable regions that a single high alpha solenoid may be divided into may be regarded as two coils of a multi coil magnet so that in this sense we have already covered a specific range of inner solenoids and field division between the two.

What of the general case of an inner solenoid in a multicoil magnet? Figure 4 shows whether any particular combination of inner coil α and field division results in a beneficial compressive stress or a detrimental tensile stress. This diagram was derived indirectly from the equations in section 2 using the graphical information in ref. 3 .

The conclusion must be reached that only narrow homogeneous inner coils are beneficial and that the greater the proportion of the field contribution from the outer coil, the narrower the inner coil should be.

THE CONCEPTS PUT INTO PRACTICE

The findings described above have been incorporated into a 30 Tesla magnet now nearing completion at the Australian National University. This magnet consists of two plane helical solenoids roughly coinciding with the two regions we have discussed. Table I lists the dimensions and characteristics of the two solenoids and their combination.

The outer solenoid described elsewhere in detail, [4] is made on the Bitter principle taken probably close to the extreme of its capacity. It is shown in Figure 5. The inner solenoid consists of eleven nesting sub coils following the principles described above. Figure 6 illustrates one of these coils. Each was wound from rectangular section wire, covered with a waterproof and insulating layer, bonded using hot curing resin into a helix of accurate pitch, and finally machined all over to size. The inside surface is smoothly finished but the outer surface has milled in it a large number of cooling grooves . It has also a machined helical groove running along the bond line which allows a certain amount of tolerance in the precision of the bonding process and in the assembly of the subcoils inside one another.

CONCLUSION

Given that the nesting subcoil arrangement described here is a practical alternative method of constructing a plane helical solenoid, homogeneous structures such as Bitter solenoids should be limited to $\alpha < 3$ and generally to the outer coils of multicoil magnets. In this application their stress distribution is likely to be more uniform than the alternative.

However the alternative is advantageous for the inner solenoids of multi-coil magnets offering in most cases a considerable improvement in stress distribution.

REFERENCES

1. Léon B 1964 Revue Gen. Elect. 12 632-6

2. Kuznetsov A A 1961 Z. tekh. fiz. 31 944-7

3. Carden P O Journal of Scientific Instruments (Journal of Physics E) 1968 Series 2, Volume 1, pp 437 -443

4. Carden P O The Design and Construction of a Bitter Solenoid having a 26 cm Diameter Bore and generating 16.6 Tesla with 26 M.W. of Power.
   Proc. 3rd International Conference on Magnet Technology - Hamburg 1970

TABLE 1

	Inner Coil	Outer Coil	Total
side diameter	2.22 inch	10.5 inch	
utside diameter	9.2 inch	26.8 inch	
ength	8.0 inch	16.25 inch	
eld Contribution	135 kilogauss	165 kilogauss	300 kilogauss
ower	4 MW	25.5 MW	29.5 MW
ooling water	0.9 cubic ft/sec	6.5 cubic ft/sec	7.4 cubic ft/sec
urrent	26.7 kA	168 kA	194.7 kA
oltage	150 V	150 V	

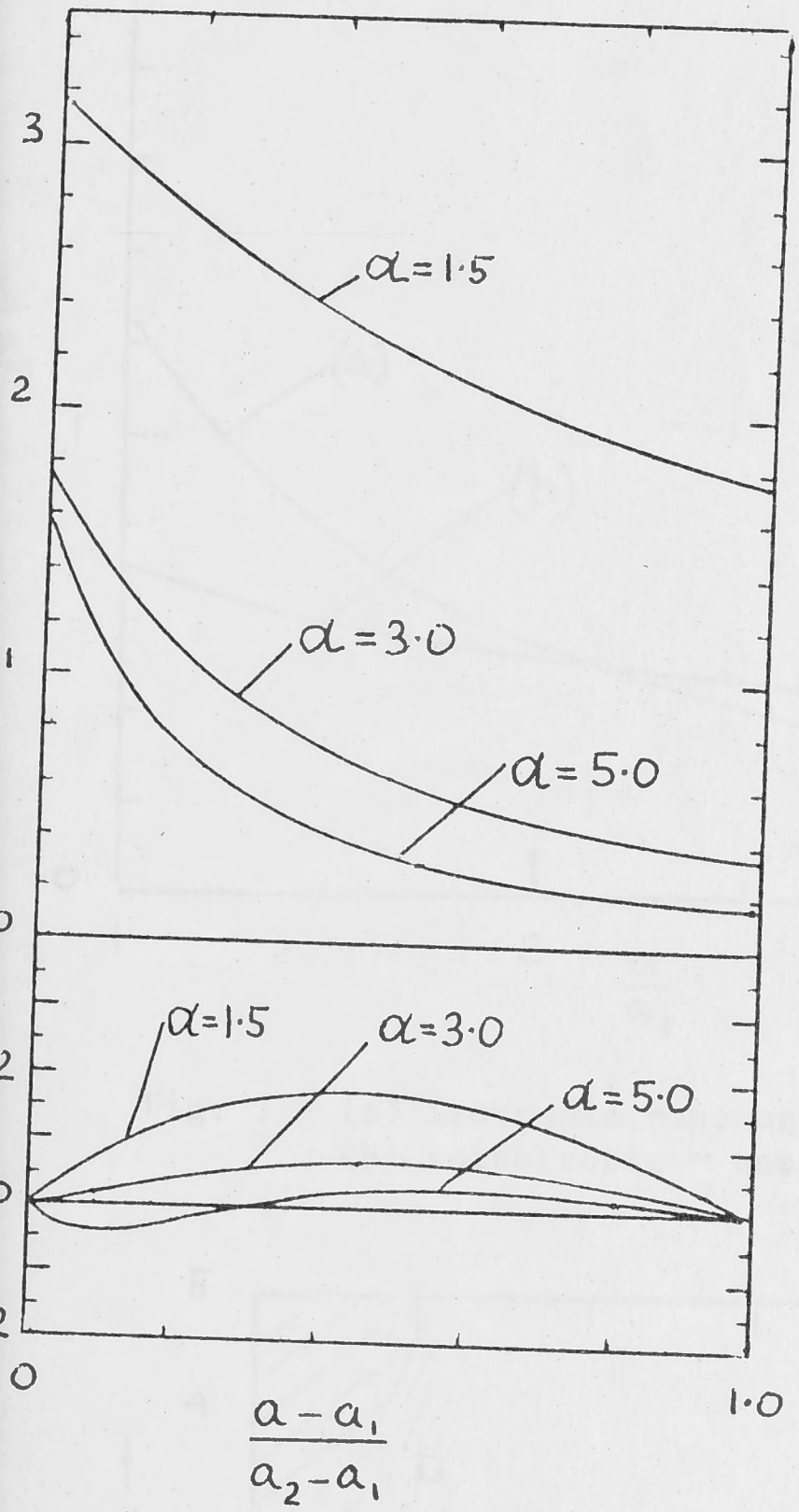

Fig. 1

a : radius

a_1 : inner radius

a_2 : outer radius

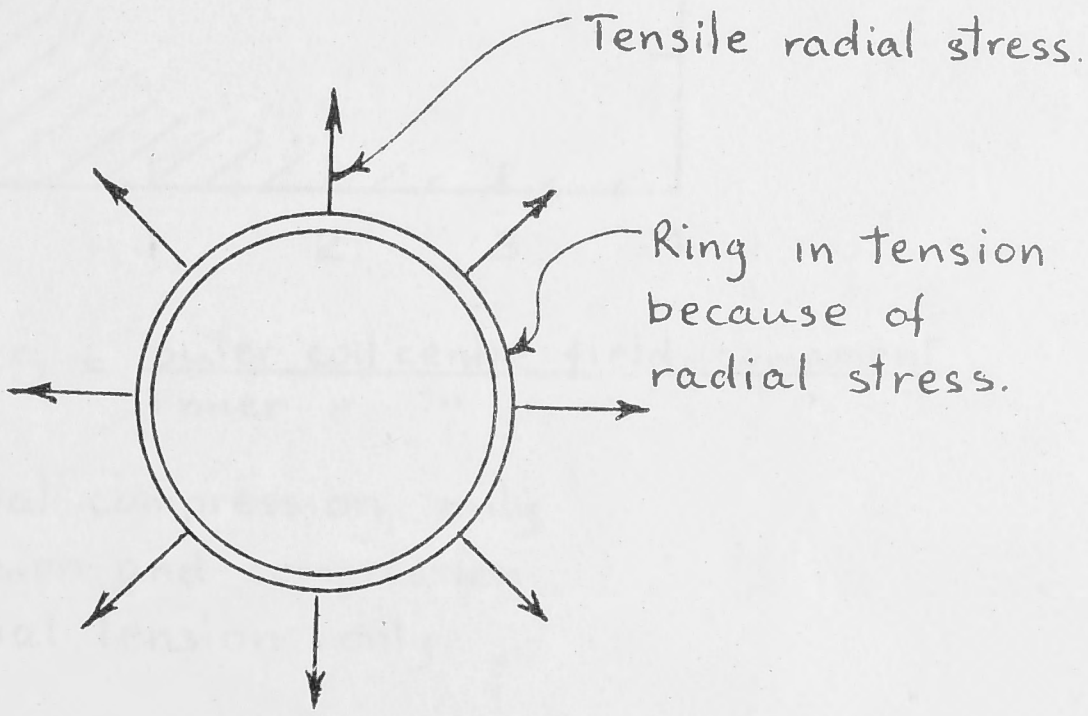

Fig. 2

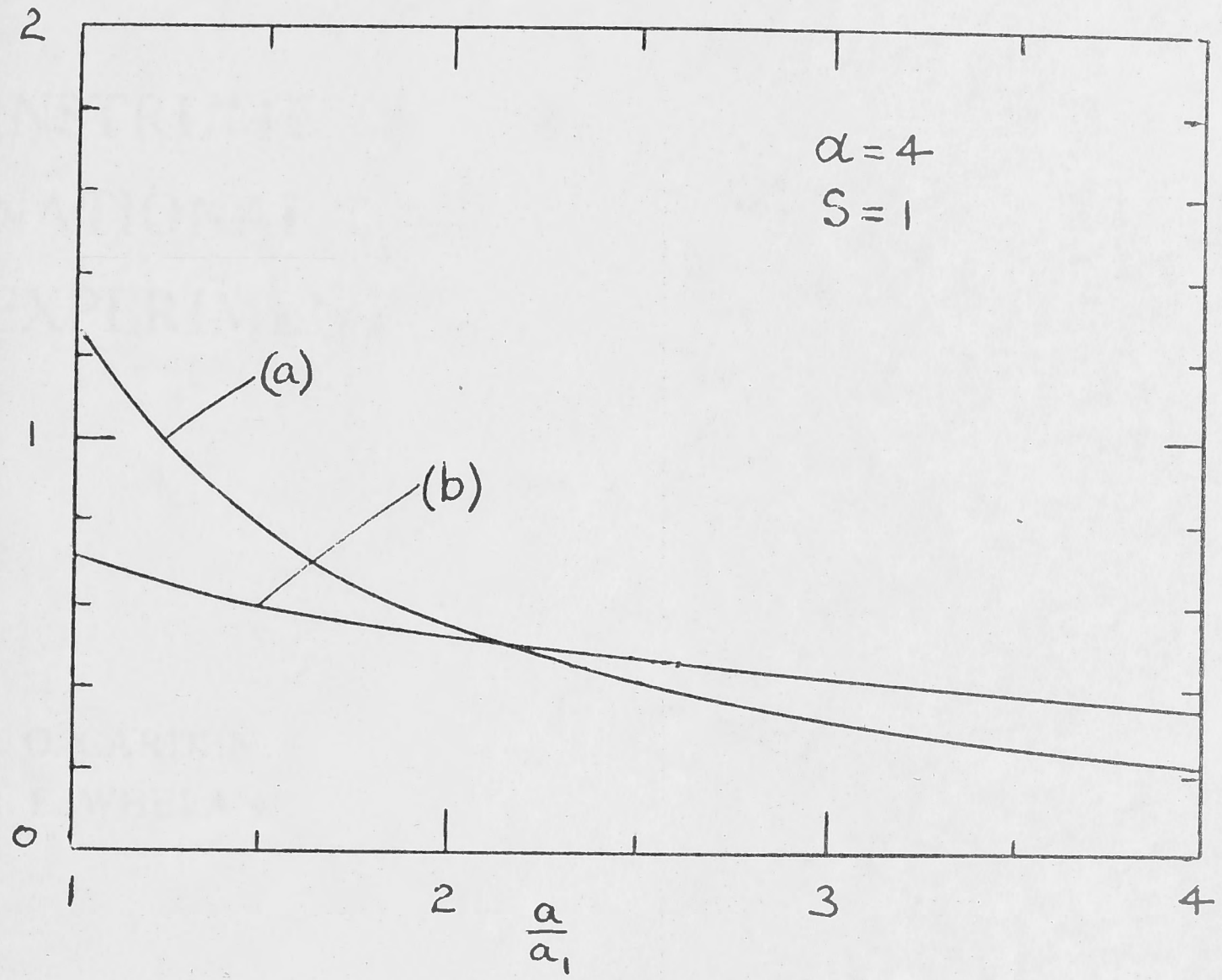

Fig. 3 (a) isotropic - homogenous
(b) anisotropic - nested sub-coils

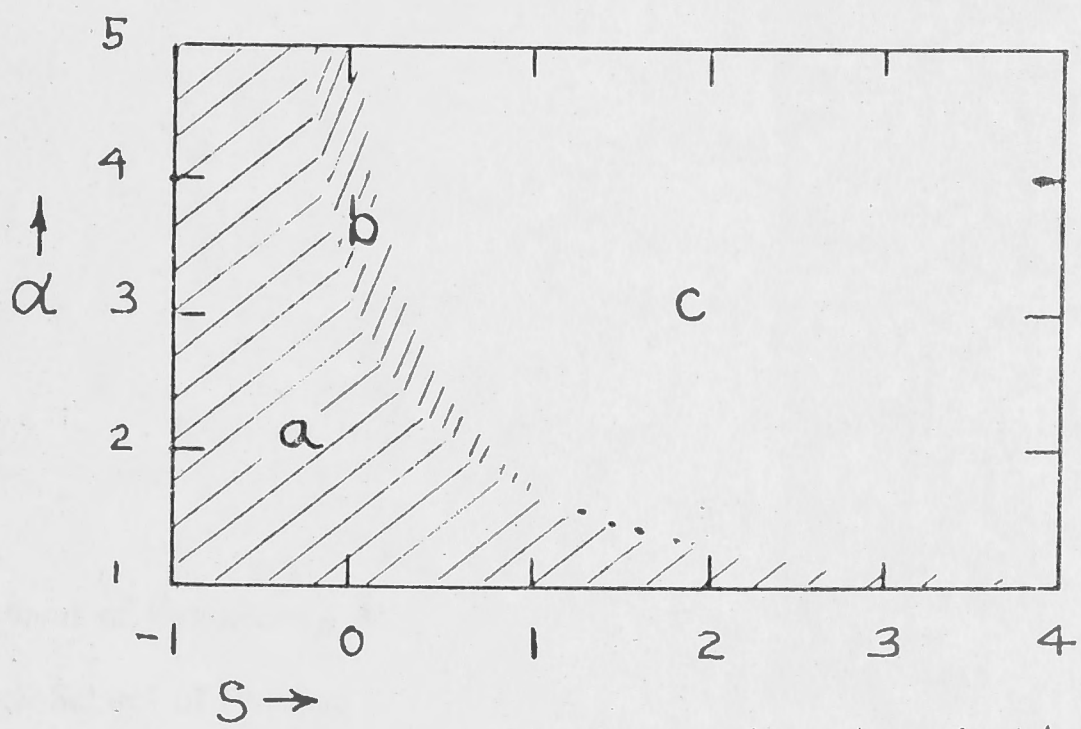

$$S = \frac{\text{outer coil centre field component}}{\text{inner " " " "}}$$

a Radial compression only
b Tension and compression
c Radial tension only

Fig. 4

(7)

INSTRUMENTATION OF THE AUSTRALIAN NATIONAL UNIVERSITY 300 KILOGAUSS EXPERIMENTAL MAGNET

EP-RR 25

P. O. CARDEN
R. E. WHELAN

December, 1969

Department of Engineering Physics
Research School of Physical Sciences
THE AUSTRALIAN NATIONAL UNIVERSITY
Canberra, A.C.T., Australia.

INSTRUMENTATION OF THE AUSTRALIAN NATIONAL UNIVERSITY 300 KILOGAUSS EXPERIMENTAL MAGNET

by

P.O. CARDEN and R.E. WHELAN

December, 1969

Publication EP-RR 25

Department of Engineering Physics
Research School of Physical Sciences
THE AUSTRALIAN NATIONAL UNIVERSITY
Canberra, A.C.T. Australia

CONTENTS

SUMMARY

The basic features of the Australian National University magnet are described, introducing critical parameters intended to be measured.

Description of the design and construction of instruments to indicate mechanical stress, temperature, pressure, relative motion, current and magnetic field, is given.

ACKNOWLEDGEMENTS

Chapter 5 is freely adapted from more complete information compiled by R. McMurtrie of the Magnet Laboratory Group, based on the work of the authors.

Figures 6 and 7 have been prepared by Mr. A. Collins, also of the group, from computed field data.

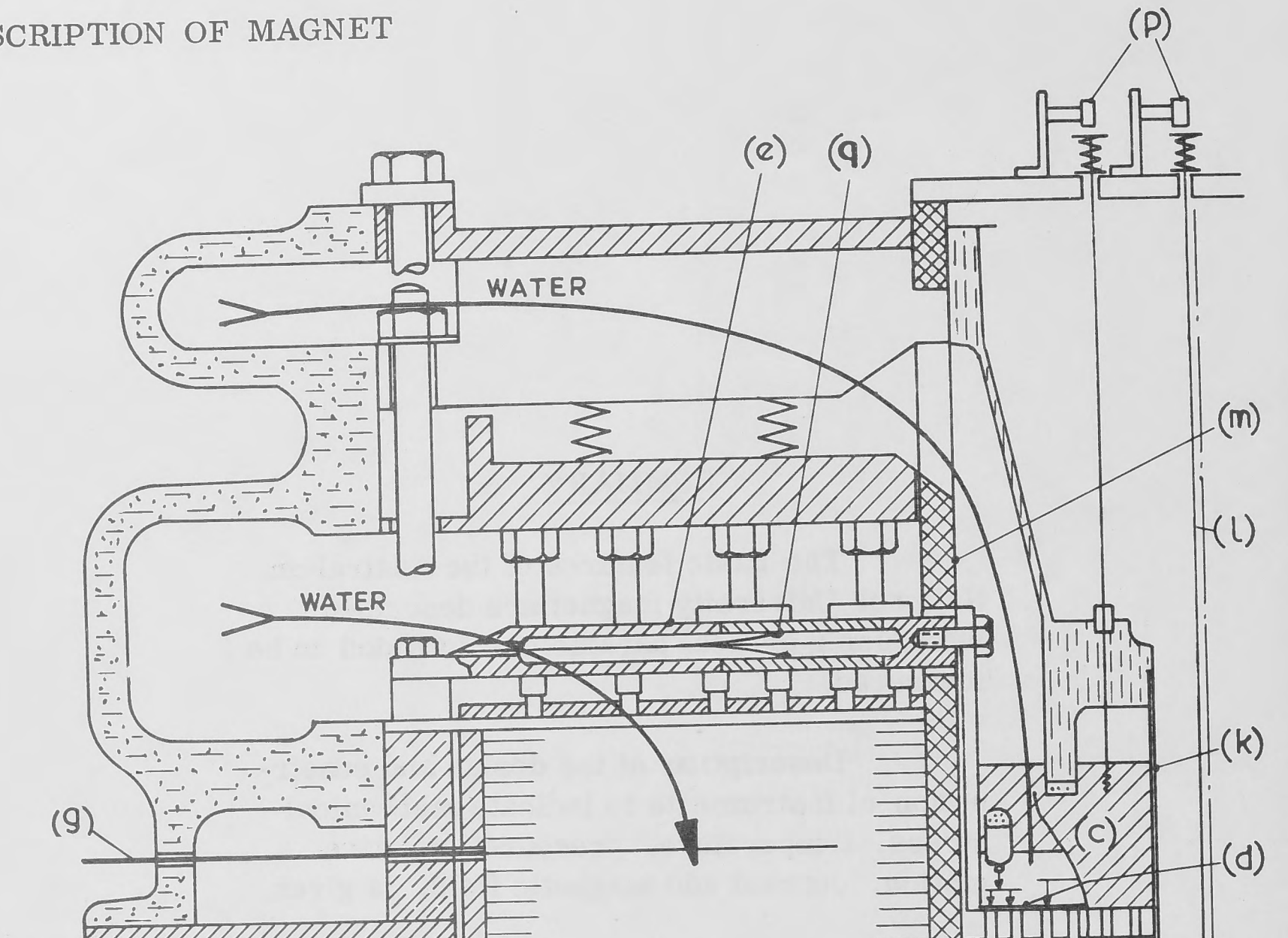

Section of Magnet

a	Inner Coil	h	Displacement Wires, Outer Coil
b	Outer Coil	j	Reference Frame
c	Inner Terminating Assembly	k	Core Tube
d	Electrodes in (c)	l	Axial Molybdenum Transfer Wire
e	Resistors	m	Clamp Tube
f	Torsion Jacket	n	Current Distributing Rings
g	Thermocouple Probes	p	Bentley Gauges
		q	Thermocouples in Resistors

1. INTRODUCTION

In 1967 work began at the A. N. U. on the design of a 300 kilogauss experimental magnet. No other such device existed, so that new ground had to be broken in theory and technology before the project looked like culminating in the creation of a practical device.

This magnet should therefore be looked upon, not merely as a new more powerful research instrument to serve, in particular, the discipline of solid state physics, but also as a piece of engineering research in its own right.

This is certainly the attitude of its builders, and it is because of this that the provision of adequate instrumentation has been regarded as a most important aspect of the work.

2. DESCRIPTION OF MAGNET

The magnet, a section of which is shown opposite, consists essentially of two concentric coils, named inner and outer, connected electrically in parallel.

The outer coil is basically a homogeneous plane helix of 48 turns, the dimensions, field rating, power consumption and cooling requirements of which are listed in Table I . The construction is based on the Bitter principle(5) of

TABLE I

	Inner Coil	Outer Coil	Total
Inside diameter	2.22 inch	10.5 inch	
Outside diameter	9.2 inch	26.8 inch	
Length	8.0 inch	16.25 inch	
Field Contribution	135 kilogauss	165 kilogauss	300 kilogauss
Power	4 MW	25.5 MW	29.5 MW
Cooling water	0.9 cubic ft/sec	6.5 cubic ft/sec	7.4 cubic ft/sec
Current	26.7 kA	168 kA	194.7 kA
Voltage	150 V	150 V	

interleaved split discs, but the principle has been developed well beyond previous practice and more is expected of the structure in terms of strength than has previously been the case. The expected stresses based on calculations derived after References 1 and 2 are graphed in Figure 1 .

The inner coil is essentially a plane helix of 96 turns and is of consid-

erably different pitch from the outer coil. However it is not mechanically homogeneous, consisting in fact of eleven concentric sub-coils all of the same

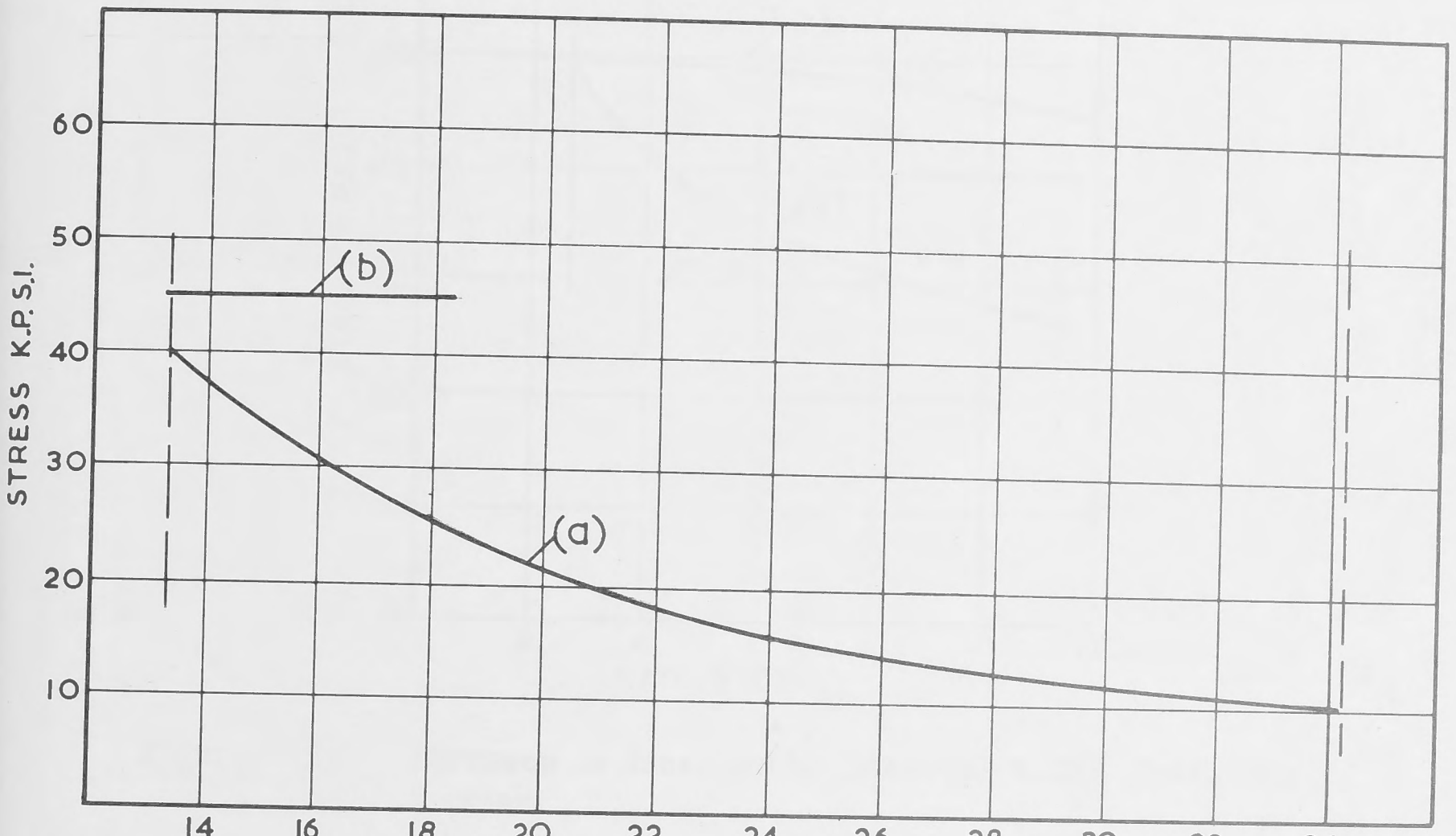

Figure 1. Stresses in outer coil. Material is .07% Ag-Cu hard temper.
(a) expected azimuthal stress.
(b) expected 0.1% proof stress.

pitch and electrically in parallel throughout the composite structure. The non-homogeneity of the inner coil is beneficial to azimuthal stress distribution which is expected to be as graphed in Figure 2 . Main parameters are listed in Table I as for the outer coil.

Cooling of both coils is by means of axial water passages - punched holes in the discs of the outer coil, and milled slots on the outer surface of each of the sub-coils of the inner coil. With the design water flow and maximum field, temperatures in the outer coil are expected to be as shown in Figure 3 and those in the inner coil as in Figure 4 .

Since the design of the magnet is based on new theory and innovations not previously verified experimentally, and since its safety depends on certain

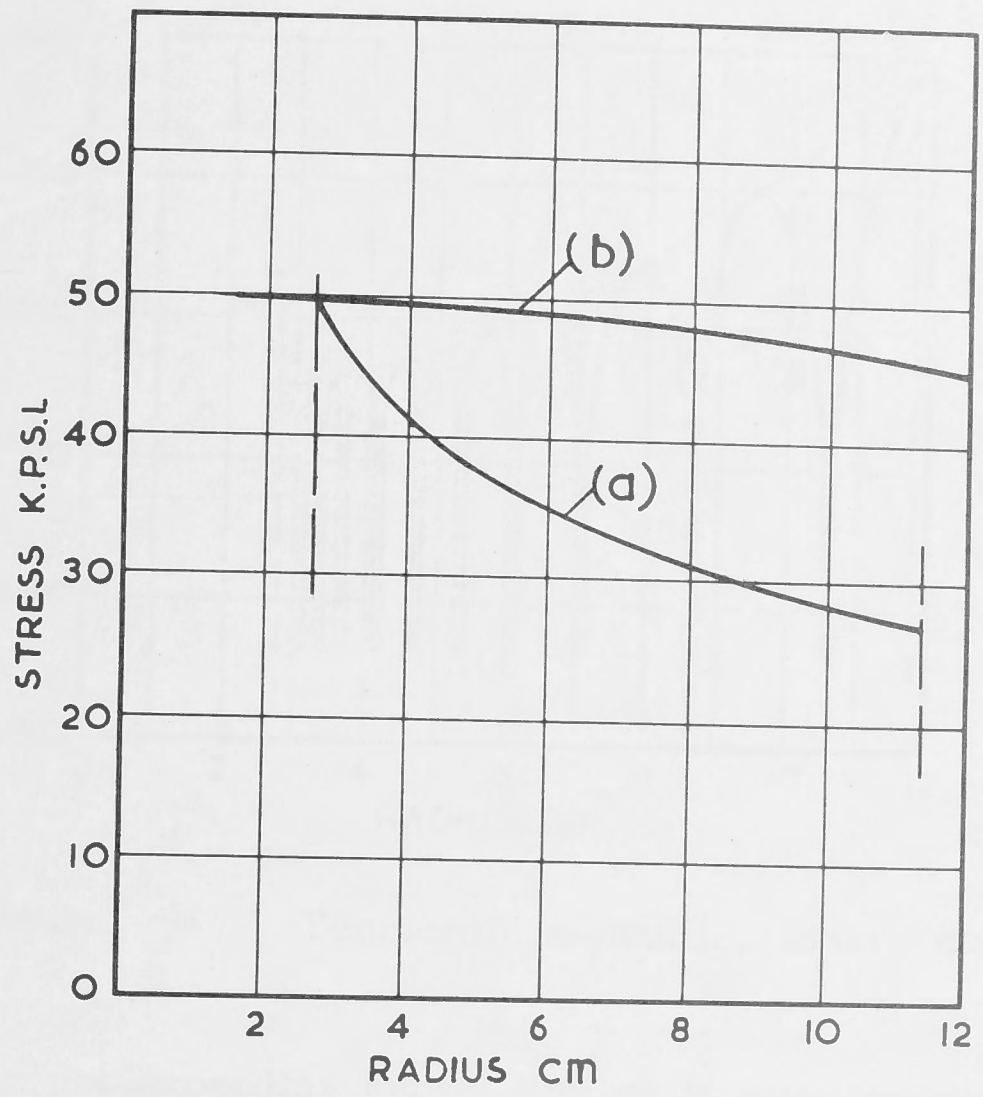

Figure 2. Stresses in inner coil. Material 0.25% Zr-Cu hard temper.
(a) expected azimuthal stress.
(b) expected 0.1% proof stress corrected for operating temperature.

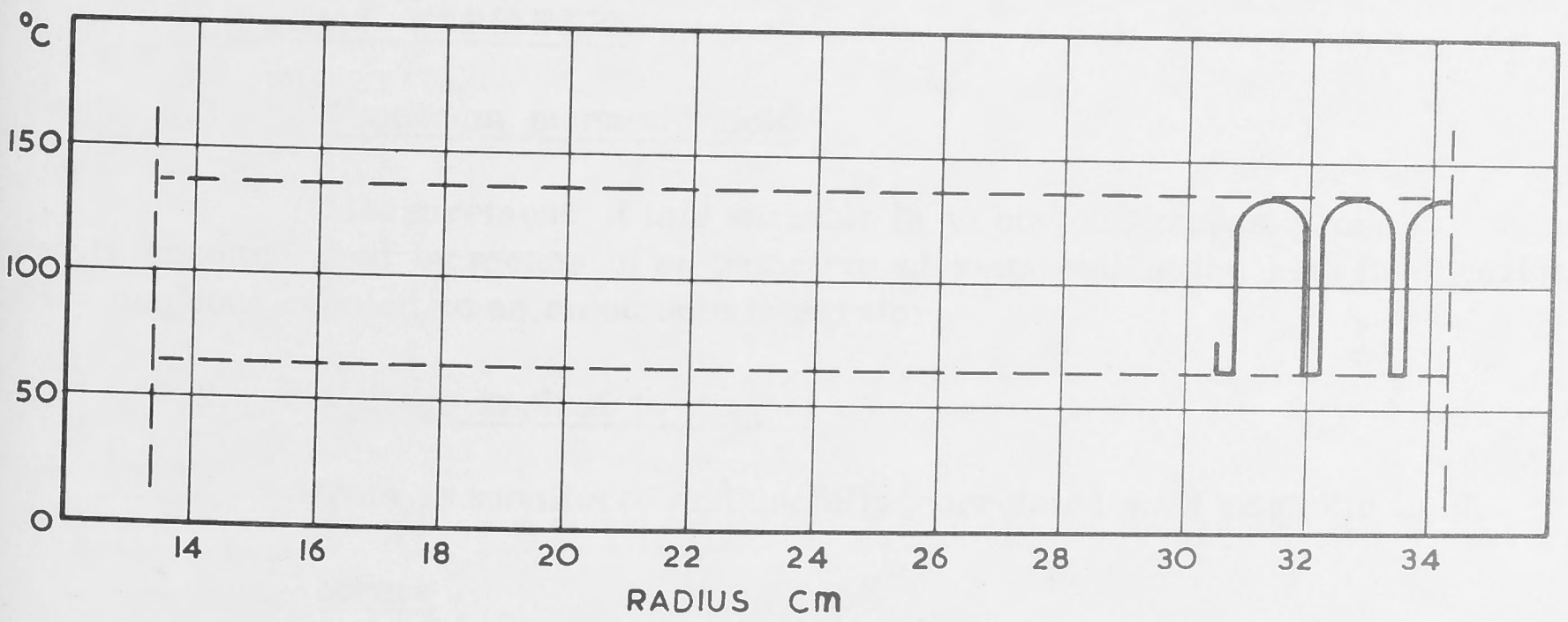

Figure 3. Temperature profile - through cooling holes, outer coil.

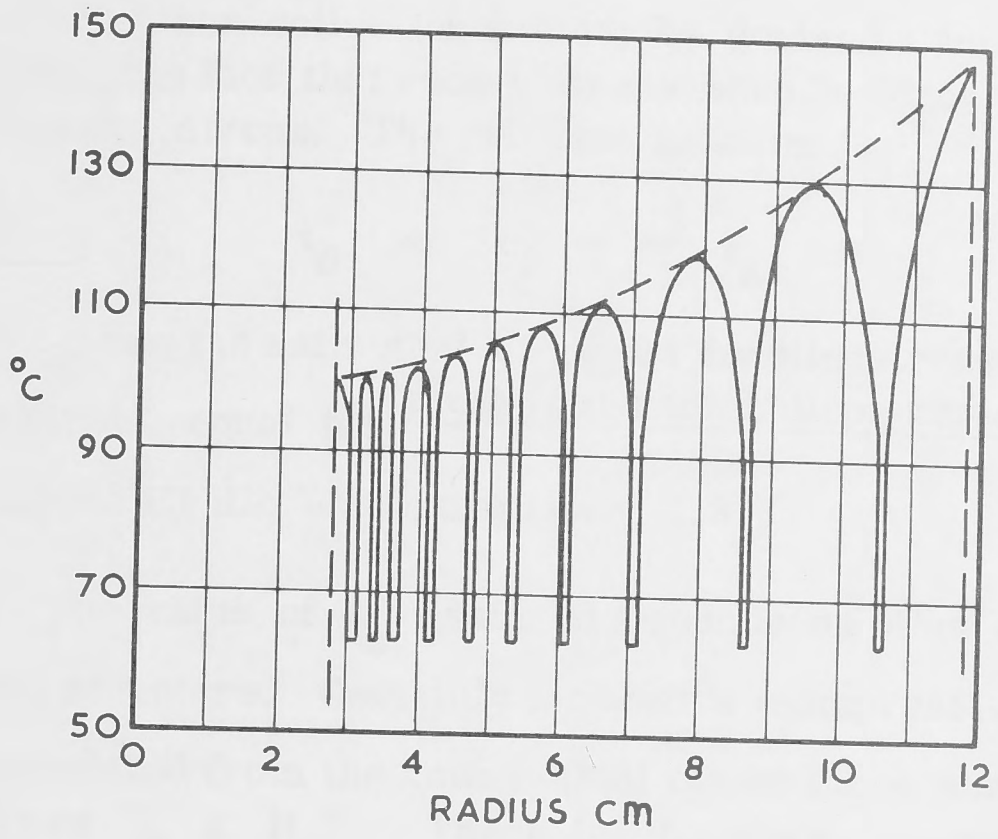

Figure 4 Temperature profile, inner coil.

critical parameters not exceeding known limits, it was considered desirable to incorporate adequate instrumentation into the magnet structure. Section 3 gives an account of the principal variables in the magnet and the practical means adopted for monitoring these variables. As will be seen, in some cases it was found impracticable to measure the desired variable directly, or in as many locations as one would like.

3. PRINCIPAL VARIABLES

3.1 Maximum magnetic field

Measurement of this variable is an obvious necessity and is readily accomplished by means of an inductive pick-up coil in the high field region of the magnet, coupled to an electronic integrator.

3.2 Voltage applied to magnet

This is monitored and usefully correlated with magnetic field.

3.3 Stress

Estimation of this variable, which is a function of position, is most important from the point of view of verifying theory, and for safety of the structure. However, the only stresses found possible to derive even approximately are the azimuthal stresses at both cylindrical surfaces of the outer coil and at the

inner surface of the inner coil. These may be derived from measurements of radial strain, using the fact that radial stress here is zero, making a reasonable assumption as to axial stress. The relevant relation is:(1, 2)

$$t_\theta = Ee_\theta + \frac{1}{m} t_z$$

where t_θ and t_z are the azimuthal and axial tensile stresses respectively, e_θ is the azimuthal strain, equal to $\frac{\text{measured radial displacement}}{\text{radius}}$, and m is the reciprocal of Poissons ratio - approximately 3.3 .

The value of t_z assumed depends on other assumptions about the rigidity of the coil structure. Certainly a negative (compressive) component of t_z can be simply calculated from the known axial clamp force and the electromagnetic axial clamping force $j_\theta \times B_r$. There is, however, a tensile component which, for rigid long solenoids, approaches a limiting value given by the equation for $\frac{t_z}{p_m}$ in Reference 2 . The appropriate value for t_z calculated from this equation for the inner surface of the outer coil is approximately 5,500 p.s.i. which makes the maximum uncertainty in t_θ from this source of the order of 1,600 p.s.i.

3.4 Forces

There are many forces about which one would like to have knowledge, but few which one can measure. The inner coil is hydraulically clamped so that there is at hand a ready means of measuring the axial force on the inner coil from hydraulic pressures. Such information is useful in determining whether the inner coil is in the magnetic centre of the outer coil and in verifying the contact and clamping force applied to the inner coil.

The current distributing rings encircle the magnet and hence experience induced currents and radial forces either inwards or outwards. In passing, it should be explained that these currents are beneficial in so far as they allow the applied current to be distributed to points around the magnet which are essentially at equal potential. This is of prime importance especially for the inner coil where the flow of current in or out of the end turns has been carefully controlled to avoid large unbalanced forces. However, it is difficult to calculate the size of the circulating currents with accuracy, and it is prudent to monitor them as directly as possible. Since for the ring

$$E = j\rho \quad ,$$

where E is the induced electric field ,
j the current density ,
and ρ the resistivity of the ring copper ,

it is possible to derive j from a measurement of E . This is done by placing a single inductive measuring loop in a representative location on the ring surface. For a loop of length l and induced voltage v ,

$$E = \frac{v}{l} .$$

The location of the loop is important because the shape of the current distributing rings is such as to suggest that there will be considerable variation in current density. The loop therefore must be located in a region where the local induced current density might be expected to be about equal to the average current density in order that the results will lead to an estimate of total induced current and nett force acting on the distributing system. The location was chosen after a computer study of fields produced by the magnet and by circulating currents in the rings.

3.5 Movement between adjustable parts

The inner coil may be moved axially by hydraulics. This ability is primarily due to the system chosen to apply axial force to the inner coil and allows adjustment of the position of the inner coil to the magnet centre of the outer coil which should enable minimisation of forces acting on it. Once the adjustment is possible, a means of monitoring must be incorporated. Such means also allows a check on axial deflection under load.

3.6 Temperatures

Together with stresses, temperatures constitute the most critical variables of the magnet because the strengths of materials used are a function of temperature. Temperatures are relatively easily measured by means of thermocouples but there is a problem of inductive pick-up in the signal leads to be investigated.

The strength most critically dependent on temperature is that of the glue bond of the inner coil. In Figure 5 is shown a graph of stress vs temperature upon which is drawn an envelope containing all points of the inner coil glue bond under all conditions of field strength up to the maximum. Also drawn is the experimentally determined strength of the composite bond developed for these coils. Clearly, a 10 or 20 degrees variation will have far more effect on the glue bond than on the strength of the metals employed. The hottest parts of each of the inner sub-coils - the top ends - are measured, using two thermocouples for each measurement to enable cross checking or to allow for a loss due to breakage during assembly of the magnet.

The outer coil is monitored by a number of fixed thermocouples and also by radially movable thermocouple probes operating in a number of slightly enlarged slits between discs of the outer coil.

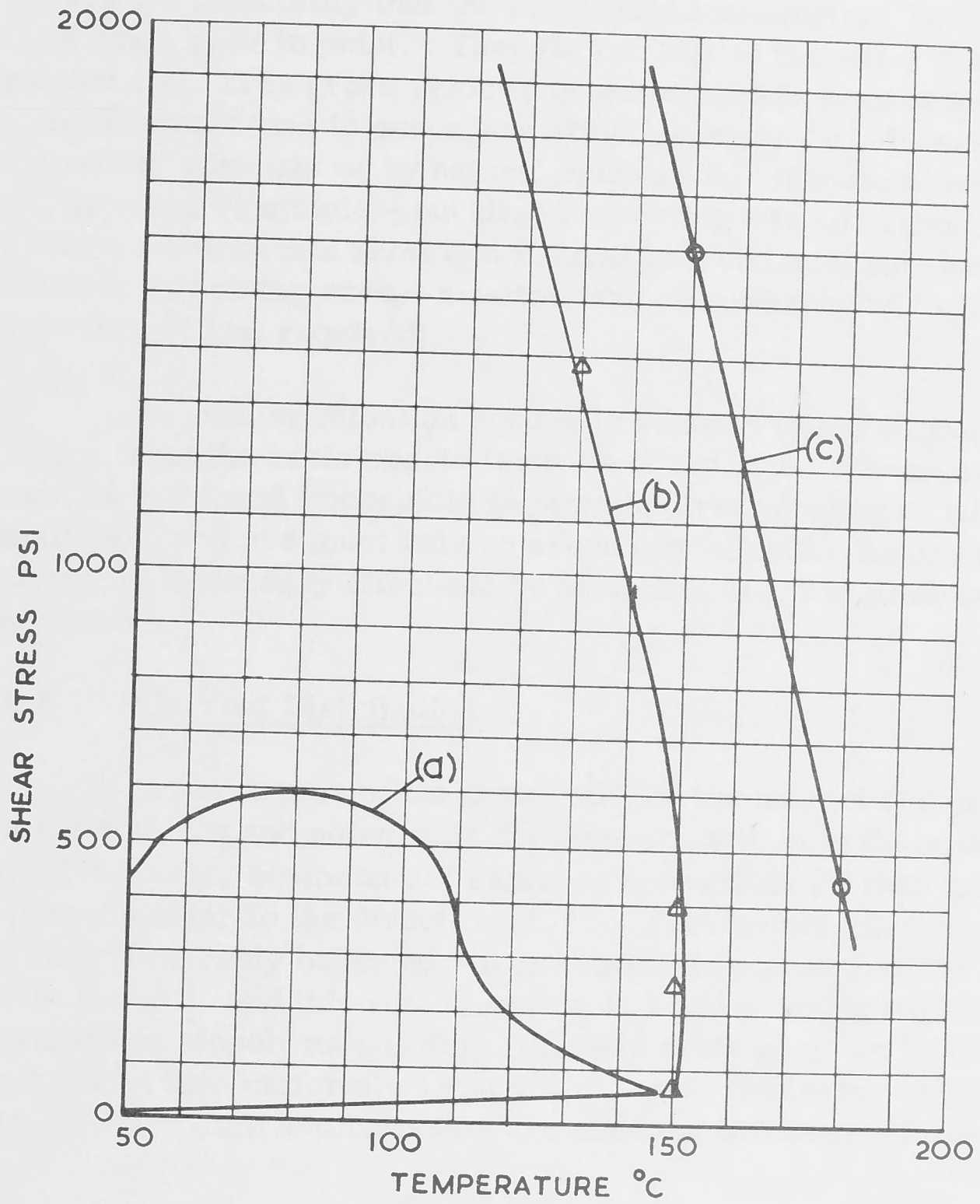

Figure 5. Inner coil glue shear stresses.

(a) envelope for all parts of the coil under all conditions of energisation.

(b) and (c) two types of epoxy resin tested.

Certain special situations require monitoring where the cooling is rather complex. All such situations have been checked experimentally by model but there is always the possibility that the model was inadequate. The resistors feeding the inner coil are a case in point. They lie radially in the water space above and below the outer coil. The gross velocity of water here is zero at the inner end of the resistors, so one must turn to secondary effects such as turbulence caused by efflux from the outer coil channels or by natural convection. If these effects prove to be insufficient, it would be simple - but time consuming - to add circulating vanes. However, model experiments show that natural convection alone should be adequate, so it is easier to do nothing except monitor temperature (hoping, with good ground, that nothing extra will be required).

A similar situation occurs in relation to the copper distributing fingers feeding from the resistors to the ends of the inner sub-coils. Due to compactness, it was found impossible to provide direct cooling to all surfaces of these components, and one must rely on secondary effects. Again, model experiments indicate the secondary effects to be adequate, but it is prudent to monitor this area, nevertheless.

3.7 Current Distribution

A large part of the complexity of the magnet design has arisen because of the complex and potentially dangerous situation at the ends of the coils. In the body of the coils, equipotential surfaces are almost vertical planes across a turn, and perpendicular to the direction of j . Fortunately, in the body of a coil, forces are very favourably balanced. It is essential to preserve this state of affairs at the ends of the coil, and this can be done only by preserving the vertical equipotential surfaces as closely as possible. This is made possible by distributing current to the first turn uniformly around it in equal, discrete, and evenly spaced increments. Twelve distribution points are used for the inner coil and four for the outer.

Monitoring of this distribution is achieved by measuring appropriate resistive voltage drops. The resistors are the obvious measuring places for the inner coil. In the outer coil the end turns are four-start and a convenient check is the voltage drop across these four sections.

3.8 Magnetic Field Distribution

The relative contributions of the two coils to maximum magnetic field is important to know since both coils are designed near the limits of strength and it would be desirable therefore not to energise the combination to full field at the expense of overloading one coil. Known variations of conductivity from the specifications suggest that there will be small differences in the contributions of field from what was intended. On the other hand it may turn out that in practice one coil is stronger than expected (the strain may be less, or the cooling better than

anticipated) enabling the contributions to be optimised for maximum central field.

The field distribution may be checked by using an inductive loop around the outer coil in conjunction with the maximum field pick up coil. The ratio of these two measurements may be correlated with the theoretical steady state ratio of the two coil currents. Figure 6 shows the approximate theoretical correlation. These measurements should also give us an indication of the transient division of currents between the two coils.

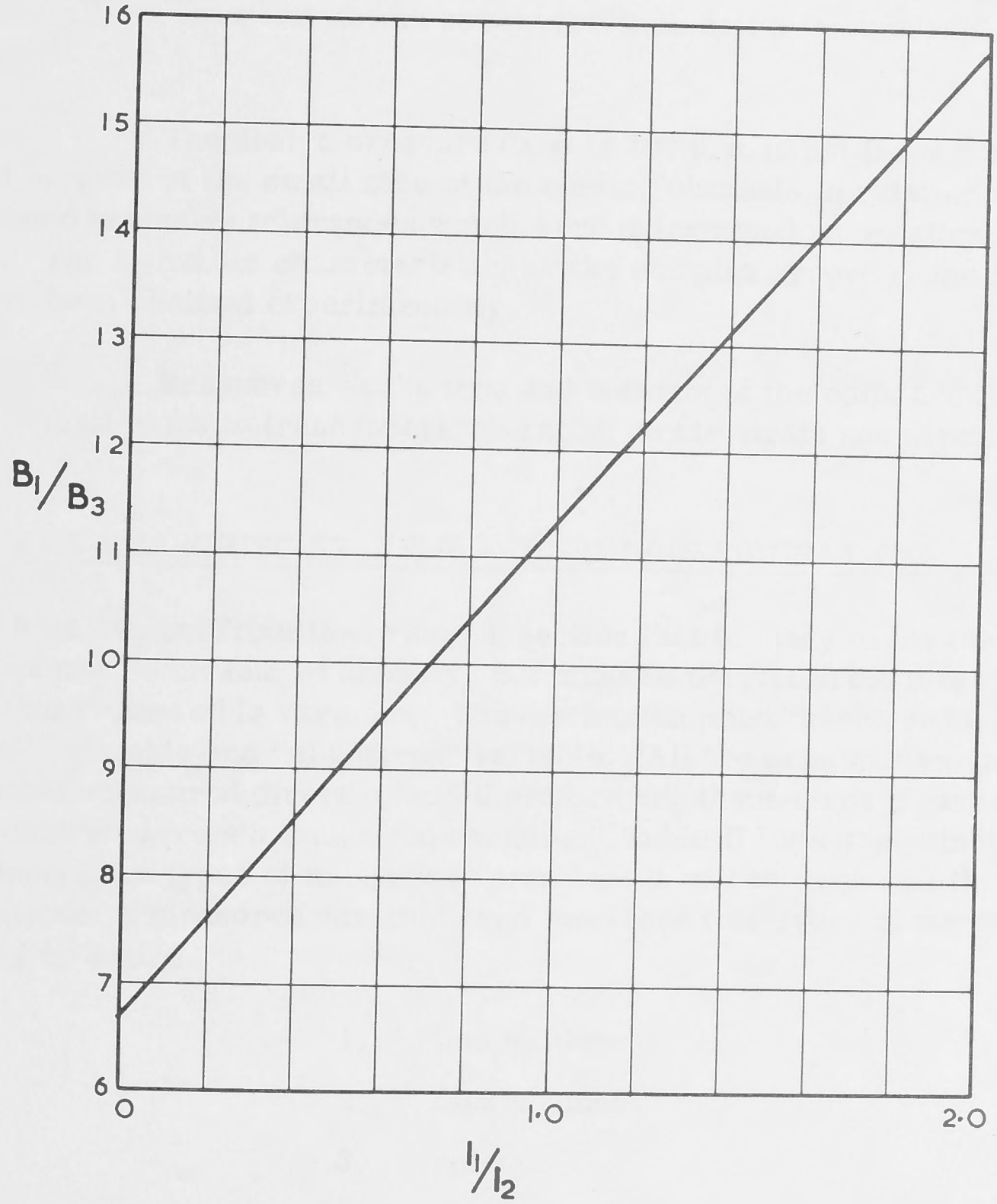

Figure 6. Theoretical relation between the average fields measured by two pick-up coils and the current distribution between the two magnet coils. B_1 is the average field in a pick-up coil in the middle of the magnet with diameter 5 cms. B_3 is the average in a coil 12 cms away from the median plane of the magnet with diameter 92 cms. I_1 and I_2 are the inner and outer currents, each normalised with respect to the design values.

3.9 Cooling Channel hydraulic characteristics

The heat transfer characteristics of the cooling channels depend on the flow velocity through the channels. The best way to monitor instantaneous water velocity is to establish the correlation between water velocity and pressure drop by a series of tests where water velocity is kept steady. The quantity of water flowing in a given time may be measured and hence the channel water velocity derived.

This correlation may be done for each of the coils separately and, once done, allows independent adjustment for each coil by means of the series valves provided.

The design pressure drop is 100 p.s.i. but large deviations are expected because of the small size of the cooling channels in relation to the manufacturing and assembly tolerances which were determined on practical and economic grounds. The hydraulic characteristics of the complex groove shape for the inner coils have been checked experimentally.

Pressures at the tops and bottoms of the coils are transferred by means of small pipes to transducers operating on the strain gauge principle.

4. THE MEASURING SYSTEMS - DESIGN CONSIDERATIONS

It is evident from the previous section that in many cases the principal variable cannot be measured directly, but must be derived from measurement of another more accessible variable. The distinction must therefore be made between "principal" variable and "measured" variable. All the principal variables discussed can be either measured directly, and therefore are themselves measured variables, or can be derived from a measured variable. Table II lists the principal variables and the associated types of measured variable. It will be seen that there are in all just four types of measured variable, and therefore four types of measuring system, which may be called

1. temperature
2. displacement
3. voltage
4. pressure

The design of these four systems will now be discussed.

TABLE II

Principal variable	Measured variable
maximum (central) magnetic field	voltage
magnet voltage	voltage
stress	displacement
force	pressure
	voltage
movement	displacement
temperature	temperature
current distribution	voltage
magnetic field distribution	voltage
cooling channel hydraulic characteristics	pressure

4.1 Temperature

All temperatures are measured by thermocouples using .003" or .008" diameter copper-constantan wires. The sensitivity of these thermocouples is only 4.2 m.V. per $100^{o}C$ so that voltages induced in the signal leads and in the thermocouple itself must be kept quite small. Thermocouples located in or on conductors must have no contact with the conductor to avoid currents that might be flowing in the conductors also partially flowing in the thermocouple. Twisted copper -constantan pairs are used to carry the signal voltage through the varying magnetic environment. A carefully twisted pair of constant pitch p (distance between cross over points) and wire diameter d may be considered as a succession of positive and negative inductive loops of area pd (actually $\frac{2pd}{\pi}$) connected in series. Two adjacent loops will have fluxes Bpd and $-\left(B + \frac{dB}{ds} \cdot p\right) pd$ respectively, where B is the field perpendicular to the direction of the wire and s is the distance along the wire. Hence the rate this flux is added to by successive pairs of loops is

$$\frac{d\phi}{ds} = -\frac{pd}{2}\frac{dB}{ds}$$

Integrating between points 1 and 2 on the twisted pair we have

$$\phi_2 - \phi_1 = - \frac{pd}{2} (B_2 - B_1)$$

This is correct provided an even number of loops lie between 1 and 2 . If there is an odd number, then an extra flux component must be added equal to $- B_1$ pd or $+ B_2$ pd depending on which end of the twisted pair the extra loop is considered to be added. The two cases are of course similar, except that one case is equivalent to the wire being twisted 180° throughout, compared with the other.

Adding the extra flux component for the odd loop case, we find

$$\phi_2 - \phi_1 = \pm \frac{pd}{2} (B_1 + B_2)$$

so that the general case may be written

$$\phi_2 - \phi_1 = \pm \frac{pd}{2} (B_1 \pm B_2)$$

The induced voltage in a twisted pair cannot therefore be greater than that induced in a single loop of that twisted pair placed in the maximum field through which it is routed.

If p = 1 cm, d = 0.07 m.m. and $\frac{dB}{dt}$ as high as 300 kilogauss per second, the induced voltage will not be greater than $\frac{1}{60}$ m. volt, equivalent to about $\frac{1}{2}$°C .

4.2 Displacement

Measurement of displacement is centred around a commercial device - a Bentley Proximator. It operates on the principle that the close proximity of a metal surface to a high frequency coil alters the coil's tuning characteristic. It has been verified experimentally that steady fields of a few thousand gauss have no effect on the proximator's calibration, but it is uncertain what effect higher fields, of the order of a hundred thousand gauss, may have, especially on the inbuilt solid state electronics. This, together with the size of the proximator ($\frac{1}{4}$" diameter x 1" long) makes it desirable to locate it well outside the structure.

The real problem with displacement measurement is then in the transfer from the point of interest within the magnet structure to the proximator. The displacement of the inner surface of the outer coil, for example, needs to be transferred through a temperature and field environment varying in time and space. Fortunately the slits between discs provide an ideal radial channel which can be made to accommodate a transfer wire of up to 0.020 inch diameter. Invar wire, 36%

Ni-Fe with a temperature coefficient of expansion of only 0.8×10^{-6}, (Reference 3) has been used under a known tension, to nullify the effects of the temperature environment, but unfortunately invar is magnetic. This property has two general effects in a space-varying magnetic field: it algebraically adds to the applied tension in the wire and it causes a side-ways force which, with the action of friction, causes an uncertainty in the tension.

The effects can be examined theoretically. We assume that the invar is magnetically saturated with a magnetisation of M_s which is fixed in value but locally takes the direction of the field B. It follows that, if B has a direction θ with the axis of the magnet (the z axis), the component of magnetization along the wire - r direction - is $M_r = M_s \sin\theta$ and the resulting longitudinal force at each point in the wire is

$$\frac{dF}{dV} = \frac{M_s \sin\theta}{\mu_o} \times \frac{dB_r}{dr} ,$$

where V is volume.

Hence the tension at any point at radius r in the wire, additional to the applied tension at radius r_2 may be expressed.

$$F_r = \frac{M_s a}{\mu_o} \int_r^{r_2} \sin\theta \cdot \frac{dB_r}{dr} \cdot dr \qquad \ldots\ldots\ldots \quad (1)$$

where a is the cross-sectional area of the wire.

Similarly the sideways force per unit length of wire may be derived, which results in an uncertainty in tension in the wire due to friction of

$$|T_r| < \frac{\gamma M_s a}{\mu_o} \int_r^{r_2} \left| \cos\theta \cdot \frac{dB_z}{dz} \right| dr \qquad \ldots\ldots\ldots \quad (2)$$

where γ is the coefficient of friction.

Here the integral of the modulus is taken because the wire is not rigid enough to allow a sideways force in one direction to be offset against a sideways force in the opposite direction several wire diameters along the wire from the first force.

The integrals in equations 1 and 2 may be obtained from computed field components of the magnet. Figure 7 shows how $\theta, \frac{dB_z}{dz}$ and

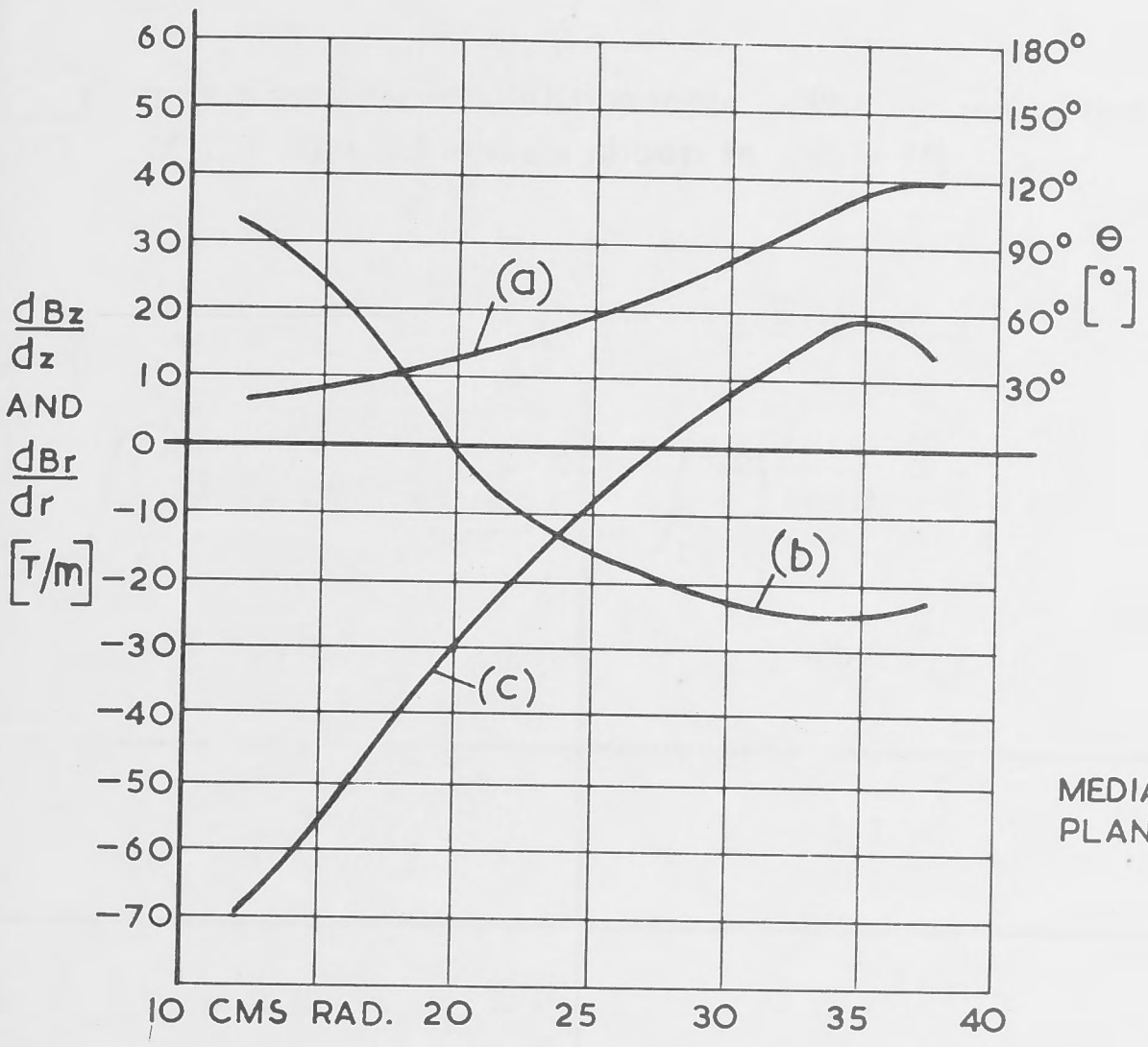

Figure 7(a)

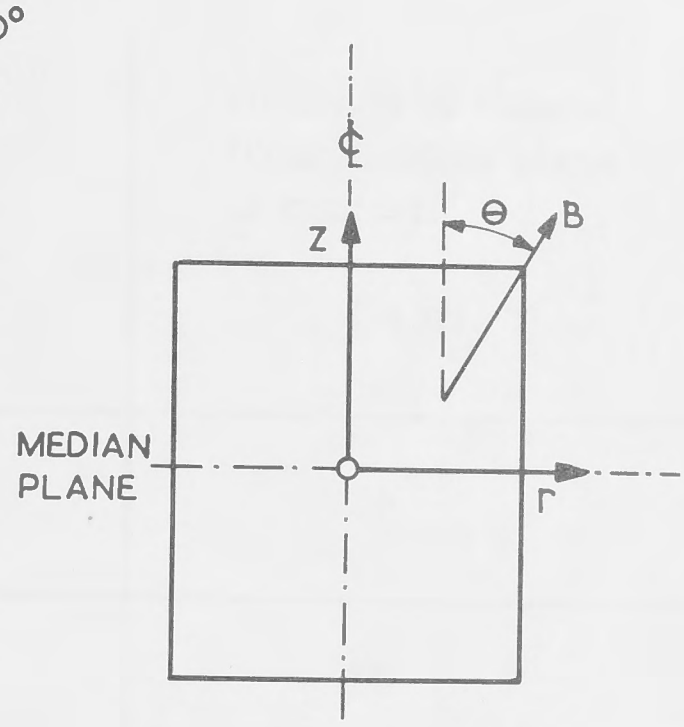

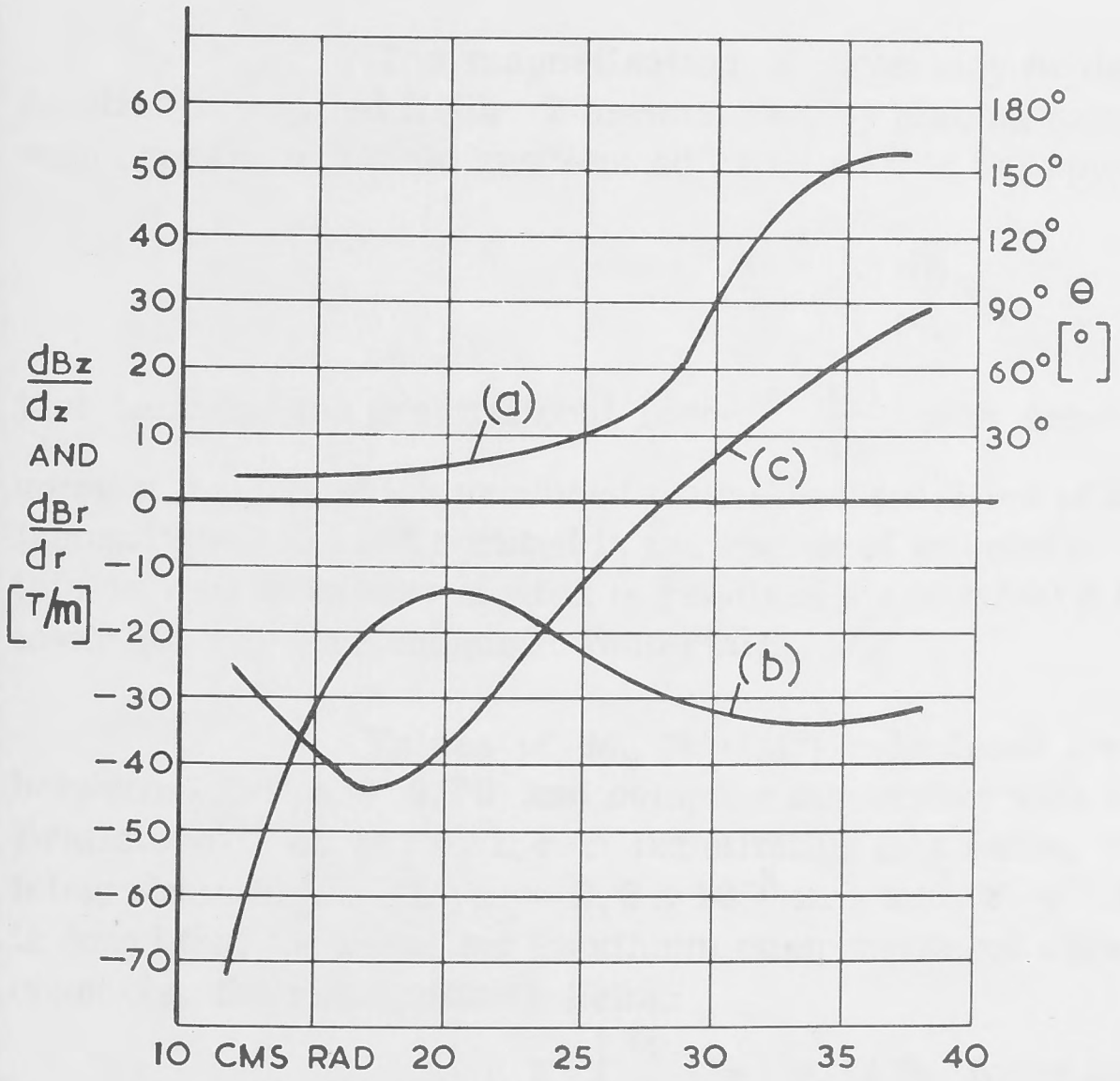

Figure 7(b)

Direction of field and magnitude of field gradients along displacement measuring channels in outer coil.

7(a) for channels 18 cms from median plane.

7(b) for channels 8 cms from median plane.

(a) angle Θ

(b) $\frac{dB_r}{dr}$

(c) $\frac{dB_z}{dz}$

The diagram defines the axes used.

$\frac{dB_r}{dr}$ vary along the radial channels. The values of the two integrals over the length of the channel are as shown in Table III .

TABLE III

$\int_{r_1}^{r_2} \sin\theta \frac{dB_r}{dr} \cdot dr$ (Wb/m^2)	$\int_{r_1}^{r_2} \left\| \cos\theta \frac{dB_z}{dz} \right\| dr$ (Wb/m^2)	Distance of channel from median plane of magnet. (cms.)
- 0.7	- 1.1	8
- 2.6	- 5.3	18

The magnetisation of invar may be determined experimentally as a function of applied field. This was done by placing samples of invar, some weighted with copper, in a field gradient adjusted so that the upward force

$$\frac{M}{\mu_o} \cdot \frac{dB}{dz} V$$

just balanced the gravitational force. $\frac{dB}{dz}$ was determined from a field plot using a magnet which produced magnetic intensities of about 8×10^4 A/m (actually 940 to 1040 oersted in the region of interest). According to Brailsford[4] this is well in excess of what is required - about 500 A/m - to produce saturation in invar (or any ferromagnetic material).

Values of M_s (Wb/m^2) calculated from these experiments ranged between 1.38 and 0.72 and compare favourably with the results given by Brailsford[4] of $M_s = 1.4$. Substituting this value, the values of the definite integrals in Table III, $a = 0.2 \times 10^{-6}\ m^2$ and $\gamma = .2$ in equations 1 and 2 , it is found that the resulting maximum components of wire tension occur in the 18 cms channels, their magnitudes being:

$$F_r \Big]_{r_1}^{r_2} = 0.13 \text{ lb. force towards magnet centre}$$

$$T_r \Big]_{r_1}^{r_2} = \pm 0.053 \text{ lb. force.}$$

These forces will cause strains which will change the length of the wire even though the applied force at the outer end is constant. The change in length for an average force of 0.05 lbs. over a wire length of 10 inches ($E = 21 \times 10^6$ p.s.i.) is about $\frac{1}{12}$ mil. (0.00008 inch) which would result in an error of 300 p.s.i. in calculated azimuthal stress at the inner radius of the outer coil if unaccounted for. It can be concluded therefore that the magnetic forces on the invar wires may be neglected and will lead to errors not exceeding a few hundred p.s.i.

Brailsford[4] also gives magnetostriction coefficients which suggest that an increase in wire length of up to about 0.2 mil. might be expected. This may also be considered insignificant, especially when it is opposite in effect to the magnetic force.

Displacement measurements of the inner coil offer a different problem. Axial displacement may be transferred from the terminating assembly at either end of the coil through either cooling water or structural material of fairly constant temperature. The radial displacement of the inner surface of the inner coil may be transferred radially inwards into the access hole. In both cases therefore the environment through which displacement is to be transferred is magnetic - with much higher field gradients than for the outer coil - but not severely thermal.
Molybdenum wire was chosen for its availability, non ferro-magnetic properties and sufficiently low thermal coefficient of expansion (4.9×10^{-6}) - Reference 3 .

4.3 Voltage

The monitoring of voltage, either induced or as a resistive drop, presents no problem as the levels are usually of the order of a volt or so. Substantial twisted pairs are used and the problem of induced noise, discussed under "temperature", is relatively insignificant.

4.4 Pressure

No particular problems arose in the design of pressure monitors. In general, pressures have been transferred through small diameter tubing to localities outside the magnet structure suitable for the installation of commerical pressure transducers. Hydrostatic pressure measurement in high velocity flows required suitably shaped pitot heads designed after N.P.L. standards.

The remainder of this paper deals with technical detailed descriptions of the instruments including the routing of signal wires and transfer devices.

5. DESCRIPTION OF INSTRUMENTS AND ROUTING OF WIRES

It will be found useful to refer to the sectional drawing of the magnet included at the beginning of Chapter 2 .

This section is divided into four sub-sections, each headed by one of the four measured variables discussed in the previous sections, viz.,

1. temperature
2. displacement
3. voltage
4. pressure

5.1 Temperature

Measurement of the temperatures of the inner and outer coils and the electrodes and resistors feeding the inner coil, is here described.

In general, thermocouples are made from .008 inch diameter copper-constantan thermocouple wire formed into a regularly twisted pair.

5.1.1 Inner coil

Each inner sub-coil is terminated at either end with a 1/8 inch thick fibre glass insulating ring (to prevent thermal discontinuities due to end cooling) through which current is taken via cylindrical contact pins. Four temperatures of each sub-coil are taken, two at each end under the fibre glass rings. This number was chosen because it is expected that there will be a significant difference in temperature between the bottom - where cooling water enters - and the top, where water exits, and because a redundancy of two is advisable for such important measurements using such fragile instruments.

The construction of each of these thermocouples is illustrated in Figure 8 . First two small holes are drilled through the fibre glass ring at right angles to each other and at 45^{o} to the coil axis, the two holes meeting close to the end surface of the coil. The separated wires of a pair are then passed along these holes to meet again where the holes coincide. Here the joint is formed using 157PA high temperature solder, and the whole made firm and insulated by means of araldite. This method of construction provides the advantage of firm anchorage. The small loop so formed is oriented so as to have no coupling with the magnetic field.

After emerging from the insulating rings, the twisted pairs are routed radially outwards to the vicinity of the outer edge of the coil, being

fixed by means of lacing twine.

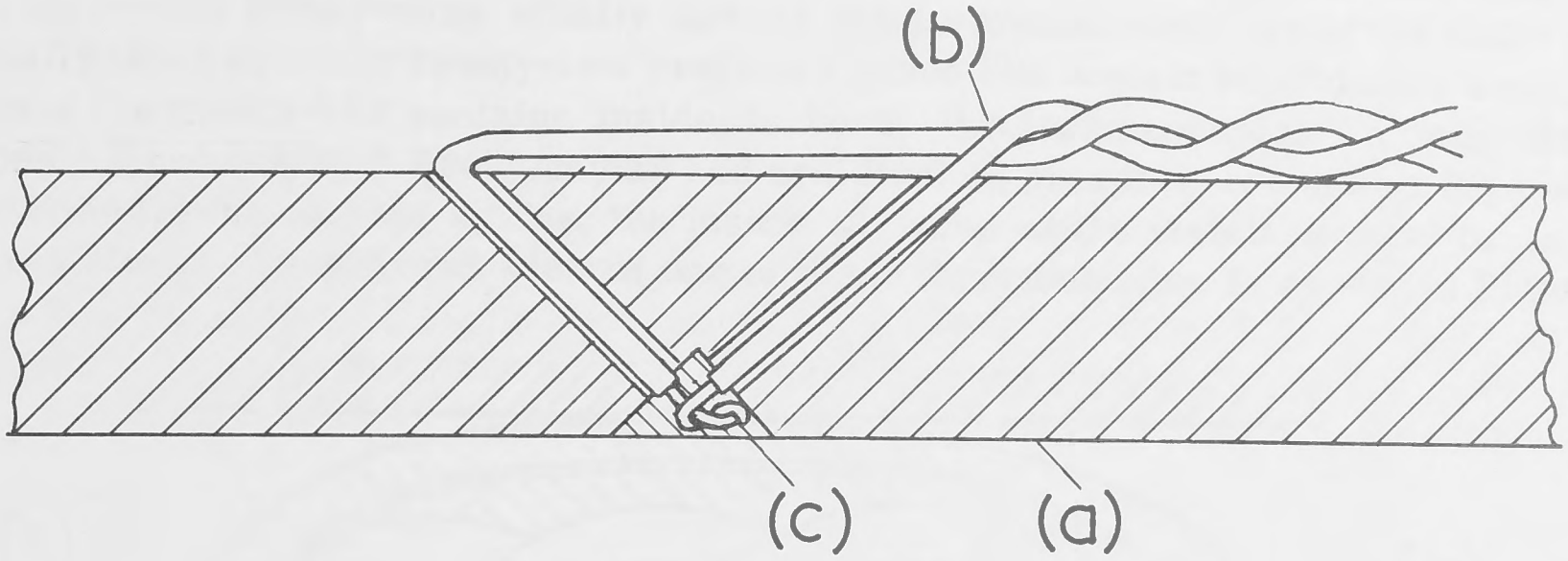

Figure 8. Construction of thermocouples for the ends of the inner coil.
(a) 1/8" fibre glass ring (section)
(b) .008" thermocouple wire
(c) araldite

The inner coil is terminated at each end by an assembly whose purpose is to provide independent contact pressure to the current-carrying contact pins, to carry the current through semiflexible conductors, and to distribute cooling water to the sub-coils. These assemblies, known as the terminating assemblies, are housed in a stainless steel body and it is through this body that the thermocouple pairs pass in 1/4" x 1/8" channels, two to an assembly. From there the wires pass through fibre glass tubes and water seals to the outside. Miniature connectors adjacent to the water seals allow ease of assembly.

5.1.2 Electrodes

Within the terminating assemblies for the inner coil described above, are twelve semiflexible conductors known as electrodes. The purpose of these is to provide connections to each of the 132 contact pins even though these may move axially as a result of temperature and stress changes. The electrodes are rather thin in order to enhance flexibility and hence tend to be hotter than most other conductors. Their temperature is monitored by means of two thermocouples to each electrode, each thermocouple being mounted on a 0.0005" mylar strip and glued to its own electrode. These pairs are routed to the channels in the terminating assemblies and thence follow the inner coil thermocouples.

5.1.3 Resistors

Feeding the electrodes, which in turn feed the inner coil, are 24 resistors, 12 at each end of the coil. These resistors are made from

stainless steel tube and copper tube, hard soldered together in various proportions to obtain the desired resistances. The purpose of the resistors is to distribute current evenly from twelve equally spaced points around each end of the coil. Actually there are only twenty-two resistors since two contain no stainless steel. Each of the twenty-two contains inside its bore, two thermocouples (a redundancy of one) insulated by 0.0005" mylar and araldited to phosphor bronze springs which press the thermocouples against the inside surfaces of the stainless steel parts of the resistors. An enlarged view of one of these thermocouples is shown in Figure 9.

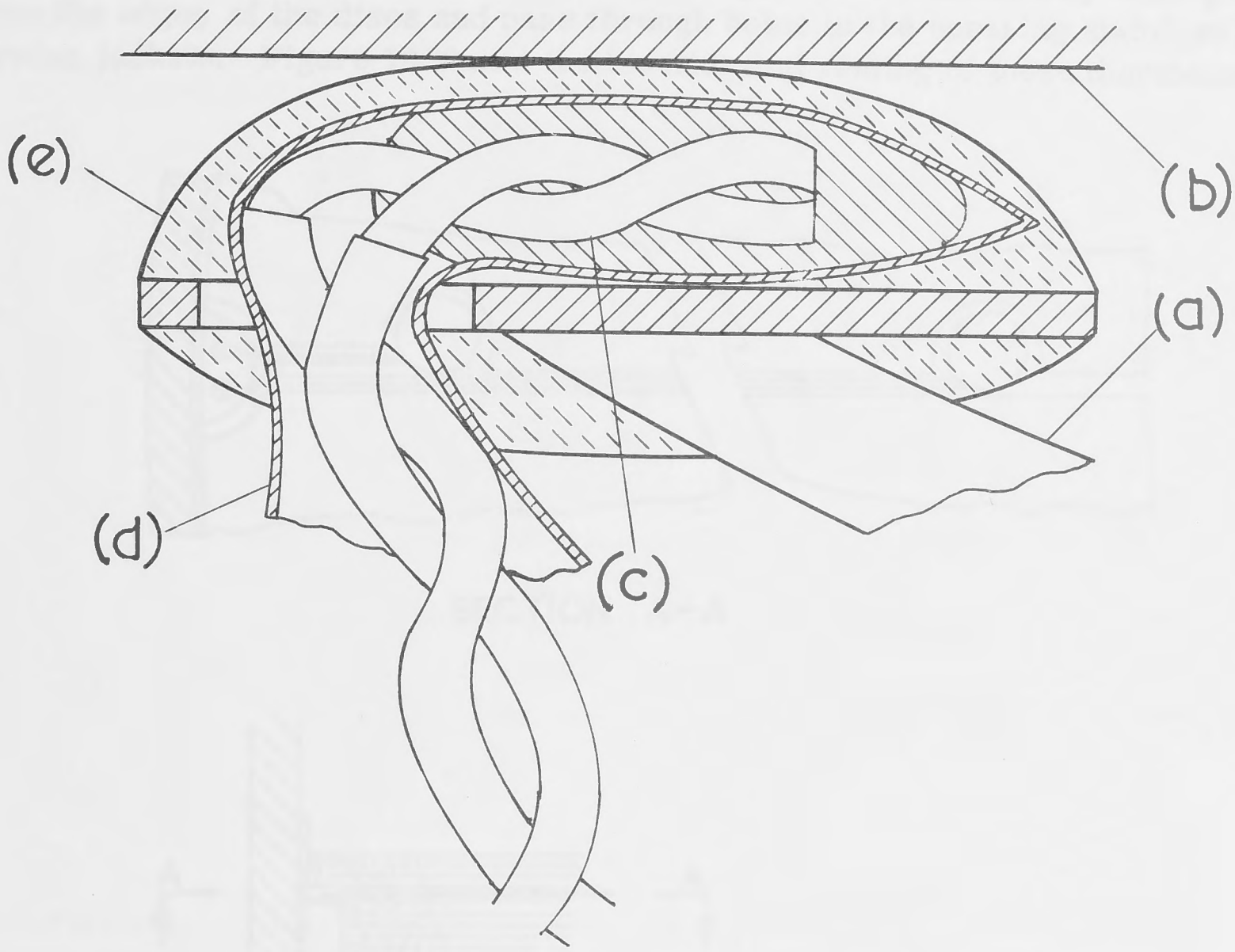

Figure 9. Construction of thermocouples used for measuring the temperature of resistors (greatly enlarged). The 0.035" phosphor bronze wire (a) presses the thermocouple (c) against the inside surface of the $\frac{1}{2}$" diameter bore of the resistor (b) .
(d) mylar
(e) araldite

5.1.4 Outer Coil

The thermocouples in the outer coil may be divided into two groups - fixed and moving. The fixed thermocouples, eight in all, monitor temperature at the inner and outer edges of the coil near the top and bottom faces.

There is again a redundancy of two.

The routing for the inside thermocouple pairs is along slits formed by two butting discs from which the coil is constructed. The discs are over 0.020 inch thick and their edges have been trimmed to provide a .025" wide rectangular section channel through which each pair runs, encased in a .020" diameter stainless steel tube. Near the outer edge, the channel is widened to take a second thermocouple. From there on, the routing for both inside and outside thermocouples is the same. They travel axially along a channel formed by scallops punched from the edges of the discs and pass through holes in the encasing stainless steel torsion jackets. Figure 10 shows the location and routing of these thermocouples.

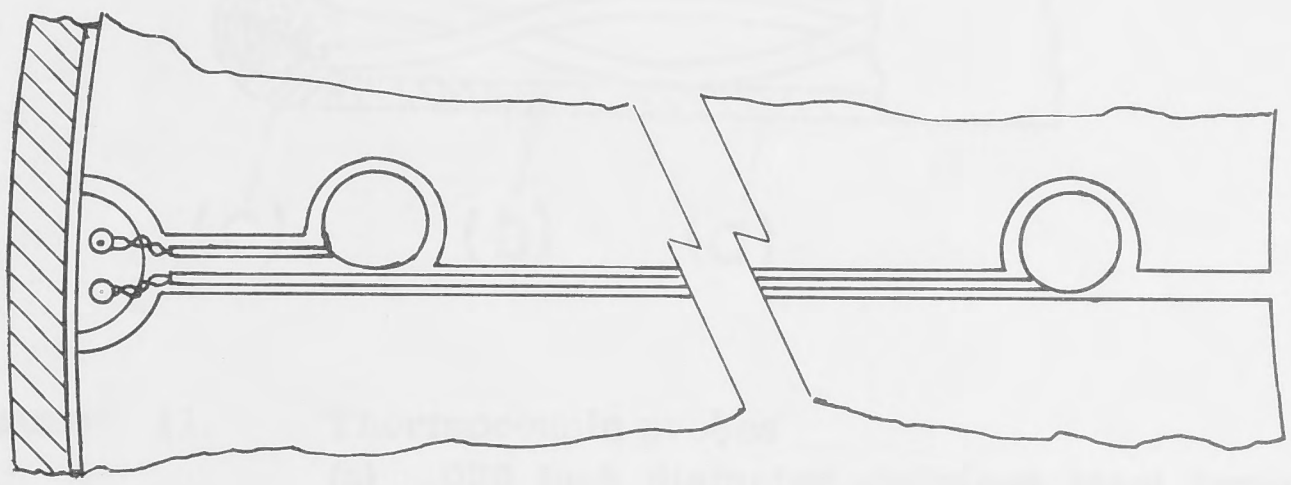

SECTION A-A

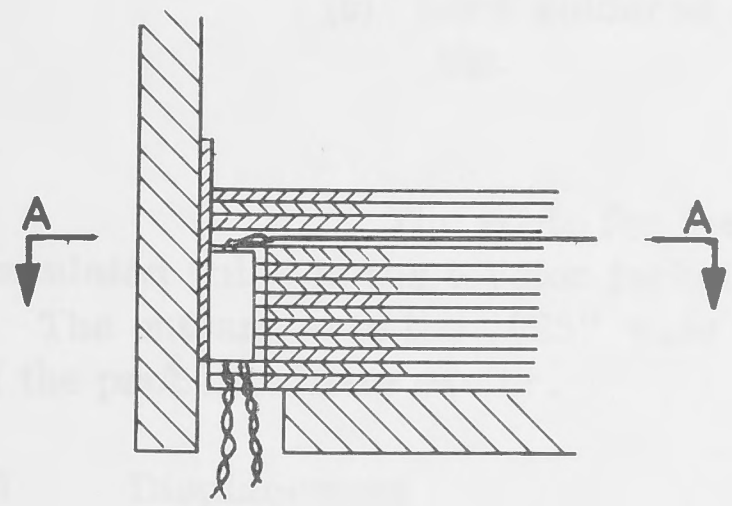

Figure 10. Construction and routing of the outer coil fixed thermocouples.

The moving thermocouples or "probes" are essentially similar to the inside fixed thermocouples but they are routed in a straight radial line to the outside of the magnet. This enables them to be moved along the .025" wide channels thus providing a complete temperature profile.

There are four levels where probes may be inserted, there being in general four positions at each level at intervals of 90° around the magnet.

Each probe comprises a .020" diameter stainless steel tube in which is a thermocouple pair soldered together at the end of the tube. The thermocouples are insulated from their tubes. The construction of these probes is shown in Figure 11. Each probe is mounted on a $\frac{1}{4}$" diameter brass tube with provision for a water seal and a means of indicating the position of the thermocouple within the coil.

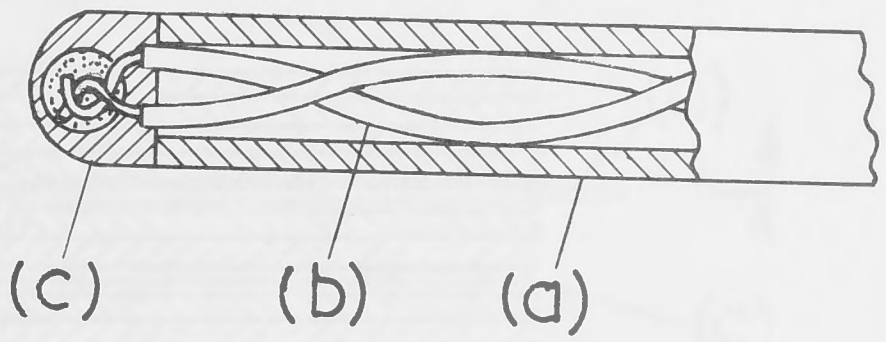

Figure 11. Thermocouple probes
(a) .020 inch diameter stainless steel approximately 8 inches long.
(b) copper-constantan thermocouple wire .003 inch diameter.
(c) hard soldered thermocouple joint in epoxy resin tip.

The route for the probes beyond the .025" wide channels is through insulated holes in the torsion jackets and through holes in the surrounding conductors. The entrances to the .025" wide channels are flared out a little to make insertion of the probes a little easier.

5.2 Displacement

Measurements are taken of the radial position of the inner and outer regions of the outer coil; the radial position of the inside surface of the inner coil and the axial position of the inner coil. In the case of the outer coil, the measurements are with respect to a circular reference frame which surrounds the magnet and which is supported independently.

5.2.1 Outer Coil

Thirty-two measurements are made, eight at each of

four levels in the coil. Of the eight at each level, four are of the inner regions and four of the outer surface of the coil, in each case spaced at 90° intervals around the coil.

For the inner regions, transfer of radial position is by means of .020 inch diameter invar wires threaded at the inner end. The outer coil is prepared with .025 inch wide radial channels similar to those used for the temperature probes. In addition, at the inner end of each of these channels is a small threaded tag formed from a disc of the coil. The invar wires may be inserted into the channels and screwed into the tags after the magnet is assembled. A wire screwed into its tag is shown in Figure 12 .

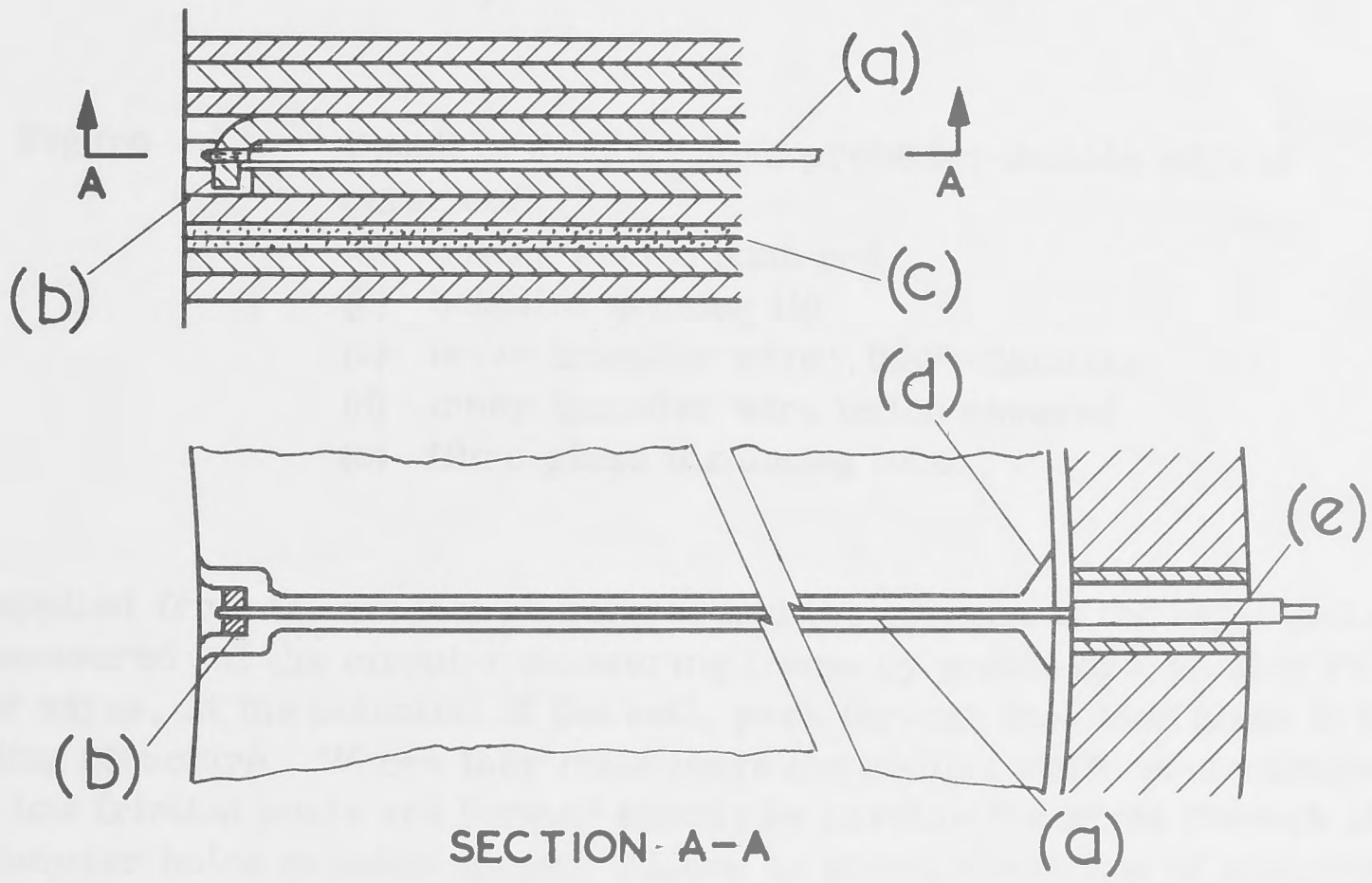

Figure 12. Details of invar displacement transfer wire from inner edge of outer coil.
(a) invar wire .020" diameter
(b) threaded tag
(c) insulation in outer coil
(d) discs shaped for easy entry of probe
(e) insulation lining access holes in torsion jacket.

At the outer edge, position is sensed by the bakelite tip of a spring loaded pusher. This is illustrated in Figure 13 . Again the position is transferred by means of invar wire through the surrounding structure to the exterior of the magnet.

In all cases, the invar wire is held under constant

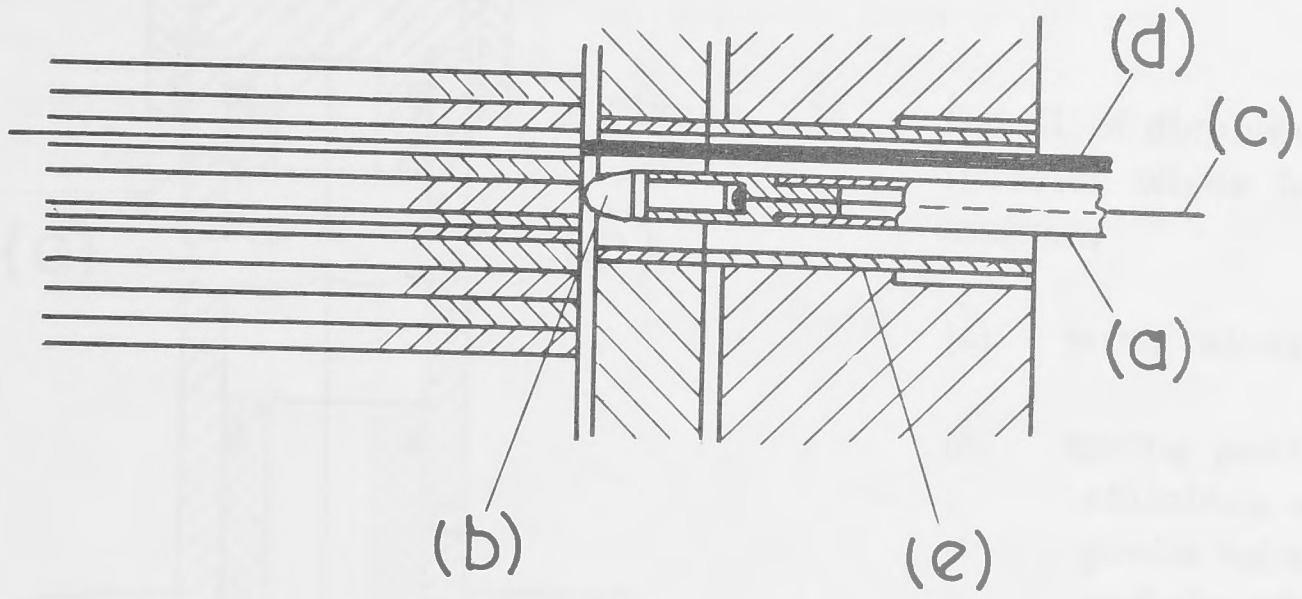

Figure 13. Detail of displacement probe for outside edge of outer coil.
(a) spring loaded push rod
(b) bakelite sensing tip
(c) invar transfer wire .020" diameter
(d) inner transfer wire teflon covered
(e) fibre glass insulating tube.

tension applied from the magnet structure, and the position of the outer end of the wire is measured off the circular measuring frame by means of a Bentley Proximator. The invar wires, at the potential of the coil, pass through insulated holes in the surrounding structure. Where they must leave the cooling water environment, effective low friction seals are formed simply by passing the wires through slightly larger diameter holes in teflon plugs. Figure 14 shows the means of applying force to the pusher which is pressed against the coil, and the teflon water seal.

5.2.2 Inner Coil

During the testing of the magnet it is intended to measure the radial position of the inside surface of the inner coil at four points spaced 90^{o} . These measurements will be relative to a compact central measuring frame placed in the access hole of the magnet. It does not seem possible to provide an alternative means of making these measurements when the access hole is required by experimenters.

The magnet access hole is within a tube, known as the core tube, placed inside the inner coil. Radial position of the coil is sensed by four small springloaded probes which pass through teflon seals in this tube. Bell cranks with jewel bearings translate radial motion from these probes to vertical motion which is transferred out of the access hole by means of four molybdenum rods.

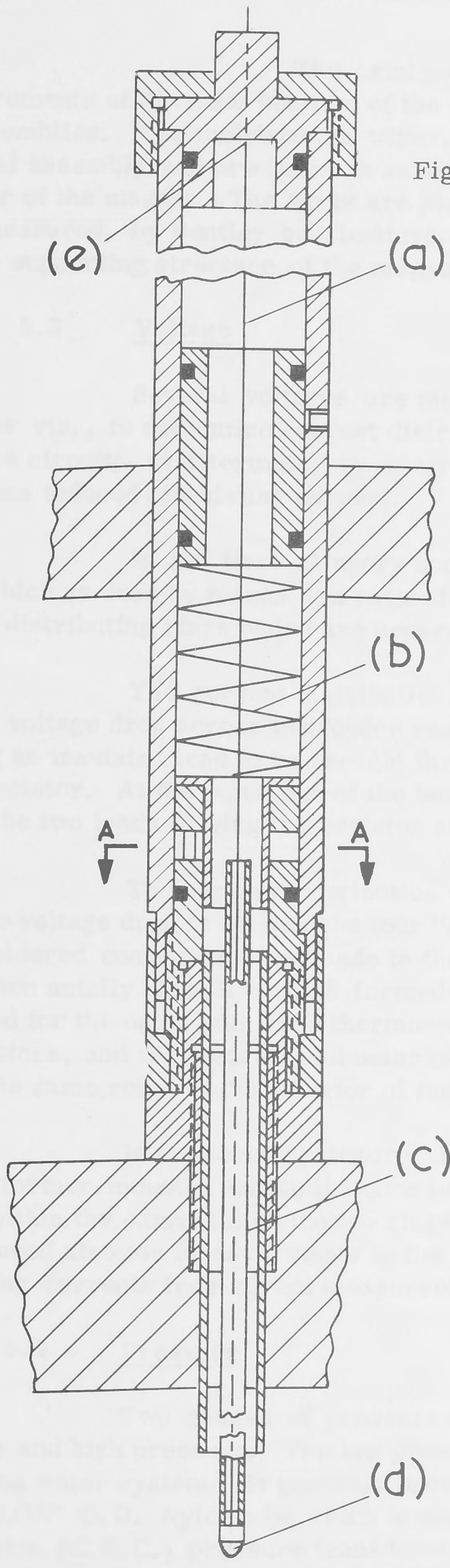

Figure 14. Detail of displacement transfer wires from the magnet.

(a) invar wires

(b) spring pushing stainless steel probe tube (c) and tip (d) against outer surface of coil.

(e) teflon water seal.

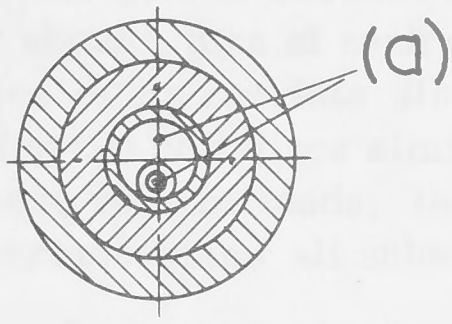

SECTION A—A

The axial position of the inner coil is determined from measurements of the axial position of the stainless steel bodies of the two terminating assemblies. Two molybdenum wires, 0.021" diameter, are attached to each terminal assembly and are taken in an axial direction through water seals to the exterior of the magnet. The wires are placed under tension and the position of their ends measured, by Bentley proximators, relative to the clamp tube which is the central supporting structure of the magnet.

5.3 Voltage

Several voltages are measured within the magnet for various purposes viz., to determine current distribution or to correlate with current in a resistive circuit; to determine, by integration, an average field strength; and to determine induced circulating current.

In the first category comes the measurement of magnet voltage itself which is done by means of a twisted pair of leads connected across the two current distributing rings which are separated by a quarter inch of insulation.

The current distribution to the inner coil is checked by measurement of voltage drop across the feeder resistors. Each of these resistors is hollow, enabling an insulated lead to be brought through the middle to connect to the inner end of the resistor. At the outer end of the bore of the resistor, another connection is made, the two leads leaving the resistor as a pair.

The current distribution within the outer coil is checked by measuring the voltage drop in each of the four "starts" for about a turn at each end of the coil. Soldered connections are made to the outer edges of appropriate discs and the leads taken axially along a channel formed by scalloping the coil discs similar to that described for the outer coil fixed thermocouples. These voltage leads, those from the resistors, and the resistor and outer coil fixed thermocouples all subsequently travel the same route to the exterior of the magnet.

In the second category, field strength, there is a coil wound on a bakelite former mounted within the core tube, and a number of single turn loops placed within the current distribution rings which surround the magnet. The latter may be used also for measurements in the third category - determination of circulating currents from direct measurement of the induced electric field.

5.4 Pressure

Two ranges of pressure are measured and may be classified as low pressure and high pressure. The low pressure measurements are all concerned with the cooling water system. In general, pressure is tapped off at the points of interest using a 3/16" O.D. Nylon tube which transfers it to Consolidated Electrodynamic Corporation (C. E. C.) pressure transducers mounted external to the magnet.

Pressures are monitored at both ends of both coils.

The high range covers water pressures, normally 2000 p.s.i. to 3000 p.s.i., which are associated with a commercial hydraulic unit used to apply the squeeze forces to both coils. Only the inner coil pressures are monitored continuously by means of C.E.C. transducers. Other hydraulic pressures are monitored by means of bourdon tube type gauges.

REFERENCES

1. CARDEN, P.O. : "Mechanical stresses in an infinitely long homogeneous Bitter solenoid with finite external field", Department of Engineering Physics, Australian National University Publication EP-RR 12, January, 1967.

2. CARDEN, P.O. : "Mechanical stresses in bonded plane helical solenoids with arbitrary external field", Journal of Scientific Instruments, 1968, Series 2, Vol. 1, pp. 437-443.

3. "Handbook of Chemistry and Physics", 44th edition, Chemical Rubber Publishing Co.

4. BRAILSFORD, F. : "Magnetic Materials", Methuen and Co. Ltd., London, 3rd edition, 1960.

5. BITTER, F. : "The Design of Powerful Electromagnets", Review of Scientific Instruments, Vol. 7, 1936, p. 479.

Publications by Department of Engineering Physics

No.	Author	Title	First Published	Re-issued
EP-RR 1	Hibbard, L. U.	Cementing Rotors for the Canberra Homopolar Generator	May, 1959	April, 1967
EP-RR 2	Carden, P. O.	Limitations of Rate of Rise of Pulse Current Imposed by Skin Effect in Rotors	Sept., 1962	April, 1967
EP-RR.3	Marshall, R. A.	The Design of Brushes for the Canberra Homopolar Generator	Jan., 1964	April, 1967
EP-RR 4	Marshall, R. A.	The Electrolytic Variable Resistance Test Load/Switch for the Canberra Homopolar Generator	May, 1964	April, 1967
EP-RR 5	Inall, E. K.	The Mark II Coupling and Rotor Centering Registers for the Canberra Homopolar Generator	Oct., 1964	April, 1967
EP-RR 6	Inall, E. K.	A Review of the Specifications and Design of the Mark II Oil Lubricated Thrust and Centering Bearings of the Canberra Homopolar Generator	Nov., 1964	April, 1967
EP-RR 7	Inall, E. K.	Proving Tests on the Canberra Homopolar Generator with the Two Rotors Connected in Series	Feb., 1966	April, 1967
EP-RR 8	Brady, T. W.	Notes on Speed Balance Controls on the Canberra Homopolar Generator	Mar., 1966	April, 1967
EP-RR 9	Inall, E. K.	Tests on the Canberra Homopolar Generator Arranged to Supply the 5 Megawatt Magnet	May, 1966	April, 1967

No.	Author	Title	First Published	Re-issued
EP-RR 10	Brady, T.W.	A Study of the Performance of the 1000 kW Motor Generator Set Supplying the Canberra Homopolar Generator Field	June, 1966	April, 1967
EP-RR 11	Macleod, I.D.G.	Instrumentation and Control of the Canberra Homopolar Generator by On-Line Computer	Oct., 1966	April, 1967
EP-RR 12	Carden, P.O.	Mechanical Stresses in an Infinitely Long Homogeneous Bitter Solenoid with Finite External Field	Jan., 1967	
EP-RR 13	Macleod, I.D.G.	A Survey of Isolation Amplifier Circuits	Feb., 1967	
EP-RR 14	Inall, E.K.	The Mark III Coupling for the Rotors of the Canberra Homopolar Generator	Feb., 1967	
EP-RR 15	Bydder, E.L. Liley, B.S.	On the Integration of "Boltzmann-Like" Collision Integrals	Mar., 1967	
EP-RR 16	Vance, C.F.	Simple Thyristor Circuits to Pulse-Fire Ignitrons for Capacitor Discharge	Mar., 1967	
EP-RR 17	Bydder, E.L.	On the Evaluation of Elastic and Inelastic Collision Frequencies for Hydrogenic-Like Plasmas	Sept., 1967	
EP-RR 18	Stebbens, A. Ward, H.	The Design of Brushes for the Homopolar Generator at The Australian National University	Mar., 1964	Sept., 1967

No.	Author	Title	First Published	Re-issued
EP-RR 19	Carden, P. O.	Features of the High Field Magnet Laboratory at the Australian National University, Canberra	Jan., 1967	
EP-RR 20	Kaneff, S. Vladcoff, A. N.	Self-Organizing teaching Systems	Dec., 1968	
EP-RR 21	Vance, C. F.	Microwave Power transmission Ratio: Its Use in Estimating Electron Density	Feb., 1969	
EP-RR 22	Smith, B. D.	An Investigation of Arcing in the Electrolytic Switch/ Test Load Used with the Homopolar Generator	Oct., 1969	
EP-RR 23	Inall, E. K.	Use of the Homopolar Generator to Power Xenon Discharge Tubes and some Associated Switching Problems	Mar., 1969	
EP-RR 24	Carden, P. O.	Pivoted Hydrostatic Bearing Pads for the Canberra Homopolar Generator	Dec., 1969	
EP-RR 25	Carden, P. O. Whelan, R. E.	Instrumentation for the Australian National University 300 kilogauss Experimental Magnet	Dec., 1969	

Copies of this and other Publications (see list inside) of the Department of Engineering Physics may be obtained from:

The Australian National University Press,
P.O. Box 4, Canberra, A.C.T., 2600.
Australia.

Price: $A1.00

National Library of Australia Card Number and ISBN 0 85584 005 6

Design principles relating to the strength and structure of the ANU 30 T electromagnet

O Carden
Department of Engineering Physics Research School of Physical Sciences, The Australian National University, Canberra, ACT, Australia

Received 6 December 1971, in revised form 21 February 1972

Abstract High magnetic fields may be generated by means of one or more concentric plane helical solenoids. The paper discusses the mechanical stresses in these solenoids when they are mechanically homogeneous and isotropic and compares them with the stresses that result when anisotropy is introduced. Under a wide range of conditions the introduction of anisotropy significantly reduces the maximum stress. The use of these principles in the ANU 30 T magnet is described.

1 Introduction

The ANU 30 T electromagnet consists of two concentric water-cooled solenoids. Probably the main difficulty in designing solenoids of this type is in accommodating the electromagnetic forces whose chief effect is to cause circumferential tensile stresses. The distribution and magnitude of these stresses depends on geometry, properties of materials and current distribution. High field solenoids are usually wide and squat with the ratio of outside diameter to inside diameter, known as alpha, typically between 3 and 6. The reasons for this are primarily bound up with the relation between power consumption and shape.

This paper is concerned solely with plane helical solenoids i.e. single layer solenoids with wide plate-like turns. They are characterized by the current density being inversely proportional to radius. An *isotropic* plane helix is one made of materials whose mechanical properties are homogeneous and isotropic, the latter being of prime significance here. The homogeneity and isotropy must extend across the bond between turns.

Although the treatment in this paper leads specifically to the application in the ANU magnet described in §7 it has been, nevertheless, kept as general as possible in order to have a wider applicability.

2 Stresses

The stresses in a long isotropic plane helical solenoid have been treated by several authors (Carden 1968, Kuznetsov 1951, Léon 1964). The results of the present author's treatment described elsewhere (Carden 1968) are reproduced here. The formulae include a superimposed field from another solenoid surrounding the one under consideration, the magnitude of which is characterized by S.

The symbols used are:

t azimuthal or hoop tensile stress;
p radial compressive stress;
B_m combined maximum magnetic field in the bore of solenoid;
p_m magnetic pressure $B_m^2/2\mu_0$;
S ratio of components of B_m,

$$S=\frac{\text{superimposed component}}{\text{solenoid component}};$$

m reciprocal of Poisson's ratio
a radius, a_1 inner radius.

The units are MKS.

$$t/p_m=\bar{A}X^2+\bar{B}X+\bar{C}(\delta^{-2}+1)+\bar{D}$$
$$p/p_m=\bar{E}X^2+\bar{F}X+\bar{G}(\delta^{-2}-1)$$

where

$$A=m/2(m-1)$$
$$\bar{B}=\frac{(1-\frac{1}{2}m)\{(S+1)\ln\alpha\}^{-1}-m}{(m-1)}$$
$$\bar{C}=\frac{-\alpha^2}{1-\alpha^2}\,\frac{m(S+\frac{1}{2})+(1-\frac{1}{2}m)/(\ln\alpha)}{(S+1)^2(m-1)}$$
$$\bar{D}=\frac{(m-2)(S+1)-(1-\frac{1}{2}m)/\ln\alpha}{(S+1)^2(m-1)\ln\alpha}$$
$$\bar{E}=-\bar{A}$$
$$\bar{F}=\frac{(1-\frac{1}{2}m)\{(S+1)\ln\alpha\}^{-1}+m}{(m-1)}$$

(compare $\bar{F}$ with $\bar{B}$)

$$\bar{G}=\bar{C}$$
$$X=\{\ln(a/a_1)\}/(S+1)\ln\alpha.$$
$$\delta=a/a_1$$

3 The two regions in high alpha solenoids

Figure 1 shows these normalized stresses plotted against normalized radius (for $S=0$) for several values of α. The

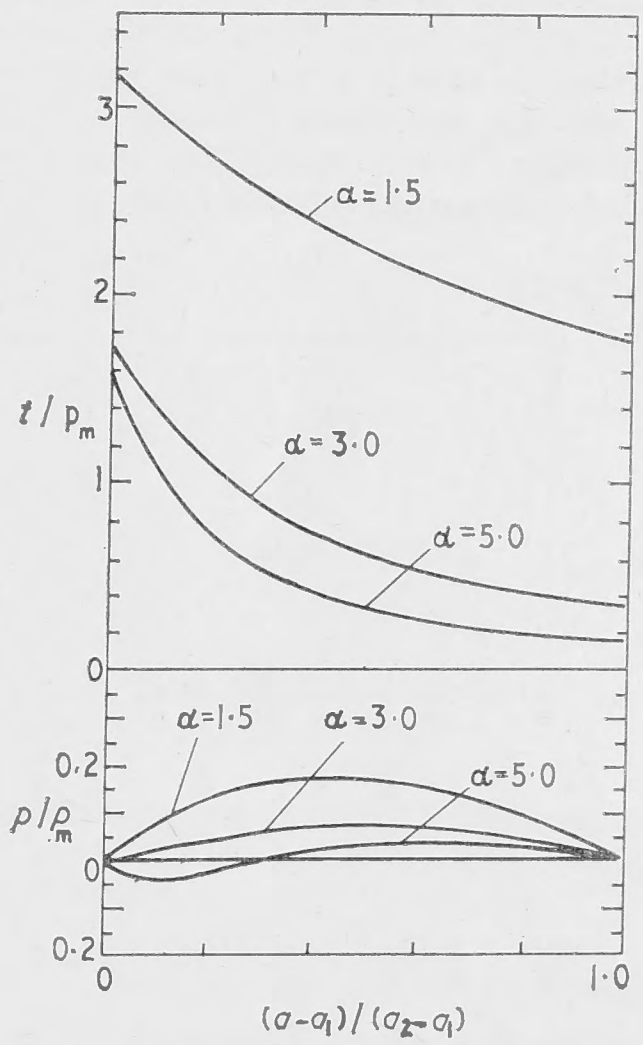

Figure 1 Normalized stresses in a long isotropic bonded helix as a function of normalized radial distance: a, radius; a_1, inner radius; a_2, outer radius

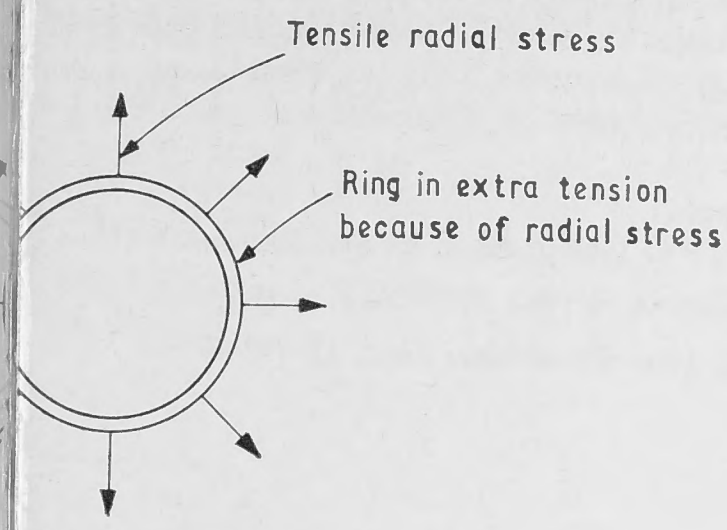

Illustrating the condition near the inner surface tropic bonded helix when radial stress is tensile

o be pointed out here is that for α less than about 3 l stress is compressive but for α greater than about 3 es tensile in an inner region before passing through ompression.

ld be possible to physically divide a solenoid with than 3 at the plane where $p=0$ without making any e to the stresses. Let us imagine that this is done so may talk of inner and outer regions as physically .

region – an alternative to isotropy

ination of the physical relation between radial and l stress reveals that, in the inner region, the tensile ess accounts for some of the peak azimuthal stress ner radius. This is simply illustrated in figure 2. If radial tension could be removed there should be a in azimuthal stress. This may be achieved by cutting id along a number of concentric cylindrical surfaces, emoving the radial strength and destroying the al isotropy.

ulting structure is a physically realizable one since simply of a number of nesting subcoils correctly with respect to one another and connected electri- arallel.

mple of the improvement in stress distribution rought about by this innovation is shown in figure 3 op stress is plotted for a homogeneous inner region he alternative arrangement of nesting subcoils. It n that in this case a factor of almost two improve- resulted.

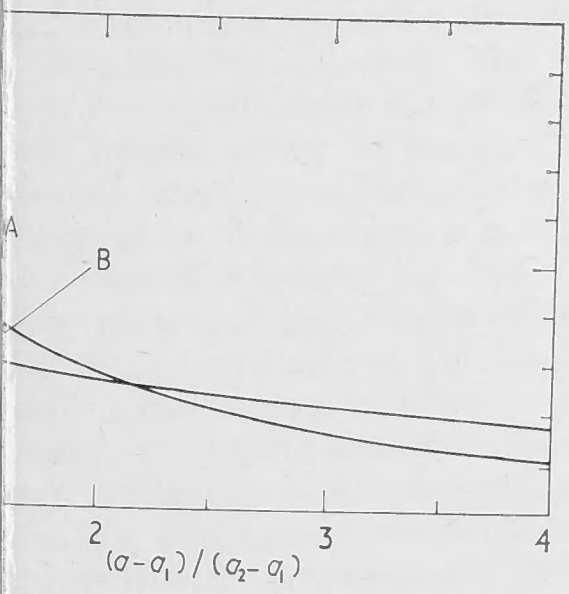

Normalized azimuthal stress plotted against radius =1: A, isotropic bonded helix; B, anisotropic ix, radial strength zero

The substitution of the subcoils makes no difference to the electrical characteristics because there is no radial current flow in the isotropic case and therefore it is immaterial whether the mating surfaces of the subcoils are in electrical contact or not.

Other advantages may be gained by division into nesting subcoils. They offer an easy way of manufacturing high alpha solenoids because it is much easier to make a number of low alpha helicies than bend metal into one of high alpha. Compared with the Bitter technique using interleaved split discs, nesting subcoils avoid the problems of providing adequate friction bond and dispersion of the slits which together require a large number of discs and high clamping forces when this method is taken to the limit of its capacity.

Assembly and replacement of damaged parts are easier in a system of subcoils than in a Bitter construction of similar strength.

5 Outer region

So far it has been shown that the stress distribution in the inner region of a high alpha isotropic solenoid can be improved upon by removing the isotropy. What of the outer region? Here, when isotropy is preserved, the radial stress is compressive which, being the reverse of the situation in the inner region, helps reduce the hoop stress at the inner radius of the region at the expense of the hoop stress at the outer radius which is in any case lower. An isotropic structure is therefore beneficial in helping to distribute stress uniformly.

6 Multicoil magnets

What has been said so far about a single isotropic solenoid applies also to the outer solenoid of a multicoil magnet since the stray fields from the inner coils are relatively small in the body of the outer solenoid.

The two physically separable regions that a single high alpha solenoid may be divided into may be regarded as two coils of a multicoil magnet so that in this sense we have already covered a specific range of inner solenoids and field division between the two.

What of the general case of an inner solenoid in a multicoil magnet? Figure 4 shows whether any particular combination of inner coil α and field division S results in a beneficial compressive stress or a detrimental tensile stress. This diagram

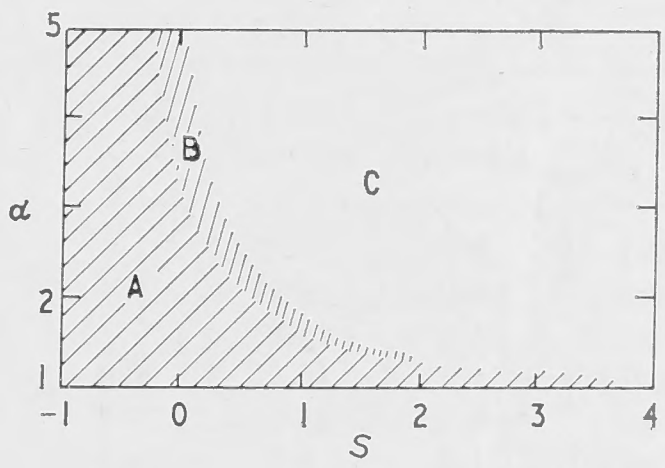

Figure 4 Radial stress conditions in the inner isotropic bonded helix of a long multicoil system as function of α_1 and S.

$$S=\frac{\text{centre field component from outer coils}}{\text{centre field component from inner coil}}$$

Region A, radial compression only; B, both tension and compression zones; C, radial tension only
An improvement in stress distribution would result from introducin g anisotropy into helicies in region C

was derived indirectly from the equations in §2 using the graphical information in Carden (1968).

The conclusion must be reached that the only isotropic inner solenoids that are beneficial are generally narrow ones and that the greater the proportion of the field contribution from the outer solenoid(s), the narrower the inner solenoid should be.

7 The concepts put into practice

The findings described above have been incorporated into the design of a 30 T magnet now operating at the Australian National University. The magnet, a photograph of which is shown in figure 5, consists of two plane helical solenoids

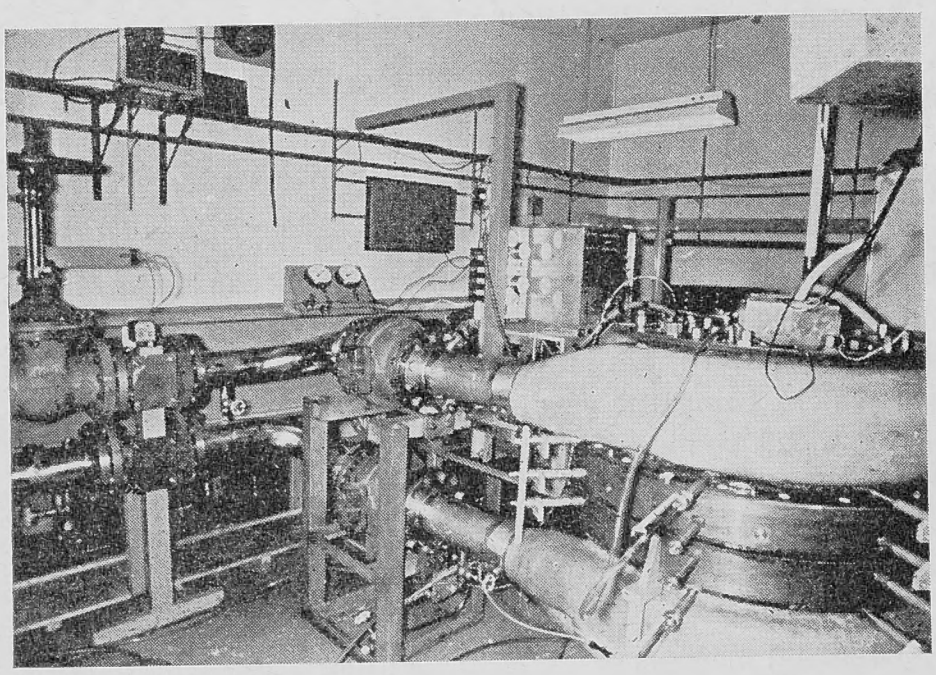

Figure 5 The ANU 30 T magnet shown connected to the busbars and cooling water system. The radial rods protruding from the girth of the magnet are instrument probes measuring temperatures and strains in the magnet

roughly coinciding with the two regions we have discussed. Table 1 lists the dimensions and characteristics of the two solenoids and their combination. The outer solenoid is made on the Bitter principle taken probably close to the extreme of its capacity whereas the inner solenoid consists of eleven nesting subcoils following the principles described above. These solenoids are the subjects of two following papers.

Table 1

	Inner solenoid	Outer solenoid	Total
Inside diameter (cm)	5·62	26·75	
Outside diameter (cm)	23·35	68·50	
Length (cm)	20·30	41·40	
Field contribution (T)	13·5	16·5	30·0
Power (MW)	4	25·5	29·5
Cooling water (kl min^{-1})	1·5	5·3	6·8
Current (kA)	26·7	168	194·7
Voltage (V)	150	150	

8 Conclusion

Given that the nesting subcoil arrangement described here is a practical alternative method of constructing a plane helical solenoid, isotropic structures such as Bitter solenoids should be limited to values of α less than 3 and generally to the outer coils of multicoil magnets. In this application their stress distribution is likely to be more uniform than the alter
However the alternative is advantageous for the inner sol
of multicoil magnets offer in most cases a consid
improvement in stress distribution.

References

Carden P O 1968 *J. Phys.* E: *Sci. Instrum.* **1** 437–43

Kuznetsov A A 1961 *Z. Tekh. Fiz.* **31** 944–7

Léon B 1964 *Revue Gen. Elect.* **12** 632–6

Journal of Physics E: Scientific Instruments 1972 V
Printed in Great Britain

sign and construction of e inner solenoid of the NU 30 T electromagnet

Carden
rtment of Engineering Physics Research School of ical Sciences, The Australian National University, berra, ACT, Australia

ceived 6 December 1971, in revised form 21 February 1972

ract The most important practical aspects of the n of the inner solenoid are described as well as details e manufacturing techniques used. Brief mention is e of other likely applications of this type of design.

ntroduction

general design principles leading to the adoption of centric nesting subcoils for the inner solenoid have been ribed in a previous paper. This paper will outline the or design and construction problems encountered in putting principles into practice and the solutions which evolved. an introductory definition one may regard a 'subcoil' as elix made from conducting wire whose turns have been d together with an insulating bonding material. The 'nesting' is meant to imply that the subcoils are made er precisely and fit closely together one inside the other form an integral unit which has certain electrical and hanical properties already described in an earlier paper.

Design of subcoils

advantage of the nested subcoil construction is the parative ease with which water cooling channels can be oduced at the interfaces between subcoils. All the cooling nnels have been made identical: basically 1 mm square, allel to the axis, and spaced evenly and as close as possible 2 mm circumferential pitch. The channels are formed ween the smooth inside surface of each subcoil and the oved outside surface of the one fitting inside it. The ess tube which passes through the innermost subcoil is grooved on its outer surface but the outermost subcoil not because it is actually only half the normal width and refore requires cooling from the inside only.

since the same hydraulic pressure is supplied to all channels, cooling characteristic of a unit area of subcoil interface constant. The subcoil widths were chosen so as to maintain nstant the heat fluxes into the cooling channels and there- re, taking into account the current distribution, subcoil lths are basically proportional to the square of their radii. follows that the cooling channel surface temperatures for points equidistant along the cooling channels should be constant and that the outermost subcoil will be the one with the hottest interior. The total number of subcoils were eleven (or ten and a half if one counts the outermost subcoil as half) ranging in overall width from 2·82 to 18·68 mm. They fit snugly one inside the other with barely an allowance of 0·02 mm for fitting.

The winding pitch and interturn insulation allowance for all the subcoils were the same, i.e. 2·12 mm and 0·125 mm respectively, chosen with regard to their effect on the resistance of the solenoid and because this pitch happened to suit the available lathes which could screw cut twelve turns per inch. There was therefore no need, in principle, for insulation between the subcoils thus offering the chance of using almost the entire surface of the water channels for heat transfer.

There was a problem however of alignment of turns between adjacent subcoils. Without taking precautions it would be almost impossible for the turns to align so that metal was opposite metal and interturn insulation opposite insulation and therefore almost certainly some turns of one subcoil

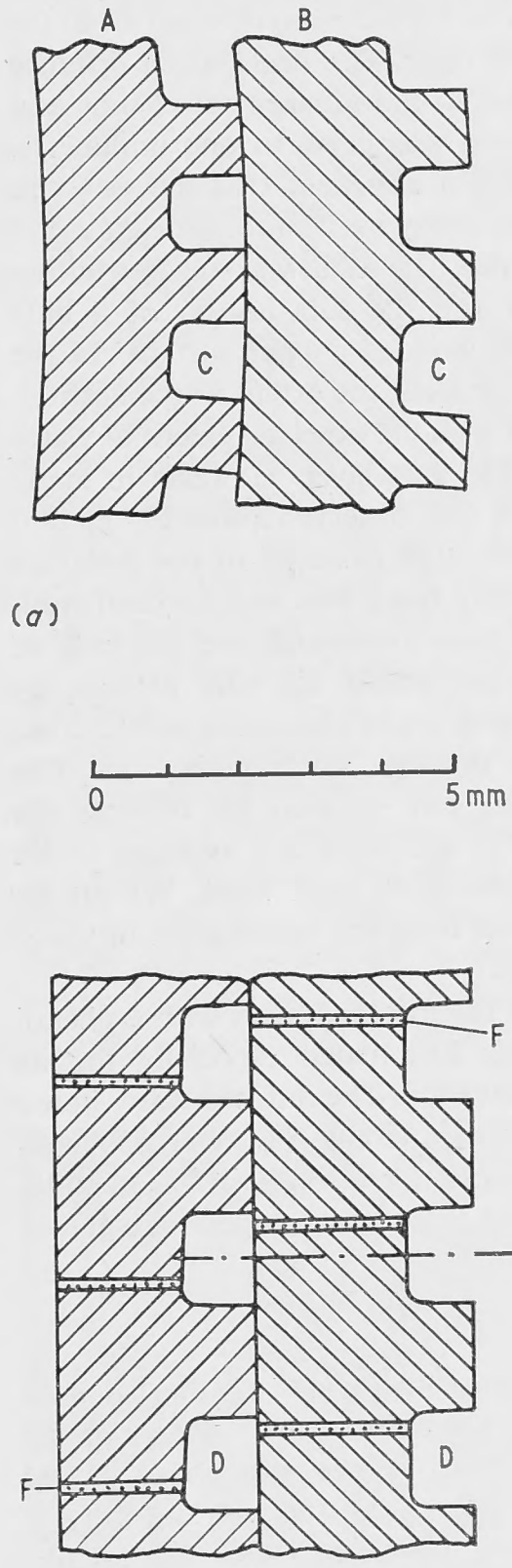

Figure 1 (*a*) Plan view of a small section of the two innermost subcoils A and B showing axial cooling grooves C (*b*) Sectional elevation showing helical grooves D with coincident centre planes E and bonding insulation F. The bond is shown at maximum permissible deviation from the groove centre

would short circuit pairs of adjacent turns of a neighbouring subcoil. This problem was avoided by carefully spacing the turns during the bonding process using a lathe and by subsequently machining in the outer surface of each subcoil a helical groove approximately 1 mm square along the bond line. The effect of this groove was to permit deviations of the bond line from the ideal position of about $\pm 0{\cdot}5$ mm. It was found that this tolerance could be achieved with moderate care during manufacture. Figure 1 shows sections of the two innermost subcoils and illustrates the tolerance permitted by the helical groove.

3 The interturn bond

The duty of the material between turns was to bond the turns together against a shear stress as great as 4·1 MPa (600 lb in^{-2}) and to provide interturn insulation. The maximum working temperature was expected to be less than 150°C but this would occur at a point where the shear stress would be only 10% of the maximum. Several types of hot curing epoxy resin were found to be suitable as far as the above requirements were concerned. However, even the most water resistant epoxy resin was found to allow the diffusion of water from the exposed edge of the adhesive layer. The penetration distance was found to be proportional to the square root of time and in six months the penetration was close to one millimetre. From numerous observations it appeared that the water in the epoxy competed with the epoxy itself in forming chemical links with the copper molecules. The result was the destruction of the copper–epoxy bond and the substitution of a blue compound on the previously bonded copper surface. In the best prepared experimental samples, the extent of the destruction of the bond agreed well with the expected extent of water diffusion from the edge of the resin layer. However in many cases a marked acceleration was observed probably caused by the free entry of water through passages in the interface region where the copper–epoxy bond was already destroyed. Any increase in bulk of the blue compound over the bulk of its original local components would aid this process by wedging open the interface and might also cause acceleration of the chemical reactions through stress activation. The significance of this problem can be seen by relating the observations to the innermost subcoil which averages about 2 mm in width and is wetted from both sides. Within six months then one might expect complete penetration of water and destruction of the bond.

The solution was to cover the metal surfaces with a phenol formaldehyde baked coating formulated especially for its high resistance to water penetration. The diffused water in the epoxy bond was not observed to have any effect on the formaldehyde–epoxy bond and in accelerated tests with this method, no deterioration was observed after the equivalent of eighteen months exposure to water.

4 Subcoil terminations

The problems associated with the ends of the subcoils probably gave more concern than any other aspect of the inner solenoid. As explained in the previous paper on the outer solenoid, it is necessary to ensure symmetrical entry of current at the ends. This is especially important for the inner solenoid where, in the worst case of asymmetric current entry, one might expect bond shear stresses to increase by 2π. Such an increased stress would, in places, exceed the strength of the bond by about 50%.

A sufficient approach to symmetry is achieved by providing at each end of the solenoid twelve equipotential entry zones, centred on twelve equally spaced radii. Each zone is fed from a resistor of such a value as to ensure that each passes

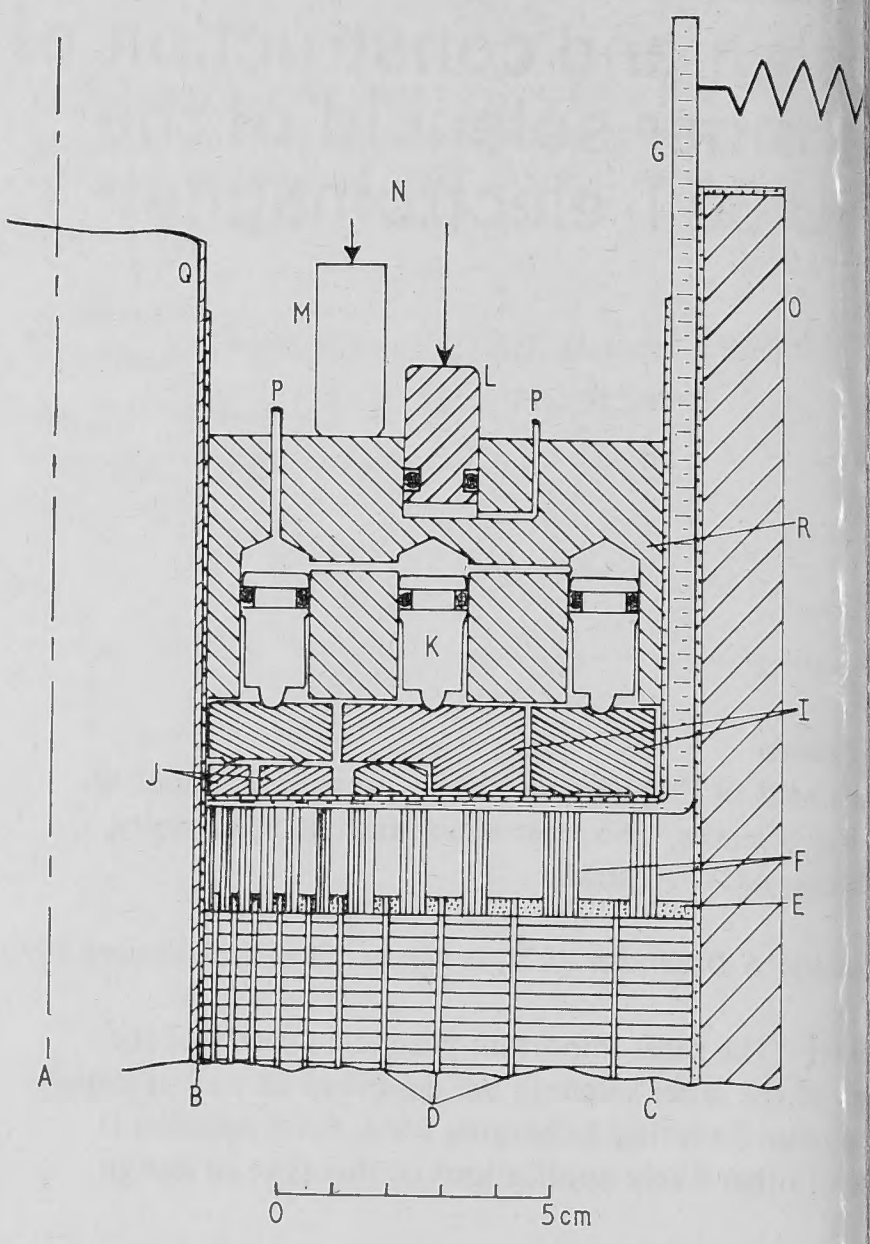

Figure 2 Sectional elevation of the upper termination of the inner solenoid, semi-schematic. A, axis of electromagn B, inner subcoil; C, outer subcoil; D, cooling water channels; E, fibre glass end caps to subcoils; F, current-contacts in one equipotential zone; G, conductor feeding equipotential zone; H, zone feed resistor; I, force distribution beams; J, force distribution discs; K, hydraul (water) source of contact force; L, hydraulic reaction to electric contact force and force on location contacts (not shown); M, fixed stops – one end only, springs at other en N, fixed restraining structure attached to support tube; O, support tube; P, hydraulic inlets – from common sourc at 17 N m^{-2} (2500 lb in^{-2}); Q, core tube providing access to high magnetic field; R, terminal assembly housing. Note: cooling water passes through the housing R in hole not shown

one twelfth of the total current. The connection betwee zone resistor and the eleven subcoils is effected by means c radially oriented slightly flexible copper conductor and ele rod-like contacts, one for each subcoil. Each contact backed by a constant force producing mechanism capable following the small movements of the contact resulting fr the axially directed expansions and contractions of the subc upon which it bears. The dimensional changes of the subco which might be as much as 0·1 mm are caused by heating a by strains which are the result of electromagnetic compressi and the Poisson effect of the azimuthal stresses. Figure illustrates the means adopted for producing the contact for The force is derived hydraulically and distributed throug system of beams, discs and fulcrums to the individual contac In addition to the current carrying contacts, an equal numb of locating contacts bear against the subcoil ends. The serve to position the subcoils correctly in relation to o another and to locate the assembly of subcoils within t superstructure.

order to eliminate thermally produced shear stresses the subcoil bonding material, it is necessary to prevent heat flow. This does not occur appreciably in the body e subcoils because current density is independent of position and because the cooled surfaces are axially ated. For the end turns, the same situation is approached achining the end surfaces flat and capping them with al insulation. The machining process causes the end to be tapered so that their cross sectional areas match rogressively increasing current in them developed by the ssive increments from the twelve contact zones. The end made from fibre glass, can be seen in figures 2 and 5. locating contacts bear upon the end caps whereas the nt contacts pass through as shown.

anufacture of subcoils

s of zirconium–copper alloy (0·25% Zr) were purchased gland and extruded and drawn into wire at Port Kembla, ralia, following an experimental programme aimed at ving the required degree of hardening in the wire-forming ess. Nine different sizes of wire were made each with a ngular cross section.

r the manufacture of each subcoil, the appropriate wire straightened and milled on the bond faces with a slight r to compensate for the deformation during coil shaping. coils were formed in a specially made continuous bending hine. At this stage care was exercised to ensure that the took the form of a true plane helix close to the desired eter. The helix was then stretched on a frame, coated the phenol formaldehyde preparation and baked. After king it was prepared for resin bonding and mounted in the having attachments which essentially applied resin een parted turns, closed them up and correctly spaced n. The helix was then placed in an oven for curing, after h the inside and outside cylindrical surfaces were mach-. This was followed in turn by milling the axial cooling oves, screw cutting the helical groove and finally facing the coil ends. The last operation was quite critical as it was ortant to obtain exactly the required number of turns,

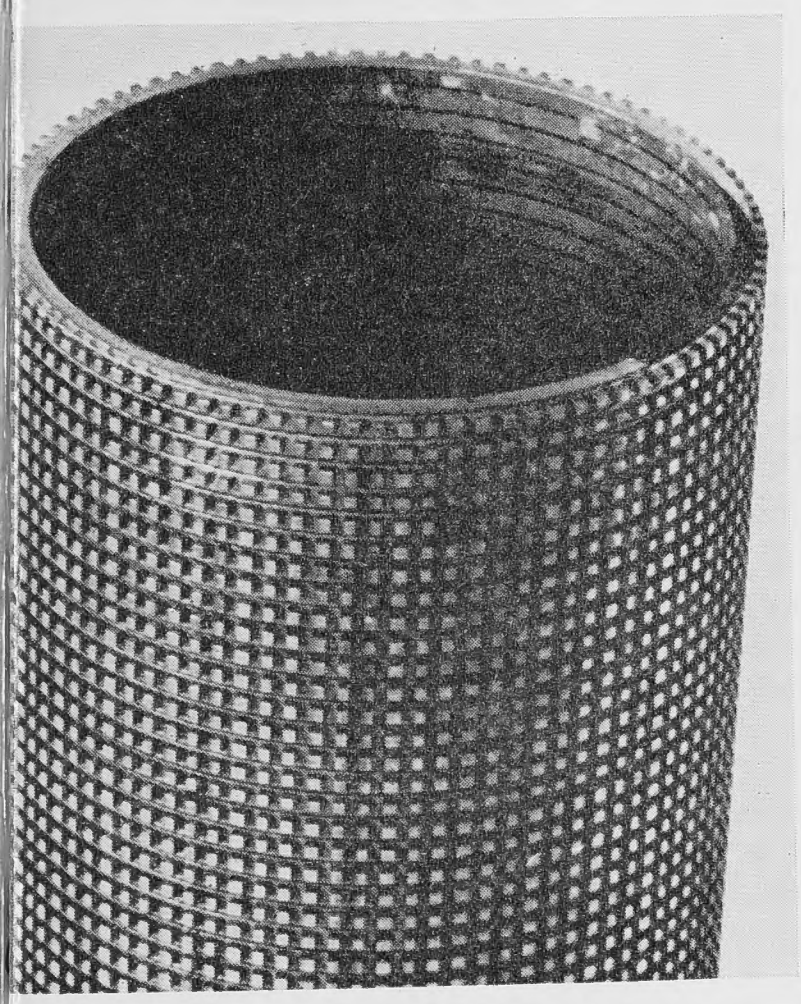

ure 3 The innermost nesting subcoil. Inside diameter 2 cm

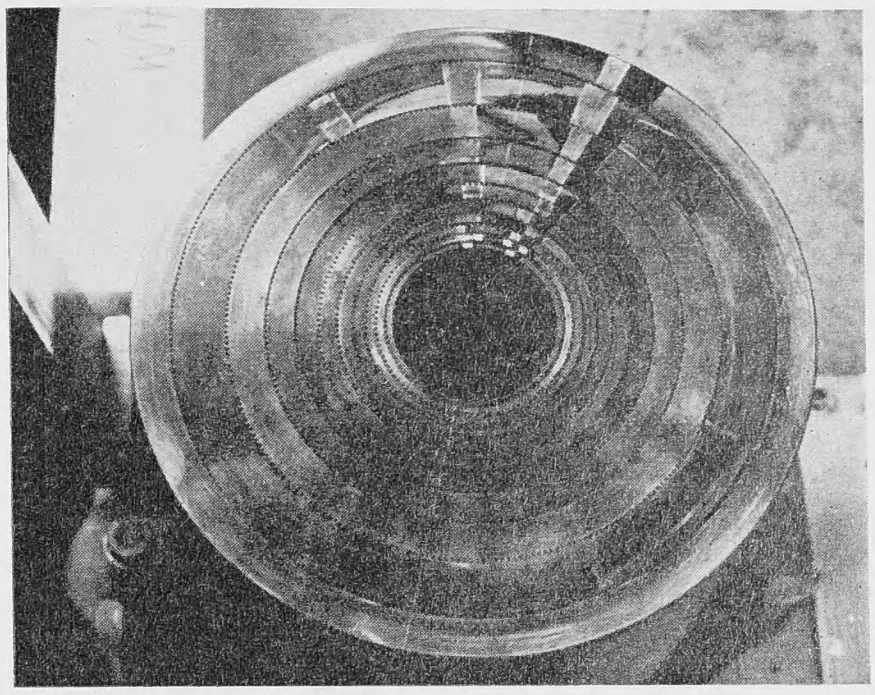

Figure 4 The eleven subcoils fitted together to form the inner solenoid. The dark areas evident on the top face of the solenoid are the bonding and insulating layers exposed by machining the ends of the subcoils. In places parts of the exposed layers can be seen to have been removed to enable contact rods to reach the underlying conductor

rather than an exact length, in order to suit the orientation of the terminating zones.

Each subcoil was checked for short circuits between turns that might have been caused by machining burrs or scratches using the principle that the magnetic field from a current passing through a fault-free subcoil should possess practically no circumferential component whereas current passing through an interturn short should. Using a lathe, AC of a few kilohertz and a small search coil mounted on the tool post, a method was found that was very sensitive to faults on the inside and outside of the subcoils. A microscope was used for final visual location and removal of the faults.

Figure 3 is a photograph of the innermost subcoil ready for assembly.

6 Assembly of subcoils

The finished subcoils were fitted one inside the other and orientated to match the contact zones. However, prior to fitting, their exact lengths were measured and also the angle on the end faces between the positions of the centres of the emergent bond line and helical groove. This information enabled the lengths of the locating contacts to be determined.

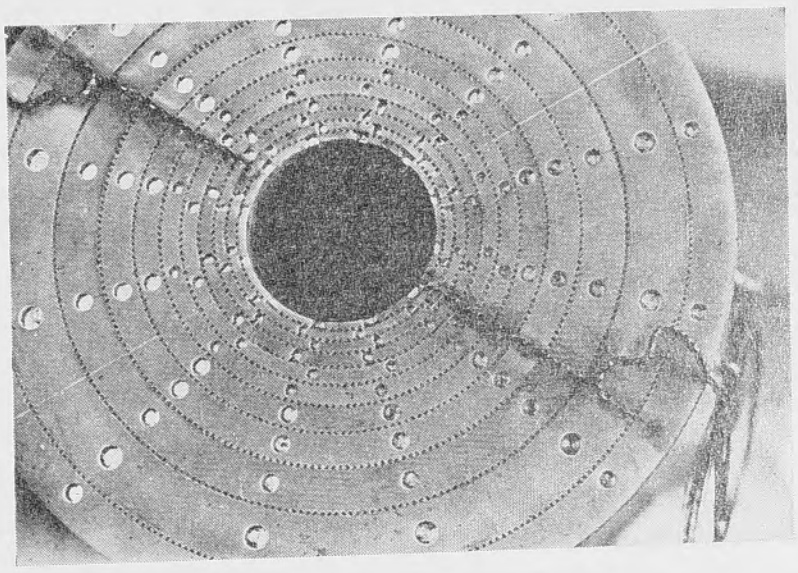

Figure 5 The solenoid fitted with fibre glass capping. Access holes from the 132 contact rods can be seen. The wires visible connect with 22 thermocouples fitted to measure the temperature of the subcoils

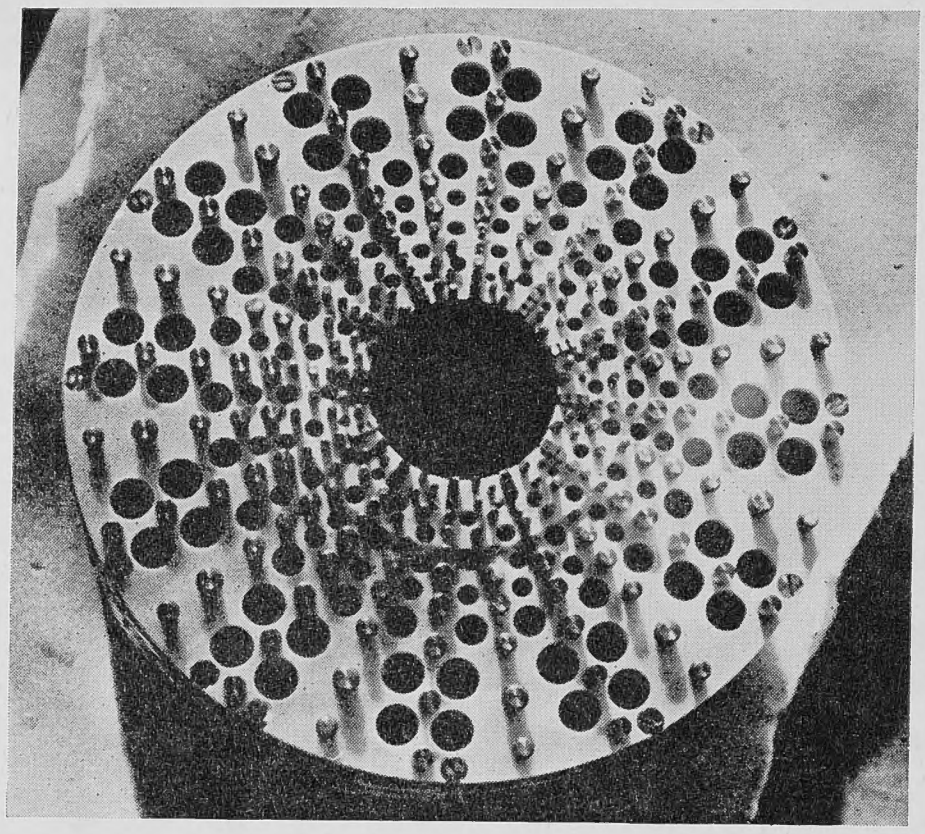

Figure 6 A view of the mating face of one of the terminal assemblies showing the protruding contact rods and locating rods

Figures 4 and 5 are photographs of the assembled inner solenoid and figure 6 shows the contact rods which mate with one end of the solenoid.

7 The complete inner solenoid assembly

Figure 7 is a photograph showing the inner solenoid between its two terminal assemblies. The unit contains all the contact rods, force distribution mechanisms and hydraulics that have been described as well as instrumentation for observing temperature and pressures. Extra instruments measuring strain and magnetic field were inserted afterwards.

8 Summary

This paper gives an account of the major considerations in design especially with reference to the subcoils. Many other aspects have not been dealt with but suffice it to say that studies were made of the electromagnetic forces associated with every part of the current path, the heating and temperature of each part, the flow of water through each passage as well as the practicability of manufacture of each part and the means of assembly of the whole. Most of these studies w concerned with steady state energization but consider attention was also paid to transient energization. In m complex situations mock-ups were constructed and stu under simulated conditions. The conclusion that might reached now following successful testing is that the desig fundamentally sound. Given this conclusion the aut believes that the same methods may be applied to proc more intense magnetic fields in conventional electromag and to produce compact and efficient solenoids for opera within superconducting solenoids. The methods may applicable to superconducting solenoids themselves now the magnetic fields being achieved by these devices are suf ently intense to cause designers to give close consideratio the mechanical stresses within them. Copper wires contain filamentary superconducting material seem to be ide suited for forming into subcoils while the enhanced ac for helium between subcoils might alleviate problems w stability and rapid field changes. The subcoils might of cou have to be energized in series necessitating layers of insulat between them but this requirement need not cause g difficulty.

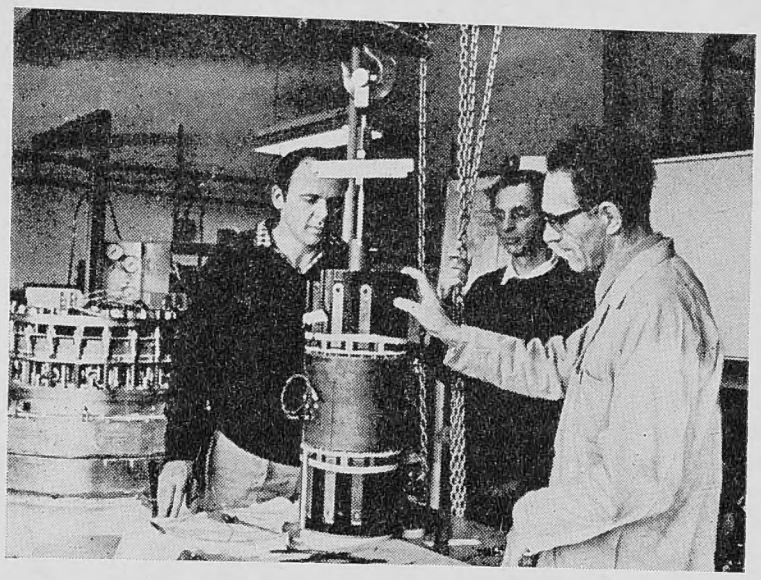

Figure 7 The inner solenoid assembly ready for fitting into the remainder of the 30 T electromagnet (visible in the left background). The assembly consists of the inner solenoid between the upper and lower terminal assemblies. In the sides of the latter can be seen the current connections, twelve each end

Journal of Physics E: Scientific Instruments 1972 Volume 5
Printed in Great Britain

The design and construction of the outer solenoid of the ANU 30 T electromagnet

D Carden

Department of Engineering Physics, Research School of Physical Sciences, The Australian National University, Canberra, ACT, Australia

Received 6 December 1971, in revised form 21 February 1972

Abstract The solenoid described here is the outer coil of a coil system for generating a 30 T magnetic field. Analysis showed that a homogeneous plane helix would be adequately strong. The Bitter principle of constructing a plane helix was chosen for practical reasons but difficulties arose due to loss of strength from the slits in the discs and from the fact that circumferential strength had to be developed through friction between the discs. The problems were overcome by adopting a design where each turn was made up of 6 discs interwound in a staggered pattern which reduced the slits and provided adequate friction bonding. The effect of the slits is small reducing the strength to 96% of an ideal continuous plane helix. It is shown that the Bitter solenoid may fail either by expansion or by unwinding. The relevant factors involved in both modes are considered and it is shown that unwinding is the most serious and cannot be remedied by increasing the number of turns per turn. A system of keying the end turns via insulating cylinders is described and illustrated. The solenoid is wound as a two-start helix with one turn each end four-start. Reasons for these features are described associated with current distribution and ease of insulation checking. The complete construction technique is described and illustrated.

1 Introduction

Some four years ago work was begun at The Australian National University on the design of a water cooled 30 T experimental electromagnet which was to be used for research in solid state physics. The design evolved into basically two concentric plane helical solenoids, electrically in parallel, the outer one of which is the subject of this paper. This solenoid requires 26 MW of power from the department's homopolar generator delivered at 150 V and 168 kA whereas the two together require 30 MW at the same voltage and 200 kA. The outer solenoid, which will henceforth be called the solenoid, requires cooling water at the rate of 6·8 $m^3 s^{-1}$ (4 $ft^3 s^{-1}$) at approximately 1·7 MPa (250 lb in^{-2}) pressure. The major dimensions of this solenoid are shown in figure 1 of Carden (1972).

2 Stresses

Stresses have been calculated using formulae and methods given by several authors (Carden 1968, Kuznetsov 1961, Léon 1964) for the case of a bonded plane helix in which the mechanical properties of the solenoid material are homogeneous, elastic and isotropic everywhere including the interface between turns. Although the design chosen is not homogeneous, elastic nor isotropic, this model is nevertheless the best available that has been mathematically analysed.

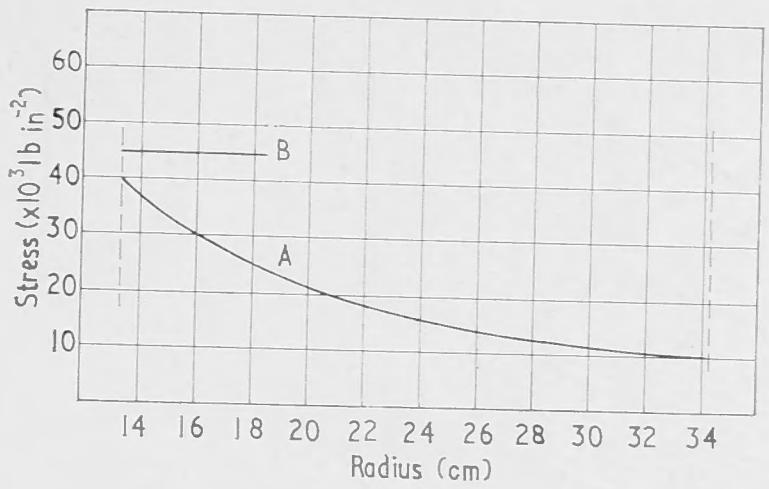

Figure 1 Stresses in outer coil. Material is 0·07 % Ag–Cu hard temper. A, expected azimuthal stress; B, expected 0·1 % proof stress

The calculated azimuthal or hoop stress is shown in figure 1. It will be seen that the maximum stress is high, this being the result of compactness which is favoured because of the economies it brings in material, power and water consumption. Axial compressive stress results from electromagnetic forces and externally applied axial forces. The electromagnetic component is zero at the ends but builds up to as high as 83 MPa (12 000 lb in^{-2}) at the median plane of the solenoid.

3 Design and construction

The construction method invented by the late Francis Bitter (1936, 1937, 1939, 1962) was chosen for the ANU solenoid as the most practical way of achieving a bonded plane helix of the size required. This method involves making a large number of thin discs each perforated with cooling holes and each having a radial cut or slit right through. The discs are interleaved in a pattern to form a helix, the holes aligning to form axial cooling channels. A solenoid constructed this way requires axial compression to provide the friction which effectively bonds the discs together. The magnitude of the axial compression required depends on the number of interleaved discs and the pattern of interleaving. In general the greater the number of discs and the greater the extent of interleaving, the less axial compression will be required.

Usually adequate axial compression resulting from electromagnetic forces prevails throughout most of the solenoid except near the ends. An external means of applying axial force is therefore necessary.

The pattern in which the discs are interleaved is best represented in a diagram obtained by projecting the solenoid radially outwards upon any cylindrical surface and developing the projection so formed. Vertical dimensions are exaggerated for clarity. Figure 2(*a*) is such a representation of the ANU solenoid. The pattern itself is believed to be unique and the number of discs per turn, sixteen, is to the author's knowledge, greater than anything attempted previously.

The pattern, identified henceforth as the ANU pattern, may be generalized for any number of discs per turn n. Its special features are that n must be even; that the slits of alternate discs appear in planes perpendicular to the axis, the planes being $n/2$ disc thicknesses apart; that the slits in each plane are spaced $4\pi/n$ radians apart; and that the slits

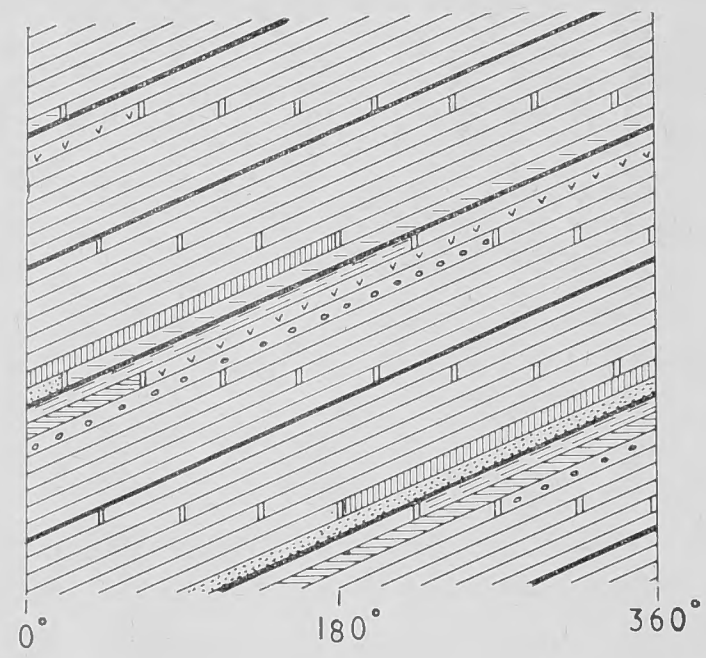

Figure 2 The ANU pattern for interleaving Bitter type split discs. (*a*) Developed diagram of pattern (vertical scale exaggerated). Shading identifies specific discs. Groups of eight discs are separated by insulation shown as a thick line. (*b*) The pattern drawn in the correct proportions (for the inner radius of the coil). Four adjacent slits shown encircled

in one plane are angularly displaced $2\pi/n$ radians from the slits in the neighbouring planes.

The discs are made from hard rolled silver–copper (0·07% Ag) of nominal thickness (0·518 mm). They arrived at the ANU workshop as full discs of approximately the finished outside diameter. All subsequent processes were carried out within the University. Cooling holes and the central hole were punched out, the outside diameters turned and the radial slits guillotined. Some of the discs were found to open or close at the slit when placed on a flat surface due to the fact that they had originally been slightly conical or buckled. This fault was corrected by pressing over the full length of selected radii using a press tool in the shape of a narrow elongated triangle. Depending on the orientation of the triangle with respect to the disc (point directed inwards or outwards) a gap or an overlap at the slit could be corrected.

Other difficulties arose because of the variation in thickness both from disc to disc and within each disc. The average thickness was found to vary between 0·483 and 0·571 mm, whereas, typically, the variation within discs was $\pm 0{\cdot}01$ mm. The former variation necessitated sorting (by weight) into sixteen groups. Members of each group butted together in the solenoid thus preventing steps and voids which would otherwise occur if discs of unequal thickness were butted. The latter variation-within-discs was unfortunately systematic which, if uncorrected, would have caused a hump in the middle of the solenoid greater than the 3·2 mm each end which could be tolerated. It was corrected by grinding the middle of each eighth disc of the solenoid.

Insulation consists of 0·08 mm 'Pyre ML' bonded glass fabric supplied by the Dupont Corporation. The material was cut into discs of the same size as the conducting discs, drilled with holes to match the cooling holes and slit radially. In the solenoid they butt together to form continuous plane helical insulating layers but their butt joints are displaced so

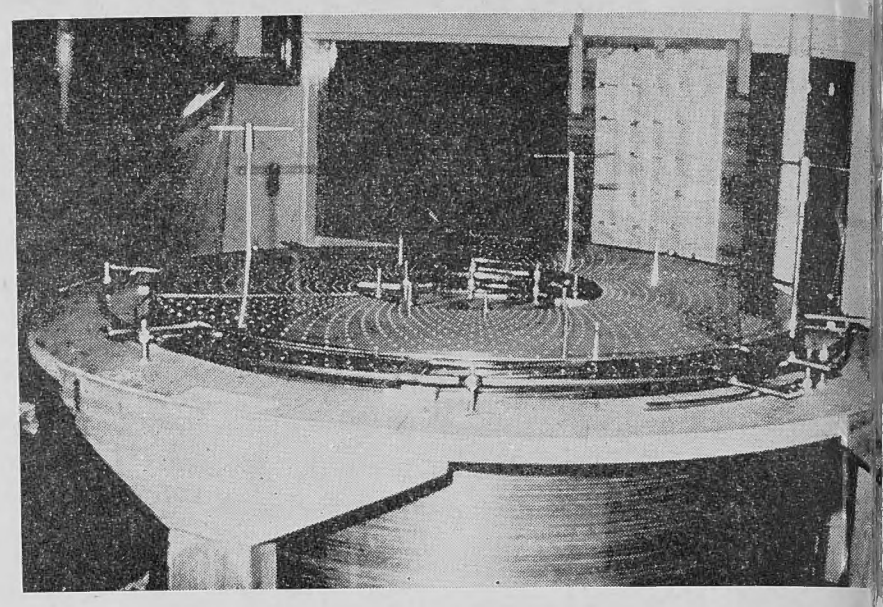

Figure 3 The ANU solenoid during assembly showing small beams supporting some discs to allow entry of the next, and three rods (with handles) in cooling holes to a location. Three other locating rods are inserted from the bottom of the solenoid and are shown protruding. The circular platform surrounding the solenoid and one in t centre are vertically adjustable

as not to coincide with the butt joints of the conducting The original plan was to divide the solenoid into four adjacent starts being separated by one layer of fabric, was soon found that, despite precautions in clean occasional metal particles had become lodged betwee glass threads of the open weave. Some of these were disc to be inside globules of resin and became evident as a circuit only after pressure was applied. This difficult overcome by inspecting every sheet on a metal table u

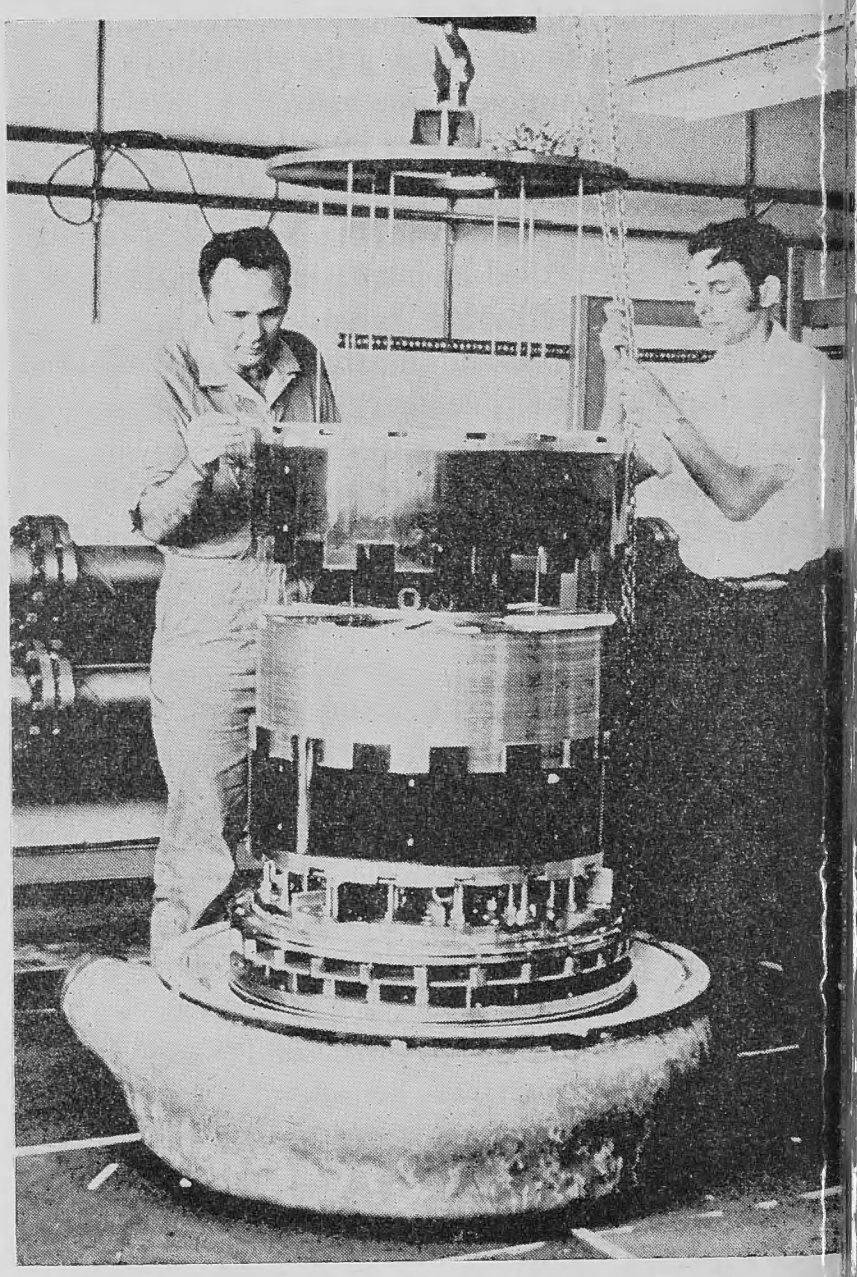

Figure 4 The solenoid in position in one torsion jack while the other is being lowered. Key bars on top of the solenoid are visible

ted roller electrically connected to the table through a which registered continuity. Once a short circuit iscovered a bearing could be drawn along the line-of-t of the roller and the fabric. The intersection of two bearings located the metal particle which was then d and removed using a microscope and another electri-connected needle-like probe. In addition to this inspec-he design was altered to two starts with double insulation ost of the solenoid.

embly was performed on a special table fitted with s aids. The method was to slide each disc in turn into usually under some discs already assembled. To perform peration accurately and without disturbing discs already bled, it was necessary to clear a passage for the next y inserting small beams which supported the assembled bove the passage. A routine for moving these supports priately for each new disc was soon worked out. Figure 3 the solenoid part way through the assembly and figure 4 the completed solenoid.

main disadvantage of the design is the large number of lual parts which have to be made and handled, and the hat with techniques developed so far assembly must d one disc at a time. The advantage of strength however standing as will become apparent in the next section.

odes of failure

as the author is aware, there are three possible modes ure of the ANU solenoid. These have been named here *ding*, *expansion* and *tensile* and they will now be discussed n.

nwinding

winding mode of failure may be defined as failure along cal fault path. Unwinding results in radial growth and g about the axis of the solenoid. In Appendix 1 helical paths involving friction bond failure are analysed. It is that the relation between azimuthal stress f_θ, axial essive stress p_z and coefficient of friction μ, for a helix ϕ is

$$p_z/f_\theta = \phi/(\mu - \phi).$$

most obvious unwinding fault path is the plane helical ce between turns. The values for the ANU solenoid

$$\left.\begin{aligned} f_\theta &= 275 \text{ MPa } (40\,000 \text{ lb in}^{-2}) \\ \mu &= 0{\cdot}2 \\ \phi &= 0{\cdot}01 \text{ rad} \end{aligned}\right\} \text{ at inner radius}$$

und that p_z must be of the order of 13·8 MPa (2000). In fact even higher values of p_z are indicated because erface between turns is not apparently the fault path he steepest helix angle. Figure 5(*a*) illustrates what is d to be the weakest unwinding fault path for the ANU . It requires approximately $(n+2)/n$ times greater p_z hat calculated above. To provide such high values of the critical end turns would be most impracticable g immense compression mechanisms and super re.

problem was overcome by attaching radial key bars discs at each end of the solenoid which keyed into riate slots in two stainless steel discs. These discs elded to two locked cylinders which encased the solen-he discs and cylinders, forming what are known as jackets, resist twisting and therefore are effective in ting failure by unwinding. These torsion jackets are in figure 4.

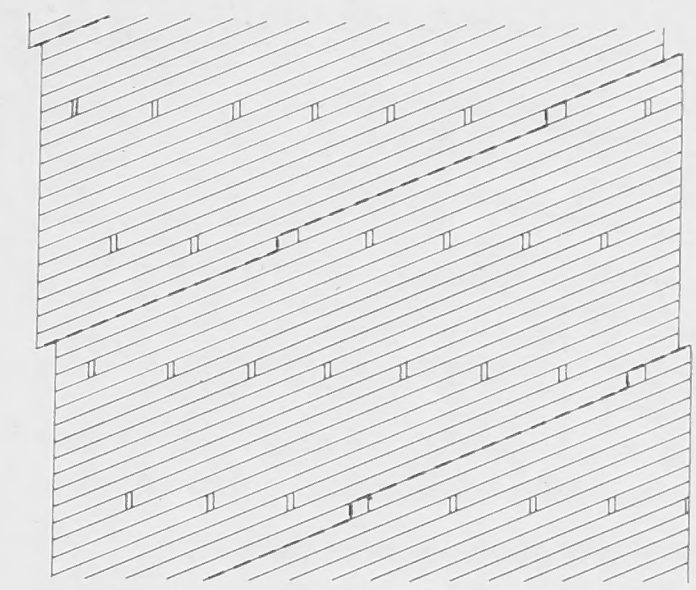

(*a*)

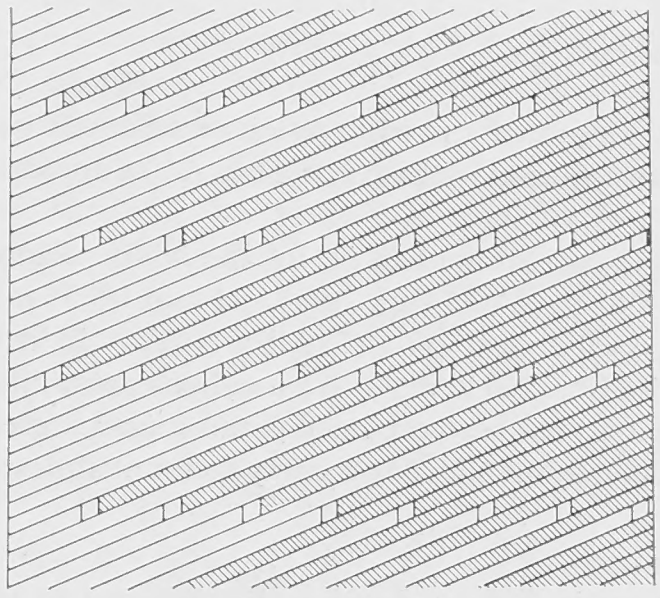

(*b*)

Figure 5 Diagrams illustrating two forms of failure: (*a*) unwinding; (*b*) expansion. The diagrams are based on the developed pattern of figure 2(*a*)

The remaining possible modes of failure are ones having axially orientated fault paths. These are the expansion and tensile modes of failure.

4.2 *Expansion*

Failure by expansion is characterized by growth in a generally radial direction without twisting about the solenoid axis. It results from failure of the friction bond between interleaved discs resulting in slipping as illustrated in figure 5(*b*) for the ANU pattern. As explained in Appendix 1, where end constraints are employed to prevent unwinding, the expansion mode of failure may be treated without regard to unwinding or the moments generated by the end constraints. The tensile strength of interleaved discs is proportional to the area of the slip planes along the fault surface and therefore the path of the fault surface will be the path of minimum length which has no net angular displacement (if the fault surface has net angular displacement, the failure is a form of unwinding which is prevented by the key-bars).

By inspection, the minimum possible path length per turn for the ANU pattern is found to be $(n^2-4)\pi/n$ rad where, as before, n is the number of discs per turn. It follows that if p_y is the compressive stress perpendicular to the slip planes at radius r, f_x the tensile stress at radius r parallel to the slip planes when failure by expansion is about to occur, μ the coefficient of friction and t is the turn thickness, then

$$p_y/f_x = nt/(n^2-4)\pi r\mu. \qquad (1)$$

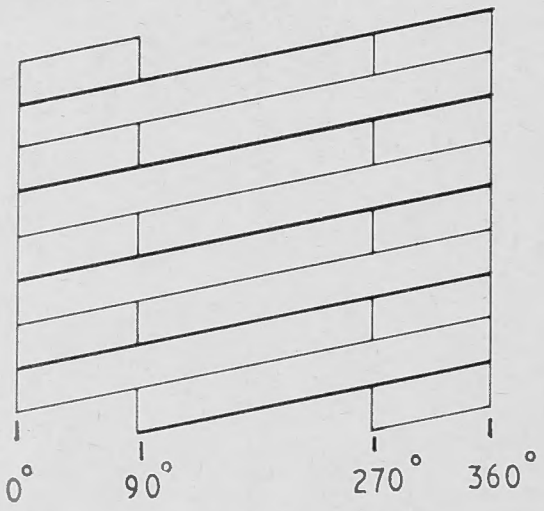

Figure 6 180° alternate overlap pattern for $n=2$

The only pattern known to have a lower ratio than this is the 180° alternate overlap pattern shown in figure 6 where the ratio is

$$p_y/f_x = t/n\pi r\mu.$$

However, as will be shown, there are serious weaknesses with this pattern and in any case, for high n, the two ratios approach one another.

The appropriate substitutions in (1) for the ANU solenoid are $n=16$, $t=8{\cdot}61$ mm (0·34 in), $r=13{\cdot}34$ mm (5·25 in) – inner radius, $\mu=0{\cdot}2$ and $f_x=275$ MPa (40 000 lb in^{-2}), whence $p_y=1{\cdot}79$ MPz (260 lb in^{-2}). An axial compression of 3·4 MPa (500 lb in^{-2}) has been provided in this region without an excessive structure thus allowing a safety factor of almost 2.

4.3 *Tensile failure*

The pattern shown in figure 6 has the slits grouped in two columns. It will be obvious that in this case the strength of the solenoid cannot exceed half of what it would be if it were homogeneous. Most known patterns suffer in this way, 50 or 25% reduction being quite common. On the other hand in figure 2(*a*), the slits are dispersed to the extent that no slits are closer than 15 disc thicknesses, i.e. the reduction in strength is only 1/16 or 6%. The wide dispersion of the slits is more apparent in the full scale developed view of the bore of the solenoid – figure 2(*b*).

5 The end treatment

Another feature of the ANU solenoid worthy of note is the end treatment. Stresses are normally calculated in a plane helical solenoid on the presupposition that current density is a function of radius only. It follows that any plane cutting the solenoid and perpendicular to its axis is not an equipotential surface due to the insulation between turns and the fact that current passes obliquely through the plane at the helix angle. In fact, following around any circle in the cutting plane one would find a uniform potential gradient everywhere except at the cut insulation line where there would be a compensating potential discontinuity equal to the turn-to-turn voltage. If these conditions are not reproduced at the ends of the solenoid, which are essentially planes perpendicular to the solenoid axis also, then one cannot expect the end stresses to be similar in nature to those in the body of the solenoid.

In most previous solenoids known to the author, the ends are simply held in contact with an equipotential electrode. Figure 7 illustrates what must happen if this is done with a simple one 'start' helix. Symmetry is destroyed in the end electrodes and current enters the solenoid along a narrow radial zone. What is usually more important, symmetry is destroyed in the end turn also, resulting in large shear stresses instead of hoop stresses.

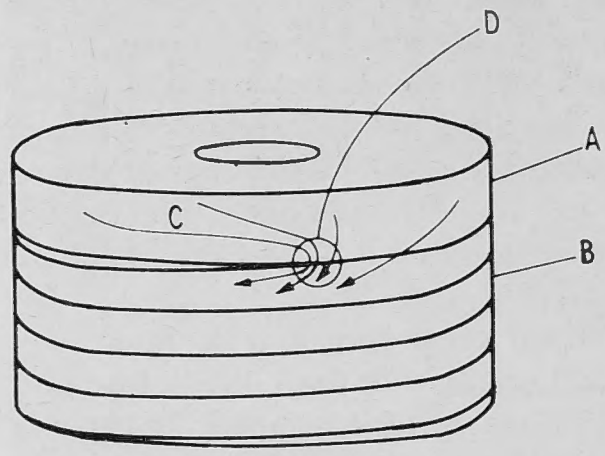

Figure 7 End effect with equipotential termination. A, equipotential electrode; B, plane helical solenoid; C, arrows showing current path; D, current concentratio and hot-spot

If the hoop force per turn is H, i.e.

$$H=\int f_\theta \, dA$$

where f_θ is hoop stress, and the integral is taken over area of the radial section of the turn then it is easily sh that the unbalanced force on the end turn is H.

The difficulty was alleviated for our solenoid by givi four starts at each end for about one turn. This provided entry and four exit points of almost equal current, and degree of balancing which resulted was found to be s factory. Away from the ends the number of starts was red to two, the insulation between them being doubled maintaining two starts it was possible to check on the in tion during assembly.

6 Conclusion

The unwinding failure mode is one to watch when desig high performance Bitter solenoids. End constraints w will resist axial twisting appear to be a practical alterna to providing large axial compression otherwise necessar develop the friction bond strength required at the end t The ANU solenoid has been tested to its design field stre with no observable deleterious effects suggesting ther that this alternative method has proved to be successfu

It would seem that there might be some advanta raising voltage and the number of turns wherever po thus reducing current and the helix angle but this mu weighed against the increased number of discs required

The unexpectedly high axial compression that woul necessary to prevent unwinding in the ANU solenoid m the author suspect that some existing Bitter solenoids w end compression appears to be rather empirically derive where end turn displacement has been reported, ma suffering from a type of failure by unwinding.

Appendix 1 Homogeneity

The analysis in this appendix requires a firm conce homogeneity which may be defined as follows. If a stru can be divided into cells of equal magnitude such th cells are identical in the number, size and magnitude o anomalies they may contain, then the structure is homoge down to the scale of the cell size. This means that analysis carried out on the basis of a homogeneous m will give the averages of the actual stresses in the cell obtain the finer structure of the stress distribution a stu the effect of the anomalies within the cells must be This will result in a 'fine structure' stress distribution may be superimposed upon the previous 'homoge

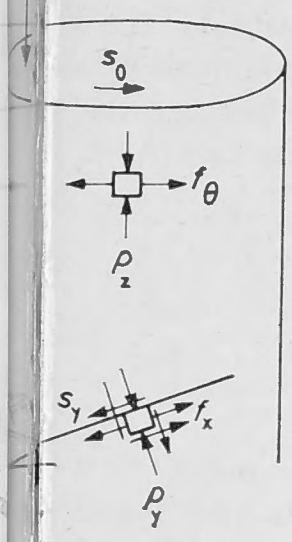

8 Illustration of terms used in the analysis

to obtain the actual stress, and which by itself averages
o throughout a cell.

he light of this concept a plane helical solenoid is now
ed. For the ANU solenoid cell size should be of the
of magnitude of the distance between slits in the θ
on, the helix pitch in the z direction and probably the
width in the r direction.

consider first the electromagnetic forces acting on the
id, i.e. the radially acting $j_\theta \times B_z$ and the axially acting
body forces. These forces result in principle stresses
p_z (f tensile, p compressive). Secondly we consider
g moments applied to the end faces of the solenoid
result in shear stress s_0 in planes at right angles to the
id axis (and in orthogonal planes containing the solenoid
These stresses are shown in figure 8. They may be
ned using Mohr's relationships which require for their
y only that the material be homogeneous (Prager 1961).
me relationship may be used to derive the stresses related
es inclined in any direction, in particular the interfaces
n the discs. These stresses, also shown in figure 8, are
shear stress along the plane, p_y the compressive stress
the plane, and f_x the tensile stress in the direction of
ne (i.e. in the direction of the helix).

components of f_x, p_y and s_y derived respectively from
inciple stresses f_θ and p_z and the applied shear stress
hown in the following table 1 where ϕ is the helix angle.
ce, making approximations for small angles

$$p_y = 2\phi s_0 + p_z \quad \text{(neglecting terms in } \phi^2\text{)} \tag{A1}$$

$$s_y = \phi f_\theta + \phi p_z - s_0 \tag{A2}$$

$$f_x = f_\theta + 2\phi s_0. \tag{A3}$$

ar we have explored the average stresses in the cells
sly defined. We may now examine the effects of
ies within the cells.

stresses whose average is f_x are subject to gross redistri-
within the cell because of the presence of the slits. This

al or stress	f_x	p_y	s_y
	$f_\theta \cos^2\phi$	$-f_\theta \sin^2\phi$	$f_\theta \sin\phi\cos\phi$
	$-p_z \sin^2\phi$	$p_z \cos^2\phi$	$p_z \sin\phi\cos\phi$
	$s_0 \sin 2\phi$	$s_0 \sin 2\phi$	$-s_0 \cos 2\phi$

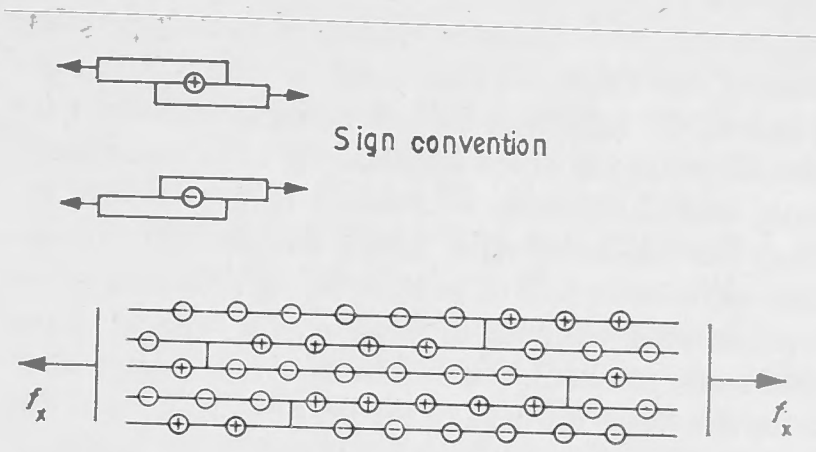

Figure 9 Illustration of the shear stresses at the disc interfaces which results from the interposition of the slits

redistribution involves shear stress components in the friction bond of magnitude kf_x where k is a factor which depends on the geometry of disc interleaving. These stresses are part of the fine structure previously referred to and are illustrated in figure 9 where, it will be seen, they alternate in sign (the sign convention is also shown in figure 9). k is defined by assuming that the strength of the turns of the solenoid in the direction of f_x is solely dependent upon the interleaving geometry and the normal force p_y. It is governed by the friction relation

$$kf_x = \mu p_y$$

and implies that

$$s_y = 0. \tag{A4}$$

Thus

$$k = \frac{\text{turn thickness}}{\text{minimum expansion mode slip path length}}$$

$$= \frac{nt}{(n^2-4)\,\pi r}$$

for the ANU solenoid. It remains to be seen what effect the inclusion of s_y has on the estimation of turn strength.

Contrary to what has been said about f_x, the average shear stress s_y, defined by equation (A2), is not affected significantly by the slits and is uniform in sign throughout the cell although, it must be noted, this sign may be positive or negative. The addition of the s_y and kf_x components results in the formation

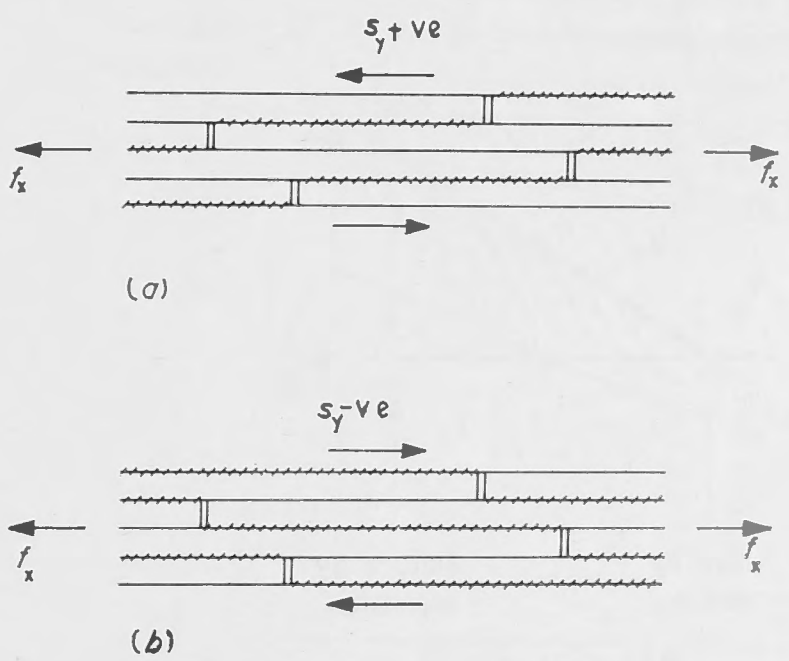

Figure 10 Illustrating the result of superimposing shear stress s_y upon the shear stresses of figure 9 (due to tensile stress f_x. (*a*) s_y positive (by sign convention of figure 9); (*b*) s_y negative. The hatched lines show the interfaces where slipping will occur. In either (*a*) or (*b*) slipping will result in the slits widening

of two possible types of continuous high stress paths depending on the sign of s_y. These are illustrated in figures 10(*a*) (s_y positive) and (*b*) (s_y negative). Failure along the former type of path results in strains which lengthen the circumference of the solenoid and is therefore referred to here as failure by 'unwinding'. For the latter type, strains shorten the circumference and the failure is said to be by 'winding'. An alternative set of definitions can be made in terms of the twisting strain experienced by the solenoid. For a right hand helix, unwinding results in the clockwise rotation of the near end relative to the far end, while the opposite rotation occurs with winding. Both of these types of failure cause widening of the slits.

For the special case $s_y=0$, both types of failure may occur simultaneously resulting in the widening of the slits but not necessarily resulting in any net twisting strain. This is the 'expansion' mode of failure referred to in the paper.

Equation for unwinding failure

The necessary condition resulting from failure of the friction bond is $s_y+kf_x=\mu p_y$. Substitution of equations (1), (2) and (3) gives

$$s_0\left(\frac{1}{\phi+k}+\frac{2\phi}{\phi+k}(\mu-k)\right)+p_z\left(\frac{\mu}{\phi+k}-\frac{\phi}{\phi+k}\right)=f_\theta. \quad \text{(A5)}$$

For relative small k and $s_0=0$, (A5) simplifies to

$$p_z/f_\theta=\phi/(\mu-\phi) \quad \text{(A6)}$$

which is a simple criterion for determining maximum unwinding strength in the absence of end face anchoring.

Equation for expansion failure

Failure by winding depends on the strength of the friction bond in the opposite direction to unwinding, the necessary condition being

$$-s_y+kf_x=\mu p_y.$$

Substitution as before results in

$$s_0\left(\frac{1}{\phi-k}-\frac{2\phi}{\phi-k}(\mu-k)\right)-p_z\left(\frac{\mu}{\phi-k}+\frac{\phi}{\phi-k}\right)=f_\theta. \quad \text{(A7)}$$

(A5) and (A7) may be thought of as defining the safe limits of s_0 as a function of f_θ (taking p_z as constant). Figure 11 shows both equations plotted in this way.

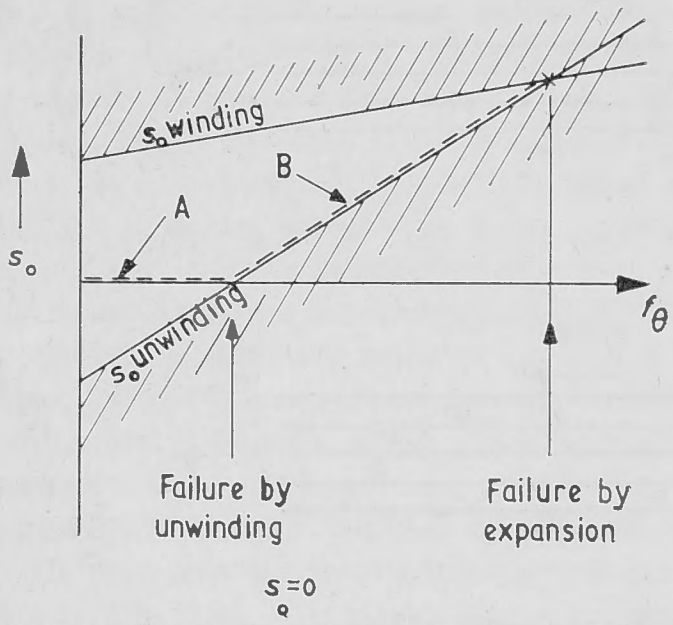

Figure 11 A–B, path followed to ultimate failure by expansion in solenoid having end face anchoring, as the magnet field is increased. B, incipient failure by unwinding which causes compensating loading of the end face anchoring

Combinations of s_0 and f_θ lying in the shaded regions lead to failure either by winding or unwinding. The intersection of the two bounding curves (if it occurs) will correspond, as explained, to $s_y=0$ and failure by expansion. The strength of the solenoid with regard to the expansion mode is therefore determined from $s_y=0$ and $kf_x=p_y$ which are the simple assumptions made when defining k (equations (A4)).

References

Bitter F 1936 *Rev. Sci. Instrum.* **7** 479

Bitter F 1936 *Rev. Sci. Instrum.* **7** 482

Bitter F 1937 *Rev. Sci. Instrum.* **8** 318

Bitter F 1939 *Rev. Sci. Instrum.* **10** 373

Bitter F 1962 *Rev. Sci. Instrum.* **33** 342

Carden P O 1968 *J. Phys.* E: *Sci. Instrum.* **1** 437

Carden P O 1972 *J. Phys.* E: *Sci. Instrum.* **5** 654–6

Kuznetsov A A 1961 *Zh. Tekh. Fiz.* (English transl. 1962 *Soviet Phys. Tech. Phys.* **6** 687–90) **31** 944–7

Léon B 1964 *Revue Gen. Elect.* (English transl. 1966 *AEI Transl.* 1056) **12** 632–6

Prager W 1961 *Introduction to Mechanics of Continua* (Boston: Ginn) pp 50–5

Journal of Physics E: Scientific Instruments 1972 Volu
Printed in Great Britain

Testing the ANU 30 T high high field magnet at Canberra

P O Carden
Department of Engineering Physics, Research School of Physical Sciences, The Australian National University, Canberra, ACT, Australia

MS *received 6 December 1971, in revised form 21 February 1971*

Abstract The test conditions of the ANU 30 T high field magnet are described and the most significant observations reported. The factor immediately limiting the maximum achievable field intensity is delineated. Conclusions are reached with regard to performance under different conditions envisaged in the future.

1 Introduction

The electromagnet whose design and construction have been described in the three preceding papers (Carden 1972a, b, c) has generated, in a series of proving tests at The Australian National University, a magnetic field of 29·4 T. This field is uniform to 0·5% within a 5 cm diameter sphere and is accessible through a 5 cm diameter axial tube. A sectional view is shown in figure 1 and the important parameters of this magnet's two solenoids are listed in table 1 of Carden (1972a). An important feature is that the inner solenoid may be removed leaving a working space 22 cm diameter at a maximum field intensity of 16·5 T. The success of these tests indicates that the Department of Engineering Physics, which is responsible for the project, is close to achieving its goal of producing a magnetic field of 30 T for the order of 10 s.

This magnet, together with a 16·5 T magnet, previously purchased from ADL Inc. are housed in the department's high field magnet laboratory. The facilities of this laboratory, including the provision of the required 120 l s^{-1} of cooling water under pressure from compressed air, are described by Carden (1968). Power for the magnets, 30 MW in the case of the new device, is derived from the department's homopolar generator (Blamey *et al.* 1962, Newstead 1967) and controlled by an electrolytic circuit breaker. The homopolar generator is an efficient energy storage device storing up to 500 MJ. It is normally fed at low power level for the order of 10 min and discharged in a matter of seconds at power levels of tens or hundreds of megawatts.

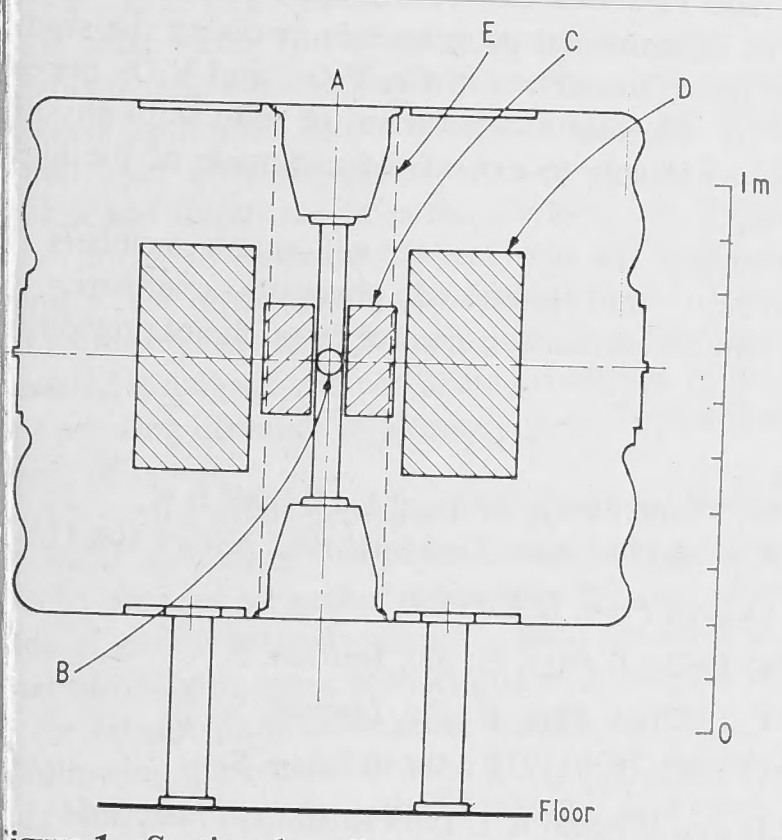

Figure 1 Sectional outline of magnet drawn to scale. A, axis of cylindrical symmetry; B, region of maximum magnetic field; C, inner coil; D, outer coil; E, boundary of central access hole with inner coil removed. Available magnetic field 16·5 T

2 Field–time characteristics

For the purposes of the proving tests the discharge cycle depicted by A in figure 2 was used. The fast rise time of this cycle resulted in certain critical electromagnetic forces in the magnet being 6% greater than they would be for a steady state current distribution yielding the same central field. To avoid this the maximum field would ideally be achieved by applying a constant voltage and allowing the field to approach the maximum value exponentially, the appropriate time constant in this case being 0·5 s. Cycles closely approaching this ideal will be available following further imminent developments of the homopolar generator and circuit breaker. However, a much greater variety of cycle shapes at lower power levels are immediately available, B in figure 2 being an example.

3 Instrumentation

The magnet has, altogether, almost 200 instruments embedded within the solenoids or attached to other parts to enable the various features to be evaluated (Carden and Whelan 1969). These instruments include thermocouples, strain-gauges, voltage probes, field pick-up coils and pressure gauges. Ultraviolet recorders and an on-line computer presented and processed the data both of which facilities are now available to experimenters.

4 Limit of performance

The maximum achievable magnetic field is governed by the magnitude of the radial electromagnetic forces acting within

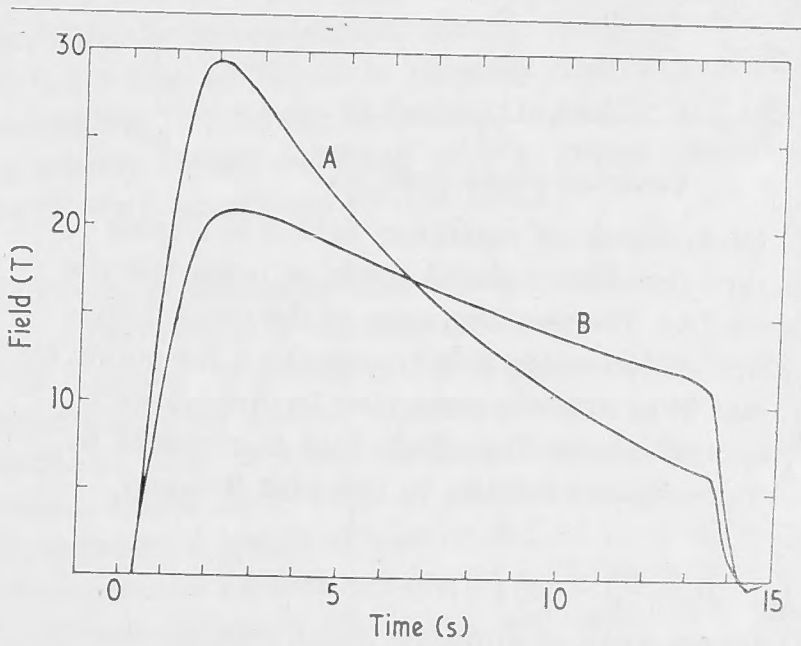

Figure 2 Magnetic field cycles. A, cycle used for proving tests; B, an example of other available cycles

the helical conductors. These cause intense circumferential tensile stresses and strains. The most severely stressed region is where the field is greatest, i.e. in the middle of the magnet at the inner surface of the inner solenoid. The conducting material here is a high strength alloy of copper and 0·25% zirconium which has an ultimate strength – even when heated – of 350 MPa. The design stress in this critical region is the '0·1% proof stress' i.e. the stress which causes a total irreversible strain of 10^{-3} and it was thought unwise to exceed this limit during the proving tests.

5 Observations of strain

Displacement gauges, specially designed for the conditions and installed in this region, measured the strain during the field cycles and also registered the amount, if any, of plastic strain through comparison of displacements before and after each cycle. A good indication of the proximity of the stress of each cycle to the ultimate strength of the material was achieved by plotting field against cumulative plastic strain (stress is proportional to field squared) and then relating the observations to known properties of the material. These properties can be represented in dimensionless form as

$$\sigma/\sigma_m = f(e)$$

where σ is the stress, σ_m the ultimate tensile strength, f the known function from sample tests and e the cumulative plastic strain. Hence, since $\sigma \propto B^2$, the relation

$$B = B_m\{f(e)\}^{1/2}, \qquad (1)$$

(where B is the field strength and B_m the field corresponding to σ_m, i.e. ultimate failure) should represent the behaviour of material in the magnet. Figure 3 shows observed values of B and e plotted for a number of cycles. Curve A is relation (1) above in which B_m has been chosen to obtain the best fit to the observations. The ratio $(B/B_m)^2$ thus indicates the stress in relation to the ultimate strength of the material. This method, employing as it does dimensionless properties of the material, enables a direct indication of the stress condition in the material under examination without requiring prior knowledge of its ultimate strength, elastic modulus or the effect of temperature or geometry on either of these. In addition, measurements of plastic strain are free from complications caused by thermal expansion.

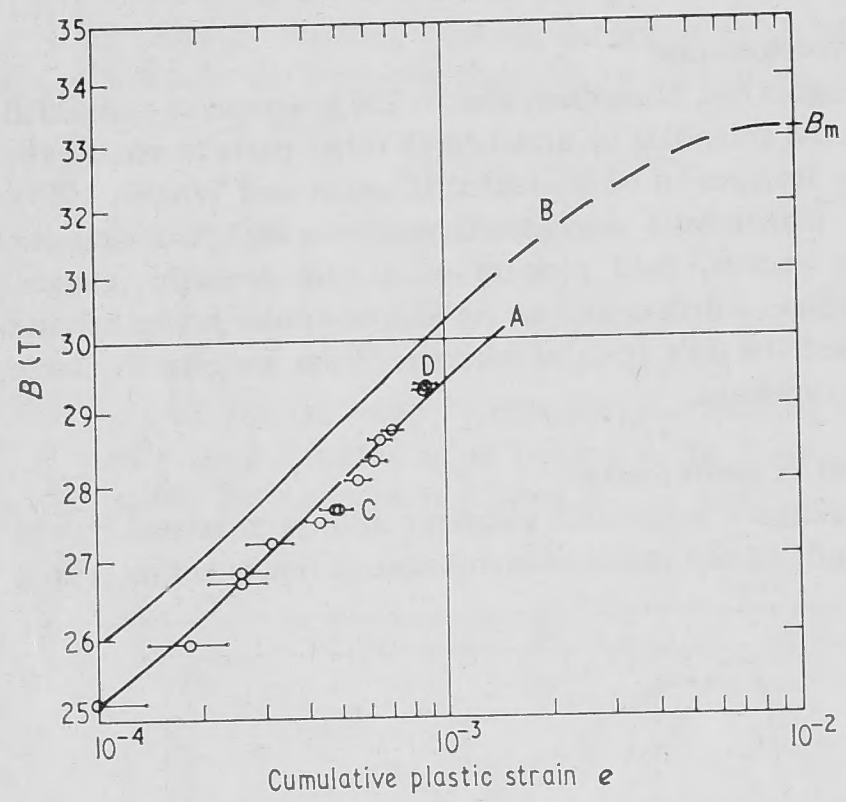

Figure 3 Observations of maximum field B in a cycle plotted against cumulative plastic strain, e, using fast rise cycles (figure 2A). The time sequence of the observations is in the order of increasing field (increasing e for points C). Curve A, best fit of material properties to observations. Curve B, implied relation for steady field B_s obtained by application of constant voltage. In this case B would approach B_s as

$$B/B_s = 1 - \exp(-t/\tau) \qquad \tau = 0{\cdot}5 \text{ s}$$

C and D are examples of duplicate cycles showing no significant change in plastic strains between first and second cycles. Design figures were $e = 10^{-3}$ for $B_s = 30$ T

It must be emphasized that the observations of plastic strain do not imply a perpetual gradual distortion and consequently a limited life of the magnet. The strain is part of the normal work hardening process and takes place substantially only upon the first application of a new high stress. The pairs of points C and D in figure 3 confirm this as do observations since the attainment of 29·4 T which show that all subsequent strains have been wholly elastic.

6 Deduction from observations

Taking into account the 6% overstressing effect earlier mentioned, one can postulate what the field–strain relation would have been, and will be, for constant voltage cycles. Curve B in figure 3 is such a postulate determined by an increase in B_m of 3% above the value used for curve A. It shows that constant voltage cycles of 30 T will cause no further plastic strain.

In the light of these observations, observations of temperatures which incidentally reach equilibrium conditions in the inner coil in less than 1·5 s, and visual inspection of the magnet, it is expected that the magnet will be satisfactory for continuous operation at 30 T and particularly for the constant voltage cycles of 10 s or more previously described.

7 Applications and conclusion

Interest has been shown in applying the inner coil design to the inner coils of 'hybrid' combinations with superconducting coils. It appears that there are limitations to Bitter disc type constructions in this situation where the requirement is for compactness and high strength.

Since the magnet was first energized in September 1970, a total of 370 cycles have been produced, 72 of which were above 20 T and 15 above 27·5 T. One quarter of these have been used in experimental programmes involving the study of magnetic phase transitions in Cr, V_2O_3, and V_2O_3 doped with Cr. Early this year a department of solid state physics was established largely to extend the use made of the high field facilities.

It is hoped that the new magnet will enable members of this department, and interested physicists elsewhere, to investigate new and rewarding areas of research not previously accessible.

References

Blamey J W, Carden P O, Hibbard L U, Inall E K, Marshall R A and Oliphant Sir Mark 1962 *Nature* **195** 113–4

Carden P O 1968 *Proc. IEE* **115** 711–5

Carden P O 1972a *J. Phys.* E: *Sci. Instrum.* **5**

Carden P O 1972b *J. Phys.* E: *Sci. Instrum.* **5**

Carden P O 1972c *J. Phys.* E: *Sci. Instrum.* **5**

Carden P O and Whelan R E 1969 *Australian National University, Dept. Engng Phys.* EP-RR 25

Newstead G 1967 *Sci. J.* **3** 55–60

Journal of Physics E: Scientific Instruments 1972 Volume 5

The ultimate possibilities of quasi-continuous high field electromagnets

P D Carden and A M Collins
Department of Engineering Physics, Research School of Physical Sciences, Australian National University

Received 3 January 1974

Abstract Design principles are described for continuously operated self supported solenoids in which the mechanical stresses in most of the conducting material are equal and approach its ultimate strength. The results of computations for a number of hypothetical solenoids are summarized showing the power, mass and distributions of current density and field intensity. Finally comments are made regarding the practicability of building such solenoids and providing the power to energize them.

1 Introduction

Generators of intense magnetic fields are important tools in many branches of experimental physics, especially the physics of the solid state. The original generators were iron-cored electromagnets, but the needs of early experimenters soon exceeded the limited field strength attained by these devices and that, ever since the pioneering days of such workers as Kapitza and Bitter, the air-cored solenoid has been the chief work horse in providing the fields of ever increasing intensity that experimental physicists demand. The exploitation of this device, though basically simple, has nevertheless presented a difficult and continuing challenge to designers to meet growing demands of strength, heat dissipation and the supply of power.

With regard to the generation of steady fields, which is the particular concern of this paper, it has been customary from time to time for an author to explore the cost of generating fields of greater intensity than has been available at the time in terms of a parameter such as power, basing his predictions on the extrapolation of existing technology.

Following the success of a 30 MW, 30 T magnet designed and built at the Australia National University (ANU) Canberra and the proven practicability of the homopolar energy storage machine used to supply its power, it seems pertinent to the present authors to make a similar exploration of the possibilities of generating steady fields of even higher intensity than already achieved by the ANU device (Carden 1972a, b, c, d). This seems especially so in view of the essentially different principles of design embodied in this magnet.

The prediction that has resulted from the present work is summarized by curve A, figure 1, and may be compared with those of two earlier groups (viz. Bitter 1961 (curves B and D) and Parkinson and Mulhall (1967, p 153 (curve F)). It is interesting to observe that very little progress has actually occurred towards achieving the preformances that have been predicted in the past, and that predictions in the higher field regions have become less optimistic as time passes.

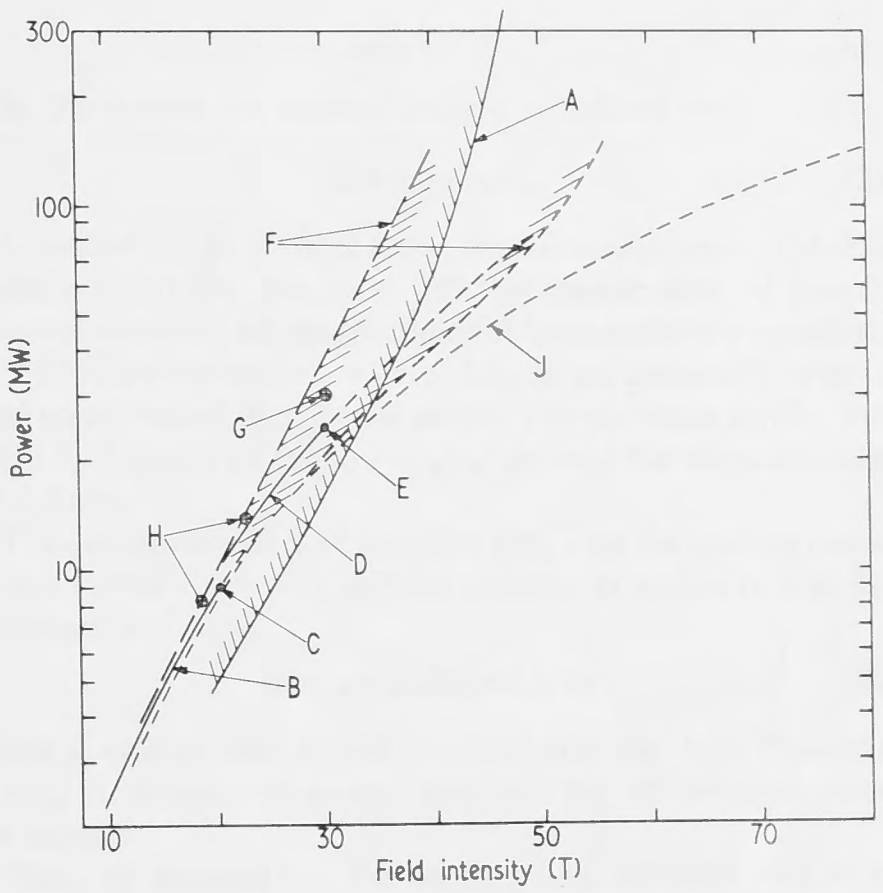

Figure 1 Field against power relations for 2·75 cm inner radius solenoid. A: strength limited Zr–Cu solenoids – the technological barrier predicted by the present authors; B: copper solenoids – predicted by Bitter 1961; C: extremity of B where stress equals elastic limit of copper; D: Zr–Cu solenoids – predicted by Bitter 1961; E: extremity of D where stress equals elastic limit of Zr–Cu; F: various solenoids based on tentative design studies compiled by Parkinson and Mulhall 1967; G: the ANU 30 T magnet; H: two existing magnets (power adjusted for differences in scale); J: $B \propto w^{1/2}$ extrapolation of curve B

Carden (1970, 1972a) has pointed out some of the limitations of solenoids of conventional design and has enunciated the several alternative design principles referred to above that have overcome these limitations in the ANU device. One of these principles is the division of a solenoid into numerous mechanically independent concentric tubular elements similar to those first employed in magnets built at the Clarendon Laboratory, University of Oxford, in which their use helped to achieve better matching with a power source of comparatively high voltage (Wood 1961).

2 Design principles for high field solenoids

2.1 *Construction of the solenoid elements*

The solenoid is composed of numerous accurately fitted, concentric, thin walled, tubular elements, each of which is machined after fabrication. Each element is, electrically, a precise single layer helix of constant pitch fabricated by edgebending a length of wire or rod into a coil, the turns of which are later bonded together by a thin layer of resin, which is strongly adhesive, insulating, and resistant to attack by the coolant. The shape of the bonded wire section is that of a rectangle or parallelogram and consequently the turns fit together in a manner that achieves a high ratio of conductor volume to insulation volume.

Bare machined conducting material is exposed at the cylindrical surfaces of each element in order to facilitate heat

r to the coolant which passes between elements, ly in machined grooves.

current density and resistivity in each tubular element e selected as independent functions of radius with axial nce and elements may be connected electrically in l or in series. In the latter case a thin insulating sleeve ired between elements at different potentials.

ermination of the elements

lements are electrically terminated in such a way as to anomalously high current densities and stresses in their To achieve this, the ends of elements are machined and a ring of constant current contacts with indepen- ressurizing mechanisms is provided at each end.

Operational stresses on the elements

eration, the elements are mechanically independent, e product (azimuthal stress) × (radius) is arranged to se from the inner element to the outer element so that, ergizing, all the very small radial gaps between elements e slightly. This arrangement, together with the small dimensions of the elements results in the radial stress he gradient of radial stress being both essentially zero herefore, the azimuthal stress is determined by a simple on of the field strength and current density in the element consideration. Axial stresses are generally secondary in itude.

practicability and validity of designs based on the above ples have been demonstrated by the performance of the 30 T magnet. In the explorative studies that we now be, it is assumed that the same principles are to be oyed and that they will continue to operate successfully dless of scale.

esign concepts and methods

of the most important considerations of a designer is fficient use of power. His goal is generally to produce ighest field intensity at the centre of a solenoid using ore than a specified maximum of power, and in order to ve this goal, he must select, within practical limits, ble spatial distributions of current density and resistivity. known that this concept of efficiency applied to the case hin walled tubular element such as we have been discus- leads to the conclusion that the efficiency is optimized the length equals the diameter, or when the half angle tended at the centre of the element is 45°†. The present rs began their studies assuming that all tubular elements ined in a solenoid were to be of the $\theta = 45°$ type, although eatment following allows for other values of θ.

solenoid, comprising a large number of tubular elements, magined to be divided into two zones by a cylindrical dary at radius r_2. The zone inside this boundary was ined to be one in which strength was the primary con- ation and was, therefore, called the 'strength' or 's-zone', one outside r_2 was regarded as being primarily governed fficiency considerations and was consequently called the iency' or 'e-zone'.

nsider now each of these zones, and the interrelation een them, for a solenoid of inner radius r_1 and outer s r_3.

the s-zone, the elemental current density j_a, element us r_a, the median field strength B_a within the element, and the material tensile strength σ are related by:

$$j_a B_a r_a = \sigma. \tag{1}$$

In the e-zone the current density is defined by:

$$j_a = j_2 (r_2/r_a)^2. \tag{2}$$

Equation (2) is derived from the known criterion (Montgomery 1969) for the most efficient distribution of power between elements whose geometrical boundaries are specified, viz. $\Delta B_0/\Delta w = \text{constant}$, where ΔB_0 is an element's central field contribution and Δw its power. For elements having the same θ, $\Delta B_0 \propto j_a \, dr$ and $\Delta w \propto j_a^2 r_a^2 \, dr$, and therefore relation (2) follows.

The component of field intensity $dB_{c,\,r}$ on the median plane at any radius r due to a tubular element at radius r_a may be expressed by:

$$dB_{c,\,r} = \mu_0 R(r/r_a) \, j_a \, dr \tag{3}$$

where j_a and dr refer to the element, and the field function $R(r/r_a)$ is dimensionless and identical for all elements with the same θ.

Thus, by summation, the median field intensity due to a zone between, for example, radii r_m and r_n and having current density distribution $j(r_a)$ for $r_n > r_a > r_m$ is derived as:

$$B_{c,\,r} = \sum_{r_a = r_m}^{r_n} \mu_0 R j \, dr_a.$$

It is convenient to express this as a new function Z, thus:

$$B_{c,\,r} = Z\,[j(r_a),\, r_a,\, r]_{r_n,\, r_m} \tag{4}$$

and it is to be noted that Z holds for computations of B_c both inside and outside the zone being considered. When equation (4) is applied to the e- or s-zone, B_c becomes either the component field distribution B_e or B_s generated by the j distributions within each respective zone.

At the boundary r_2 between the two zones, both equations (1) and (2) must apply and the correct solutions to the current density and field distributions must provide for continuity here. However it was found convenient to employ an iterative method of solution in which it was necessary to allow a temporary discontinuity in j in trial solutions. Accordingly equations (1) and (2) were combined to give:

$$j_{e,\,2}(B_{e,\,2}/f)\, r_2 = \sigma \tag{5}$$

in which $j_{e,\,2}$ and $B_{e,\,2}$ refer specifically to values in, or generated by, the e-zone at r_2, and the dimensionless factor f is used to relate the total boundary field strength B_2 to the component $B_{e,\,2}$; i.e. $f = B_{e,\,2}/B_2$.

Equation (4) applied specifically to the e-zone gives:

$$B_{e,\,2} = j_2 Z \left[\left(\frac{r_2}{r_a} \right)^2, \frac{r_a}{r_2}, 1, \right]_{1,\, r_3/r_2}$$

which, when combined with equation (5) gives an operating equation for $j_{e,\,2}$

$$j_{e,\,2} = \left[\frac{\sigma f}{Z r_2} \right]^{1/2}. \tag{6}$$

Equation (6) permits the study of a solenoid in which the three radii r_1, r_2 and r_3 are fixed and where a trial value of f has been selected. It enables, in turn, the computation of a trial B_e distribution throughout the solenoid, a necessary first step in computing conditions in the s-zone.

Conditions within the s-zone are defined by equation (1) with $B_r = B_{s,\,r} + B_{e,\,r}$ and by using equation (4) to relate $B_{s,\,r}$ to the s-zone current density. The successful iterative method

Klerk 1965 *The Construction of High Field Electromagnets* port Instruments Ltd, p 45.

of solution of these relationships may be summarized by the following procedure:

(i) select arbitrarily a j distribution in the s-zone, j_s

(ii) compute $B_{s,\,r}$ for $0<r<r_2$ using equation (4)

(iii) compute B_r from $B_r=B_{s,\,r}+B_{e,\,r}$ (using the previously obtained B_e distribution with arbitrary value of f).

(iv) compute a new s-zone j distribution using equation (1): j_s (new) $=\sigma/B_r$.

(v) compare j_s (new) with j_s and if sufficiently alike the computation is completed. Otherwise go to (ii) substituting $[j_s\text{ (new)}+j_s]/2$ for j_s.

In every case this process evolved a stable j_s and B_s distribution. To achieve a final solution for the whole solenoid it only remained to compare $j_{s,\,2}$ with $j_{e,\,2}$ derived from equation (6) and to proceed with further trial values of f until continuity at the zone boundary was established.

The solenoid power was then computed using the incremental equation

$$dw=4\pi \tan\theta\, \bar{\rho}\, j^2 r^2\, dr$$

where $\bar{\rho}$ is an effective resistivity, and the mass of the solenoid was also computed.

4 Preliminary studies

The initial goal was to establish the relationship between central field and solenoid power for a series of solenoids all having the same physical boundaries and mass. This entailed fixing r_1, r_3 and θ ($=45°$) and inserting successive values of r_2 in the computations described. In order to establish the effect of changing the outside radius, three such studies were performed, each with identical r_1 but different r_3. The results of these studies are shown in figure 2. The curves A, B and C are for $r_1=2{\cdot}75$ cm, and $r_3=30{\cdot}25$ cm, $50{\cdot}25$ cm and $70{\cdot}25$ cm respectively. In all these and successive studies the material constants were given the following values which took reasonable account of the space occupied by cooling passages and insulation; $\bar{\rho}=2{\cdot}8\times10^{-8}\ \Omega\,m$; $\sigma=3{\cdot}0\times10^{8}\ N\,m^{-2}$ (corresponding to zirconium copper alloy with 0·9 space f
density 8930 kg m^{-3}.

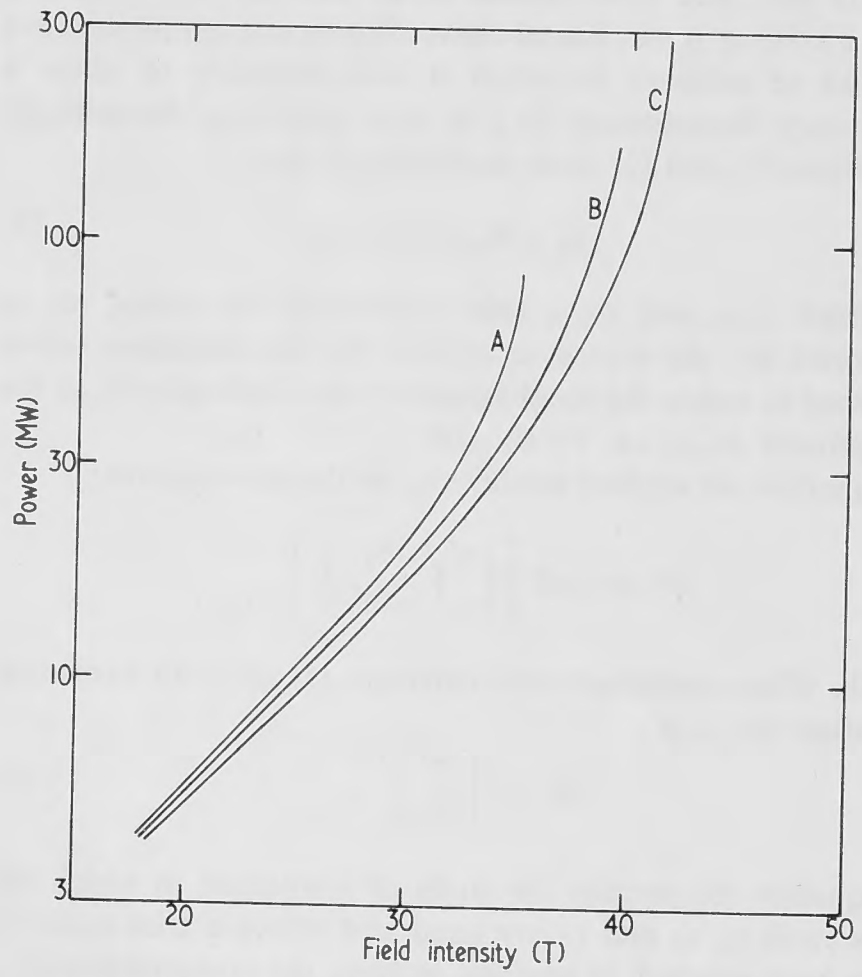

Figure 2 Power against field for three series of identical mass solenoids. In every case $\theta=45°$ and $r_1=2{\cdot}75$ cm. A: $r_3=30{\cdot}25$ cm, mass $=1030$ kg; B: $r_3=50{\cdot}25$ cm, mass $=4750$ kg; C: $r_3=70{\cdot}25$ cm, mass $=13\,000$ kg

The studies showed clearly that gains in field could
by increasing r_3 but only at the expense of an eno
increase in mass. Consequently all further studies were
on $r_3=50{\cdot}25$ cm which was regarded as a reasonable co
mise. Nevertheless, it is useful to consider all three cur
part of a family of curves of constant mass. The mass
useful measure of monetary cost and such a set of curv
be used as a yardstick against which other designs c
measured. For instance if a design modification lead
point to the right of the family member of equivalent
then it can be regarded as an 'improvement'. Further st
now to be described, lead to significant improvements
judged this way.

5 Further optimization

It was observed with each of the curves of figure 2 t
increased more rapidly with B_0^2 than the linear relatio
characteristic of solenoids with constant efficiency.
implied that gains in B_0 were to be had only at the expe
efficiency and therefore allowed the possibility that pert
tions of the design, based as it was on maximum effi
concepts, might result in an improvement in the sense al
defined. For although such a perturbation would inev
lead to a decrease in efficiency, it might still repres
improvement provided it increased B_0 sufficiently.

The two possible perturbations to investigate were:
departure from the most efficient j distribution in the e-
viz. that defined by equation (2); (ii) a departure from θ
in both zones.

A clue that both of these perturbations might result
improvement is to be had by considering the field compo
B_c produced within any radius r_4 by the region outsid
It is generally always true that $B_{c5}>B_{c0}$ for $r_4>r_5>0$
degree of inequality depending on j and θ in the region ou
r_4 (e.g. $B_{c5}\to B_{c0}$ as $\theta\to90°$). Since any reduction in
while still keeping B_{c0} unchanged, will result in allowin
increased j_5 if it occurs in the s-zone, it follows that su
reduction will result in an increase in the total field
However it could only be brought about by changes i
region outside r_4 that would reduce efficiency there.

An investigation of the first of the above-menti
perturbations was not pursued vigorously since the sole
of greatest interest, viz. the highest field ones, had relat
small e-zones. However, some evidence was gathered to s
that marginal improvements are to be had in this way.

On the other hand preliminary investigations into
effect of varying θ from 45° showed that significant impr
ments were possible. Curves D, E, F, and G of figure 3 s
the results of further studies in which r_3 was fixed at 50·25
and θ was made respectively $\tan^{-1}0{\cdot}5$, $\tan^{-1}1{\cdot}5$, $\tan^{-1}2{\cdot}5$
$\tan^{-1}3{\cdot}5$ throughout the solenoid. Comparison of t
results with the original set A, B and C will reveal that s
segments of the new curves represent improvements,
above 30 T curve E is a definite improvement on C (E
less mass and produces more field for a given power), al
36 T, F is a definite improvement on E, and above al
40 T, G also represents an improvement. It is evident
a new set of constant mass curves for solenoids of optin
θ, could now be drawn considerably to the right of the orig
set of figure 2, thus constituting a new yardstick aga
which further improvement in design might be gauged.

The obvious next step was to consider the effect of vary
θ with radius in a given solenoid. Unfortunately the definit
of 'improvement' that we adopted was not quantifiable
therefore it was not possible to establish a programme t

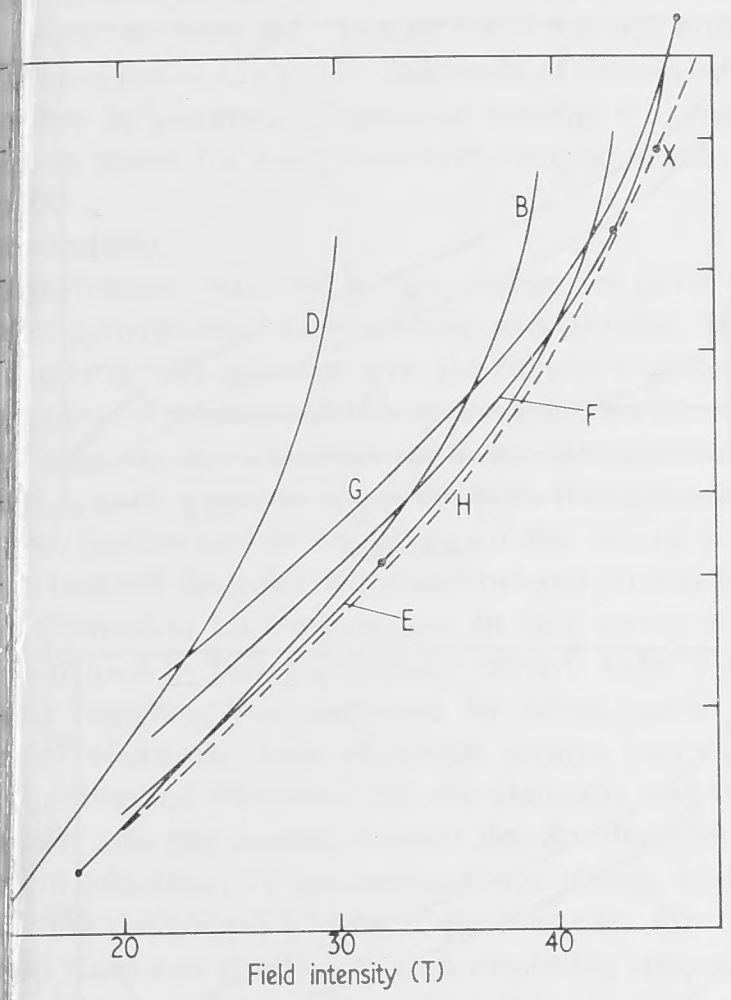

3 Power against field for several series of constant
noids. In every case $r_1 = 2{\cdot}75$ cm, $r_3 = 50{\cdot}25$ cm.
$\tan^{-1} 1$, mass = 4750 kg; D: $\theta = \tan^{-1} 0{\cdot}5$,
2370 kg; E: $\theta = \tan^{-1} 1{\cdot}5$, mass = 7120 kg;
$\tan^{-1} 2{\cdot}5$, mass = 11 900 kg; G: $\theta = \tan^{-1} 3{\cdot}5$,
16 600 kg; X: 8 constant θ zones mass = 7210 kg,
4·7 T, $w = 185$ MW; H: approximate limit of
mance of Zr–Cu solenoids of mass 7200 kg. The five
shown correspond to the distributions shown in
5

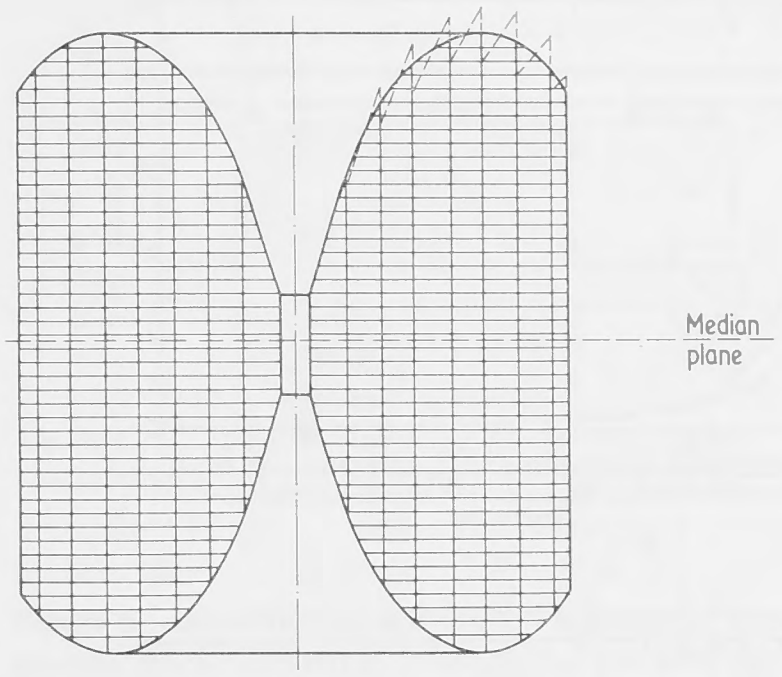

Figure 4 Smoothed-out line of the eight segment solenoid whose performance is shown as point X on figure 3. The dashed outline is the one whose performance was actually computed; mass = 7210 kg; $B_{0\,max} = 44{\cdot}7$ T; $w = 185$ MW. The outer segment is e-zone; the others are all s-zone

evolve an optimum function for θ. However, in view
differing aims of magnet designers there seemed to be
merit in trying to define an improvement any more
y than had been done, for our primary aim was to
what was possible rather than what was best. This
sophy appears to be in line with the conclusions reached
by the designers of iron-cored magnets who also had
ulty in making comparisons on the basis of mass, power
field (Kroon 1968). Accordingly, we chose simply to
arily select a function for θ and to test whether it was
nprovement relative to our new yardstick. A selected
ion which passed this first test was further refined by
g whether any local perturbations of θ could be dis-
ed which could lead to a further improvement defined
simultaneous increase in field, reduction in power and
tion in mass.

e point X on figure 3 represents the performance of one
tedious computation for a solenoid divided into eight
entric constant θ zones (outlined in figure 4). This result,
her with the results of several three-zone studies indicated
only marginal gains in performance were possible by
ng θ with radius. However, clearly, a considerable
tion in mass is possible. This is exemplified by point X
h has a mass of about half of the optimum constant θ
noid of equal performance. It is important to note, how-
that the significant saving in weight is related to the fact
any solenoid with the performance of X must have a
ively large volume of s-zone, and it is only because of the
ence of an s-zone that the perturbations which we have
discussing are effective. Therefore it must not be expected
that the saving in weight exhibited by our example X can be repeated at lower fields where the s-zone is relatively smaller, and the optimum θ tends towards 45°. In fact if one considers only 7200 kg solenoids there is every reason to believe that the optimum series of designs can be represented by a curve such as H in figure 3 running through X and very close to the right hand envelope of the other curves in figure 3.

It is evident from these results that there appears to be a technological barrier to further improvement which might be represented by an empirically derived curve such as H in figure 3. This question is further pursued after the section on scaling laws.

6 Current density and field distributions

Perhaps the most unusual feature of the solenoid designs proposed here are the cusp-like current density distributions illustrated in the selection of four examples of optimum constant θ solenoids (figures 5(*a*)–(*d*)), and for the eight segment 'X' solenoid shown in figure 5(*e*). These figures also show the total field distributions and the e-zone and s-zone component field distributions. The gradual migration of the zone boundary outwards as higher maximum fields are designed for, is evident in figures 5(*a*)–(*d*). An important observation is that the magnitude of the maximum value of j in any solenoid is never impractically high and in fact reduces as higher design fields are attained, e.g. in figure 5(*e*), j_{max} is 22·36 kA cm^{-2} which is substantially lower than the maximum value in the ANU 30 T magnet, viz. 39 kA cm^{-2}.

Another point worthy of note is that, although higher fields are attained by increasing the radius of the zone boundary, there must always remain a finite e-zone. This is because B must reverse sign somewhere inside the solenoid, but it is not permissible for this to occur in the s-zone because of the consequent implication of infinite power.

7 Scaling

In all the studies that we carried out, the inner radius, and the material strength and resistivity were fixed. This, however, does not preclude our results from being applied to solenoids of other sizes and materials, because it is a simple matter to derive appropriate scaling factors from the three proportionalities listed below. In these relationships B, j and r are

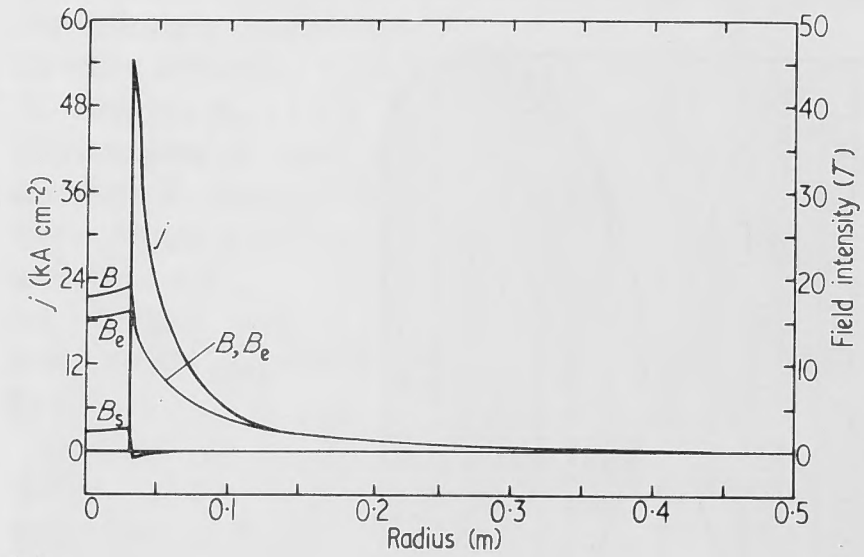

(a)

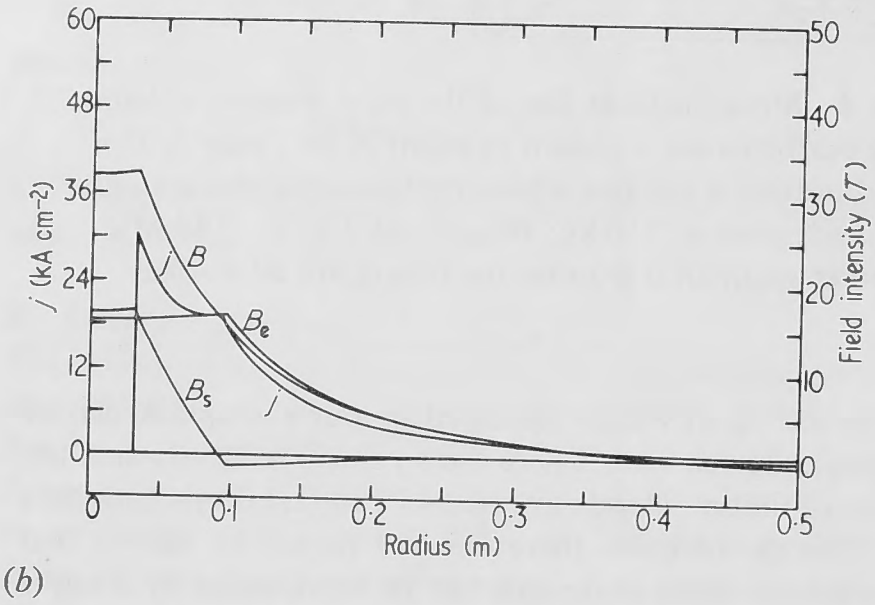

(b)

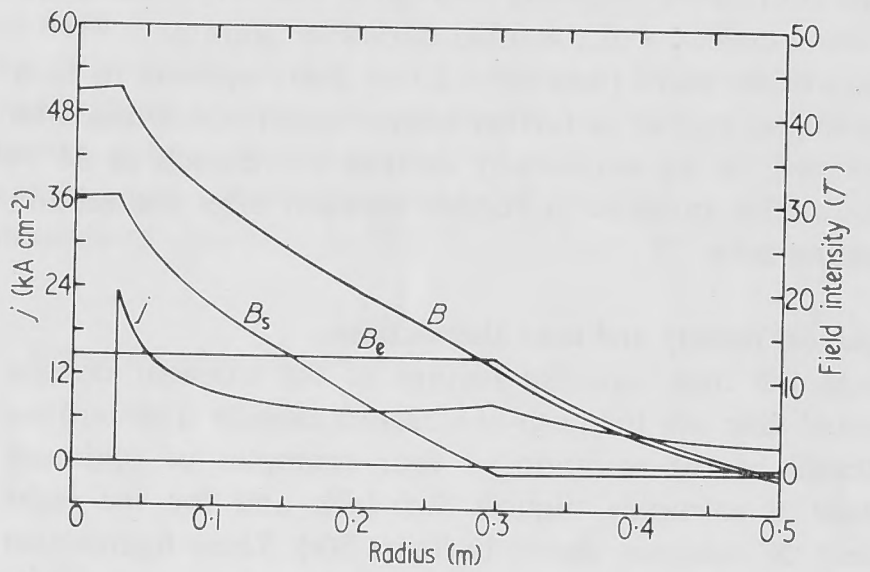

(c)

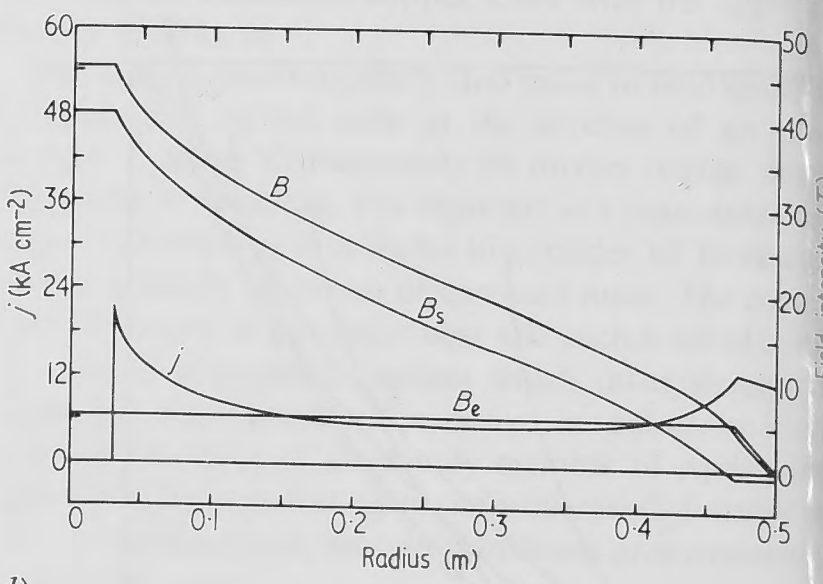

(d)

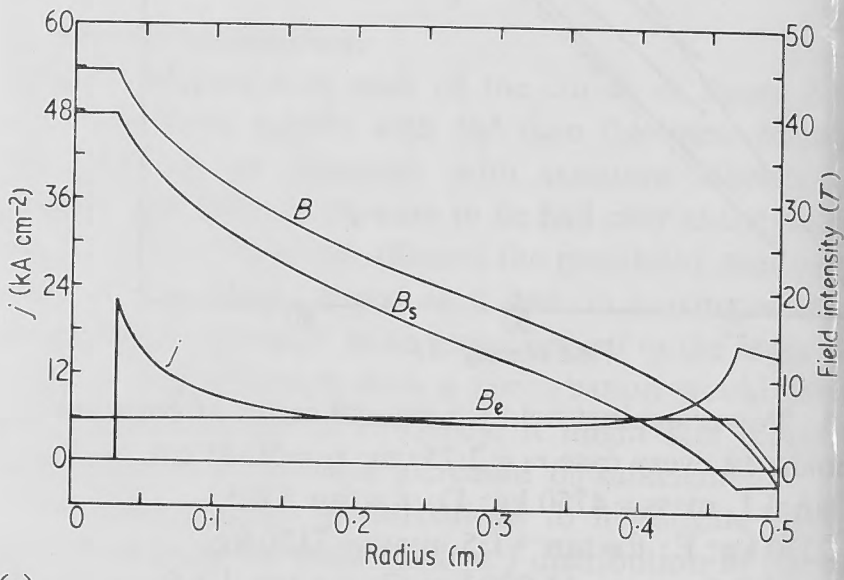

(e)

Figure 5 Examples of current density and field distribu ($r_1=2{\cdot}75$ cm, $r_3=50{\cdot}25$ cm). (*a*) $\theta=\tan^{-1}1{\cdot}0$, $r_2=3{\cdot}25$ c $B_0=17{\cdot}9$, $w=4{\cdot}2$; (*b*) $\theta=\tan^{-1}1{\cdot}5$, $r_2=10{\cdot}25$ cm, $B_0=32$ $w=21{\cdot}3$; (*c*) $\theta=\tan^{-1}2{\cdot}5$, $r_2=30{\cdot}25$ cm, $B_0=42{\cdot}7$, $w=1$ (*d*) $\theta=\tan^{-1}3{\cdot}5$, $r_2=47{\cdot}25$ cm, $B_0=45{\cdot}7$, $w=372$; (*e*) po X figure 3, $r_2=47{\cdot}25$ cm, $B_0=44{\cdot}7$, $w=185$

characteristic values of maximum field, maximum current density and radius of the particular solenoid being considered, while σ and ρ are material parameters. The proportionalities relate B, w and j to those of the variables, ρ, σ and r that each is dependent upon.

(i) $B^2 \propto \sigma$

(ii) $w \propto \rho\sigma r$

(iii) $j^2 \propto \sigma/r^2$

These relations reveal that a compromise in material properties is necessary: relations (ii) and (iii) require the lowest available values of $(\rho\sigma)$ in order to minimize power and power density, whereas (i) requires the highest value of σ. There is no figure of merit applicable to all materials, which will point to a single best material for these types of solenoid. In fact the choice of a material and a design is seen to be a matter of careful compromise which cannot be arrived at independently in any particular case.

An interesting point that bears mentioning while on the subject of materials is that a new series of improved solenoid designs might result from the use of different materials with optimum properties for the regions in which they are u We have not done any work in this direction but remar passing that the large variation in current density distribu within a solenoid that we have already noted, may ha significance when considering graded materials.

It was mentioned earlier that there appeared to be a tec logical barrier to any significant improvement upon solenoid performances so far achieved, and that it migh useful to derive an empirical relation between w, B_0 and o parameters, which described this barrier. Our attemp derive such an equation is given below, equation (7); curve H in figure (3) is the graph of this equation for particular values of ρ, σ and r used in our studies. The equa is:

$$w=\frac{a\rho r_1}{\sigma^7}B^{16}+\frac{b\rho r_1}{\sigma}B^4+c\rho r_1\sigma$$

where $a=1{\cdot}34\times10^{50}$, $b=6{\cdot}06\times10^{18}$, $c=1{\cdot}17\times10^7$, r_1 is solenoid internal radius and ρ and σ are effective value resistivity and strength respectively. Equation (7) may written in more manageable form by dividing throughou $(\rho r_1 B^2/\mu_0{}^2)$ which has the dimensions of power, and making the substitution $\sigma'=2\mu_0\sigma/B^2$ in which σ' is normalized stress with respect to the 'magnetic pressure'

$$w'=\frac{\mu_0{}^2 w}{\rho r_1 B^2}=\frac{1}{G^2}=\left(\frac{0{\cdot}751}{\sigma'}\right)^7+\frac{24{\cdot}0}{\sigma'}+7{\cdot}36\times\sigma'$$

where G is the well known 'Fabry factor' (Parkinson Mulhall 1967, p 15).

equations are for solenoid masses of about $350\,r_1^3$ kg ould be true for $26\times10^{-4}\,\sigma^{1/2} > B > 12\times10^{-4}\,\sigma^{1/2}$. ts are consistently MKS. Solenoids of masses other than can be assumed to produce roughly 6% more field ven power for every four-fold increase in mass.

cticability

istribution indicated by our studies are quite different ne conventional ones usually encountered. However, ay be simply achieved with the tubular element type of ction by appropriately adjusting the width and pitch helix in each element and by interconnecting the ts in such a way as to satisfy both the requirements of istribution and of matching to the power source. A d recently designed by the authors and built in Australia Clarendon Laboratory has, in fact, partly embodied rinciples in that a particular current density distribu- nd matching was achieved by series connecting six of elements, three of which groups contained two l connected elements. All the elements had the same itch and the desired current density distribution (for um efficiency) in this instance was closely approached cting the correct widths of the elements. Groups were ed from one another by thin insulating sleeves, but no ion was needed between elements in the same group.

wer supplies

olenoids discussed in this paper require very large nts of power in the range of a few hundred megawatts. gh powers of this magnitude are occasionally used for mental purposes, it is hardly likely that these levels generally available on a continuous basis, so that one turn to some form of 'burst mode' of operation, using ergy storage system. From an experimenter's point of his method of operation seems to be acceptable, pro- the bursts can supply several seconds of steady field m to work in. In some experiments, temperature control prove to be a problem because of eddy current heating g the period of field growth. However it is probable that of these difficulties can be alleviated through changes design of experiments and through the use of more sticated techniques (Olsen 1966).

e of the least expensive energy storage devices is the polar generator and several authors have remarked on itability for powering electromagnets (Fakan 1961, ly 1961, Blamey *et al.* 1970). The basic components of levice are a rotating conducting mass, a source of etic excitation field and a means of making electrical ct to the rotor. Probably the largest and most practical of machines is the one at Canberra. (Blamey *et al.* 1970). 500 MJ of energy can be stored and released in a few ds at power levels of a few hundred megawatts. This ine is used to supply 30 MW to power the 30 T magnet nberra.

e Canberra machine evolved from components available e time, and does not represent the optimum that can be ved. This is particularly so with regard to the size of the ine. A completely new design might achieve the same d energy and power with only a fraction of the bulk – gh the use of stronger rotor materials, a superconducting r-cored magnet and a rotor design commensurate with stronger materials. A very significant feature of the erra machine is the simple and practical means of nt collection through the use of solid brushes made to ct only when required to carry the discharge current shall 1966). As an example of what can be achieved follows a brief description of a hypothetical machine

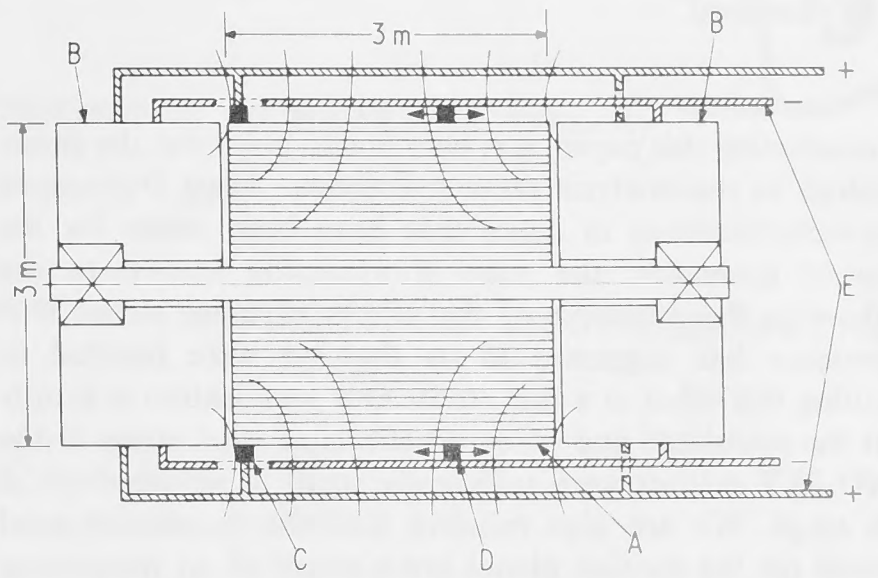

Figure 6 Hypothetical self-excited homopolar energy storage machine capable of supplying 200 MW for 8 s at controlled voltage. A: rotor; B: two excitation air-cored solenoids; C: fixed brush ring; D: sliding (control) brush ring; E: coaxial terminals

that could store 2245 MJ (figure 6). The rotor consists of a number of concentric non magnetic tubes keyed together so that all turn together, but each is free to expand radially independently of the others. Only the outer tube conducts current, and it sustains the highest stress of all, viz. 420 MPa due to centrifugal action. All tubes are 3 m long, and the largest is 3 m diameter. The maximum angular speed is 437 rad s^{-1}. Placed adjacent to each end of the rotor are two large air-cored excitation magnets, each of which produces an average axial field of 1 T over the rotor end faces. Two brush rings surround the outer tube, one fixed at one end and the other capable of being slid axially along the rotor (Marshall 1973). When the brush rings are at the ends of the rotor tube a maximum of 981 V is developed. The excitation magnets are water cooled and are energized from the machine itself. They are assumed to require together a maximum of 50 MW. In operation the position of the sliding set of brushes is automatically varied in order to maintain the desired output voltage. The kinetic energy is transferred from the inner tubes to the outer conducting tube by means of a keying system which needs to withstand only a very small shear stress (averaged over the whole interface). The rotor is mostly of duralumin composite and the energizing magnets are notionally similar to figure 5(*b*), medianly split.

The energizing magnets are connected in parallel with the load (a high field solenoid such as we have been discussing) across the brush rings. At the commencement of a power burst the rotor spins at full speed and the sliding brush ring is positioned to produce one quarter of full voltage, viz. 245 V. As energy is transferred to the load and energizing magnets, this voltage is maintained by sliding the movable brush ring along the rotor until it reaches its limiting position, at which time the speed will have reduced to one quarter of the initial speed, and only one sixteenth of the original stored energy will remain in the rotors. Thus substantially all the stored energy (in fact 2105 MJ), is extracted at constant voltage. Allowing for the 50 MW required for the excitation magnets, this performance would allow the energizing of a 200 MW high field magnet for more than eight seconds.

The above description of a hypothetical machine, although omitting mention of many of the important engineering problems that would be encountered, nevertheless makes the point that the generation of large powers for substantial periods of time can be achieved with equipment of moderate

size and complexity in comparison to the high field solenoids to be energized.

10 Conclusions

In concluding this paper, it is only fair to point out the shortcomings in the analysis presented above. Apart from some over-simplifications in detail that have been made for the sake of generality, the main shortcoming known to the authors is the omission of the effects of axial stress. Our experience has suggested to us that we were justified in omitting this effect in a first study. Our justification is simply that the calculated and observed effects of axial stress in the ANU 30 T magnet were sufficiently small to ignore them at this stage. We are also mindful that the maximum axial stresses (at the median plane) are a result of an integrating process over the axial length and, therefore, the tapered magnet profiles that are proposed here would tend to offset the shortening axial length on the one hand, against the increasing field on the other, as the central high field region is approached.

In our view, these studies have demonstrated that the feasibility of producing quasi-continuous 45 T fields in practically useful volumes is much greater than we had anticipated. Many of the problems which had been imagined, particularly those relating to current density, e.g. cooling, have been shown to be less than generally thought.

References

Bitter F 1961 *Proc. Conf. on High Magnetic Fields* (Cambridge, Mass: MIT and New York: Wiley) pp 85–99

Blamey J W, Carden P O, Inall E K, Marshall R A and Newstead G 1970 *Proc. Int. Conf. on Magnet Technology* Hamburg 1970, pp 1293 (Hamburg: Deutsches Elektronen–Synchrotron DESY)

Carden P O 1970 *Proc. Int. Conf. on Magnet Technology* Hamburg pp 271–8 (Hamburg: Deutsches Elektronen–Synchrotron DESY)

Carden P O 1972a *J. Phys.* E: *Sci. Instrum.* **5** 654–6

Carden P O 1972b *J. Phys.* E: *Sci. Instrum.* **5** 657–62

Carden P O 1972c *J. Phys.* E: *Sci. Instrum.* **5** 663–6

Carden P O 1972d *J. Phys.* E: *Sci. Instrum.* **5** 667–8

Fakan J C 1961 *Proc. Conf. on High Magnetic Fields* (Cambridge, Mass: MIT and New York: Wiley) pp 211–6

Klaudy P 1961 *Proc. Conf. on High Magnetic Fields* (Cambridge, Mass: MIT and New York: Wiley) pp 218–34

Kroon D J 1968 *Laboratory Magnets* Phillips Technical Library pp 133–9

Marshall R A 1966 *IEEE Trans. of Power Apparatus and Systems* **PAS-85** 1177–88

Marshall R A 1973 *Australian National University Department of Engineering Physics Research Report* EP-RR **27**

Montgomery D B 1969 *Solenoid Magnet Design* (New York: Wiley-Interscience) p 20

Olsen J L 1966 *Proc. Conf. on Megagauss Magnetic Field Generation by Explosives and Related Experiments* (Brussels: Euratom) pp 483–90

Parkinson D H and Mulhall B E 1967 *The Generation of High Magnetic Fields* (London: Heywood)

Wood M 1961 *Proc. Conf. on High Magnetic Fields* (Cambridge, Mass: MIT and New York: Wiley) pp 387–92

Journal of Physics E: Scientific Instruments 1974 Volume 7

13

PAPER PRESENTED TO FIFTH INTERNATIONAL CONFERENCE ON MAGNET TECHNOLOGY

FRASCATI (ROME), 21-25 APRIL 1975

EPTIONAL ASPECTS OF HIGH POWER RESISTIVE SOLENOIDS IN RELATION TO THEIR USE IN HYBRID MAGNET SYSTEMS

r A. Hudson - Clarendon Laboratory, Parks Road, Oxford, U.K.
r E. Hanley - Oxford Instrument Co. Ltd., Osney Mead, Oxford, U.K.
r O. Carden - Department of Engineering Physics, A.N.U., Canberra, Australia.

Combined resistive and superconductive magnet systems offer an economical approach to higher fields for ratories that possess a large power supply and have adequate refrigeration/liquefaction capacity. Such "hybrid" ems have the advantage that they can produce magnetic fields much larger than can be generated alone by either of component parts. Experience with the first generation of hybrid magnets is being accumulated in establishments in ada (McGill University), the U.K. (Clarendon Laboratory, University of Oxford), the U.S.A. (Francis Bitter onal Magnet Laboratory) and the U.S.S.R. (Kurchatov Institute of Atomic Energy, Moscow). Whilst the next eration of hybrid magnets will perhaps become increasingly ambitious in respect of the design of the superconducting on, problems associated with the inner magnet being exposed to increasingly higher stress levels will be a dominant or in dictating the overall efficiency of the system.

INTRODUCTION

In a paper presented to the conference "High magnetic fields; their production and their applications" in 1966, d and Montgomery[1] examined the feasibility of combining superconductors with resistive windings to form a "hybrid" net. The potential of this approach is to provide the means to higher magnetic fields for laboratories with er-limited installations, and in the absence of any major breakthrough in superconductor technology, to offer the economical approach to the generation of steady fields above 20 tesla[2]. Hybrid systems permit also a greater ational flexibility in laboratories with a large amount of installed power, 10 or 12 MW.

The logical hybrid arrangement is shown in fig. 1. The superconducting windings in which the maximum current ity is a function of magnetic field, are providing a background field in which the resistive insert operates. The iency of the resistive part will depend on the distribution of current density which in some regions may be limited by s and the considerations that are given to power dissipation and cooling. At fields greater than approximately esla, the Lorenz force begins essentially to dominate the design[3].

RESISTIVE MAGNETS

Bitter Magnets. The most widely used construction for high field resistive coils is that due to the late Francis r. The Bitter technique involves the manufacture of a large number of thin discs of copper or a high strength copper , each disc being perforated with a pattern of small diameter holes and having a radial slit such that by assembling a of interleaved discs, a helical coil can be built up, the small holes aligning to form axial cooling channels (fig. 2). resultant distribution of current density, which varies inversely with radius, yields greater field per unit power than can btained with a coil of uniform current density.

The discs are effectively bonded together by friction, but near the ends of the coil the electromagnetic forces do not ide sufficient axial compression and an external means of applying ping force is necessary to prevent unwinding. It is convenient to inate the helix on two equipotential electrodes, but this practice ts in unbalanced shear forces at the points of current entry and exit. solutions to these particular problems of Bitter magnets are readily eved but if this type of construction is to be used as an insert coil hybrid arrangement, the space occupied by clamping structures and training members could result in a larger, costlier superconducting ing than perhaps might otherwise be necessary. However, the cipal problem in the design of a hybrid coil system is the support of nteractive forces between the two coils.

Under normal conditions, a small axial displacement produces a ring force and by careful alignment, making some allowance for ive motion, this need not cause difficulty. However, during an eme asymmetrical failure of the copper magnet resulting in a ficant displacement of magnetic centres, the peak accelerating e can attain alarming proportions[4]. The forces in the radial ction are unstable, a radial displacement producing an increasing e, and it is thus necessary to provide radial location and not to allow relative radial movement. Radial forces are in general small enough o seriously influence the efficiency of cryostat design[5].

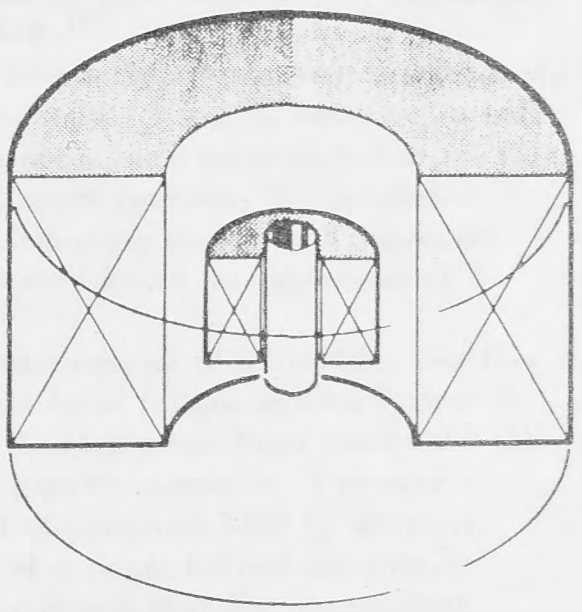

Fig. 1.
Hybrid magnet arrangement.

A alternative method of magnet construction which should lead to a reduction in magnitude of the peak accelerating
wh ch could develop when single stack Bitter magnets are used in hybrid systems, and which should also overcome
t e earlier difficulties mentioned is the polyhelix scheme.

P yhelix Magnets. The concentric nesting arrangement of bonded helices was first used by Wood in 1962(6)
co e the difficulty of designing improved efficiency resistive coils to match the relatively high impedance of the
pe erator at the Clarendon Laboratory, Oxford. By adopting Wood's technique and dividing the winding volume
nu ber of discrete single layer coils, (fig. 3), it is possible to achieve any desirable distribution of current density
t the constraints of available power, limitations of cooling and considerations of strength(7). By series, parallel
m nation series/parallel electrical arrangement of sub-coils, impedance matching is greatly facilitated.
A advantage of the polyhelix construction is the ease with which cooling channels can be introduced at the
i between coils. Cooling of Wood's early magnets was achieved by the insertion of pre-formed corrugated
g ss-reinforced-plastic (grp) into the enlarged annular gaps between adjacent coils. More recently Carden
(ence 8) has described an elegant development of this technique in which axial grooves are machined into
i surface of each sub-coil, electrical insulation, where necessary, being provided by tightly fitting a cylinder of
l d grp. This precise arrangement has been selected for the inner magnet of the Clarendon hybrid system which
r e later. Where coils are grouped in parallel arrangements, an additional degree of freedom is given to the
r that the optimisation computation can take account of the variation of the space factor with radius due to the
t n of the cooling channels. This results in slight departures from a $^{1}/_{r}$ current density distribution.

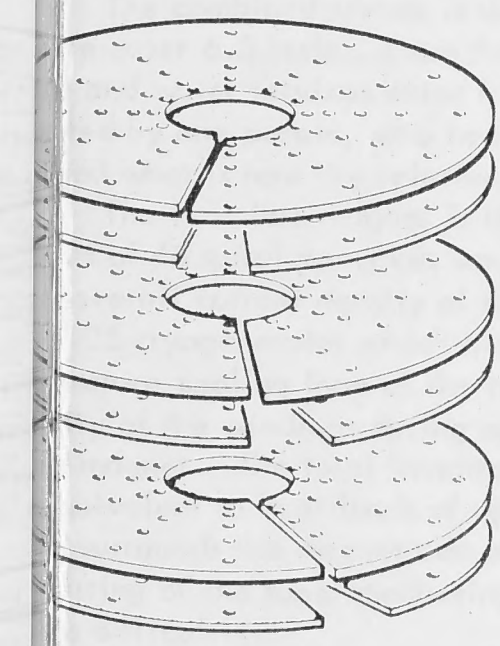

Fig. 2 Bitter magnet.

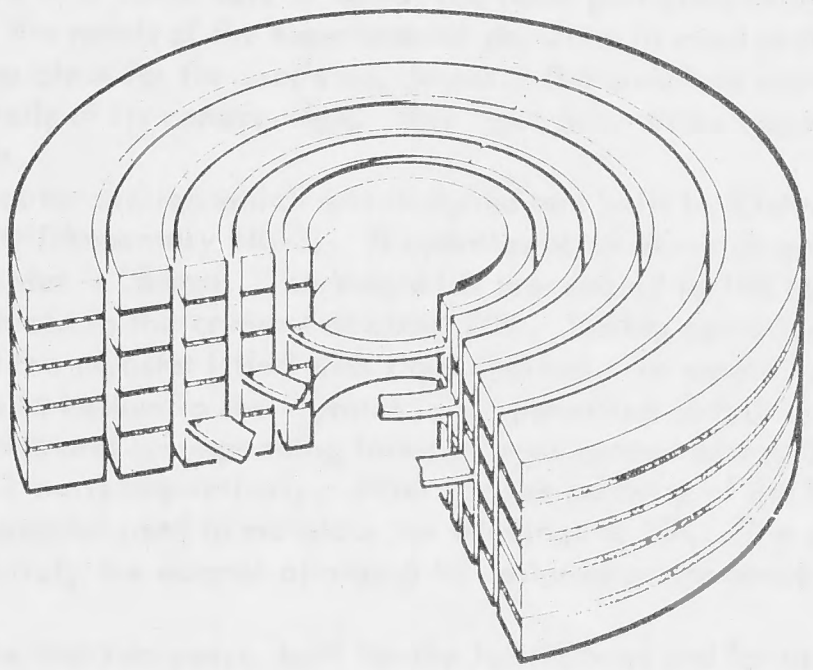

Fig. 3 Polyhelix magnet.

T ere are a number of features which make the polyhelix arrangement particularly suited to use in high field hybrid

T e first of these is that the design of the whole magnet is not limited by the stresses that appear at the inner radius
w dings. Thus while the current density in the innermost sub-coils may be limited by local stress levels, the current
i the outer coils can be selected to make the most efficient use of available power.(8)
T e second is that by bonding the adjacent turns of each sub-coil together, and introducing the current progressively
f st turn, the need for the massive clamping arrangements of Bitter magnets is avoided. There is, however, a net
s rce on each sub-coil due to end effects, but these forces can be arranged to oppose each other such that the total
f e complete magnet is small. Because of the absence of large peripheral mechanical features, the polyhelix
c on results in a compact geometry which minimises the size of the outer superconducting magnet and allows all
p cooling services to the copper magnet to be introduced from below - an important feature for experimental
e e.
T e third advantage to be gained by incorporating this type of winding for the insert magnet of a hybrid system lies
m hanical independence of each sub-coil. It is likely that the propagation of any local failure will be limited to
a il or group of electrically parallel coils and that the maximum force that can develop under fault conditions will
c rably smaller than if the insert magnet consisted of a single coil, of the Bitter type for example. (Hanley
[5] calculates for the Clarendon hybrid system a maximum force in the axial direction of 1400 kg which is
w s approximately one-sixth of the force which could arise if the coil consisted of a single helical winding.).
c yogenic requirements of the vessel which houses the superconducting winding demands that the two magnets
s ectly coupled together and thus any significant reduction in force leads to a more efficient cryostat design and
i ed reliability.

This cornucopia of desirable features cannot be obtained without some disadvantages and problems, many of which from the added complexity of the polyhelix arrangement.

The coils themselves are difficult to manufacture requiring the edge bending of copper strip, often of high aspect into small diameters, and the consequent need to avoid winding distortion. The demands placed on the medium used to the turns are stringent. The bond must be capable of maintaining constant spacing between turns, it must also be tant to the effects of deionised water and heat on its insulating properties and mechanical strength over long periods of

Serious design problems arise when considering the electrical termination of the sub-coils. Carden has chosen to number of discrete pressure contacts onto the machined end faces of the coils, both in the A.N.U. magnet [8] and the endon magnet. An alternative scheme which has been studied at the Clarendon Laboratory is to use interference - copper caps, but this annuls the above mentioned feature of being able to introduce the current progressively into rst turn of each coil. Soldering or welding techniques are ruled out by the damage they would cause to the -turn bonding.

The use of discrete contact points results in considerable mechanical complexity, as each contact has to be able to endently follow up distortions in the coil produced by thermal effects and electromagnetic forces. Individual current ing contact rods have to be able to withstand appreciable sideways forces in the radial field at the ends of the magnet.

THE CLARENDON MAGNET

This hybrid system has been described in depth previously[5], but since its installation considerable experience has gained which merits further description, with particular reference to the inner magnet.

The combined system is designed to produce 16 tesla in a 50mm bore of which the inner part contributes 9.5 tesla, he outer 6.5 tesla. From the outset it was built with the needs of the experimental physicist in mind so that all the r and water services enter from below, leaving the top clear for the user's equipment. The complete system can be ted by one person, who need not be aware of the details of its construction. This "user orientation" perhaps ted what is now the relatively modest field of 16 tesla.

The complete magnet is illustrated in fig. 4. The outer section which was designed and built by Oxford Instruments, sts of 46 spiral pancakes wound from fully-stable, multifilamentary Nb-Ti. It operates at 617A which corresponds overall current density of 63A/mm^2. The inner diameter is 284mm. This magnet is pre-cooled to 18K by a Philips 105 cryogenerator which also maintains a radiation shield in the cryostat at about 70K. During operation, the low- erature cooling loop of the refrigerator is shut off and the cryostat filled with liquid helium. To ensure full ity of the windings during operation, the level of liquid helium in the cryostat is not permitted to fall below the top e magnet. The total inventory is approximately 65 litres and corresponding losses at zero current and at 617 amps quivalent to heat loads of approximately 2 watts and 3 watts respectively. After use the majority of the helium h surrounds the magnet can be recovered and the refrigerator used to maintain the windings at 18K. The construction esting of the superconducting magnet has been uneventful, the magnet attaining its designed performance without us difficulties.

It has been cooled and operated repeatedly over the last two years, both for the hybrid tests and for use in high magnetic separation experiments.

The inner magnet, designed and built by P.O. Carden of A.N.U. and Research Technology, Canberra, follows olyhelix principle outlined above. It consists of 10 coils arranged in six electrically serial groups. Each coil is m long and has 40 turns. The radial thickness of the coils ranges from 2mm to 16mm and their inner diameters from to 184mm. They are made from hard-temper copper with ·05% silver. As in the A.N.U. magnet, the coils are nated by pressure contacts, with an arrangement of rocking copper bridges and copper rods to transmit the clamping which is obtained hydraulically (fig. 5). This arrangement is fed with current through twelve pairs of tudinal leads arranged around the outside of the magnet. In this way all external electrical terminations are at the m. The members of each pair of leads of opposite polarity are bonded together so there is no azimuthal force - a n which places stringent requirements on insulation. Each lead has a small resistor in series with it, whose value is n so that they carry approximately equal current.

The inner magnet also reached its designed field of 9.5 tesla shortly after installation. However, after only brief tion, one of the lead pairs referred to above burnt out and some damage occurred to the innermost sub-coil. It is ved that this damage to the coil was due to arcing when contact pressure was momentarily lost, but the exact anism of failure was not clear. After repairs were completed, similar lead damage was again experienced and the eventually traced to insulation failure resulting from water absorption. Extensive insulation tests led to a new design being developed which has so far proved to be satisfactory. A number of problems were also encountered in ning reproducible contact resistances. These were resolved by gold-plating the relevant areas, by careful attention to ng of the contacts and also by ensuring that the moving parts of the assembly were perfectly free. In connection with oint, it was found that the glass-fibre housings of the mechanism swelled after long immersion in water, thus reducing learances.

The inner magnet has now been repeatedly operated at full field and it has been found that the contact resistances eliably repeatable. However, immediately after reassembly, the contacts have to be "bedded-in" at a relatively low nt before it can be safely run quickly to its maximum. If the magnet has not been dismantled, then this does not apply.

With an inlet water temperature of 20°C, 9.5 tesla is produced for a power consumption of 1.6 MW at
The temperatures of the individual sub-coils range from 27°C to 57°C above the inlet water temperature.
During tests, it was found useful to monitor the voltage across each of the sub-coil groups and also the current
each of the twenty-four leads. Thus a change in contact resistance or a recurrence of the lead damage could
diately recognised.

A number of hybrid runs have taken
cently with gradually increasing total
. To do this the field centres of each
ad to be established with a precision
than 1 millimetre. It was found that
d best be done by plotting the field
rge region with a low precision
be (about 1%) rather than by highly
measurements over a small region,
M.R. for example. This is because
odd-order gradients displace the
field centre by as much as several
es, when making the high accuracy
nents.

To date, a combined field of 15.4T
reached without incident and the full
ld of 16T will probably be attained
ext test.

ACKNOWLEDGEMENTS

The authors thank all those who have
ed their skill and care and patience
oject, who are too numerous to
by name.

The project is supported by the Science
Council.

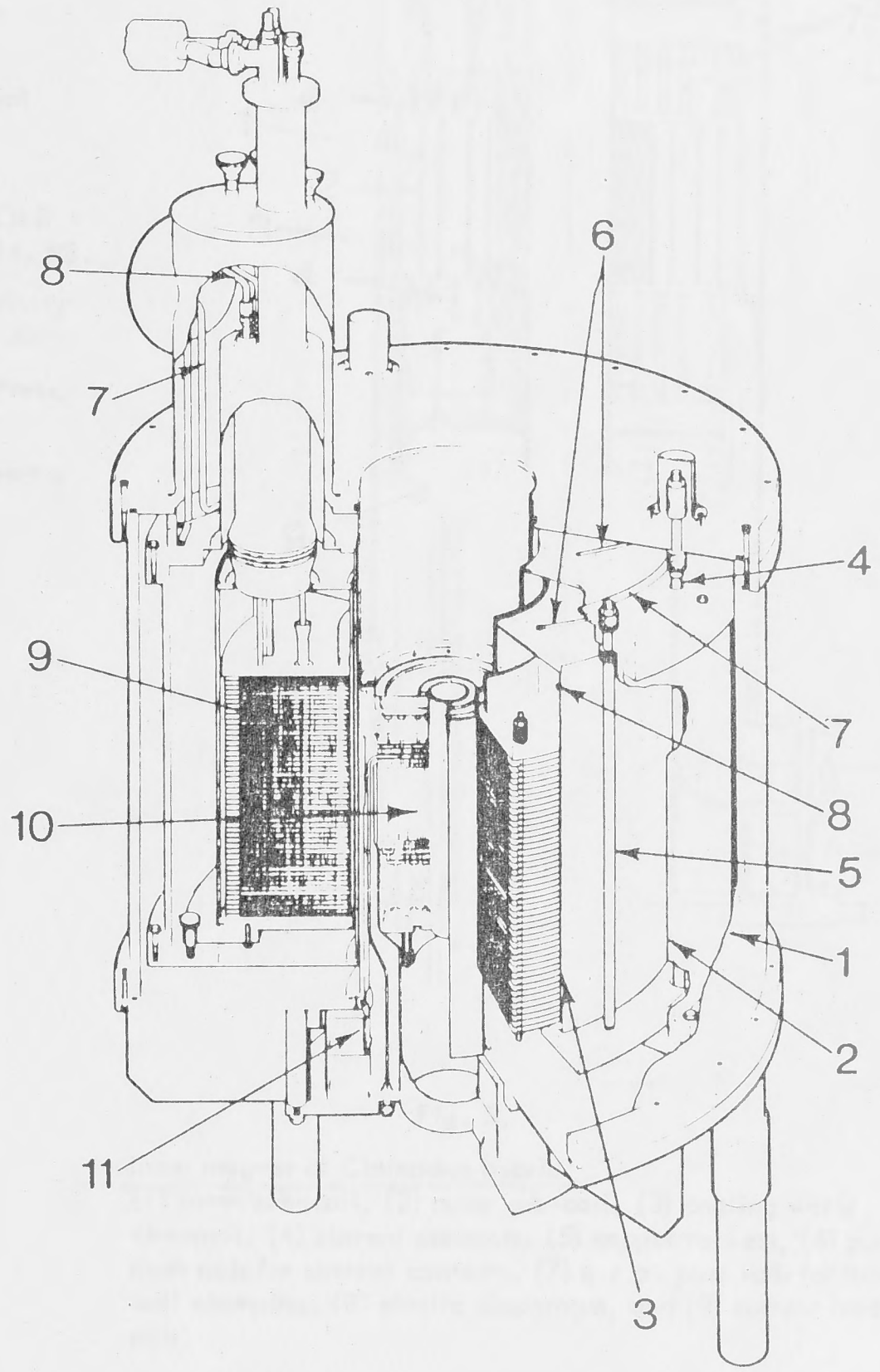

Fig. 4.
General arrangement of hybrid magnet.
(1) Outer vacuum case, (2) radiation shield, (3) liquid helium can, (4) support tube - outer case to radiation shield, (5) support tube - radiation shield to helium can, (6)radial support rods, (7) 50K refrigeration lines, (8) 20K refrigeration lines, (9) superconducting magnet, (10) water-cooled magnet, and (11) cooling water manifold and current terminals.

EI RENCES

) M.F. WOOD and D.B. MONTGOMERY - High magnetic fields: their production and their applications, Grenoble 1966 (editions du CNRS, Paris, 1967), 91.

) see eg. R.J. WEGGEL and D.B. MONTGOMERY - Proc. IV Int. Conf. on Magnet Technology, 1972 (US Atomic Energy Commission AEC CONF-720908), 18.

) P.O. CARDEN and A.M. COLLINS - Journal of Physics E: Sci. Instrum., 1974, 7, 750.

) D.B. MONTGOMERY, J.E.C. WILLIAMS, N.T. PIERCE, R. WEGGEL and M.J. LEUPOLD - Advances in Cryogenic Engineering, 1969, 14, 88.

) P.E. HANLEY - Proc. Applied Superconductivity Conf., Annapolis, 1972 (New York:IEEE), 302.

) M.F. WOOD - High Magnetic Fields, MIT Press, Cambridge, Mass., 1962, 387.

) P.A. HUDSON - Proc. Physics in High Magnetic Fields, Grenoble, 1974.

) P.O. CARDEN - Journal of Physics E: Sci. nstrum., 1972, 5, 654.

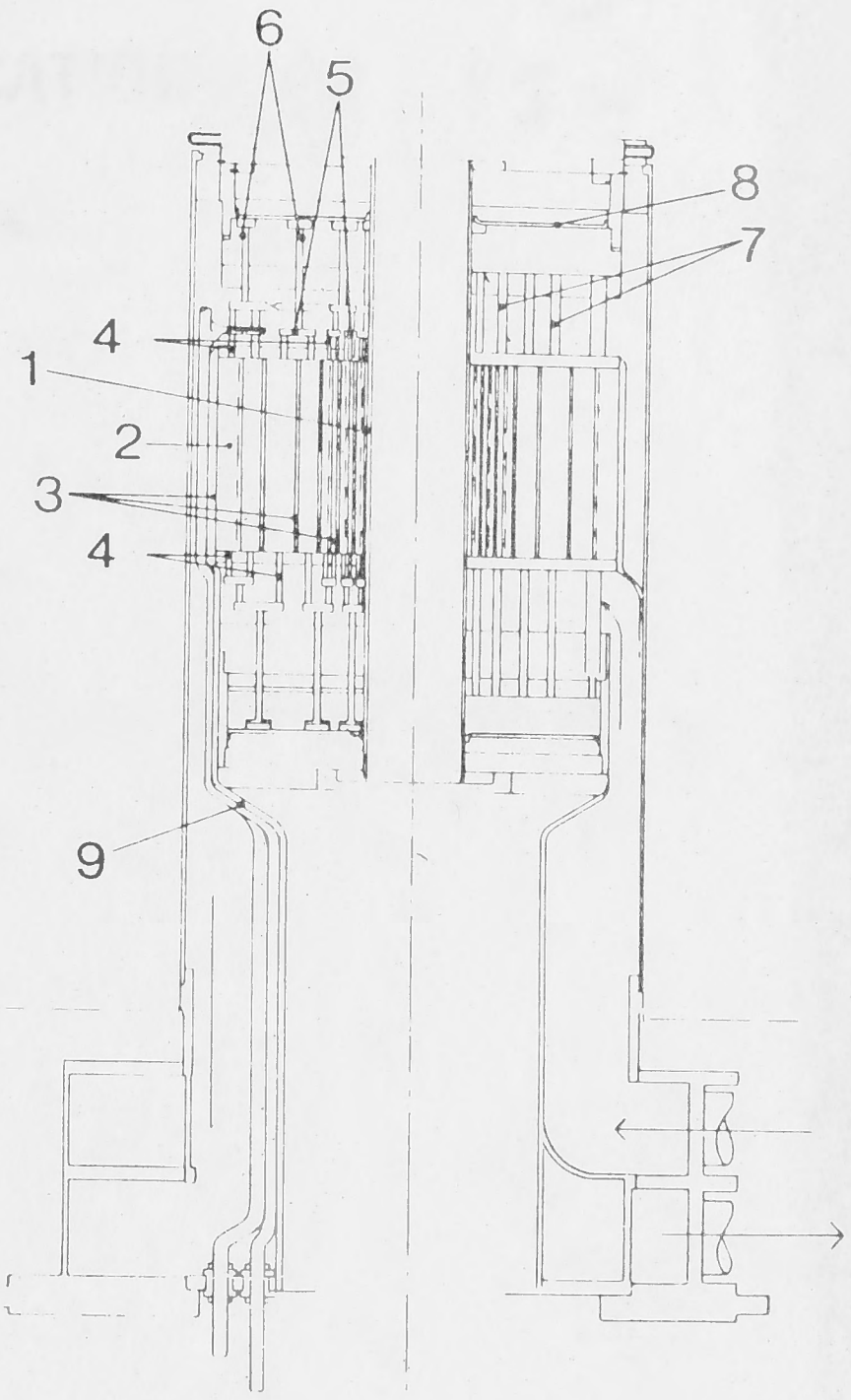

Fig. 5.

Inner magnet of Clarendon hybrid.
(1) inner sub-coil, (2) outer sub-coil, (3) cooling water channels, (4) current contacts, (5) copper rockers, (6) g.r.p. push rods for current contacts, (7) g.r.p. push rods for axial coil clamping, (8) elastic diaphragm, and (9) current lead pair.

(11) 416635

(14)

COMMONWEALTH OF AUSTRALIA

PATENT SPECIFICATION (21) 44,033/68

Class (52) 73.1; 02.1; 02.6; 47.7; 79.3.

Int. Cl. (51) C08g; H01f.

Application Number (21) 44,033/68.
Lodged (22) 30th September, 1968.
(Accompanied by a
Provisional Specification)

Complete Specification
entitled (54) A METHOD OF BONDING METAL TO METAL OR OTHER MATERIALS.

Lodged (23) 29th September, 1969.
Accepted (44) 27th August, 1971.
Published (41) 15th January, 1970.

Convention Priority (30) -

Applicant (71) THE AUSTRALIAN NATIONAL UNIVERSITY.

Actual Inventors (72) PETER O'NEIL CARDEN, JOHN CECIL HARRIS and YARKO LADYZHYNSKY.

Related Art (56)

293,544(51,144/64)	09.4; 79.3; 47.7; 73.1; 09.10
17,515/67	73.1
51,145/64	73.1.

The following statement is a full description of this invention, including the best method of performing it known to us :

W. G Murray, Government Printer, Canberra

19682/71—L

134-ND-23/9/71-25P.C.

This invention relates to the bonding together of two surfaces at least one of which is a metal, alloy, or metal-based compound (the term metal will hereinafter be taken to include the alloy or metal-based compound).

Epoxy resin has hitherto been used to bond metals to metals and metals to synthetic resin-bonded materials. In general, use of this convenient bonding agent has provided a bond of adequate strength for most purposes, but when such a bond is in contact with water, the water diffuses into the epoxy layer and in due course destroys the bond between the epoxy material and the metal.

The object of the present invention is to provide a bond to metal surfaces which is many times more resistant to the effects of water than the plain epoxy bond.

According to the present invention, a method of bonding a metal component to a second component comprises: coating the surface of said metal component with at least one layer of a synthetic resin as hereinafter defined; baking said coated metal component after the application of the or each layer of synthetic resin; preparing, after baking, the surface of such coated metal component for an epoxy bond by cleaning and, if necessary, roughening same; preparing the surface of said second component for an epoxy bond by cleaning and, if necessary, roughening same; and bonding said coated metal component and said second component together using an epoxy resin.

The term "synthetic resin" as used herein is defined as meaning a resin which:

a) when baked forms a coating which is substantially impervious to moisture;

b) requires mixing with a solvent in order to be effectively applied as a coating, with such solvent being a substance that evaporates during the baking process;

c) exhibits a strong bond to metal surfaces when applied as a coating thereto and baked; and

d) does not form a sound adhesive bond between two surfaces which are impervious to the solvent.

In the method of this invention, the synthetic resins used act purely as a coating, or a water-proofing agent, on the metal surfaces and do not contribute to the bonding together of the two components. These snythetic resins are accordingly chosen primarily for their imperviousness to moisture and for their bond strength to metal. These resins are applied with the aid of a solvent and, after application, are baked at a high temperature, e.g. 300°F or 400°F. in order to evaporate the solvent and cause chemical cross-linking of the resin. Examples of synthetic resins which are suitable for use as coating agents in the method of this invention are phenol formaldehyde resins and phenolic-epoxy resins.

The water resistance of the bond obtained using this invention is presumably due to the fact that the synthetic resin coating is more impervious to water than epoxy resin and the bond between the synthetic resin coating and epoxy resin is little affected by water diffused into the epoxy material.

It has been found that a bond made in accordance with the method of this invention is less brittle, and usually stronger, than the plain epoxy bond. An additional advantage of the present invention in some electrical applications is that the coating of synthetic resin provides a layer of insulation which may be inspected before the bond is complete. A further advantage, in some cases, of the present invention is that the metal coated with synthetic resin may be heated in air in order to cure the resin before bonding with the epoxy material without fear of oxidation of the metal. Previously, a metal which would have oxidised under such heating had to be heated in an inert atmosphere.

A particular application of the present invention is to the fabrication of electrical solenoids employing high power densities, for example, the solenoids used to generate high magnetic fields for experimental purposes. It is therefore appropriate to describe a preferred embodiment of the invention as used for this purpose.

The coils referred to in the previous paragraph are usually cooled by water in direct contact with the conductor of the coil. The water in such cases must necessarily come into contact with the bonding agent used to bond adjacent turns of the solenoid together.

For the particular application to be described,

copper wire of rectangular cross-section is first formed into the helical shape of the solenoid. The helix is then pulled axially so that it stretches elastically, exposing the surfaces to be bonded. The surfaces to be bonded are than sand blasted and coated with phenol formaldehyde resin by a known process. Whilst one coat is sufficient for some applications, several coats of phenol formaldehyde are normally applied, with a baking period after each coat. It has been found that two coats, each 0.001 inch thick, gives a very satisfactory result. The surfaces are examined for flaws after each coat of phenol formaldehyde has been baked.

When the required number of coats of phenol formaldehyde resin have been applied and baked, the surface of the phenol formaldehyde is lightly sanded with a fine sand paper or lightly sand blasted, care being taken not to expose the conductor. The turns of the helix are then correctly located with respect to one another to provide the space between them for the intrusion of epoxy resin and to ensure that the bonded helix has the desired pitch. A jig and several strips temporarily bonded longitudinally to the external surface of the solenoid may be conveniently used for this purpose.

The helix is now ready for bonding using the epoxy resin, which is generally a hot curing type chosen for its high water resistance.

In the preferred method of forming the epoxy resin bond, the helix is heated before applying the epoxy resin to give a quick and practical method of intruding the epoxy resin between the surfaces to be bonded. This is done by placing it in a cylindrical canister which is spun adjacent to the coils of a radio

frequency heater or a set of gas burners.

When the helix is at the correct temperature, approximately 70°C, the cold epoxy resin is rapidly introduced into the canister where it is quickly made fluid by being subjected to large distorting forces (i.e. epoxy resin is a thixotropic material) and by contact with the hot helix. The mobile fluid resin then easily intrudes between the turns of the helix and is spread by centrifugal action.

It has been found that a spinning speed of 2000 r.p.m. is adequate to perform the above operation when the inside diameter of the helical coil is 2 inches and where the spacing between the coated turns is no greater than 0.001 inch. The necessary spinning speed for different sized helical coils is inversely proportional to the square root of the inside diameter of the helix.

After sufficient epoxy resin has been applied to fill all the spaces between the turns of the helix and the spaces between the helix and the capsule, the temperature of the helix is raised to promote rapid curing and the spinning is continued for the curing time recommended by the epoxy resin manufacturers.

The canister is then removed from the helix by machining, which will also remove any resin from the outer surface of the helix as it is important for the cooling of the helix that the cooling water comes into direct contact with the copper of the solenoid.

It will be understood that a particular way in which the present invention may be utilized has been described. It is not essential to carry out all of these steps in other applications of this invention; in particular, it will rarely be necessary to assemble the resultant product in a jig if a single bond is to

be formed.

If a metal surface is to be bonded to the surface of a synthetic resin-bonded material, that material needs no coating treatment before using the epoxy resin to effect the bond, but needs only to be cleaned and, in some instances, roughened, by way of preparation for the actual bonding. In this context, the term "synthetic resin-bonded material" means a resin reinforced by the inclusion of threads or sheets of any substance which will bond to the resin. Essentially the resin encases the reinforcing and gives form and rigidity to the composite material. The resin is usually a thermosetting plastic and the reinforcing will include metal threads as well as the more usual glass strands, linen or glass cloth, paper, mica flakes and carbon strands. An example of a synthetic resin-bonded material is polyester bonded fibreglass and epoxy bonded fibreglass.

The claims defining the invention are as follows:

1. A method of bonding a metal component to a second component which comprises: coating the surface of said metal component with at least one layer of a synthetic resin as hereinbefore defined; baking said coated metal component after application of the or each layer of synthetic resin; preparing, after baking, the surface of said coated metal component for an epoxy bond by cleaning and, if necessary, roughening same; preparing the surface of said second component for an epoxy bond by cleaning and, if necessary, roughening same; and bonding said coated metal component and said second component together using an epoxy resin.

2. A method as claimed in claim 1, in which said second component is a metal component and said preparing of the surface of said second component comprises: coating said surface with at least one layer of said synthetic resin; baking said coated second component after the application of the or each layer of synthetic resin; preparing, after baking, the surface of said second component for an epoxy bond by cleaning and, if necessary, roughening same.

3. A method as claimed in claim 1, in which said second component comprises a synthetic resin-bonded material.

4. A method as claimed in any one of claims 1 to 3, in which said synthetic resin is a phenol formaldehyde resin.

5. A method as claimed in any one of claims 1 to 3, in which said synthetic resin is a phenolic epoxy resin.

6. A method as claimed in any preceding claim, in which the surface of the or each metal component is sand-